universität wien

DISSERTATION / DOCTORAL THESIS

Titel der Dissertation /Title of the Doctoral Thesis

„Stratigraphic paleobiology of *Terebratula* (Brachiopoda) in the Pliocene of south-east Spain“

verfasst von / submitted by

Ing. Diego A. García-Ramos

angestrebter akademischer Grad / in partial fulfilment of the requirements for the degree of

Doktor der Naturwissenschaften (Dr.rer. nat.)

Wien, 2020 / Vienna 2020

Studienkennzahl lt. Studienblatt / degree programme code as it appears on the student record sheet:	UA 796 605 426
Dissertationsgebiet lt. Studienblatt / field of study as it appears on the student record sheet:	Erdwissenschaften
Betreut von / Supervisor:	Univ.Prof. Mag. Dr. Martin Zuschin

A mi madre

Vida en Piedra

A golpes de mar, clastos derrumbados,
lientos y deshechos, eternos ratos
de ese mar a hachazos, capas, estratos
ya rendidos, ya desenterrados.

Rendidos a un tiempo, los derribados
restos de piedra ven otro destino,
atrás quedó la vida en el camino,
atrás los sedimentos devastados.

Morir, tal vez, de nuevo, en las arenas,
volver siempre y para siempre al mar,
o quizás, sólo, nada entre la nada.

Sólo es eso. Vida en piedra en la piedra
por siempre condenada a retornar
a una historia triste y olvidada.

DAGR, Lorca, 1998

Table of Contents

Acknowledgements

My fascination with fossils grew in me when I was seven years old. I took a few steps in Paleontology as an amateur, but the vicissitudes of life made me think that my dream of doing a PhD about brachiopods was just that: a dream. For this reason I massively thank my supervisor Professor Martin Zuschin, first off for trusting me for the position in the beautiful city of Vienna and for granting me this incredible opportunity in my life (a dream come true!). Not least I express my gratitude to him for his wisdom, constant generosity, support, patience, and encouragement throughout the course of this thesis. He openly encouraged me from the beginning to work on brachiopods, which are my passion. Vielen Dank!
The fantastic moments with numerous friends at the Department of Paleontology will remain forever in my memory, as well as the numerous field trips to the Carnic Alps, the Aquitaine Basin (that was electric!), Eggenburg, Eisenstadt, Tuscany, the North Adriatic, Trieste, the Dinaric Alps, Serbia, Bosnia and the Eastern Betics.

A special mention should be made to Professor Michael Joachimski, Yadong Sun and Emilia Jarochowska for their kind hospitality in Erlangen and for the fruitful discussions about oxygen isotope ratios from brachiopod calcite. Yadong was always very kind and supportive in every step of the way. Emilia is a source of inspiration as a model for early career scientists. I appreciate her advice and the moral support to navigate the winding roads of a PhD.

My gratitude goes also to Stjepan Ćorić for his kindness and for sharing his incredible knowledge of calcareous nannoplankton during our collaboration!

I want to thank many friends and colleagues too numerous to count, who crossed paths with me at the Department. With Alex Haselmair and Ivo Gallmetzer I shared my first experience during my stay in Vienna. Doing field work in the North Adriatic was a fantastic experience! My gratitude goes to them for our numerous invaluable talks, moral support, for keeping my health in check with their delicious dishes and for sharing their vast knowledge of the marine habitats in the North Adriatic, as well as on the taxonomy and ecology of mollusks.

To Rafał Nawrot for the numerous discussions and suggestions on many paleontological aspects and for the beers we had. His perspicacity with quantitative methods in paleobiology was inspiring. I also want to thank him for his invaluable help with programming every time I got stuck with R, for his help with the taxonomy and paleoecology of Neogene

mollusks and for the abundant literature he made available to me. I also want to thank our room mate Jelena Vidović for her support, our talks during lunch breaks and for the discussions on extant foraminifera. Likewise, I would like to thank her supervisor Vlasta Ćosović for sharing her extensive knowledge on foraminifera, stratigraphy and paleoenvironments and for her advice. We had a fantastic time visiting the geological wonders of Istria!

The "Foram" colleagues made me feel like one of their own: I warmly thank Professor Johann Hohenegger for sharing his second-to-none knowledge of statistics and multivariable methods, and resolving many doubts about the biology, ecology and taxonomy of foraminifera and for his reprints! I was also lucky to enjoy the friendship, discussions and coffee/lunch/beer breaks with Wolfgang Eder, Patrick Bukenberger, Anna Binczewska, Ana Torres, Julia Wukovits, Sunichi Kinoshita "Kino", Julia Wöger and Erik Wolfgring. They have also helped me on numerous occassions by sharing their knowledge, with SEM pictures or with literature.

I particularly would like to thank Paolo Albano for his supervision, advice and constant support regarding numerous scientific aspects, and putting his inmense expertise on mollusks at my disposal for the study of the complex molluscan life and death assemblages from the Persian Gulf. I extend my gratitude to Jan Steger for his camaraderie and for the numerous discussions and company during lunch breaks. He solved numerous doubts regarding the taxonomy, ecology and distribution of mollusks with his unique and incredible expertise!

I have had the privilege to enjoy numerous discussions with Adam Tomašových about brachiopods among other diverse paleontological topics. His profound knowledge and analytical depth is a source of inspiration for all of us. I also thank him for his help on many occasions with R code which was out of my depth.

No me olvido de agradecer a "Javi" Souto y a Andrei Ostrovsky por compartir en numerosas discusiones su profundo conocimiento sobre la taxonomía y la ecología de los briozoos, así como por la identificación de algunas especies del Plioceno de mi zona de estudio. ¡Muchas gracias también por tu ayuda con las imágenes de microscopio electrónico!

Tampoco me olvido de mis amigas griegas, Danae Thivaiou y Konstantina Agiadi, por los simpáticos momentos que pasamos discutiendo sobre moluscos miocenos y sobre la Crisis de Salinidad del Messiniense, entre otras cuestiones. ¡A veces en español!

I can neither forget the help from Kai-Uwe Hochhauser fixing technical problems with my laptops and for encouraging me to become a Linux user!

I am massively grateful to “Michi” Berensmeier (Huhu!), Angelina Ikvić, Marija Bošnjak (Hvala!) and “Bee” Dunne for their friendship and support, and for so many wonderful times that we shared during the last year!

I am warmly grateful to Martin Maslo for being a great friend, for the uncountable occasions he helped me and for our wonderful field trips in this fantastic country!

I extend my gratitude to all the colleagues and students I met during these years, too many to name of all them here. Thank you all!

Finally, I conclude with special thanks to my family, in particular to my mother, for believing in me when I didn’t. Without their support this journey would have been impossible.

Chapter 1

Introduction

Diversity and history of the Brachiopoda

Brachiopods are a phylum of exclusively marine invertebrate metazoans with a characteristic bivalved shell. They are filter feeders, most are stenohaline, and most have a benthic sessile lifestyle (James et al., 1992; Álvarez et al., 2005a; Bitner and Cohen, 2013). About 30.000 fossil species representing approximately 5.000 genera have been described (Richardson, 1986; Lee, 2008; Santagata, 2015), and their temporal distribution spans the Early Cambrian through to the present day. Today about 400 species allocated in 118 genera are known (making up only ~ 5% of all described genera), which are distributed worldwide (Logan, 2007; Emig et al., 2013).

Brachiopod-dominated Paleozoic world

Brachiopods are the most diverse and abundant animals preserved in the Paleozoic marine fossil record. In terms of sustained familial richness through time, brachiopods rank third among marine metazoans of all time (Thayer, 1986). Their dominance of Paleozoic benthic ecosystems in terms of taxonomic richness has long been thought to come to an end after the most devastating mass extinction of life's history on Earth, at the end of the Permian, which wiped out > 90% of marine skeletonized species (Erwin, 1994). This event was especially dramatic for brachiopods, the second largest group having been affected by this biotic crisis (Erwin, 1994; Chen et al., 2005). Indeed, the end-Permian mass extinction marked a turnover from the Paleozoic Evolutionary Fauna (dominated by rhynchonelliform brachiopods) to the Modern Evolutionary Fauna dominated by bivalves and gastropods (Sepkoski, 1981; Clapham et al., 2006).

Brachiopod-Bivalve ecologic switch

To explain the overall pattern of waning brachiopod diversity coupled with waxing bivalve

diversity, early hypotheses (e.g., Simpson, 1953) invoked the "geometric argument" (i.e., one taxon decreases in diversity as the other increases because of direct biotic competition for resources) (Sepkoski, 1996). Alternative views of this problem, however, suggest that both groups simply displayed differential response, in terms of taxononomic losses, to the end-Permian mass extinction. The event reset diversities, and each group pursued its characteristic and different history without mediation of competition; like 'ships that pass in the night' (Gould and Calloway, 1980). Therefore, one interpretation for the Triassic brachiopod-bivalve turnover has been posed as a case of pre-emptive exclusion by incumbent bivalves that took over vacant post-extinction ecospace (Walsh, 1996; Kowalewski et al., 2002); something sort of like 'move your feet, lose your seat'. Along these lines, it has been pointed out that the life habits displayed by Early Triassic bivalves evolved already during the Paleozoic, and the subsequent morphological innovations that fueled the Mesozoic bivalve radiation are not deemed to be responsible for the Early Triassic brachiopod-bivalve ecologic switch (Frasier and Bottjer, 2007). Because traditionally most studies dealing with the brachiopod-bivalve problem have focused on the Early Triassic recovery after the end-Permian mass extinction, some recent studies have set the scope at refining the knowledge on brachiopod-molluscan diversity and ecological trends during the Permian (Clapham and Bottjer, 2007a). These studies conclude that the brachiopod-bivalve diversity shift developed stepwise, beginning already around the Guadalupian-Lopingian boundary, with a second shift that occurred in the Late Jurassic (Clapham and Bottjer, 2007a,b). These results contrast with the tacit assumption of a single ecologic shift associated with the end-Permian mass extinction. Moreover, there is evidence that, from the metabolic activity standpoint, dominance of bivalves in Paleozoic ecosystems predates the end-Permian mass extinction by 150 m.y., and their increasing metabolic rates during the Phanerozoic might have operated by acquisition of new food resources rather than by displacing brachiopods (Payne et al., 2014; Hsieh, 2019).

Disproportional environmental distribution of brachiopods through the Phanerozoic

An interesting pattern arises if we consider the whole Phanerozoic: brachiopods have colonized a plethora of environments encompassing the intertidal to abyssal (Ager, 1965; Zezina, 2008; Bitner and Cohen, 2013), including hydrocarbon seeps, hydrothermal vents (e.g., Sandy, 2010; Peckmann et al., 2011) and seamounts (Vörös, 1986; Ager, 1993; Gischler et al., 2004). The Phanerozoic distributional patterns of brachiopods are, however, disproportional (Tomašových, 2006). During the Paleozoic, brachiopods were diverse and abundant in tropical to subtropical shallow-water environments, often in soft-bottom habitats (Tomašových, 2006). On the contrary, nowadays brachiopods are abundant in hard substrates of sheltered habitats: shaded fjords (Grange et al., 1981; Tunnicliffe and Wilson, 1988; Dawson, 1991; Försterra et al., 2008), sea-lochs (Curry, 1982), caves (Logan and Zibrowius, 1994; Taddei Ruggiero, 2001; Motchurova-Dekova et al., 2002; Álvarez et al., 2005b), polar regions from shallow to deep waters (Foster, 1974; Barnes and Peck, 1997), and they are relatively rich in pelagic seamounts (Logan, 1998; Gaspard, 2003; Bitner, 2008). Dense brachiopod-dominated communities occur in the outer platform in the Mediterranean Sea (Emig, 1987) and the Pacific coast off California (Pennington et al., 1999), but these are temperate regions. The only example of extant abundant brachiopods in tropical shelves is known from Brazil (Kowalewski et al., 2002). It is interesting that these assemblages contain one endemic genus while the others are cosmopolite, occurring in other climatic settings (Simões et al., 2004). In shallow-water tropical regions brachiopods are micromorphic and occupy cryptic, shaded areas in crevices and undersides of corals (Jackson et al., 1971; Logan, 1975; Asgaard and Stentoft, 1984; Zuschin and Mayrhofer, 2009; Peck and Harper, 2010).

Latitudinal diversity gradient

A decrease of extant brachiopod diversity toward the tropics was pointed out by Rudwick (1970) and Walsh (1996), the latter who suggested that this pattern was already being shaped during the Jurassic. This is striking if we consider that taxonomic richness of many clades peaks in the

tropics (Roy et al., 2000; Macpherson, 2002; Jablonski et al., 2013). Although four out of nine brachiopod orders in the Permian survived the end-Permian mass extinction through to the Jurassic (Vörös, 2010), athyridid and spiriferidid brachiopods, severely affected by the end-Triassic extinction, went extinct in the Early Toarcian, probably because of the Toarcian global anoxic event (Vörös, 2002; Baeza-Carratalá et al., 2015). Diversity of terebratulid and rhynchonellid brachiopods, however, conspicuously rebounded during the Triassic and Jurassic (Sepkoski, 1996; Lee, 2008; Allroy, 2010; Hsieh, 2019). This suggests that the end-Permian mass extinction alone cannot explain this shifting brachiopod distribution toward sheltered habitats either in shallow (caves, undersides of boulders or corals) or deeper water (Tomašových, 2006).

Biotic factors: Escalation and Biological Disturbance

Several lines of evidence point to the appearance of high-metabolism durophagous predators (e.g., jawed fishes and malacostracans) in the middle Devonian, evolving through to the Carboniferous. The occurrence of these predators is accompanied by a concomitant increase in repair marks (from unsuccessful crushing attacks) and drilling predation intensity in brachiopods and other shelled organisms (Signor and Brett, 1984; Leighton, 1999; Leighton et al., 2013). These authors likewise identify morphological changes to more ornamented shells of brachiopods toward the equator, and interpret this trait as an adaptive response to a latitudinal gradient of increasing predation pressure (Dietl and Kelley, 2001). It is possible that this trend was disrupted during the end-Permian mass extinction (Leighton, 1999), which is consistent with the rebounds of brachiopod diversity in the Triassic and Jurassic. There is cogent evidence that predators and bioturbating/bulldozing organisms radiated in the Jurassic (Thayer, 1983; Bambach, 2002; Aberhan et al., 2006). Grazing and bulldozing have very deleterious effects on the survival of attached brachiopod larvae, because once dislodged, they are unable to re-attach to the substrate (Thayer, 1979; Collins, 1991). In parallel to this predator radiation, brachiopods in shallow-water habitats developed stronger ribbed ornamentation, which conforms to the ‘escalation hypothesis’ (e.g.,

Vermeij, 2013), while coeval brachiopods that were adapted to seamounts remained smooth (Vörös, 2005), exhibiting morphologies comparable to those of Paleozoic counterparts inhabiting the same environments (Gischler et al., 2004). Eventually, shallow water, strongly ribbed brachiopods gave up the 'arm race' and gradually disappeared after the mid-Jurassic, retreating toward deeper water habitats (Vörös, 2005; 2010) where the predation pressure was presumably lower (Harper and Peck, 2016). The gradual retreat of brachiopods toward deep water refugia or cryptic oligotrophic habitats is consistent with a decrease of their metabolic rate by about 50% during the Phanerozoic (Payne et al., 2014), a trait that makes brachiopods fitter to cope with low- or seasonal nutrient input, and low levels of oxygen (Tunnicliffe and Wilson, 1988; Peck et al., 2005). Study cases of extant brachiopods in shallow-water habitats show that neutral models (Hubbell, 2001) of community dynamics alone do not explain variation in community composition (Tomašových, 2008a), and that these brachiopods thrive in complex substrates where grazing pressure is lower, being less competitive than co-occurring epibyssate bivalves in bare surfaces (Tomašových, 2008b; but see Zuschin and Mayrhofer, 2009). Several studies have suggested that brachiopods may be unpalatable and not a preferred prey (Thayer, 1985; McClintock et al., 1993; Mahon et al., 2003), but Tyler et al. (2013), however, reached the conclusion, based on experimental results and field surveys, that this might not be the case. There is a wealth of evidence in the fossil record that brachiopods have been preyed upon in the Paleozoic (Kowalewski et al., 2005; Leighton et al., 2013), the Mesozoic (Kowalewski et al., 1998; Harper and Warton, 2000), the Cenozoic (Baumiller and Bitner, 2004; Baumiller et al., 2006; Schimmel et al., 2012) and the Recent (Delance and Emig, 2004; Taddei Ruggiero et al., 2006; Evangelisti et al., 2012).

Abiotic factors

An array of perturbations of marine communities is, however, related to changing environmental parameters associated with sea-level changes (Brett, 1995, 1998; Gahr, 2005). Physico-chemical factors (e.g., substrate composition/consistency, oxygen availability, temperature,

light irradiance, sedimentation rates, fluctuations in salinity, etc.), have been likewise recognized as an important factor in shaping the composition, distribution and abundance of marine benthic assemblages (Fürsich, 1995; Fürsich et al., 2001; Gahr, 2005; Reolid, 2005; Pérez-Huerta and Sheldon, 2006; Tomašových, 2006) because stressful conditions foster changes in community composition (e.g., decrease of diversity, vanishing or replacement of taxa, and dominance of opportunistic species) (Abdelhady and Fürsich, 2014).

Temperature and brachiopod distribution

Overall, for marine invertebrates, the upper and lower thermal tolerance is associated with geographical and depth distribution, and metabolic rate (James et al., 1992). The ranges of thermal tolerance of most individual species of extant brachiopods are not well known thus far (Rudwick, 1970; Richardson, 1997; Manceñido and Damborenea, 2008). Nevertheless, a large list of some extant species from different latitudes, and the temperature range of the waters where they were found, is gathered by Brand et al. (2003). In a number of cases, however, brachiopod species display a rather localized distribution, and many tolerate cold water (-1.9º C) (Foster, 1974; Manceñido and Damborenea, 2008), and as much as 32ºC (Lee, 2008; Brand et al., 2013). It has likewise been pointed out that some organo-phosphatic brachiopods (i.e., Linguliformea) are better represented in shallow subtropical to tropical water, whereas calcareous brachiopods (Craniiformea and Rhynchonelliformea) occur more commonly in temperate water, and when they are represented in lower latitudes, they occur in deeper environments taking advantage of the depth/temperature gradient (Rudwick, 1970; Helmcke fide Ziegler, 1975; Manceñido and Damborenea, 2008; Giles, 2012) or they are micromorphic. Latitudinal taxonomic richness of brachiopods at genus level from Cambrian to Recent was calculated by Powell (2009) based on Doescher's extensive brachiopod literature database, concluding that brachiopods did not change their latitudinal distribution during the Phanerozoic. James et al. (1992) suggested that brachiopods, in comparison with mollusks, are expected to be stenothermal, according to their subtidal and cryptic distribution. James et al. (1992)

also mentioned some examples of temperature tolerance of extant brachiopods: a majority of New Zealand brachiopods appear to tolerate temperatures ranging from 8º to 18º C (Lee, 1991), while intertidal species from New Zealand display tolerance to a temperature range in excess of 15º C (6.1º C in winter to 21º C in summer). Paine (1963) observed that the lingulid brachiopod *Glottidia* would not respond to stimuli at 10º C, while its activity is resumed at 12º C (see also Rudwick, 1970). Peck (1989) also recorded an upper tolerance temperature of 4.5º C for the terebratulidine brachiopod *Liothyrella uva* from Antarctica. Richardson (1997), in an essay on the ecology of extant rhynchonelliform brachiopods, argues that temperature and food supply are unlikely to limit their distribution, based on the widespread latitudinal and bathymetric distribution of examples such as *Macandrevia americana* and *Platidia anomioides*. Then Pennington et al. (1999), based on laboratory experiments, showed that the proportion of *Laqueus erythraeus* larvae that successfully settled was dependent on temperature range.

Influence of temperature on organisms survival

There are three main ways for organisms to cope with environmental change: 1) To use the physiological capacity to survive; including modification of their behavior or activity; 2) To evolve or adapt to the new conditions through selection of mutations which are consistent with survival; 3) To migrate to areas which are suitable for continued survival (Peck, 2007).Under normal conditions, organisms display a capacity or flexibility to meet biological requirements. The capacity not used for essential functions can be regarded as spare capacity available for other requirements, or to cope with the environmental variability (e.g., seasonality) in the area where these organisms thrive. If the range of environmental variability shifts with time, organisms might survive because the environmental shift took place within the range of physiological capacity, at the expense of reducing the spare capacity remaining after the shift in environmental conditions. However, if the shift in environmental range moves beyond the limits of physiological capacity, survival remains time limited (Peck, 2007). Adaptation of organisms to a shift in environmental range would mean a

concomitant shift in the upper and/or lower boundary of capacity limit that would encompass the new range of environmental conditions. If the organisms cannot evolve to withstand the change in environmental conditions, the only way out is migration to more suitable areas for survival.

On one hand, when temperature rises, ectothermic organisms cope with the new conditions by raising their metabolic rates, usually through oxygen consumption, to cover the costs of increased body temperatures (Pörtner et al., 2007; Peck, 2007).Extant brachiopods are considered to have poor abilities to raise their metabolic rates and have poor metabolic scopes (i.e., minimum (standard) rate of oxygen consumption minus maximum aerobic metabolic rate) (Peck, 2007). On the other hand, when temperature drops between the lower temperature threshold for metabolic activity and the survival threshold, the organism is in a state of suspended animation, but can resume metabolism once the temperature increases and re-crosses the lower temperature metabolic threshold (Clarke et al., 2013), which is consistent with the observations by Paine (1963) on *Glottidia*. However, the survival for sexually reproducing eukaryotes depends on temperature not dropping below the metabolic threshold necessary for completion of the life cycle from zygote to zygote (Clarke et al., 2013). This means that a climate change involving a drop of temperature below the metabolic threshold for reproduction of a species will result in its extinction if it cannot migrate to more suitable areas (Monegatti and Raffi, 2001).

Pleistocene cooling as a trigger for the extinction of Terebratulinae?

The Cenozoic-Quaternary genus *Terebratula*, like other representatives of the family Terebratulinae such as *Pliothyrina* and *Maltaia*, thrived in relatively shallow-water environments (as shallow as 30 m based on the height of Gilbert-type delta clinoforms (Reolid et al., 2012)). This taxon has been found in detritic-bottom habitats of neritic settings in the Paratethys and the Mediterranean realms in an era dominated by mollusks and bulldozing marine organisms. Attaining a big size (up to 9.5 cm in length for *Terebratula scillae*) (Taddei Ruggiero, 1994) might have

served as a size-refuge strategy (Doherty, 1979; Harper et al., 2009) against the high biotic disturbance in these habitats. The genus existed under subtropical to warm-temperate conditions during the Miocene and Pliocene (e.g., Brébion et al., 1978; Taviani, 2002; Kroh et al., 2003; Nalin et al., 2010) (see also climatic variability for the Neogene in Zachos et al., 2001, Kocsis et al., 2008, Juan et al., 2016). Although *Terebratula* survived the Gelasian cooling (Borghi, 2001; Malz and Jellinek, 1984), it went extinct in the Mediterranean region during the Calabrian (Middle Pleistocene) (Gaetani and Saccà, 1985; Lee et al., 2001), coinciding with a second cooling climatic event (Crippa et al., 2016; 2019). In particular, two species of *Terebratula* occur in the Pleistocene: *Terebratula terebratula* occurring in the Calabrian deposits of the sections at the Arda and Stirone rivers in the Emilia Romagna Region (northern Italy) (Brocchi, 1814; Borghi, 2001; Dominici, 2001; 2004; Bertolaso et al., 2009; Pervesler et al., 2011; Crippa et al., 2015; 2016). This taxon is also recorded in the Gelasian of the Apulia Region (southern Italy) (e.g., Taddei-Ruggiero and Raia, 2014). The other species, *T. scillae* (restricted to Sicily, Calabria and Apulia in southern Italy), died out also during the Calabrian.

Bathyal brachiopods associated with cold-water coral assemblages described from the Pleistocene of Sicily (Seguenza, 1865; 1871; Gaetani and Saccà, 1984; Borghi et al., 2014) no longer exist in the present-day Mediterranean, but some of the same species and some other closely related species occur in the Atlantic nowadays. The extinction of these taxa in the Mediterranean is thought to have been triggered by progressive uplift of the Gibraltar Sill (Logan, 1979). The hypothesis implies that these taxa thrived under psycrospheric conditions (e.g., Gaetani and Saccà, 1984; Borghi et al., 2014). The warmest periods of the Pleistocene probably annihilated them from the Mediterranean realm, and subsequently they were unable to re-enter it due to the onset of homothermic conditions (Logan, 1979; Gaetani and Saccà, 1984; Taviani, 2002; Logan et al., 2004).

In contrast, the only hypothesis posed for the extinction of the relatively shallow-water taxon *Terebratula* is progressive cooling during the Pleistocene (Lee et al., 2001). This hypothesis

implies that *Terebratula* displayed a metabolic threshold for reproduction incompatible with the climatic conditions during the Calabrian between 30º and 45º latitudes. Members of the family Terebratulinae have been reported from the Eastern Atlantic. The genus *Pliothyrina* persisted up to the Pleistocene in the Red Crag Formation of the United Kingdom (Muir-Wood, 1938; Wood et al., 2009). Dollfus and Cotter (1909) reported terebratulidines (identified as *Terebratula ampulla*) from the Pliocene north of the Tagus river in Portugal. The internal characters of this taxon are not known, therefore at present it is difficult to assess whether this taxon belongs either to *Terebratula* or to *Pliothyrina*. Toscano et al. (2010) identified *Maltaia pajaudi* = *M. moysae* (Mayer-Eymar, 1898) from the Pliocene of Huelva (SW Spain). González-Álvarez (2013) recently illustrated Pliocene specimens of *Maltaia moysae* from the Gran Canaria Island (identified by the former author as *Terebratula sinuosa*). Bitner and Moissette (2003) reported the taxon *Terebratula* sp. from the Pliocene of Morocco. The extinction of these terebratulidines, evaluating the hypothesis that cooling affected deleteriously their metabolic ability for reproduction, implies that some ecological barriers prevented their migration toward warmer areas in lower latitudes of the Eastern Atlantic (e.g., Monegatti and Raffi, 2001; Taviani, 2002).

Light

The vertical distribution of extant brachiopods has only been reliably established for about 200 species (Zezina, 2008). The maximum species richness of extant brachiopods is attained between 100 and 150 m depth (Zezina, 2008). The latter author commented that, overall, most brachiopod species live below 30-50 m, beyond the limits of the phytal zone or in its lower boundaries. James et al. (1992) summarized some studies on brachiopod larval behavior, stressing that the analyzed species were positively phototactic during early swimming stages to become negatively phototactic just prior to settlement. In the terebratellidine *Laqueus erythraeus*, however, there is no evident response to vertical or horizontally directed lights, and their larvae are probably geotactic (Pennington et al., 1999). It appears that larvae of these species display rugophilic,

explorative and selective behavior for substrate settlement (James et al., 1992), which would explain the observed propensity of some brachiopods to settle on irregular surfaces or crevices in very shallow-water environments (James et al., 1992). The influence of biotic and abiotic disturbances, such as grazing pressure, substrate failure, selective predation or near-substrate fluid dynamics, has been unsufficiently explored (James et al., 1992). In this regard, it is interesting to recall the observations described by Savage (1972) from his studies of a sandy rocky platform close to Durban, South Africa. In researching the brachiopod *Megerlina pisum*, Savage (1972) commented that only one boulder, out of several dozens surveyed, contained brachiopods and other organisms in its underside. The boulder was carefully relocated and, upon new inspection after two weeks, the boulder had been moved several meters away by wave action, and the brachiopods torn off.

Relationship with substrate

As mentioned earlier, brachiopods are sessile epibenthic to semi-endobenthic organisms (although there are infaunal inarticulate brachiopods such as the lingulids), which leads to the consideration that the importance of the substrate for brachiopod distribution is crucial. Gaspard (1997) provided some examples of adaptive solutions displayed by brachiopods to inhabit a range of different substrates (rocks, shell fragments, other organisms –including congeners-, and exceptionally even unconsolidated pelitic sediments) (e.g., Manceñido & Damborenea, 2008). Lee (1978) distinguished between *macrosubstrate*, which refers to the type of sediment where the brachiopod is found, and the *microsubstrate*, which may coincide with the latter or not, and refers to the substrate where the pedicle is actually attached. In this thesis I discuss the macrosubstrate and its relationship the brachiopod species considered. In some especial cases it is possible to identify the microsubstrate as well (in the study area, I have identified pedicle traces –*Podichnus obliquus*- in congeners of the terebratulidines *Terebratula* spp. and *Maltaia moysae*, which suggest that these taxa facultatively formed clusters). In the study area, specimens of the inarticulate brachiopod

Novocrania anomala have often been found cemented to shells of *Terebratula*, scallops or oysters in the *Terebratula* biostrome. In the Carboneras and Mazarrón areas (SE Spain), an assemblage composed of small gryphine brachiopod species, *Megerlia truncata*, *Terebratulina retusa*, *Lacazella mediterranea* and the small terebratulidine *Ceramisia meneghiniana* have been identified associated with octocorals of the genus *Keratoisis* (Barrier et al., 1991). This latter case suggests that these brachiopod assemblages found proper hard substrates for attachment in other organisms within this deep-water paleocommunity, which is found associated with very fine-grained deposits, which otherwise would seem unsuitable for attachment. Brachiopod species can either be *generalists* or *specialists* (e.g., Richardson, 1986). The different species can be ascribed to either type by analyzing the association with different macrosubstrates where they are found and the anatomical features that can be deduced from their morphological traits. I have likewise observed that at the top of a thick and conspicuous *Terebratula* biostrome of Pliocene age in the study area, the onset of coarse siliciclastic sedimentation coincides with a turnover in dominance favoring the scallop *Aequipecten scabrellus*. Abdelhady & Fürsich (2014), in a paleoecological study of Middle Jurassic sections, observed that increasing terrigenous input was coincident with an abundance of bivalves and dwindling presence of brachiopods. These authors explain that the terrigenous influx may turn the substrate soupy, making it unstable for brachiopods to thrive. Conversely, these authors observed an abundance of brachiopods associated with carbonate lithologies, an observation similar to that reported by Kowalewski et al. (2002) for extant Brazilian shelf brachiopods. In the study area, the macrosubstrate for *Terebratula* is most often made up of mixed-carbonate siliciclastic fine-grained sands.

Oxygenation of the bottom

Brachiopods are often labeled as minimalist organisms (Ghallager, 2003), because their low metabolic rates allow them for a low oxygen comsumption (e.g., Peck, 1996; Tunnicliffe & Wilson, 1988). Consequently, several authors have explained the success and extraordinary abundance of

brachiopods in particular environments as the result of their tolerance of low oxygen concentrations, conditions which might be rather adverse for organisms with higher metabolic demands, such as bivalves (competitors) or possible predators (e.g., Tomašových et al., 2006; Abdelhady & Fürsich, 2014). However, in the context of understanding this presumable superiority of brachiopods over bivalves during biotic crises in the Earth's history, some studies suggest that bivalves might withstand similar levels of hypoxia, or even more than brachiopods (Ballanti et al., 2012).

Paleoproductivity and hydrodynamic conditions

Alméras & Elmi (1983, 1985) have suggested that primary production along with a well established deep ocean circulation, fostering upwelling and downwelling currents, are among the main factors controlling brachiopod distribution. This hypothesis is supported by the observations of Emig & García-Carrascosa (1991), who mapped the populations of the terebratulidine *Gryphus vitreus* in the Corsican platform, and found that maximum densities were coincident with the highest velocities of bottom-currents which run perpendicular to isobaths, and depend on the steepness of the continental platform and its physiography. Reolid et al. (2012) likewise held that warm and more saline currents flowing towards the Atlantic through a Miocene seaway, in southern Spain, might explain the spectacular abundance of *Terebratula* in that locality. Kowalewski et al. (2002) found that high densities of brachiopods in the Brazilian Ubatuba Bay (outnumbering bivalves and gastropods combined) coincide with nutrient rich, well-oxygenated and relatively cold ($T<20^{o}C$) upwelling currents at a depth of 100-120 m, in the shelf break. The reports of nutrient rich environments as suitable for brachiopods might appear to be contradicting the examples where brachiopods successfully thrive in remarkably oligotrophic conditions (Peck et al., 2005). Both types of observations suggest the hypothesis that while low metabolic rates of brachiopods and their versatility to feed on different sources of food makes them successful colonizers of oligotrophic habitats, they might not be exclusively limited to nutrient poor environments.

Sedimentation rates and sequence stratigraphy

Sedimentation rates are often invoked as another critical factor controlling brachiopod distribution (e.g., Abdelhady & Fürsich, 2014; Alméras & Elmi, 1985; Garcia & Dromart, 1997). It can be envisaged that, overall, the sessile character of brachiopods makes them incompatible with high sedimentation rates. Three examples from the literature can be put forth to understand the effects of high sedimentation rates: Emig (1989) observed that fires started in the Corsica Island triggered episodes of high terrigenous influx into the continental platform because unsheltered soils were subjected to erosion. The eventual increase in terrigenous particles reaching bathyal depths is claimed to be responsible for high mortalities of *Gryphus vitreus* (up to 90% of individuals).. Following the same rationale, He et al. (2007) posed the hypothesis that turbid conditions associated with a cycle of marine regression might explain the phenomena of miniaturization in brachiopods (Liliput effect). All these three examples are supposed to involve the clogging of the lophophore with fine terrigenous particles, which prevents normal feeding and respiration, either leading to miniaturization in the long run or to starvation and death if the shift and intensity in sedimentation rate is very sharp (Laurin and García Joral, 1990). Thin pavements of *Terebratula* in the study area, associated with fine-grained sediments and displaying very high articulation ratio as well as pristine preservation, might be interpreted as obrution deposits triggered by a substantial increase of sedimentation rates. The abundance of tubes of the polychaete *Ditrupa arietina* in these deposits is consistent with this interpretation, because this taxon is considered as a proxy for unstable substrates and high sedimentation rates (e.g., Sanfilippo, 1999).

Conversely, Garcia & Dromart (1997) interpreted brachiopod marker beds of Jurassic age to be related to maximum flooding surfaces corresponding to cycles of different orders. These marker beds are characterized by being spatially very widespread, and by displaying biofabrics of densely packed brachiopod concentrations. Maximum flooding surfaces are characterized by very low sedimentation rates because during this stage of the sea level, the accommodation space is maximal. There are localities of Cenozoic age reported in the literature which record brachiopod shell beds

extending across several kilometers, often associated with glauconitic sands (Feldman, 1977; Pedley, 1976). The general features of these shell beds might suit the model proposed by Garcia & Dromart (1997) to explain their formation. In the study area, localities recording the early Pliocene transgression, over the local metamorphic basement or over older Miocene deposits, are generally rich in brachiopods.

Taxonomic remarks on Terebratulinae from the Pliocene of Águilas

Large-sized terebratulids from the European Cenozoic have a long and complex nomenclatorial and taxonomic history (e.g., Bitner and Martinell, 2001; Lee et al., 2001; Dulai et al., 2020), which is still unresolved today. To a great extent, this uncertainty is due to the loss of type specimens, lack of topotypical material (or poorly preserved material when topotypes are available), and vague original descriptions regarding the type localities (mostly from 19th century and earlier works). To justify the taxonomy used in this dissertation, it is necessary to comment on the state of the art of the problem. During the preparation of the revised volume of the Treatise on Invertebrate Paleontology, part H, chapter 6 (Lee et al., 2006), it was necessary to formally designate the type species of the genus *Terebratula* Müller, 1776 and select a neotype. This was accomplished by Lee and Brunton (1998) and Lee et al. (2001), who designated the species *Terebratula terebratula* (Linnaeus, 1758) as the type of the genus, and erected a neotype to act as the name bearer for the Order Terebratulida (Lee et al., 2001). The neotype is a planoplicate (= trapezoidal uniplication *sensu* Nath, 1932 *fide* Muir-Wood, 1936) coming from the Pliocene of Andria (Apulia, Italy). Unfortunately, the insufficient original definitions of species such as *T. terebratula*, *Terebratula sinuosa* (Brocchi, 1814), *Terebratula pedemontana* Valenciennes *in* Lamarck, 1819 and *Terebratula ampulla* (Brocchi, 1814) led to multiple and different interpretations of these and other species in the subsequent literature (see review in García-Ramos, 2006). For example, both Linnaeus (1758) and Brocchi (1814) referred to a strongly folded specimen of unknown locality depicted in Colonna (1616) as the reference to their respective

species *Anomia terebratula* and *Anomia sinuosa*. Although the Pliocene specimens from Andria are described as smooth to secondarily and anteriorly folded (unlike the Colonna specimen, which is strongly folded since very early ontogentic stages), *T. sinuosa* was placed into the synonymy of *T. terebratula* by Lee et al. (2001). This action was justified due to an objective synonymy (both nominal species had the same type, i.e., the Colonna specimen). As a result, Lee et al. (2001) argued that the strong plication depicted in the Colonna illustration was probably an exaggeration of the artist, and presumably considered that the less strongly folded taxa *Terebratula calabra* Seguenza, 1871 and *Terebratula costae* Seguenza, 1871 were conspecific with the Andria specimens (the latter which are usually planoplicate), and regarded them as synonyms of *T. terebratula*. Lee et al. (2001) were possibly unaware that other authors, most notably Boni (1933; 1934), Marasti (1973), De Porta et al. (1979) and Calzada (1978), had illustrated Miocene specimens very similar to the Colonna specimen. Because of the objective synonymy of *T. terebratula* and *T. sinuosa* pointed out by Lee et al. (2001), García-Ramos (2006) proposed the binomen *Terebratula maugerii* Boni, 1933 (a junior synonym of *T. sinuosa*) to accommodate the Miocene strongly folded specimens, which were clearly non-conspecific with the Andria taxon. Recently, Taddei Ruggiero et al. (2019) proposed to revalidate the name *T. sinuosa* for the strongly folded taxon by invoking the long – albeit confusing– history of the binomen in the literature. This revalidation was also proposed because the concept of *T. terebratula* had changed forever following the 2001 designation of a neotype from Andria; thereby the Colonna specimen was no longer representative of the concept of *T. terebratula*.

After studying population samples from many Miocene and Pliocene outcrops in southern Spain, García-Ramos (2006) concluded that the anteriorly folded specimens from the Pliocene were attributable to *T. calabra*, rejecting a synonymy with *T. terebratula* from Andria as proposed by Lee et al. (2001) and subsequent authors. This sulciplicate taxon with folding restricted to the anterior half of the shell is best represented in classical localities from Piedmont, Calabria and south-east Spain. In Piedmont the species is abundant in the Asti area (e.g., Valle Botto, Capriglio

and Montafia), and was illustrated under different names by Sacco (1902), Caretto (1963), Taddei Ruggiero (1983), Pavia and Zunino (2008), Taddei Ruggiero et al. (2008) and Taddei Ruggiero and Raia (2008). This taxon from Asti has usually been confused with *T. ampulla* (see subsequent discussion about this species). *T. calabra* was defined from Calabria in southern Italy (Nasiti and Terreti). Illustrations of specimens from this area are included in Seguenza (1871), Taddei Ruggiero (1983) and Gaetani and Saccà (1985), whereas the stratigraphy and the paleoenviroments were studied in detail by Barrier et al. (1987) based on the Pavigliana section, which is located relatively close to the type locality. *T. calabra* is also abundant in southern Spain, and it was illustrated under different names by Pajaud (1976; 1977), Bitner and Martinell (2001), and García-Ramos (2004; 2006). It should be noted that the specimens from Terreti are, on average, somewhat smaller than those from the Asti and Águilas areas (Gaetani and Saccà, 1985). This difference in size can probably be understood in the context of the slightly different ages of the different populations. On the contrary, I have seen a few specimens from Montafia, and these are indistinguishable from those of Águilas.

The attribution of the late Zanclean Asti specimens to *T. ampulla* goes back to Sacco (1902), as far as I am aware. The Asti area is not included in the original localities referred to by Brocchi (1814) for *T. ampulla*. Brocchi (1814) cited "Fossile nel Piacentino, a San Geminiano, e a Lajatico nella Toscana, e nella Calabria". It seems clear that Brocchi had in mind a planoplicate taxon, at best weakly biplicate, for *T. ampulla*. This is evidenced, besides his description, by his reference to the terebratula illustrated by Scilla (1670, Tav. 'XIIII') as an example of *T. ampulla*. The Scilla specimen most probably corresponds with *Terebratula scillae* Seguenza, 1871, which is another mainly planoplicate taxon. Besides, Brocchi (1814, p. 467) described a variety of *T. ampulla* from Crete Senesi south of Siena, in Tuscany, as "prominently folded and with a sinuous inferior margin". This "variety" from Tuscany highlights that Brocchi (1814) did not consider the typical *T. ampulla* as a notably biplicate taxon. The variety from Tuscany, instead, seems to agree with the features of *T. calabra*. Brocchi (1814), however, was more explicit about a locality for *T. ampulla*

in page 467 of his work: "Nelle colline di Castell'Arquato presso Piacenza trovasi sepolta questa anomia in una marna bigia che ne riempie la cavità interna…" A detailed taxonomic revision of the terebratulids from the Arda and Stirone rivers was conducted by Borghi (2001). This author described the Castell'Arquatto and Stirone terebratulas as mainly uniplicate (also E. Borghi, personal communication, 2005; and personal observation at the Geological Museum of Castell'Arquatto, 2018). The typical specimens from these localities fit closely the description of *T. ampulla* by Brocchi (1814). Hence, if we accept Castell'Arquatto as the type locality of *T. ampulla*, then this latter binomen would be a junior synonym of *T. terebratula*, because the specimens from the Arda River (Calabrian in age) are hardly distinguishable from the specimens coming from Andria and other localities of the Gravina Calcarenites (García-Ramos, 2006; Bertolaso et al., 2009).

Also in relation to the Asti terebratulas I should discuss the species *T. pedemontana*. This species was insufficiently described (without illustration) by Valenciennes *in* Lamarck (1819). It was described as a biplicate species, and the only indication about is provenance or age was "Fossile de Turin". Davidson (1850, 1870) traced the original specimen housed at the museum of the Garden of Plants in Paris, and illustrated it for the first time, but only in dorsal view, hampering its comparison with other biplicate species such as *T. sinuosa*. Davidson (1850, 1870) further mentioned that it was collected by Sig. Bonelli in the "tertiary beds near Turin, Italy". Subsequently, Sacco (1902) reinterpreted the species as a "variety" (a morphotype) of *T. sinuosa*, and stated that it is frequent in the Miocene of Turin (Colli Torinesi). On December the 18th, 2009 I received a message from Jean Michel Pacaud, from the Muséum National d'Histoire Naturelle, Paris, mentioning that the syntype of *T. pedemontana* was housed in said institution. This specimen is curated with register number MNHN.F. A32406 coll. Bonelli, and it is said to be of Miocene age (Pacaud, 2015). Recently available online photographs of such syntype[1] show a terebratulid very

[1] http://coldb.mnhn.fr/catalognumber/mnhn/f/a32406

similar to the Pliocene specimens from the Asti area mentioned above, which occur as close as 27 km away from Turin (e.g., Capriglio). It is, therefore, feasible that *T. calabra* might be a junior synonym of *T. pedemontana*, the latter probably coming from the Pliocene of the Asti area. The uncertainty about the exact provenance and the geological horizon of the syntype, along with the lack of further syntypes, however, complicates further assessments about the synonymy of *T. calabra* with *T. pedemontana*. For this reason, I have opted here to attribute the Águilas specimens to *T. calabra*, as I did in my former review (García-Ramos, 2006), awaiting further clarification about *T. pedemontana*.

Systematics

Phylum **Brachiopoda** Duméril, 1806
Subphyllum **Rhynchonelliformea** Williams, Carlson, Brunton, Holmer y Popov, 1996
Class **Rhynchonellata** Williams, Carlson, Brunton, Holmer y Popov, 1996
Order **Terebratulida** Waagen, 1883
Suborder **Terebratulidina** Waagen, 1883
Superfamily **Terebratuloidea** Gray, 1840
Family **Terebratulidae** Gray, 1840
Subfamily **Terebratulinae** Gray, 1840
Genus ***Terebratula*** Müller, 1776
Type species: ***Terebratula terebratula*** (Linnaeus, 1758)

Terebratula calabra Seguenza, 1871
FIG.TEXT 1

?	1814	*Anomia ampulla.Var.* (*plicis ementioribus, margine inferne sinuoso*). Brocchi, p.467.
?	1819	*Terebratula pedemontana*. Valenciennes *in* Lamarck, p. 252. (*)
?	1850	*Terebratula pedemontana* Val. in Lamk. Davidson, p. 440, pl. 14, fig.34.
Pars	1864	*Terebratula sinuosa* (Brocchi, 1814). Davidson, p.6, pl. 1, figs. 1,2
	1865	*Terebratula sinuosa*. Seguenza, p. 36, pl.4, figs.2-3.
?	1870	*Terebratula pedemontana* (Lamarck). Davidson, p. 365, pl. 18, fig. 5.
	1871	*Terebratula philippii* Seg. Seguenza, p. 128, pl. 4, figs.6-11.
*	1871	*Terebratula calabra* Seguenza. Seguenza, p. 138, pl. 5, figs.5-8.
	1902	*Terebratula ampulla* var. *complanata* Sacc. Sacco, p. 12, pl.2, figs. 9-11. (juveniles)
Pars	1902	*Terebratula ampulla* var. *plicata* Sacc. Sacco, p. 13, pl.2, figs.22-24.
	1902	*Terebratula ampulla* var. *plicatolata* Sacc. Sacco, p. 14, pl.2., fig. 26.
	1902	*Terebratula ampulla* var. *perstricta* Sacc. Sacco, p.14, pl.3, figs. 1-2.
	1963	*Terebratula ampulla* var. *plicatolata* Sacco. Caretto, pl. 4, figs. 1a-b.
	1976	*Terebratula terebratula* (Linné, 1758). Pajaud, p. 100, pl. 3, figs. A-C.
	1977	*Terebratula terebratula* (Linné). Pajaud, p. 6, pl. II, figs. C-E.
	1983	*Terebratula ampulla*. Taddei Ruggiero, p.178, pl.1, figs. 4a-d.
	1983	*Terebratula sinuosa*. Taddei Ruggiero, p.178, pl.1, figs. 5a-c.
	1983	*Terebratula sinuosa* Brocchi. Cooper, pl. 4, figs. 17-19.
	1985	*Terebratula calabra* Seguenza 1871. Gaetani and Saccà, p. 7, fig. 5 (text), pl. 1, figs. 7-

12.
1988 *Terebratula terebratula* (Linné). Gómez-Alba, p. 142, fig. 7.
1994 *Terebratula calabra* Seguenza, 1871. Taddei Ruggiero, p. 206, pl. 1, figs. 3-5.
1999 *Terebratula terebratula* (Linné, 1758). Iñesta, p. 22, pl.5, fig.2.
2001 *Terebratula terebratula* (Linnaeus, 1758). Bitner and Martinell, p. 181, fig.3 M-T.
2004 *Terebratula ampulla*. Rico-García, p. 254, pl. 5, figs. D-E.
v 2004 *Terebratula terebratula* (Linnaeus, 1758). García-Ramos, p. 25, figs.4-6 (text); pl.5, figs.3-10; pl.6, figs.1-3; pl.7, figs. 2, 8, 10.
v 2006 *Terebratula calabra* Seguenza, 1871. García-Ramos, pl.2, figs. 1-7; pl.7, figs. 7-8, 10; pl.8, figs. 11-29.
2008 *Terebratula ampulla* (Brocchi). Taddei Ruggiero and Raia, p.322, fig. 2 A-I.
2008 *Terebratula ampulla*. Taddei Ruggiero et al., p.211, fig. 1H-M.
2012 *Terebratula terebratula*. Reolid et al., p. 10, fig.7a-b.
? 2016 *Terebratula ampulla* (Brocchi, 1814). Dulai, p. 83, figs. 19-21.
2018 *Terebratula* cf. *calabra* Seguenza. Giannetti et al., p. 24, fig. 6.11a-c.

*****Muséum national d'Histoire naturelle, Paris (France), Collection: Paleontology (F), Fossil specimen MNHN.F.A32406

Diagnosis. *Terebratula* of medium to large size; oval to rounded subpentagonal outline; maximum width somewhat displaced anteriorly from midvalve; adults usually sulciplicate, with dorsal folds developing at- or more usually anterior to midvalve; antero-ventral region smooth or with short, gently developed ventral fold. Juveniles with a tendency to be subrhomboidal in outline; with the maximum width often displaced posteriorly ('high-shouldered' *sensu* Middlemiss, 1976), plano-convex to concavo-convex and slightly sulcate.

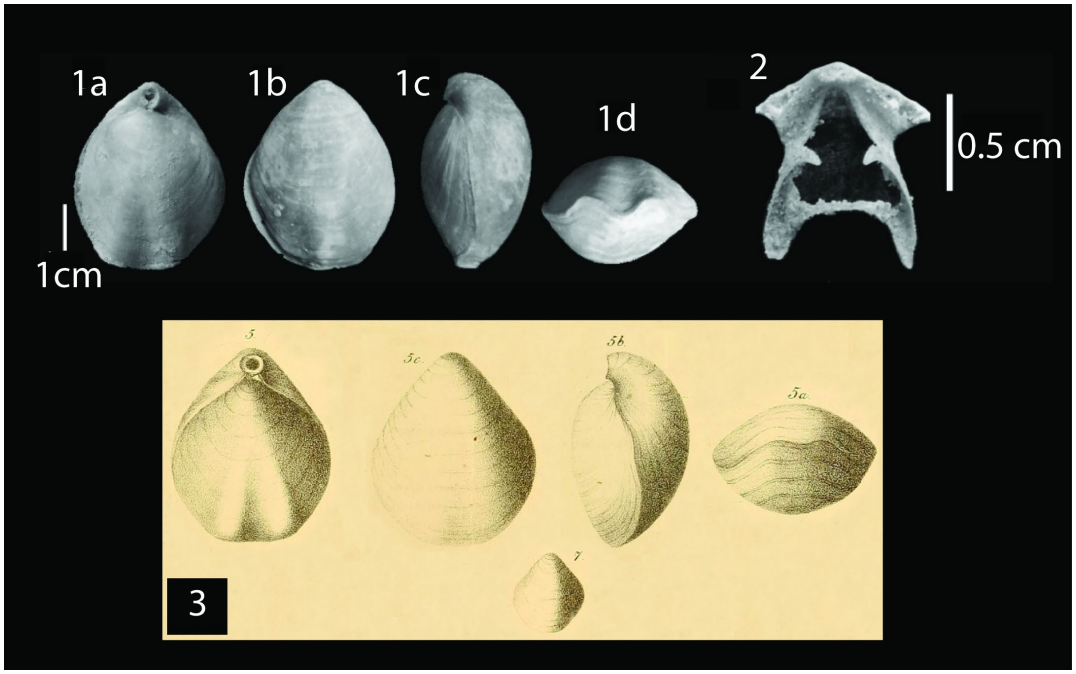

FIGURE 1. 1, 2, Specimens of *Terebratula calabra* from the biostrome in the Águilas Basin

(modified from García-Ramos, 2006). 1a-d, specimen showing dorsal, ventral, lateral and frontal views. 2, brachidium of another specimen, displaying long terminal points. 3, original specimens of *T. calabra* from Nasiti (Calabria) (modified from Seguenza, 1871).

Remarks. The specimens from Santa Pola (Alicante, Spain) and from Cuatro Calas (Águilas Basin, Spain) illustrated by Pajaud (1976; 1977) were attributed to *T. terebratula* when the concept of the species was that of a relatively strongly folded taxon as interpreted by Buckman (1907).The latter author was based on a notably plicated, but deformed, specimen from the Pleistocene deposits of Monte Mario (near Rome, Italy). This specimen was also reproduced by Thomson (1927) and by Muir-Wood *in* Moore (1965). As shown by Cooper (1983), the Monte Mario specimens (which he identified as *T. ampulla*) can be planoplicate. It seems that the Buckman specimen was an extreme morphotype, untypical for the population. The Monte Mario specimens are most probably conspecific with the Andria specimens (and with specimens from other Apulian localities from the Gravina Calcarenites Fm), and are, therefore, attributable to *T. terebratula*. *T. calabra* differs from *T. terebratula* overall in being less elongate in outline, smaller, and in the tendency of adults to be sulciplicate; displaying better defined folds on the dorsal valve. *T. terebratula* can be rectimarginate to sulciplicate but the typical morphotype is planoplicate in adulthood. In the Paratethys there are taxa that resemble *T. calabra*. These were identified under different names, such as *Terebratula grandis* (Blumenbach, 1803) or *Terebratula styriaca* Dreger, 1889 (Kudrin, 1961; Barczyk and Popiel-Barczyk, 1977). Their internal features are poorly known but the Polish and Ukranian specimens can probably be referred to as *"Terebratula" makridini* Kudrin, 1958. This latter taxon can at best be considered a heterochronous homeomorph of *T. calabra*. The attribution of the Polish specimens to *T. styriaca* is unlikely, since the topotypical material of *"T." styriaca* from Kleinhöflein near Eisenstadt (Austria) that I have seen are notably smaller and more strongly plicated, as faithfully illustrated in the original publication of Dreger (1889). *T. calabra* is easily distinguishable from *T. sinuosa* (in the sense of Marasti, 1973 and Taddei Ruggiero et al., 2019) or

from "*Terebratula*" *hoernesi* Suess, 1866 because the latter two are very strongly folded, with a ventral fold developed from the posterior to the anterior margins of the shell. The Tortonian (late Miocene) specimens identified by Calzada (1978; 1984) as *T. ampulla*, from Ceutí (Spain), are larger than *T. calabra*, and tend to be planoplicate, but there are also specimens with well-developed sulciplication. The folding patterns in this taxon, also identified by García-Ramos (2006) in Barranco de Cavila, near Caravaca (Spain), start to develop posterior to midvalve, when compared with either *T. calabra* or *T. terebratula*. These latter Miocene specimens are similar to *T. sinuosa* var. *pseudoscillae* Sacco, 1902 from the Miocene of Monte Vallassa (Italy), which García-Ramos (2006) considered to be a valid species. In late Miocene outcrops there are anteriorly plicated specimens which are difficult to distinguish from *T. calabra*. They are known from Malta (Cooper, 1983, who identified them as *T. sinuosa*), from the late Tortonian of the Guadix Basin, Spain (García-Ramos, 2006; Reolid et al., 2012; Giannetti et al., 2018) and from the late Tortonian-early Messinian of the Sorbas Basin, Spain (Videt, 2003; García-Ramos, 2006; Puga-Bernabéu et al., 2008).

Genus ***Maltaia*** Cooper, 1983

Type species: ***Maltaia maltensis*** Cooper, 1983

Maltaia moysae (Mayer-Eymar, 1898)
FIG.TEXT 2

	1865	*Terebratula pedemontana*. Lamk. Seguenza, 1865, p.39, pl. 4, fig. 5.
*	1898	*Terebratula moysae*. Mayer-Eymar, p. 72, pl.12, figs. 20 a, b.
	1898	*Terebratula biplicata* (Brocchi, 1814). Almera and Bofill, p.167-168, pl. 6, figs. 2a-2b.
	1898	*Terebratula biplicata* var. *lata*. Almera and Bofill, p.168, pl. 6, fig.3.
	1902	*Terebratula ampulla* var. *plicatoparva* Sacc. Sacco, p., pl. 2, fig. 13.
	1902	*Terebratula ampulla* var. *incavata* Sacc. Sacco, pl.2. fig. 25.
	1988	*Terebratula sinuosa* (Brocchi, 1814). Gómez Alba, pl. 71, fig. 9.
	1988	*Terebratula terebratula*. Calzada, p. 248, fig. 225
	1989	*Terebratula calabra* Seguenza, 1871. Spano, p. 160, pl. 9, figs. 2-4.
v,pars	2004	*Terebratula sinuosa* (Brocchi, 1814). García-Ramos, p.23, figs. 2, 3 (text); pl. 4, figs.1-8; pl. 6, figs. 5-7,11, 13.
v	2006	*Maltaia pajaudi*. García-Ramos, 2006, p. 61, fig. 19.1a-g (text); pl.6, figs. 1-13; pl.8, figs.1-10.
v	2010	*Maltaia pajaudi* García-Ramos, 2006. Toscano et al., 2010, p. 257, figs. 3 e-h.
	2011	*Terebratula sinuosa* Brocchi 1814. Betancort, p. 90, pl. 5, figs. 1-4.
	2013	*Terebratula sinuosa* (Brocchi, 1814). González-Álvarez, p. 14, fig. 1a-b.

Diagnosis. Provided in García-Ramos (2006).

Remarks. This taxon is very abundant in some Mediterranean localities but has drawn the attention of a few authors only. I erected the species *Maltaia pajaudi* in 2006 without having a copy of the works of Mayer-Eymar (1898) and Almera and Bofill (1898), both of whom described and illustrated the same species. I now consider *M. pajaudi* to be a junior synonym of *M. moysae*. This species is characterized by being remarkably smaller than other Mediterranean species, by a strong subpentagonal to subrhomboidal outline, and by the presence in most specimens of well-developed dorsal folds located anterior to midvalve. Some specimens display a conspicuous pedicle collar. The most characteristic feature of the species, however, is a ventral sulcus. This is displayed by many specimens from population samples coming from many different localities. Other rare specimens can display a smooth antero-ventral region or develop an inconspicuous ventral fold. The loop of adults of this species (with very short terminal points, and a low-arched, rounded transverse band) is like that of juveniles of different species of *Terebratula*. These morphological features can be considered, therefore, as paedomorphic traits. That was the reason why I argued (García-Ramos, 2006) that the species can be included in *Maltaia* Cooper, 1983. Different species of *Terebratula* display much longer terminal points and usually a high-arched, trapezoidal transverse band. The trapezoidal shape in frontal view is produced by a narrow bridge (*sensu* Arcelin and Roché, 1936) on the ventral side of the transverse band of *Terebratula*. The species *M. moysae* was first defined from Egypt (Mayer-Eymar, 1898) and is cited from there in a few works (e.g., Sandford and Arkell, 1933; Little, 1936) without illustrations. It is also described from Egypt by Hamza (1972 *non vidi*). The brachiopods mentioned by Aigner (1983) from the Pliocene cliff-line near the Giza pyramid plateau likely refer to the same species. I have found *M. moysae* in several similar outcrops from southern Spain. Elsewhere, the species is described from Italy, under different names, by Sacco (1902) (notably *T. ampulla* var. *incavata*). Enrico Borghi has shown me pictures of this species from Ciuciano (Tuscany). Seguenza (1865) identified a possibly conspecific specimen from San Filippo inferiore (Messina, Sicily) as *T. pedemontana*, whereas Spano (1989) illustrated a most likely conspecific specimen from the lower Pliocene of Capo di San Marco in Sardinia.

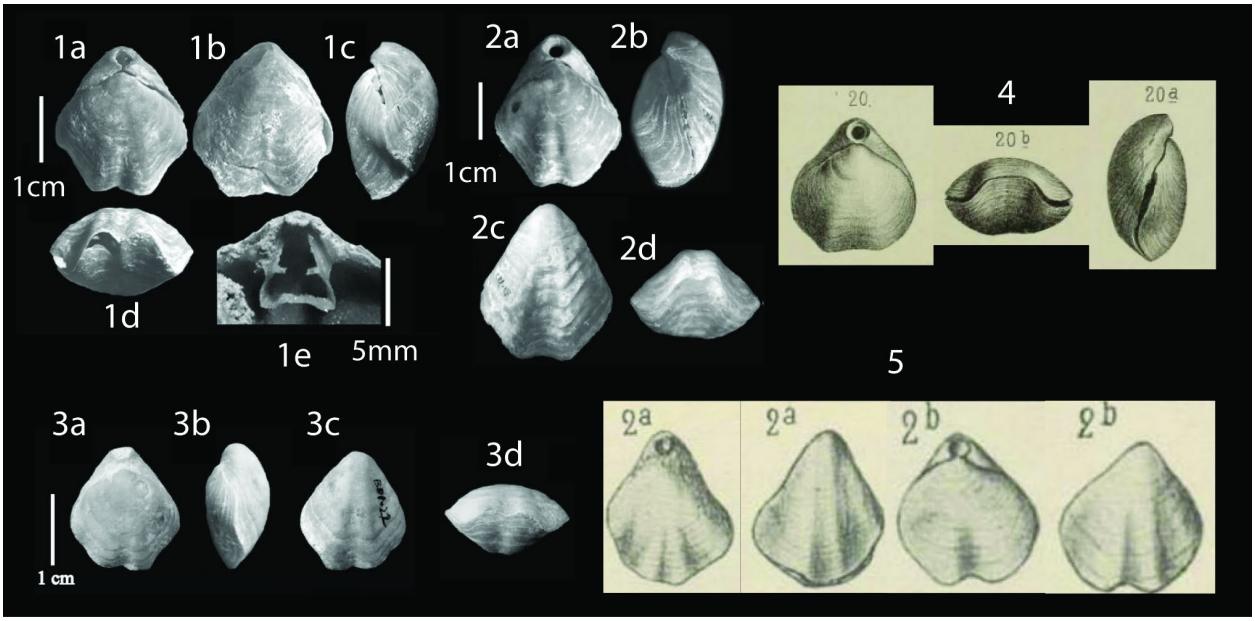

FIGURE 2. Specimens of *Maltaia moysae* (Mayer-Eymar, 1898). 1-3, Specimens in dorsal, ventral, lateral and frontal view. They come from the lower Pliocene of Bolnuevo (1), Cabo Cope (2) and Playa de Piedra Mala (3); all in the Province of Murcia. 4, original illustrations of "*T. moysae"*, modified from Mayer-Eymar (1898). 5, original illustrations of *Terebratula biplicata* var. *lata,* modified from Almera and Bofill (1898).

In Spain I have found *M. moysae* in many localities in the provinces of Almería, Murcia and Alicante, always in Zanclean sediments. It certainly occurs also in Málaga (Guillermo Díaz-Medina, personal communication, 2019) and in the Guadalquivir Basin (Toscano et al., 2010). It was described and illustrated from some localities in Catalonia by Almera and Bofill (1898) either as *Terebratula biplicata* or *T. biplicata* var. *lata*. Later authors attributed specimens from Vilacolum to *T. terebratula* (Calzada, 1988; Encinas, 1992 *non vidi*). It has recently been illustrated, under the name *T. sinuosa*, from Gran Canaria (Canary Islands) by Betancort (2011) and by González Álvarez (2013). The ventral sulcus of the Pliocene specimens enables an easy distinction from relatively similar forms such as *Maltaia* aff. *costae* (*sensu* García-Ramos, 2006), *"T." styriaca*, *"Terebratula" kemenczeiensis* Majer, 1915 and *M. maltensis*. The latter four taxa are

probably heterochronous quasi-homeomorphs.

Thesis aims

Terebratulide brachiopods are considered the "supreme survivors" of all brachiopod clades, since nowadays they are the dominant brachiopod clade in modern oceans in terms of abundance, diversity and biomass (95% of brachiopod biomass), when compared with rhynchonellide and thecideide brachiopods (Lee, 2008). The genus *Terebratula* is a good example of success as reflected in Neogene sediments in terms of species richness and abundance (e.g., Pedley, 1976; Reolid et al. 2012). The genus, however, strikingly went extinct in the Calabrian. The aim of this dissertation is to help constrain the optimal ecological niche of *Terebratula* and analyze the environmental conditions that once drove its success, because these questions have been insufficiently explored, and because improving our knowledge on this specific question can contribute to better understanding the dramatic demise of other examples of once successful organisms.

In this thesis I address the above question by discussing how the distribution of *Terebratula* was influenced by a number of environmental variables associated with depth-related gradients, such as the type of macrosubstrate, oxygenation of the bottom, productivity, sedimentation rates, hydrodynamic conditions, and light. All these paleobiological analyses are integrated in a framework of detailed sedimentological and sequence stratigraphic models.

Literature Overview

Abdelhady, A.A. and Fürsich, F.T. 2014. Macroinvertebrate palaeo-communities from the Jurassic succession of Gebel Maghara (Sinai, Egypt). *Journal of African Earth Sciences* 97: 173–193.

Aberhan, M., Kiessling, W. and Fürsich, F.T. 2006. Testing the role of biological interactions in the evolution of mid-Mesozoic marine benthic ecosystems. *Paleobiology* 32 (2): 259–277.

Ager, D.V. 1965. The adaptation of mesozoic brachiopods to different environments. *Palaeogeography, Palaeoclimatology, Palaeoecology* 1: 143–172.

Ager, D.V. 1993. Mesozoic brachiopods and seamounts. *In*: Pálfy, J. and Vörös, A. (eds.), *Mesozoic Brachiopods of Alpine Europe*, 11–13. Hungarian Geological Society, Budapest.

Aigner, T. 1983. A Pliocene cliff-line around the Giza pyramids plateau, Egypt. *Palaeogeography, Palaeoclimatology, Palaeoecology* 42 (3–4): 313–322.

Almera, J. and Bofill i Poch, A. 1898. Moluscos fósiles recogidos en los Terrenos pliocénicos de Cataluña : descripciones y figuras de las formas nuevas y enumeración de todas las encontradas en dichos yacimientos. *Boletín de la Comisión del Mapa Geológico de España* 24: 1–223.

Alméras, Y. and Elmi, S. 1983. Influence de la production primaire organique et de la circulation océanique profonde sur la distribution des Brachiopodes (Jurassique, Actuel). *Comptes-rendus des séances de l'Académie des sciences. Série 2, Mécanique-physique, chimie, sciences de l'univers, sciences de la terre* 297 (10): 779–782.

Almeras, Y. and Elmi, S. 1985. Le contrôle des peuplements de brachiopodes: comparaisons des données du Jurassique et de l'Actuel. *Ann. Soc. géol. Nord, Villeneuve d'Ascq* 104: 127–140.

Alroy, J. 2010. The Shifting Balance of Diversity Among Major Marine Animal Groups. *Science* 329 (5996): 1191–1194.

Álvarez, F., Martínez, A., Nuñez, L. and Fraga, J.N. 2005. Sobre la presencia en Canarias de varias especies de braquiópodos (Brachiopoda: Rhynchonellata) en cuevas y cornisas submarinas. *Vieraea: Folia Scientarum Biologicarum Canariensium* (33): 261–280.

Álvarez, F.Á. and Emig, C.C. 2005. Brachiopoda. *In*: *Lophophorata, Phoronida, Brachiopoda*, 57–177. Museo Nacional de Ciencias Naturales. CSIC., Madrid.

Arcelin, F. and Roché, P. 1936. Les Brachiopodes bajociens du Monsard. *In Travaux du Laboratoire de géologie de la Faculté des sciences de Lyon*. Lyon.

Asgaard, U. and Stentoft, N. 1984. Recent micromorph brachiopods from Barbados: Palaeoecological and evolutionary implications. *Geobios* 17: 29–37.

Baeza-Carratalá, J.F., García Joral, F., Giannetti, A. and Tent-Manclús, J.E. 2015. Evolution of the last koninckinids (Athyridida, Koninckinidae), a precursor signal of the early Toarcian mass extinction event in the Western Tethys. *Palaeogeography, Palaeoclimatology, Palaeoecology* 429: 41–56.

Ballanti, L.A., Tullis, A. and Ward, P.D. 2012. Comparison of oxygen consumption by *Terebratalia transversa* (Brachiopoda) and two species of pteriomorph bivalve molluscs: implications for surviving mass extinctions. *Paleobiology* 38 (4): 525–537.

Bambach, R.K., Knoll, A.H. and Sepkoski, J.J. 2002. Anatomical and ecological constraints on Phanerozoic animal diversity in the marine realm. *Proceedings of the National Academy of Sciences* 99 (10): 6854–6859.

Barczyk, W. and Popiel-Barczyk, E. 1977. Brachiopods from the Korytnica basin (Middle Miocene; Holy Cross Mountains, Poland). *Acta Geologica Polonica* 27 (2): 157–168.

Barnes, D.K.A. and Peck, L.S. 1997. An Antarctic shelf population of the deep-sea, Pacific brachiopod *Neorhynchia strebeli*. *Journal of the Marine Biological Association of the United Kingdom* 77 (2): 399–407.

Barrier, P., Zibrowius, H., Lozouet, P., Montenat, C., d'Estevou, P.O., Serrano, F. and Soudet, H.-J. 1991. Une faune de fond dur du bathyal supérieur dans le Miocène terminal des cordillères bétiques (Carboneras, SE Espagne). *Mésogée* 51: 3–13.

Baumiller, T.K. and Bitner, M.A. 2004. A case of intense predatory drilling of brachiopods from the Middle Miocene of southeastern Poland. *Palaeogeography, Palaeoclimatology, Palaeoecology* 214 (1): 85–95.

Baumiller, T.K., Bitner, M.A. and Emig, C.C. 2006. High frequency of drill holes in brachiopods from the Pliocene of Algeria and its ecological implications. *Lethaia* 39 (4): 313–320.

Bertolaso, L., Borghi, E. and García-Ramos, D. 2009. Brachiopodi neogenici e pleistocenici dell'Emilia (Parte seconda). *Parva Naturalia* 8 (2007–2009): 3–42.

Betancort-Lozano, J.F. 2011. Fósiles marinos del Neógeno de Canarias (Colección de la ULPGC): dos neotipos, catálogo y nuevas aportaciones (Sistemática, Paleoecología y Paleoclimatología). PhD Thesis, 377 pp.

Bitner, M.A. 2008. New data on the recent brachiopods from the Fiji and Wallis and Futuna islands, South-West Pacific. *Zoosystema* 30 (2): 419–461.

Bitner, M.A. and Martinell, J. 2001. Pliocene brachiopods from the Estepona area (Málaga, south Spain). *Revista Española de Paleontología* 16 (2): 9–17.

Bitner, M.A. and Moissette, P. 2003. Pliocene brachiopods from north-western Africa. *Geodiversitas* 25 (3): 463–479.

Bitner, M.A. and Cohen, B.L. 2013. Brachiopoda. *In*: *ELS*, American Cancer Society.

Blumenbach, J.F. 1803. *Specimen Archaeologiae Telluris Terrarumque Inprimis Hannoveranarum*. Dieterich.

Boni, A. 1933. Fossili miocenici del Monte Vallassa. *Bollettino della Società Geologica* 52: 73-156.

Boni, A. 1934. Studi statistici sulle popolazioni fossili; *Chlamys scabrella* Lam. e *Terebratula sinuosa* Brocchi. *Revista Italiana di Paleontologia (Pavia)* 1 (Supplement) (40): 1–275.

Borghi, E. 2001. Osservazioni sui Brachiopodi neogenici e pleistocenici dell'Emilia. *Parva Naturalia* 2001: 45–81.

Borghi, E., Garilli, V. and Bonomo, S. 2014. Plio-Pleistocene Mediterranean bathyal echinoids: evidence of adaptation to psychrospheric conditions and affinities with Atlantic assemblages. *Palaeontologia Electronica* 17 (3): 1–26.

Brand, U., Logan, A., Hiller, N. and Richardson, J. 2003. Geochemistry of modern brachiopods: applications and implications for oceanography and paleoceanography. *Chemical Geology* 198 (3): 305–334.

Brand, U., Azmy, K., Bitner, M.A., Logan, A., Zuschin, M., Came, R. and Ruggiero, E. 2013. Oxygen isotopes and MgCO3 in brachiopod calcite and a new paleotemperature equation. *Chemical Geology* 359: 23–31.

Brébion, P., Lauriat-Rage, A., Pajaud, D., Pouyet, S. and Roman, J. 1978. Les faunes pliocènes des environs d'Aguilas (provinces d'Almeria et de Murcia, Espagne méridionale). *Bulletin du Muséum national d'Histoire naturelle* 68: 55–76.

Brett, C.E. 1995. Sequence stratigraphy, biostratigraphy, and taphonomy in shallow marine environments. *Palaios*: 597–616.

Brett, C.E. 1998. Sequence stratigraphy, paleoecology, and evolution; biotic clues and responses to sea-level fluctuations. *Palaios* 13 (3): 241–262.

Brocchi, G.B. 1814. *Conchiologia fossile subapennina; con osservazioni geologische sugli apennini e sul suolo adiacente. 2 Vols. 71 Pages, 15 Pls*. Milan.

Buckman, S.S. 1907. Brachiopod nomenclature: the genotype of *Terebratula*. *Annals and Magazine of Natural History* 19 (114): 525–531.

Calzada, S. 1978. Braquiópodos tortonienses de Murcia. *Estudios Geológicos* 34 (3–6): 351–358.

Calzada, S. 1984. Notas sobre Braquiópodos Miocénicos. *Trabajos del Museo Geologico del Seminario Conciliar de Barcelona* 214: 14.

Calzada, S. 1988. Introducció al coneixement dels braquiòpodes fòssils. *In*: *Història Natural Dels Països Catalans*, Vol. 15, 239–252. Barcelona.

Caretto, G. 1963. Nuovi dati sull'estensione della formazione a facies piacenziana a ovest della città di Asti. *Atti Soc. It. Sc. Nat. e del Museo Civ. St. Nat. di Milano* 52: 1–33.

Chen, Z.-Q., Kaiho, K. and George, A.D. 2005. Early Triassic recovery of the brachiopod faunas from the end-Permian mass extinction: A global review. *Palaeogeography, Palaeoclimatology, Palaeoecology* 224 (1): 270–290.

Clapham, M.E. and Bottjer, D.J. 2007a. Permian marine paleoecology and its implications for large-scale decoupling of brachiopod and bivalve abundance and diversity during the Lopingian (Late Permian). *Palaeogeography, Palaeoclimatology, Palaeoecology* 249 (3): 283–301.

Clapham, M.E. and Bottjer, D.J. 2007b. Prolonged Permian–Triassic ecological crisis recorded by molluscan dominance in Late Permian offshore assemblages. *Proceedings of the National Academy of Sciences* 104 (32): 12971–12975.

Clapham, M.E., Bottjer, D.J., Powers, C.M., Bonuso, N., Fraiser, M.L., Marenco, P.J., Dornbos, S.Q. and Pruss, S.B. 2006. Assessing the ecological dominance of Phanerozoic marine invertebrates. *PALAIOS* 21 (5): 431–441.

Clarke, A., Morris, G.J., Fonseca, F., Murray, B.J., Acton, E. and Price, H.C. 2013. A low temperature limit for life on Earth. *PLoS One* 8 (6): e66207.

Collins, M.J. 1991. Growth rate and substrate-related mortality of a benthic brachiopod population. *Lethaia* 24 (1): 1–11.

Colonna, F. 1616. *Purpura: Hoc est de Purpura ab Animali testaceo fusa, de hoc ipso Animali, aliisquibus rarioribus Testaceis quibusdam*. J. Mascardo, Rome.

Crippa, G., Angiolini, L., Bottini, C., Erba, E., Felletti, F., Frigerio, C., Hennissen, J.A.I., Leng, M.J., Petrizzo, M.R. and Raffi, I. 2016. Seasonality fluctuations recorded in fossil bivalves during the early Pleistocene: Implications for climate change. *Palaeogeography, palaeoclimatology, palaeoecology* 446: 234–251.

Crippa, G., Azzarone, M., Bottini, C., Crespi, S., Felletti, F., Marini, M., Petrizzo, M.R., Scarponi, D., Raffi, S. and Raineri, G. 2019. Bio-and lithostratigraphy of lower Pleistocene marine successions in western Emilia (Italy) and their implications for the first occurrence of *Arctica islandica* in the Mediterranean Sea. *Quaternary Research*: 1–21.

Curry, G.B. 1982. Ecology and population structure of the Recent brachiopod *Terebratulina* from Scotland. *Palaeontology* 25 (2): 227–246.

Davidson, T. 1850. Notes on an examination of Lamarck's species of fossil Terebratulæ. *The Annals and Magazine of Natural History* 30 (2, tome 5): 433–449.

Davidson, T. 1864. On the Brachiopoda of the Maltese Islands. *L. Adams, Outline of the Geology of the Maltese Islands. Annals and Magazine of Natural History (London), Ser* 3 (14): 5–11.

Davidson, T. 1870. On Italian Tertiary Brachiopoda. *Geological Magazine* 8 (74, tome 7): 359–370.

Dawson, E.W. 1991. The systematics and biogeography of the living Brachiopoda of New Zealand. *In*: MacKinnon, D.I., Lee, D.E. and Campbell, J.D. (eds.), *Brachiopods through Time*, 431–437. Balkema, Rotterdam.

Delance, J.H. and Emig, C.C. 2004. Drilling predation on *Gryphus vitreus* (Brachiopoda) off the French Mediterranean coasts. *Palaeogeography, Palaeoclimatology, Palaeoecology* 208 (1): 23–30.

Dietl, G.P. and Kelley, P.H. 2001. Mid-Paleozoic latitudinal predation gradient: Distribution of brachiopod ornamentation reflects shifting Carboniferous climate. *Geology* 29 (2): 111–114.

Doherty, P.J. 1979. A demographic study of a subtidal population of the New Zealand articulate brachiopod *Terebratella inconspicua*. *Marine Biology* 52 (4): 331–342.

Dollfus, G.F. and Cotter, J.C.B. 1909. *Mollusques tertiaires du Portugal: Le Pliocène au nord du Tage (Plaisancien). Pelecypoda, précédée d'une notice géologique*. Vol. 1. Commission du service géologique du Portugal, Imprimerie Nationale, Lisbonne.

Dominici, S. 2001. Taphonomy and paleoecology of shallow marine macrofossil assemblages in a collisional setting (late Pliocene–early Pleistocene, western Emilia, Italy). *Palaios* 16 (4): 336–353.

Dominici, S. 2004. Quantitative taphonomy in sandstones from an ancient fan delta system (Lower Pleistocene, Western Emilia, Italy). *Palaios* 19 (3): 193–205.

Dreger, J. 1889. Die tertiären Brachiopoden des Wiener Beckens. *Beiträge zur Paläontologie Österreich-Ungarns* 7: 179–192.

Dulai, A. 2016. Sporadic Pliocene and Pleistocene brachiopods in Naturalis Biodiversity Center (Leiden, the Netherlands): records from the Mediterranean, and the North Sea Basin. *Fragmenta Palaeontologica Hungarica* 33: 65–98.

Dulai, A. and Hocht, F.V.D. 2020. Upper Oligocene Brachiopods from NW Germany, with Description of a New Platidiinae Genus, *Germanoplatidia* N. Gen. *Rivista italiana de Paleontologia e Stratigrafia*126 (1).

Emig, C.C. 1987. Offshore brachiopods investigated by submersible. *Journal of Experimental Marine Biology and Ecology* 108 (3): 261–273.

Emig, C.C. 1989. Observations préliminaires sur l'envasement de la biocoenose à *Gryphus vitreus* (Brachiopoda), sur la pente continentale du Nord de la Corse (Méditerranée). Origines et conséquences. *Comptes Rendus de l'Académie des Sciences Paris* 309: 337–342.

Emig, C.C. and García-Carrascosa, M.A. 1991. Distribution of *Gryphus vitreus* (Born, 1778) (Brachiopoda) on transect P 2 (Continental margin, French Mediterranean coast) investigated by submersible. *Sci. Mar.* 55 (2): 385–388.

Emig, C.C., Bitner, M.A. and Alvarez, F. 2013. Phylum brachiopoda. *Zootaxa* 3703 (1): 75–78.

Encinas, A. 1992 (non vidi). Paleobiología de los braquiópodos de la cuenca neógena del Empordà. Unpublished MSc. Thesis, Universitat de Barcelona, barcelona, 180pp.

Erwin, D.H. 1994. The Permo–Triassic extinction. *Nature* 367 (6460): 231–236.

Evangelisti, F., Albano, P.G. and Sabelli, B. 2012. Predation on two brachiopods, *Joania cordata* and *Argyrotheca cuneata*, from an offshore reef in the Tyrrhenian Sea. *Marine Biology* 159 (10): 2349–2358.

Feldman, H.R. 1977. Paleoecology and morphologic variation of a Paleocene terebratulid brachiopod (*Oleneothyris harlani*) from the Hornerstown Formation of New Jersey. *Journal of Paleontology*: 86–107.

Försterra, G., Häussermann, V. and Lüter, C. 2008. Mass occurrence of the recent brachiopod *Magellania venosa* (Terebratellidae) in the fjords Comau and Reñihué, northern Patagonia, Chile. *Marine Ecology* 29 (3): 342–347.

Foster, M.W. 1974. *Recent Antarctic and Subantarctic Brachiopods*. *In Antarctic Research Series*. Vol. 21. American Geophysical Union, Washington, .

Fraiser, M.L. and Bottjer, D.J. 2007. When bivalves took over the world. *Paleobiology* 33 (3): 397–413.

Fürsich, F.T. 1995. Approaches to palaeoenvironmental reconstructions. *Geobios* 28: 183–195.

Fürsich, F.T., Berndt, R., Scheuer, T. and Gahr, M. 2001. Comparative ecological analysis of Toarcian (Lower Jurassic) benthic faunas from southern France and east-central Spain. *Lethaia* 34 (3): 169–199.

Gaetani, M. and Saccà, D. 1984. Brachiopodi batiali nel Pliocene e Pleistocene di Sicilia e Calabria. *Rivista Italiana di Paleontologia e Stratigrafia* 90 (3): 407–458.

Gaetani, M. and Saccà, D. 1985. Brachiopodi neogenici e pleistocenici della provincia di Messina e della Calabria meridionale. *Geologica Romana* 22: 1–43.

Gahr, M.E. 2005. Response of Lower Toarcian (Lower Jurassic) macrobenthos of the Iberian Peninsula to sea level changes and mass extinction. *Journal of Iberian Geology* 31 (2): 197–215.

Gallagher, W.B. 2003. Oligotrophic oceans and minimalist organisms: collapse of the Maastrichtian marine ecosystem and Paleocene recovery in the Cretaceous-Tertiary sequence of New Jersey. *Netherlands Journal of Geosciences* 82 (3): 225–231.

Garcia, J.-P. and Dromart, G. 1997. The validity of two biostratigraphic approaches in sequence stratigraphic correlations: brachiopod zones and marker-beds in the Jurassic. *Sedimentary Geology* 114 (1–4): 55–79.

García-Ramos, D. 2004. Braquiópodos pliocenos de Águilas. *Boletín de la Asociación Cultural Paleontológica Murciana* 3: 18–39.

García-Ramos, D. 2006. Nota sobre Terebratulinae del Terciario de Europa y su relación con los representantes neógenos del sureste español. *Bol. Asoc. Cult. Paleont. Murciana* 5: 23–83.

Gaspard, D. 1997. Stratégies de fixation etde positionnement chez les brachiopodes. Relation avec le substrat. *Geobios* 30: 121–133.

Gaspard, D. 2003. Recent brachiopods collected during the "SEAMOUNT 1" CRUISE off Portugal and the Ibero-Moroccan Gulf (Northeastern Atlantic) in 1987. *Geobios* 36 (3): 285–304.

Giannetti, A., Baeza-Carratalá, J.F., Soria-Mingorance, J.M., Dulai, A., Tent-Manclús, J.E. and Peral-Lozano, J. 2018. New paleobiogeographical and paleoenvironmental insight through the Tortonian brachiopod and ichnofauna assemblages from the Mediterranean-Atlantic seaway (Guadix Basin, SE Spain). *Facies* 64 (3): 24.

Giles, P.S. 2012. Low-latitude Ordovician to Triassic brachiopod habitat temperatures (BHTs) determined from $\delta^{18}O$ [brachiopod calcite]: A cold hard look at ice-house tropical oceans. *Palaeogeography, Palaeoclimatology, Palaeoecology* 317–318: 134–152.

Gischler, E., Balinski, A., Fuchs, A. and Heidelberger, D. 2004. Famennian brachiopod and gastropod occurrences on top of Devonian seamounts, Elbingerode and Iberg Reefs, Harz Mts., Germany. *Senckenbergiana lethaea* 84 (1): 125–139.

Gómez Alba, J.A.S. 1988. *Guía de Campo de los Fósiles de España y de Europa*. Omega, Barcelona.

González Álvarez, E. 2013. Braquiópodos Pliocenos y Pleistocenos de las Canarias Orientales con mención de los actuales.Master, Universidad de las Palmas de Gran Canaria, Las Palmas, Spain, 27 pp.

Gould, S.J. and Calloway, C.B. 1980. Clams and brachiopods—ships that pass in the night. *Paleobiology* 6 (4): 383–396.

Grange, K.R., Singleton, R.I., Richardson, J.R., Hill, P.J. and Main, W. deL. 1981. Shallow rock-wall biological associations of some southern fiords of New Zealand. *New Zealand Journal of Zoology* 8 (2): 209–227.

Hamza, F.H. 1972. A study on some Pliocene fauna from Egypt. Unpublished MSc. Thesis, Ain Shams University, 228 pp.

Harper, E.M. and Wharton, D.S. 2000. Boring predation and Mesozoic articulate brachiopods. *Palaeogeography, Palaeoclimatology, Palaeoecology* 158 (1): 15–24.

Harper, E.M. and Peck, L.S. 2016. Latitudinal and depth gradients in marine predation pressure. *Global Ecology and Biogeography* 25 (6): 670–678.

Harper, E.M., Peck, L.S. and Hendry, K.R. 2009. Patterns of shell repair in articulate brachiopods indicate size constitutes a refuge from predation. *Marine Biology* 156 (10): 1993–2000.

He, W., Shi, G.R., Feng, Q., Campi, M.J., Gu, S., Bu, J., Peng, Y. and Meng, Y. 2007. Brachiopod miniaturization and its possible causes during the Permian–Triassic crisis in deep water environments, South China. *Palaeogeography, Palaeoclimatology, Palaeoecology* 252 (1): 145–163.

Hsieh, S., Bush, A.M. and Bennington, J.B. 2019. Were bivalves ecologically dominant over brachiopods in the late Paleozoic? A test using exceptionally preserved fossil assemblages. *Paleobiology* 45 (2): 265–279.

Hubbell, S.P. 2001. *The Unified Neutral Theory of Biodiversity and Biogeography*. Princeton University Press, Princeton and Oxford, .

Iñesta, M. 1997. Presencia de *Terebratula sinuosa* (Brocchi) en el Mioceno superior de Monforte del Cid (Alicante). *Noveldiana* 2: 11–18.

Jablonski, D., Belanger, C.L., Berke, S.K., Huang, S., Krug, A.Z., Roy, K., Tomasovych, A. and Valentine, J.W. 2013. Out of the tropics, but how? Fossils, bridge species, and thermal ranges in the dynamics of the marine latitudinal diversity gradient. *Proceedings of the National Academy of Sciences of the United States of America* 110 (26): 10487–10494.

Jackson, J.B.C., Goreau, T.F. and Hartman, W.D. 1971. Recent Brachiopod-Coralline Sponge Communities and Their Paleoecological Significance. *Science* 173 (3997): 623–625.

James, M.A., Ansell, A.D., Collins, M.J., Curry, G.B., Peck, L.S. and Rhodes, M.C. 1992. Biology of Living Brachiopods. *In*: Blaxter, J.H.S. and Southward, A.J. (eds.), *Advances in Marine Biology*, Vol. 28, 175–387. Academic Press.

Juan, C., Ercilla, G., Javier Hernández-Molina, F., Estrada, F., Alonso, B., Casas, D., García, M., Farran, M., Llave, E., Palomino, D., Vázquez, J.-T., Medialdea, T., Gorini, C., D'Acremont, E., El Moumni, B. and Ammar, A. 2016. Seismic evidence of current-controlled sedimentation in the Alboran Sea during the Pliocene and Quaternary: Palaeoceanographic implications. *Marine Geology* 378: 292–311.

Kocsis, L., Vennemann, T.W., Fontignie, D., Baumgartner, C., Montanari, A. and Jelen, B. 2008. Oceanographic and climatic evolution of the Miocene Mediterranean deduced from Nd, Sr, C, and O isotope compositions of marine fossils and sediments. *Paleoceanography* 23 (4).

Kowalewski, M., Dulai, A. and Fürsich, F.T. 1998. A fossil record full of holes: The Phanerozoic history of drilling predation. *Geology* 26 (12): 1091–1094.

Kowalewski, M., Simões, M.G., Carroll, M. and Rodland, D.L. 2002. Abundant Brachiopods on a Tropical, Upwelling-Influenced Shelf (Southeast Brazilian Bight, South Atlantic). *Palaios* 17 (3): 277–286.

Kowalewski, M., Hoffmeister, A.P., Baumiller, T.K. and Bambach, R.K. 2005. Secondary Evolutionary Escalation Between Brachiopods and Enemies of Other Prey. *Science* 308 (5729): 1774–1777.

Kroh, A., Harzhauser, M., Piller, W.E. and Rögl, F. 2003. The Lower Badenian (Middle Miocene) Hartl Formation (Eisenstadt – Sopron Basin, Austria). *In*: Piller, W.E. (ed.), *Stratigraphia Austriaca*, 87–109. Österreichische Akademie der Wissenschaften.Schriftenreihe der Erdwissenschaftlichen Kommission, Vienna.

Kudrin, L.N. 1961. Miocene terebratulides of the south-western outlying district of the Russian Platform [*In Russian*]. *Paleontol. Sbornik Ivovskogo Geol. Obshchestva* 1: 51–59.

Lamarck, J.-B. de M. de. 1819. *Histoire naturelle des animaux sans vertèbres: présentant les caractères généraux et particuliers de ces animaux, leur distribution, leurs classes, leurs familles, leurs genres, et la citation des principales espèces qui s'y rapportent : précédée d'une introduction*. Vol. 6, part 1. Verdière, Paris, France.

Laurin, B. and García-Joral, F. 1990. Miniaturization and heterochrony in *Homoeorhynchia meridionalis* and *H. cynocephala* (Brachiopoda, Rhynchonellidae) from the Jurassic of the Iberian Range, Spain. *Paleobiology* 16 (1): 62–76.

Lee, D.E. 1978. Aspects of the ecology and paleoecology of the Brachiopod *Notosaria nigricans* (Sowerby). *Journal of the Royal Society of New Zealand* 8 (4): 395–417.

Lee, D.E. 1991. Aspects of the ecology and distribution of the living Brachiopoda of New Zealand. *In*: MacKinnon, D.I., Lee, D.E. and Campbell, J.D. (eds.), *Brachiopods through Time*, 273 – 279. A. A. Balkema Publishers, Rotterdam, The Netherlands.

Lee, D.E. 2008. The terebratulides: the supreme brachiopod survivors. *Fossils and Strata* 54: 241–249.

Lee, D.E. and Brunton, C.H.C. 1998. *Terebratula* Müller, 1776 (Brachiopoda): proposed designation of *Anomia terebratula* Linnaeus, 1758 as the type species. *Bulletin of Zoological Nomenclature* 55: 220–223.

Lee, D.E., Dagys, A.S., Smirnova, T.N. and Dong-Li, S. 2006. Part H, Brachiopoda (Revised), vol. 5, ch. 6, p. 2082–2162. *Digital Treatise*.

Lee, D.E., Brunton, C.H.C., Ruggiero, E.T., Caldara, M. and Simone, O. 2001. The Cenozoic brachiopod *Terebratula*: its type species, neotype, and other included species. *Bulletin of the Natural History Museum London, Geology Series* 57 (2): 82–94.

Leighton, L.R. 1999. Possible latitudinal predation gradient in middle Paleozoic oceans. *Geology* 27 (1): 47–50.

Leighton, L.R., Webb, A.E. and Sawyer, J.A. 2013. Ecological effects of the Paleozoic-Modern faunal transition: Comparing predation on Paleozoic brachiopods and molluscs. *Geology* 41 (2): 275–278.

Linnaeus, C. von. 1758. *Systema Naturae sive Regna tria Naturae systematice proposita per Classes, Ordines, Genera et Species*. Vol. 1, Regnum Animale (part. II). Stockholm.

Little, O. 1936. Recent geological work in the Fayum and in the adjoining portion of the Nile Valley. *Bull Institut d'Égypte* 18: 201–240.

Logan, A. 1975. Ecological Observations on the Recent Articulate Brachiopod *Argyrotheca bermudana* Dall from the Bermuda Platform. *Bulletin of Marine Science* 25 (2): 186–204.

Logan, A. 1979. The Recent Brachiopoda of the Mediterranean Sea. *Bulletin de l'Institut océanographique de Monaco* 72: 1–112.

Logan, A. 1998. Recent Brachiopoda from the oceanographic expedition SEAMOUNT 2 to the north-eastern Atlantic in 1993. *Zoosystema* 20 (4): 549–562.

Logan, A. 2004. The present-day Mediterranean brachiopod fauna: diversity, life habits, biogeography and paleobiogeography. *Scientia Marina* 68 (Extra 1): 163–170.

Logan, A. 2007. Geographic distribution of extant articulated brachiopods. *In*: Seldon, P.A. (ed.), *Treatise on Invertebrate Paleontology*, Vol. 6, 3082–3115. Geological Society of America and University of Kansas, Boulder, Colorado and Lawrence, Kansas,.

Logan, A. and Zibrowius, H. 1994. A New Genus and Species of Rhynchonellid (Brachiopoda, Recent) from Submarine Caves in the Mediterranean Sea. *Marine Ecology* 15 (1): 77–88.

Macpherson, E. 2002. Large-scale species-richness gradients in the Atlantic Ocean. *Proceedings of the Royal Society B: Biological Sciences* 269 (1501): 1715–1720.

Mahon, A.R., Amsler, C.D., McClintock, J.B., Amsler, M.O. and Baker, B.J. 2003. Tissue-specific palatability and chemical defenses against macropredators and pathogens in the common articulate brachiopod Liothyrella uva from the Antarctic Peninsula. *Journal of Experimental Marine Biology and Ecology* 290 (2): 197–210.

Malz, H. and Jellinek, T. 1984. Marine Plio-/Pleistozän-Ostracoden von SE-Lakonien (Peloponnes, Griechenland). *Senckenbergiana biologica* 65 (1–2): 113–167.

Manceñido, M.O. and Damborenea, S.E. 2008. Brachiopoda. *Los invertebrados fósiles: Buenos Aires, Vázquez Mazzini Editores*: 243–292.

Marasti, R. 1973. La fauna tortoniana del T. Stirone: limite Parmense-Piacentino. *Bollettino della Società Paleontologica Italiana* 12 (1): 76–120.

Mayer-Eymar, K. 1898. Systematisches Verzeichniss der Fauna des unteren Saharianum (marines Quartaer) der Umgegend von Kairo; nebst Beschreibg der neuen Arten. *Palaeontographica* 30: 61–90.

McClintock, J.B., Slattery, M. and Thayer, C.W. 1993. Energy content and chemical defense of the articulate brachiopod Liothyrella uva (Jackson, 1912) from the Antarctic Peninsula. *Journal of Experimental Marine Biology and Ecology* 169 (1): 103–116.

Middlemiss, F.A. 1976. Lower Cretaceous Terebratulidina of northern England and Germany and their geological background. *Geologisches Jahrbuch* 30: 21–104.

Monegatti, P. and Raffi, S. 2001. Taxonomic diversity and stratigraphic distribution of Mediterranean Pliocene bivalves. *Palaeogeography, Palaeoclimatology, Palaeoecology* 165 (3): 171–193.

Motchurova-Dekova, N., Saito, M. and Endo, K. 2002. The Recent rhynchonellide brachiopod *Parasphenarina cavernicola* gen. et sp. nov. from the submarine caves of Okinawa, Japan. *Paleontological Research* 6 (3): 299–319.

Muir-Wood, H.M. 1936. A Monograph on the Brachiopoda of the British Great Oolite Series. Part I. The Brachiopoda of the Fuller's Earth. *Monographs of the Palaeontographical Society* 89 (404): 1–144.

Muir-Wood, H.M. 1938. Notes on British Eocene, and Pliocene Terebratulas. *Annals and Magazine of Natural History* 2 (8): 154–181.

Muir-Wood, H.M. 1965. Mesozoic and Cenozoic Terebratulidina. *In*: Moore, R.C. (ed.), *Treatise on Invertebrate Paleontology. Part H, Brachiopoda*, 762–816. Geological Society of America & University of Kansas Press, New York.

Nalin, R., Ghinassi, M. and Basso, D. 2010. Onset of temperate carbonate sedimentation during transgression in a low-energy siliciclastic embayment (Pliocene of the Val d'Orcia Basin, Tuscany, Italy). *Facies* 56 (3): 353–368.

Nath, R. 1932. Terminology of some Types of Folding in Brachiopods. *Journal of the Geological, Mineralogical and Metallurgical Society of India* 4: 189–193.

Pacaud, J.M. 2015. Catalogue des types de brachiopodes conservés dans les collections de Paléontologie du Muséum National d'Histoire Naturelle de Paris. *Revue française de paléontologie* (5): 82–98.

Paine, R.T. 1963. Ecology of the Brachiopod *Glottidia pyramidata*. *Ecological Monographs* 33 (3): 187–213.

Pajaud, D. 1976. Les Brachiopodes du Pliocène I de la Sierra de Santa Pola (sud d'Alicante, Espagne): *Terebratula terebratula* (Linné, 1758) et *Phapsirhynchia sanctapaulensis* nov. gen., nov. sp. *Annales de la Société géologique du Nord* 96: 99–106.

Pajaud, D. 1977. Les Brachiopodes du Pliocène I de la région d'Aguilas (sud d'Almeria, Espagne). *Annales de Paléontologie (Invertébrés)* 63: 59–75.

Pavia, G. and Zunino, M. 2008. Progetto di Geoconservazione del sito a Brachiopodi del Pliocene inferiore di Capriglio (Asti). *Geologica Romana* 41: 19–24.

Payne, J.L., Heim, N.A., Knope, M.L. and McClain, C.R. 2014. Metabolic dominance of bivalves predates brachiopod diversity decline by more than 150 million years. *Proceedings of the Royal Society B: Biological Sciences* 281 (1783): 20133122.

Peck, L.S. 1996. Metabolism and feeding in the Antarctic brachiopod *Liothyrella uva*: a low energy lifestyle species with restricted metabolic scope. *Proceedings of the Royal Society of London. Series B: Biological Sciences* 263 (1367): 223–228.

Peck, L.S. 2005. Prospects for survival in the Southern Ocean: vulnerability of benthic species to temperature change. *Antarctic Science* 17 (4): 497–507.

Peck, L.S. 2007. Brachiopods and climate change. *Earth and Environmental Science Transactions of The Royal Society of Edinburgh* 98 (3–4): 451–456.

Peck, L.S. and Harper, E.M. 2010. Variation in size of living articulated brachiopods with latitude and depth. *Marine Biology* 157 (10): 2205–2213.

Peck, L.S., Barnes, D.K.A. and Willmott, J. 2005. Responses to extreme seasonality in food supply: diet plasticity in Antarctic brachiopods. *Marine Biology* 147 (2): 453–463.

Peck, L.S., Curry, G.B., Ansell, A.D. and James, M. 1989. Temperature and starvation effects on the metabolism of the brachiopod, *Terebratulina retusa* (L.). *Historical Biology* 2 (2): 101–110.

Peckmann, J., Kiel, S., Sandy, M.R., Taylor, D.G. and Goedert, J.L. 2011. Mass Occurrences of the Brachiopod *Halorella* in Late Triassic Methane-Seep Deposits, Eastern Oregon. *The Journal of Geology* 119 (2): 207–220.

Pedley, H.M. 1976. A palaeoecological study of the Upper Coralline Limestone, *Terebratula-Aphelesia* bed (Miocene, Malta) based on bryozoan growth-form studies and brachiopod distributions. *Palaeogeography, Palaeoclimatology, Palaeoecology* 20 (3): 209–234.

Pennington, J.T., Tamburri, M.N. and Barry, J.P. 1999. Development, Temperature Tolerance, and Settlement Preference of Embryos and Larvae of the Articulate Brachiopod *Laqueus californianus*. *The Biological Bulletin* 196 (3): 245–256.

Pérez-Huerta, A. and Sheldon, N.D. 2006. Pennsylvanian sea level cycles, nutrient availability and brachiopod paleoecology. *Palaeogeography, Palaeoclimatology, Palaeoecology* 230 (3): 264–279.

Pervesler, P., Uchman, A., Hohenegger, J. and Dominici, S. 2011. Ichnological Record of Environmental Changes in Early Quaternary Gelasian-Calabrian Marine Deposits of the Stirone Section, Northern Italy. *Palaios* 26 (9): 578–593.

De Porta, J., Martinell, J. and Llovera, J.C. 1979. Datos paleontológicos y tafonómicos de la formación Turre en Cortijada de Arejos (Almería). *Studia geologica salmanticensia* (15): 63–84.

Pörtner, H.-O., Bock, C. and Mark, F.C. 2017. Oxygen- and capacity-limited thermal tolerance: bridging ecology and physiology. *Journal of Experimental Biology* 220 (15): 2685–2696.

Powell, M.G. 2009. The Latitudinal Diversity Gradient of Brachiopods over the Past 530 Million Years. *The Journal of Geology* 117 (6): 585–594.

Puga-Bernabéu, A., Martín, J.M. and Braga, J.C. 2008. Sistema de canales submarinos en una rampa de carbonatos templados, Cuenca de Sorbas, sureste de España. *Geogaceta* 44: 203–206.

Reolid, M. 2005. Asociaciones de braquiópodos del Oxfordiense medio-Kimmeridgiense inferior en la zona prebética (Sureste de España): relación con los litofacies y el gradiente proximal-distal de la plataforma. *Revista española de paleontología* 20 (1): 21–36.

Reolid, M., García-García, F., Tomašovỳch, A. and Soria, J.M. 2012. Thick brachiopod shell concentrations from prodelta and siliciclastic ramp in a Tortonian Atlantic–Mediterranean strait (Miocene, Guadix Basin, southern Spain). *Facies* 58 (4): 549–571.

Richardson, J.R. 1986. Brachiopods. *Scientific American* 255 (3): 100–107.

Richardson, J.R. 1997. Ecology of articulate brachiopods. *In*: Kaesler, R. (ed.), *Treatise of Invertebrate Paleontology, Brachiopoda (Rev.) Part H*, Vol. 1, 441–462. Geological Society of America and University of Kansas, Colorado.

Rico-García, A. 2004. Estudio paleontológico del Neógeno superior de Vejer de la Frontera (Cádiz). Bachelor Thesis, Universidad de Salamanca, Salamanca, 247 pp.

Roy, K., Jablonski, D. and Valentine, J.W. 2000. Dissecting latitudinal diversity gradients: functional groups and clades of marine bivalves. *Proceedings of the Royal Society B: Biological Sciences* 267 (1440): 293–299.

Rudwick, M.J.S. 1970. *Rudwick: Living and fossil brachiopods*. Hutchinson University Library, London, .

Sacco, F. 1902. *I brachiopodi dei terreni terziarii del Piemonte e della Liguria*. C. Clausen, Torino.

Sandford, K.S. and Arkell, W.J. 1933. *Paleolithic Man and the Nile-Faiyum Divide in Nubia and Upper Egypt: A Study of the Region during Pliocene and Pleistocene Times*. *In* Breasted, J.H. (ed.) *Oriental Institute Publications*. Vol. 1. University of Chicago Press, Chicago.

Sandy, M.R. 2010. Brachiopods from Ancient Hydrocarbon Seeps and Hydrothermal Vents. *In*: Kiel, S. (ed.), *The Vent and Seep Biota: Aspects from Microbes to Ecosystems*, 279–314. Springer Netherlands, Dordrecht.

Santagata, S. 2015. Brachiopoda. *In*: Wanninger, A. (ed.), *Evolutionary Developmental Biology of Invertebrates 2: Lophotrochozoa (Spiralia)*, 263–277. Springer, Vienna.

Savage, N.M. 1972. Some observations on the behaviour of the Recent brachiopod *Megerlina pisum* under laboratory conditions. *Lethaia* 5 (1): 61–67.

Schimmel, M.K., Kowalewski, M. and Coffey, B.P. 2012. Traces of predation/parasitism recorded in Eocene brachiopods from the Castle Hayne Limestone, North Carolina, USA. *Lethaia* 45 (2): 274–289.

Scilla, A. 1670. La vana speculazione disingannata dal senso. A. Coliccia, Naples.

Seguenza, G. 1871. Studii paleontologici sui brachiopodi terziarii dell'Italia meridionale. *Bollettino Malacologico Italiano* 4: 1–74.

Seguenza, Giuseppe. 1865. *Paleontologia malacologica dei terreni terziarii del distretto di Messina*. *Memorie della Società Italiana Di Scienze Naturali* 6: 1-88.

Sepkoski, J.J. 1981. A factor analytic description of the Phanerozoic marine fossil record. *Paleobiology* 7 (1): 36–53.

Sepkoski, J.J. 1996. Patterns of Phanerozoic Extinction: a Perspective from Global Data Bases. *In*: Walliser, O.H. (ed.), *Global Events and Event Stratigraphy in the Phanerozoic: Results of the International Interdisciplinary Cooperation in the IGCP-Project 216 "Global Biological Events in Earth History"*, 35–51. Springer, Berlin, Heidelberg.

Signor, P.W. and Brett, C.E. 1984. The mid-Paleozoic precursor to the Mesozoic marine revolution. *Paleobiology* 10 (2): 229–245.

Simões, M.G., Kowalewski, M., Mello, L.H.C., Rodland, D.L. and Carroll, M. 2004. Recent brachiopods from the southern Brazilian shelf: palaeontological and biogeographical implications. *Palaeontology* 47 (3): 515–533.

Simpson, G.G. 1953. *Life of the Past*. Yale Univ. Press, New Haven, Connecticut.

Spano, C. 1989. Macrofauna circalitorale del Pliocene inferiore di Capo S. Marco (Sardegna occidentale). *Rivista Italiana di Paleontologia e Stratigrafia (Research In Paleontology and Stratigraphy)* 95 (2): 137–172.

Taddei Ruggiero, E. 1983. Struttura del guscio dei generi *Gryphus* e *Terebratula* (Terebratulidae, Brachiopoda). *Societa dei Naturalisti in Napoli, Bollettino* 90: 177–201.

Taddei Ruggiero, E. 1994. Neogene Salento brachiopod palaeocommunities. *Bollettino della Società Paleontologica Italiana* 33 (2): 197–213.

Taddei Ruggiero, E. 2001. Brachiopods of the Isca submarine cave: observations during ten years. *In*: Brunton, C.. H.C., Cocks, Robin.L. and Long, S.L. (eds.), *Brachiopods, Past and Present*, 261–267. Taylor and Francis, New York, NY.

Taddei Ruggiero, E. and Raia, P. 2008. Ontogeny in *Terebratula* species. Functional convergence and allometry but not heterochrony. *Proceedings of the Royal Society of Victoria* 120 (1): 318–329.

Taddei Ruggiero, E.T., Buono, G. and Raia, P. 2006. Bioerosion on Brachiopod Shells of a Thanatocoenosis of Alboràn Sea (Spain). *Ichnos* 13 (3): 175–184.

Taddei Ruggiero, E. and Raia, P. 2014. Oichnus taddeii, a new fossil trace produced by capulids on brachiopod shells. *Spanish journal of palaeontology* (1): 15–24.

Taddei Ruggiero, E., Raia, P. and Buono, G. 2008. Geometric morphometrics species discrimination within the genus *Terebratula* from the Late Cenozoic of Italy. *Fossils and Strata* (54): 209–217.

Taddei Ruggiero, E.T., Serio, C. and Raia, P. 2019. On the validity of *Terebratula sinuosa*. *Rivista Italiana di Paleontologia e Stratigrafia* 125 (3): 631-636.

Taviani, M. 2002. The Mediterranean benthos from late Miocene up to present: ten million years of dramatic climatic and geologic vicissitudes. *Biologia marina mediterranea* 9 (1): 445–463.

Thayer, C.W. 1979. Biological Bulldozers and the Evolution of Marine Benthic Communities. *Science* 203 (4379): 458–461.

Thayer, C.W. 1983. Sediment-Mediated Biological Disturbance and the Evolution of Marine Benthos. *In*: Tevesz, M.J.S. and McCall, P.L. (eds.), *Biotic Interactions in Recent and Fossil Benthic Communities*, 479–625. Springer US, Boston, MA.

Thayer, C.W. 1985. Brachiopods versus Mussels: Competition, Predation, and Palatability. *Science* 228 (4707): 1527–1528.

Thayer, C.W. 1986. Are Brachiopods Better Than Bivalves? Mechanisms of Turbidity Tolerance and Their Interaction with Feeding in Articulates. *Paleobiology* 12 (2): 161–174.

Thompson, A. 1927. *Brachiopod morphology and genera (Recent and Tertiary)*. *In New Zealand Board of Science and Art, Manual*.

Tomašových, A. 2006. Brachiopod and Bivalve Ecology in the Late Triassic (Alps, Austria): Onshore-Offshore Replacements Caused by Variations in Sediment and Nutrient Supply. *Palaios* 21 (4): 344–368.

Tomašových, A. 2008a. Evaluating neutrality and the escalation hypothesis in brachiopod communities from shallow, high-productivity habitats. *Evolutionary Ecology Research* 10: 667–698.

Tomašových, A. 2008b. Substrate exploitation and resistance to biotic disturbance in the brachiopod *Terebratalia transversa* and the bivalve *Pododesmus macrochisma*. *Marine Ecology Progress Series* 363: 157–170.

Tomašových, A., Fürsich, F.T. and Wilmsen, M. 2006. Preservation of Autochthonous Shell Beds by Positive Feedback between Increased Hardpart-Input Rates and Increased Sedimentation Rates. *The Journal of Geology* 114 (3): 287–312.

Toscano-Grande, A., García-Ramos, D., Ruiz-Muñoz, F., González-Regalado, M.L., Abad, M., Civis-Llovera, J., González-Delgado, J.Á., Rico-García, A., Martínez-Chacón, M.L. and Xiomara García, E. 2010. Braquiópodos neógenos del suroeste de la depresión del Guadalquivir (sur de España). *Revista mexicana de ciencias geológicas* 27 (2): 254–263.

Tunnicliffe, V. and Wilson, K. 1988. Brachiopod populations: distribution in fjords of British Columbia (Canada) and tolerance of low oxygen concentrations. *Marine Ecology Progress Series* 47 (2): 117–128.

Tyler, C.L., Leighton, L.R., Carlson, S.J., Huntley, J.W. and Kowalewski, M. 2013. Predation on modern and fossil brachiopods: Assessing chemical defenses and palatability. *Palaios* 28 (10): 724–735.

Vermeij, G.J. 2013. On Escalation. *Annual Review of Earth and Planetary Sciences* 41 (1): 1–19.

Videt, B. 2003. Dynamique des paléoenvironnements à huîtres du Crétacé supérieur nord-aquitain (SO France) et du Mio-Pliocène andalou (SE Espagne): biodiversité, analyse séquentielle, biogéochimie.PhD Thesis, Université Rennes, 304 pp.

Vörös, A. 1986. Brachiopod palaeoecology on a Thethyan Jurassic Seamount (Pliensbachian, Bakony Mountains, Hungary). *Palaeogeography, Palaeoclimatology, Palaeoecology* 57 (2): 241–271.

Vörös, A. 2002. Victims of the Early Toarcian anoxic event: the radiation and extinction of Jurassic Koninckinidae (Brachiopoda). *Lethaia* 35 (4): 345–357.

Vörös, A. 2005. The smooth brachiopods of the Mediterranean Jurassic: Refugees or invaders? *Palaeogeography, Palaeoclimatology, Palaeoecology* 223 (3): 222–242.

Vörös, A. 2010. Escalation reflected in ornamentation and diversity history of brachiopod clades during the Mesozoic marine revolution. *Palaeogeography, Palaeoclimatology, Palaeoecology* 291 (3): 474–480.

Walsh, J.A. 1996. No Second Chances? New Perspectives on Biotic Interactions in Post-Paleozoic Brachiopod History. *In*: Copper, P. and Jin, J. (eds.), *Brachiopods*, 281–288. A.A. Balkema, Rotterdam.

Wood, A.M. 2009. The Phylogeny and Palaeozoogeography of Cold-Water Species of Ostracod (Crustacea) from the Pre-Ludhamian Stage (Late Pliocene-Early Pleistocene), Red Crag Formation, East Anglia, England; with Reference to the Earliest Arrival of Pacific Species. *Paleontological Research* 13 (4): 345–366.

Zachos, J., Pagani, M., Sloan, L., Thomas, E. and Billups, K. 2001. Trends, Rhythms, and Aberrations in Global Climate 65 Ma to Present. *Science* 292 (5517): 686–693.

Zezina, O.N. 2008. Biogeography of the recent brachiopods. *Paleontological Journal* 42 (8): 830–858.

Ziegler, B. 1975. *Einführung in die Paläobiologie*. Teil 1. Allgemeine Paläontologie. E. Schweizerbart, Suttgart, .

Zuschin, M. and Mayrhofer, S. 2009. Brachiopods from cryptic coral reef habitats in the northern Red Sea. *Facies* 55 (3): 335–344.

Chapter 2

MANUSCRIPT 1

High-frequency cycles of brachiopod shell beds on subaqueous delta-scale clinoforms (south-east Spain)

Authors: Diego A. García-Ramos and Martin Zuschin

Publication status: published online the 26th september 2018 in *Sedimentology,* vol. 66, 5, August 2019, https://doi.org/10.1111/sed.12541

SEDIMENTOLOGY the journal of the International Association of Sedimentologists

Sedimentology (2019) doi: 10.1111/sed.12541

High-frequency cycles of brachiopod shell beds on subaqueous delta-scale clinoforms (early Pliocene, south-east Spain)

DIEGO A. GARCÍA-RAMOS and MARTIN ZUSCHIN
Department of Palaeontology, University of Vienna, Althanstrasse 14, A-1090, Vienna, Austria

Associate Editor – Christopher Fielding

ABSTRACT

During the early Pliocene, subaqueous delta-scale clinoforms developed in the Águilas Basin, in a mixed temperate carbonate–siliciclastic system. The facies distribution is consistent with the infralittoral prograding wedge model. Stacking patterns and bounding surfaces indicate that the clinoforms formed during the highstand and falling sea-level stages of a high rank cycle. Twenty-two prograding clinothems were recognized over a distance of ≥1 km. Biostratigraphic data indicate a time span shorter than 700 kyr for the whole unit (MPl3 biozone of the Mediterranean Pliocene). Cyclic skeletal concentrations and occasional biostromes of suspension feeders (terebratulid brachiopods, modiolid bivalves and adeoniform bryozoan colonies), slightly evolved glauconite and occasional *Glossifungites* ichnofacies formed on the clinoforms during high-frequency pulses of relative sea-level rise. During such stages, increased accommodation space in the topsets of the clinoforms caused a strong reduction of terrigenous input into the foresets and bottomsets. This provided favourable conditions for the development of these suspension feeder palaeocommunities. During stillstand stages, however, reduced accommodation space in the topsets eventually resumed progradation in the foresets. There, the abundance of *Ditrupa* tubes indicates frequent siltation events that extirpated the terebratulid populations and other epifaunal suspension feeders in the foreset and bottomset subenvironments. The occurrence of shell beds on the clinoforms suggests that this case study represents lower progradation rates than standard examples where shell beds bound the clinobedded units at their base and top only. Importantly, the distributions of biofacies and ichnoassemblage associations contribute significantly to the understanding of the effects of relative sea-level fluctuations on the evolution of subaqueous delta-scale clinoform systems.

Keywords Brachiopods, clinoforms, high-frequency sea-level changes, mixed carbonate–siliciclastic systems, sequence stratigraphy, shell beds.

INTRODUCTION

The duration of cycles is the traditional criterion to discriminate the hierarchical order of stratigraphic sequences (Mitchum & Van Wagoner, 1991; Vail *et al.*, 1991). The assignment of sequences to orders, however, can be difficult and arbitrary because the structure of the sedimentary record conforms to a continuum rather than to distinct modes of abundance classes of cycle duration (Drummond & Wilkinson, 1996; Schlager, 2004, 2010). Many authors advocate analyzing hierarchy based on the relative scale and magnitude of sequences (Embry, 1993, 1995; Catuneanu, 2006; Neal & Abreu, 2009; Catuneanu *et al.*, 2011). Accordingly, high rank (low frequency) and low rank (high frequency) sequences are established on a case by case basis using observations from the rock record. For example, the sequence of largest magnitude in a particular

basin can be designated by the generic rank 'N', and successively lower rank sequences can be designated by ranks 'N-1', 'N-2', etc. (e.g. Massari & Chiocci, 2006). Such hierarchical systems can serve as a template for comparison with other study areas and, if good chronological control is available, these ranks can be evaluated in light of cycle duration to reconcile both approaches (Schlager, 2010). The physical expression of sequences can include the relative extension of unconformities, depth of incision of fluvial valleys, geometric relationships between the building blocks of composite sequences, magnitude of facies shifts, relative scale of clinoforms (Thorne, 1995; Helland-Hansen *et al.*, 2012; Patruno *et al.*, 2015), or the development of onlap, backlap, downlap and toplap shell beds (Kidwell, 1991; Abbott, 1997; Naish & Kamp, 1997; Kondo *et al.*, 1998; Di Celma *et al.*, 2005; Hendy *et al.*, 2006; Zecchin & Catuneanu, 2013). Except for large-scale outcrops, however, where the relationships between the rank of sequences and the distribution of shell beds can be directly traced (Beckvar & Kidwell, 1988; Massari & D'Alessandro, 2012; Zecchin & Catuneanu, 2017) (Fig. 1A), exposures with limited spatial extent hamper the observation of clinoforms. In such cases, the rank of sequences defined by the position and geometric relationship of condensed shell beds with the sequence building blocks can be difficult to elucidate (Fürsich *et al.*, 1991; Ruffell & Wach, 1998).

This study documents the distribution of cyclically arranged brachiopod shell beds in the Águilas Basin (south-east Spain) in extensive outcrops of Pliocene sediments. These pavements formed on the distal part of lower rank delta-scale (i.e. tens of metres high) clinoforms (Fig. 1B and C). Importantly, this contrasts with other examples where onlap and backlap shell beds bound lower rank delta-scale clinoforms (e.g. Massari & D'Alessandro, 2012) (Fig. 1A). Determining the scale of clinoforms in the current study area enables the identification of low rank onlap and backlap shell beds. Moreover, the development of condensed shell beds on clinoforms implies lower progradation rates than those where clinoforms of comparable scale/rank lack such hiatal concentrations.

NOMENCLATURE

Clinoforms, clinothems and scale

Clinoforms are sloping depositional surfaces commonly associated with prograding strata (Pirmez *et al.*, 1998; Patruno *et al.*, 2015, and references therein). These surfaces consist of gently dipping topset and bottomset parts bounded by a basinward steeper-dipping portion termed the foreset (Gilbert, 1885) (Fig. 2A). The sedimentary deposits (or stratal packages) bounded by two successive clinoforms of the same hierarchy/rank are termed 'clinothems' (Rich, 1951; Anell & Midtkandal, 2015; Patruno *et al.*, 2015) (Fig. 2A). In short, clinoforms are surfaces and clinothems are the deposits between them. Depending on the geometry of the clinoform, there are one or two slope break points of maximum curvature, known as 'rollovers'. An 'upper rollover' connects the topset with the foreset and a 'lower rollover' connects the foreset and the bottomset (Walsh *et al.*, 2004; Mitchell, 2012; Patruno *et al.*, 2015) (Fig. 2A). The rollover separating the topset and foreset has also been referred to as shoreline break, breakpoint, brinkpoint, offlap break or shelfbreak, depending on the scale of the clinoform and the sedimentary environment (Vail *et al.*, 1991; Hernández-Molina *et al.*, 2000; Soria *et al.*, 2003). Concerning the spatial scale, clinoforms are fractal structures that display a huge vertical range, in the order of centimetres to thousands of metres (Thorne, 1995; Pirmez *et al.*, 1998; Patruno *et al.*, 2015). Accordingly, in a proximal to distal transect, large clinoforms have been classified as subaerial delta and subaqueous delta clinoforms (both tens of metres high), shelf prisms (*ca* 100 to 500 m high) and continental margin clinoforms (thousands of metres high) (Helland-Hansen *et al.*, 2012; Patruno *et al.*, 2015) (Fig. 2B).

In rare cases, all four types are found to prograde synchronously in the same basin, forming a compound clinoform system (Patruno *et al.*, 2015) (Fig. 2B and C). In physical-accommodation dominated systems (*sensu* Pomar & Kendall, 2008), the relative progradation rates decrease from subaerial and subaqueous deltas, to shelf prisms and then to continental margin clinoforms (Patruno *et al.*, 2015) (Fig. 2B). This is important because the relative progradation rates can help to reconcile the duration of relative sea-level cycles and their physical expression in the rock record.

Delta-scale clinoforms

Both subaerial and subaqueous delta-scale clinoforms display a vertical range of tens of metres. Subaerial and subaqueous deltas should not be confused, because the former have a topset entirely or partially above sea-level (Postma,

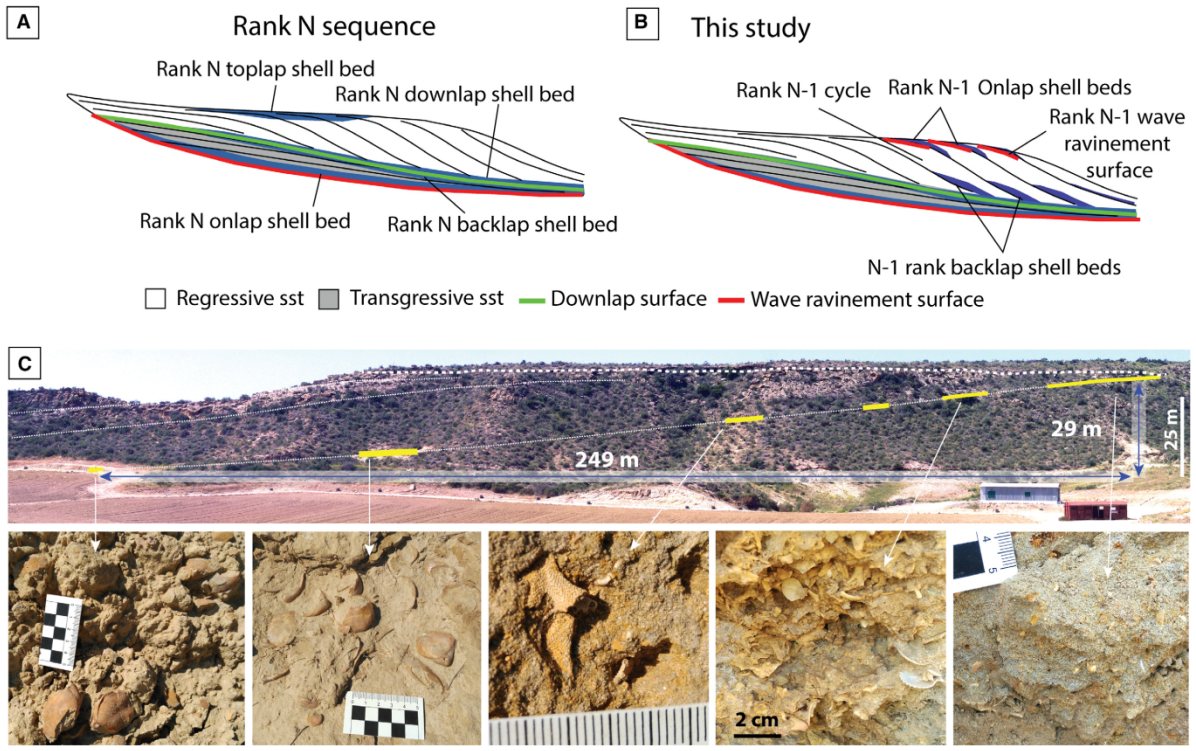

Fig. 1. Idealized sketch of the sequences with the location of condensed shell beds and the conceptual framework for a hierarchical classification of ranks based on geometry and scale. (A) Rank N sequence with indication of rank N onlap, backlap, downlap and toplap shell beds (adapted from Zecchin, 2007). (B) Rank N sequence indicating the position of both rank N and rank N-1 shell beds as described in this study. (C) Outcrop example of rank N-1 shell beds on a Pliocene subaqueous delta-scale clinoform (low rank) in the Águilas Basin (from proximal to distal: *Schizoretepora* – rhodolith debris, *Schizoretepora* and *Terebratula* facies).

1990), whereas the latter have the whole clinoform (topset, foreset and bottomset) submerged (Fig. 2C). Moreover, the rollover in subaerial deltas can be coincident with or very close to the shoreline, whereas in subaqueous deltas the rollover is on average several kilometres away from the shoreline.

In a meta-analytical study of clinoform geometry and scale, Patruno *et al.* (2015) differentiated two types of subaqueous delta-scale clinoforms: sand-prone and mud-prone. This distinction is relevant because the former display higher foreset gradients and their rollovers are closer to the shoreline than in the latter (Patruno *et al.*, 2015). The terminology of Patruno *et al.* (2015) focuses on the geometric description of clinoforms. Similar terms related to geometric aspects include 'distally steepened ramp' (Read, 1985) for carbonate environments (see also Pomar, 2001).

Other terms have been proposed following a genetic approach. For example, Hernández-Molina *et al.* (2000) introduced the term 'infralittoral prograding wedge' (IPW) for a morpho-sedimentary system characterized by narrow, shore-parallel, sigmoidal-shaped sedimentary bodies that prograde below the wave base in the offshore transitional zone of wave-dominated coasts. Geometrically, this system belongs to the category of sand-prone subaqueous delta-scale clinoforms of Patruno *et al.* (2015). Such a distinction is helpful because prograding reef platforms also produce subaqueous delta-scale clinoforms (Franseen & Mankiewicz, 1991; Pomar & Ward, 1994; Braga & Martín, 1996; Cuevas-Castell *et al.*, 2007; Kleipool *et al.*, 2017) but the genetic factors and resulting facies are quite different from those of an IPW (Pomar & Kendall, 2008).

Mixed carbonate–siliciclastic 'hybrid' deposits

For mixed carbonate–siliciclastic systems, the term 'hybrid' is often used in the literature to

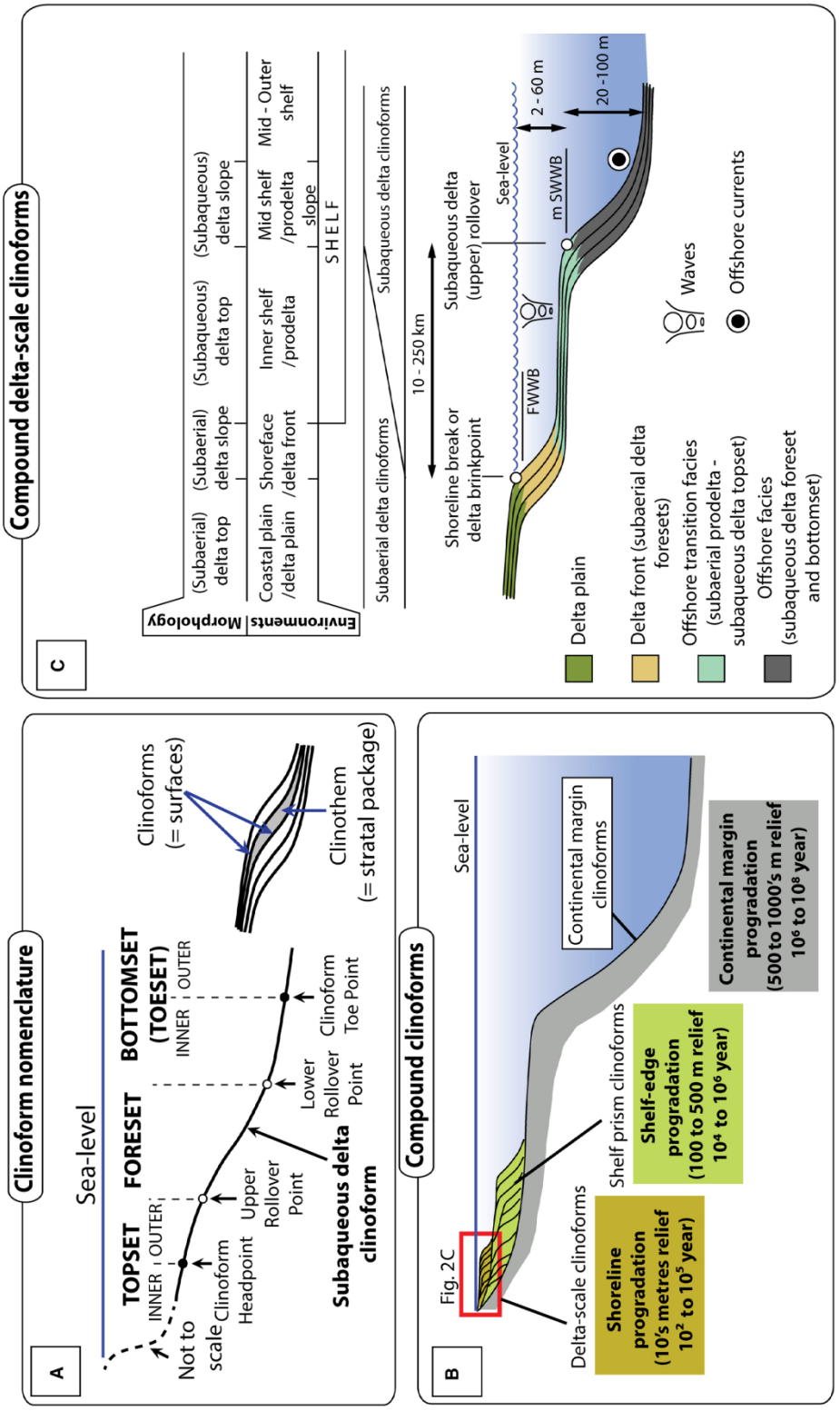

Fig. 2. (A) Terminology for the different parts of a clinoform using a subaqueous delta-scale clinoform (adapted from Patruno *et al.*, 2015). (B) A compound system with subaqueous delta-scale, shelf prism and continental margin clinoforms. The range of relief and progradation rates is indicated in insets (adapted from Patruno *et al.*, 2015). (C) Compound delta-scale clinoform system with either shoreline or subaerial delta-scale, and subaqueous delta-scale clinoforms (adapted from Patruno *et al.*, 2015): m SWWB, mean storm weather wave base; FWWB, fair weather wave base.

quickly convey the mixed character of sediments with fractions of both carbonate and siliciclastic components (Mount, 1984; Flügel, 2004; Tomassetti & Brandano, 2013; Nalin *et al.*, 2016; Zecchin & Catuneanu, 2017). Nalin *et al.* (2016) used this term for mixed deposits with a siliciclastic fraction, in particular, between 20% and 50%.

Synthem

A synthem is an unconformity-bounded unit (Ruban, 2015). In this study, the term refers to the units bounded by the local high rank unconformities.

'Pristine' preservation

This study uses the term 'pristine' as a shortcut to refer to bioclasts that barely display any signs of biostratinomic alteration. These bioclasts are articulated and complete, with well-preserved ornamental features, and have not been subject to macrobioerosion and/or encrustation by epizoan organisms.

GEOLOGICAL SETTING

The Águilas Arc (south-east Spain) (Fig. 3A), which belongs to the Inner Zones of the Betic Cordillera, is a tectonic megastructure that extends onshore over a distance of 60 km along a south-west/north-east axis. The megastructure resulted from a north–south or north-west/south-east rigid-plastic indentation of a crustal block that began in the Early Miocene due to collision of the African and Eurasian plates in the Western Mediterranean and is still active today (Coppier *et al.*, 1989; Griveaud *et al.*, 1990). This arc is delimited to the south-west and north-east by systems of left-lateral and right-lateral strike slip faults (Palomares, Cocón-Terreros and Moreras fault systems) (Coppier *et al.*, 1989; Silva *et al.*, 1993). The internal sector of this arc comprises five small basins that are open to the Mediterranean (Bardají *et al.*, 1999); their opening was probably caused by an important collapse of the southern margin of the arc, associated with transtension (Coppier *et al.*, 1989). These basins probably acted as rias (i.e. estuaries encased in high-relief fluvial valleys) and then as coastal embayments during the early Pliocene (Dabrio *et al.*, 1991; García-Ramos *et al.*, 2014). This study focuses on the southwestern sector of the Águilas Basin (Fig. 3B and C), located some 5 km south-west of the town of Águilas, where the succession of Pliocene marine sediments is most complete (Montenat *et al.*, 1978).

STRATIGRAPHIC FRAMEWORK

Pliocene deposits in the current study area can be attributed to three synthems: SP0 (MPl1–MPl2 *pro parte* biozones), SP1 (MPl3 biozone) and SP2 (possibly MPl4) (Fig. 3D). The focus here is on the prograding succession of synthem SP1. The topmost part of SP1 consists of carbonates of an isolated platform abutting a volcanic ledge, that is an entirely different morpho-sedimentary system and therefore beyond the scope of this study (Fig. 3C and D). To provide a stratigraphic framework, SP0, SP1 and SP2 are briefly outlined.

The SP0 synthem is represented by glaucony-rich condensed deposits. At the 14 m thick El Barcelón section (Fig. 3C), beds are oriented N79°E/8°SE. A sharp transgression over metamorphic rocks of the Palomas Unit (Alpujárride Complex, Inner Betic Zones) (Álvarez & Aldaya, 1985) is recorded at the base. Planktonic foraminifera from SP0 indicate the MPl1 and MPl2 biozones of the Mediterranean Pliocene (Montenat *et al.*, 1978; García-Ramos *et al.*, 2012). Based on benthic and planktonic foraminifera, García-Ramos *et al.* (2014) proposed a shallowing upward trend evolving up-section to assemblages of shallow-water benthic foraminifera, devoid of planktonic foraminifera. In this section, the top of SP0 is truncated and overlain by Quaternary conglomerates, and the transition from SP0 to SP1 is not exposed. An angular, erosive unconformity is inferred because of the different strike and dip of the two synthems and a conspicuous shift in benthic and planktonic foraminiferal assemblages from shallow-water to a relatively deep-water, offshore environment between the top of SP0 and the base of SP1. This unconformity crops out in a section north-east of Castillo de Terreros (Montenat *et al.*, 1978) (Fig. S1).

Synthem SP1 consists of a succession of clinobedded units that prograded over a distance of about 2 km starting from the hillock of Cabezo Alto across the area of Cañada Brusca and the Cuatro Calas coves (Fig. 3D). In SP1, clinoforms have a strike of N57°E with a variable dip (a few degrees to over 14°SE) along a north-

west/south-east transect. The unconformity between SP1 and SP2 eroded part of the upper interval of SP1, which is either missing on the surface or covered by colluvial deposits. The uppermost part of SP1 crops out again, however, in the Cuatro Calas coves sector (Fig. 3C); there, the top of SP1 is also truncated and overlain by Quaternary conglomerates. The SP2 synthem was described and interpreted as a wave-dominated Gilbert-type delta system (Dabrio *et al.*, 1991): SP2 is also truncated at the top by an unconformity and covered by Quaternary marine and terrestrial units, one of which has been dated to the oxygen isotopic stage 5e based on the occurrence of the gastropod *Persististrombus latus* (Bardají *et al.*, 2001).

Biostratigraphy

The co-occurrence of *Globorotalia puncticulata* and *G. margaritae* from the base to the top of the synthem SP1 (Fig. 3D) indicates that it was deposited entirely during the MPl3 planktonic foraminiferal biozone of the Mediterranean Pliocene (4·52 to 3·81 Myr) (Iaccarino *et al.*, 2007; Violanti, 2012; Corbí & Soria, 2016). Because of truncation at the base and the top of the synthem, the exact duration of SP1 is uncertain, but must be <700 kyr.

MATERIAL AND METHODS

Fluvial incision has revealed laterally continuous outcrops oriented subparallel and subperpendicular to the depositional strike that enabled the stratal geometries and stacking patterns to be studied. Clinoforms and clinothems were mapped using outcrop panoramic photomosaics while stratigraphic contacts and facies were checked in the field. Two main sections (Figs 3C, 3D and 4), 44 m thick (Cabezo Alto) and 77 m thick (Cañada Blanca), were logged in detail, for lithology, sedimentary structures, macrofossil composition, biofabrics and ichnoassemblages to evaluate the vertical variation and stacking of facies. These sections were complemented by smaller sections to show details of stratigraphic features. The macrofauna was identified to species level whenever possible, except for most bryozoans, for which only the zooarial morphology was noted. The abundance of macrofaunal taxa was estimated in the field by distinguishing between dominant (26 to 100%), common (11 to 25%) and rare (1 to 10%) categories. This qualitative approach was conducted by visually inspecting each sampling site for 30 min (cf. time-picking of Ceregato *et al.*, 2007). Skeletal concentrations were described using qualitative criteria (Kidwell *et al.*, 1986), while biofabrics follow the semi-quantitative charts of Kidwell & Holland (1991). Macroscopic descriptions of lithofacies were complemented with representative thin sections. Some bulk samples of uncemented sediment were sieved through 500 μm, 125 μm and 63 μm meshes to explore qualitatively the content of benthic and planktonic foraminifera in the 125 μm fraction, to aid in a palaeoenvironmental interpretation and biostratigraphic characterization of the studied synthem. For 26 samples of the Cabezo Alto section, >200 benthic foraminifera were identified and counted. Taxa with >3% proportional abundance are reported.

Magnetic susceptibility, a proxy of terrigenous input (Davies *et al.*, 2013), was measured in the field, with a SM-20 magnetic susceptibility meter (Gf Instruments, Brno-Medlénky, Czechia) for the Cabezo Alto (34 sampling sites) and Cañada Blanca (68 sampling sites) sections. Five to six replicate measurements per sampling site (*ca* 1 sec measuring time) were taken on flat rock surfaces, and the mean value reported.

Carbonate content was quantified at the Institute of Geography and Regional Research (University of Vienna) with a Scheibler calcimeter for 34 samples in the Cabezo Alto section and 48 samples at the Cañada Blanca section. The procedure specified in ISO 10693:1995 has been followed (ÖNORM L 1084, 2006).

Glauconite maturity has been categorized into four stages, based on the K_2O content (Amorosi

Fig. 3. Location of the study area in south-east Spain. (A) Tectonic Águilas Arc (modified from Bardají *et al.*, 2001). (B) Detail of the Águilas Basin with indication of outcrops of Pliocene age. (C) Cartographic sketch of the studied sector in the Cañada Brusca area, including Pliocene synthems (SP0, SP1 and SP2), the main facies associations in SP1 (FA1 to FA4), and location of the studied sections or those mentioned in the text. (D) Schematic cross-section of the studied sector to show the relationship of the identified Pliocene synthems, with indication of the studied sections (CA, Cabezo Alto; CBr W, Cañada Brusca W; CBL, Cañada Blanca). Biostratigraphically relevant planktonic foraminiferan taxa indicate the MPl3 biozone (Zanclean) for the whole synthem SP1. Vertical scale exaggerated.

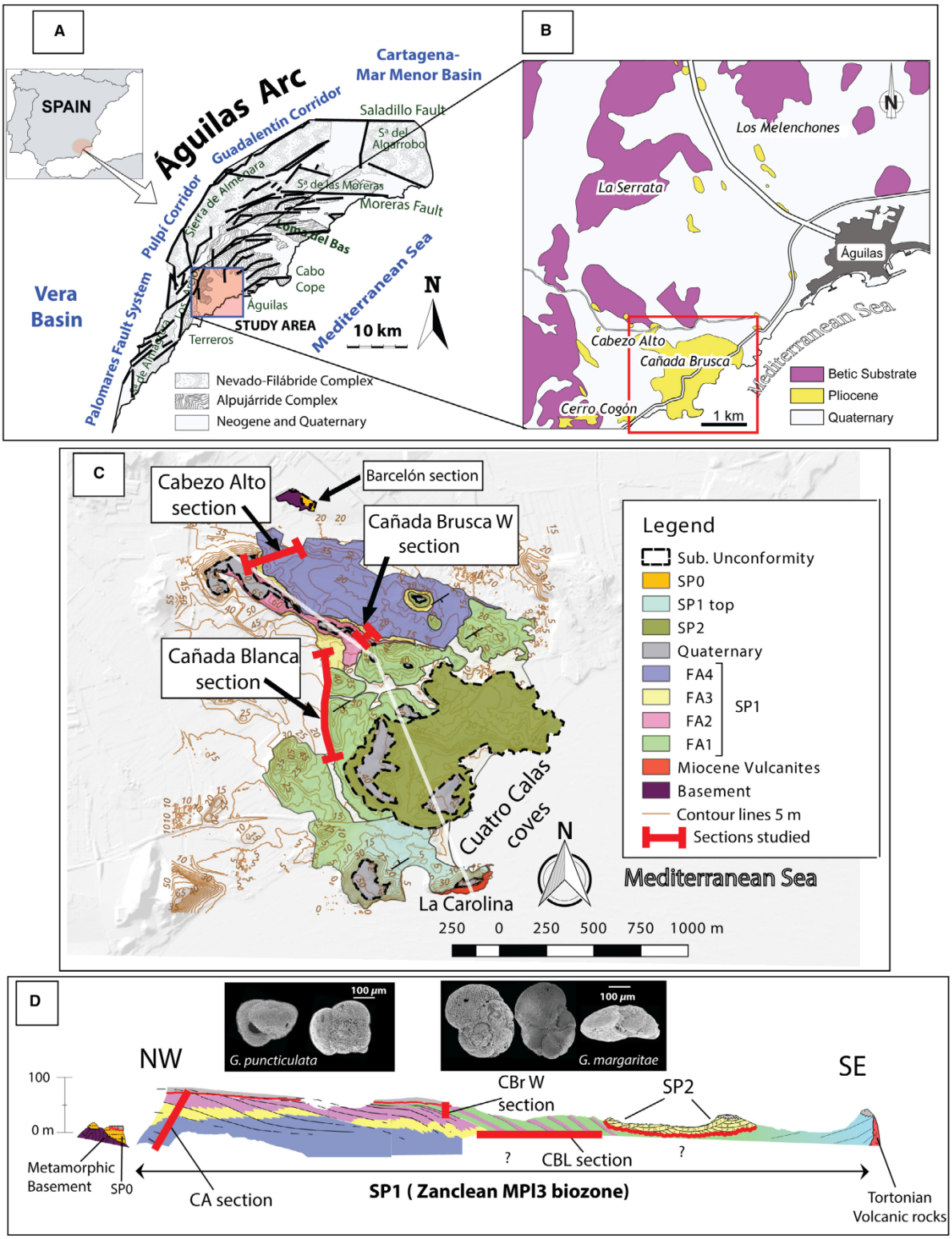

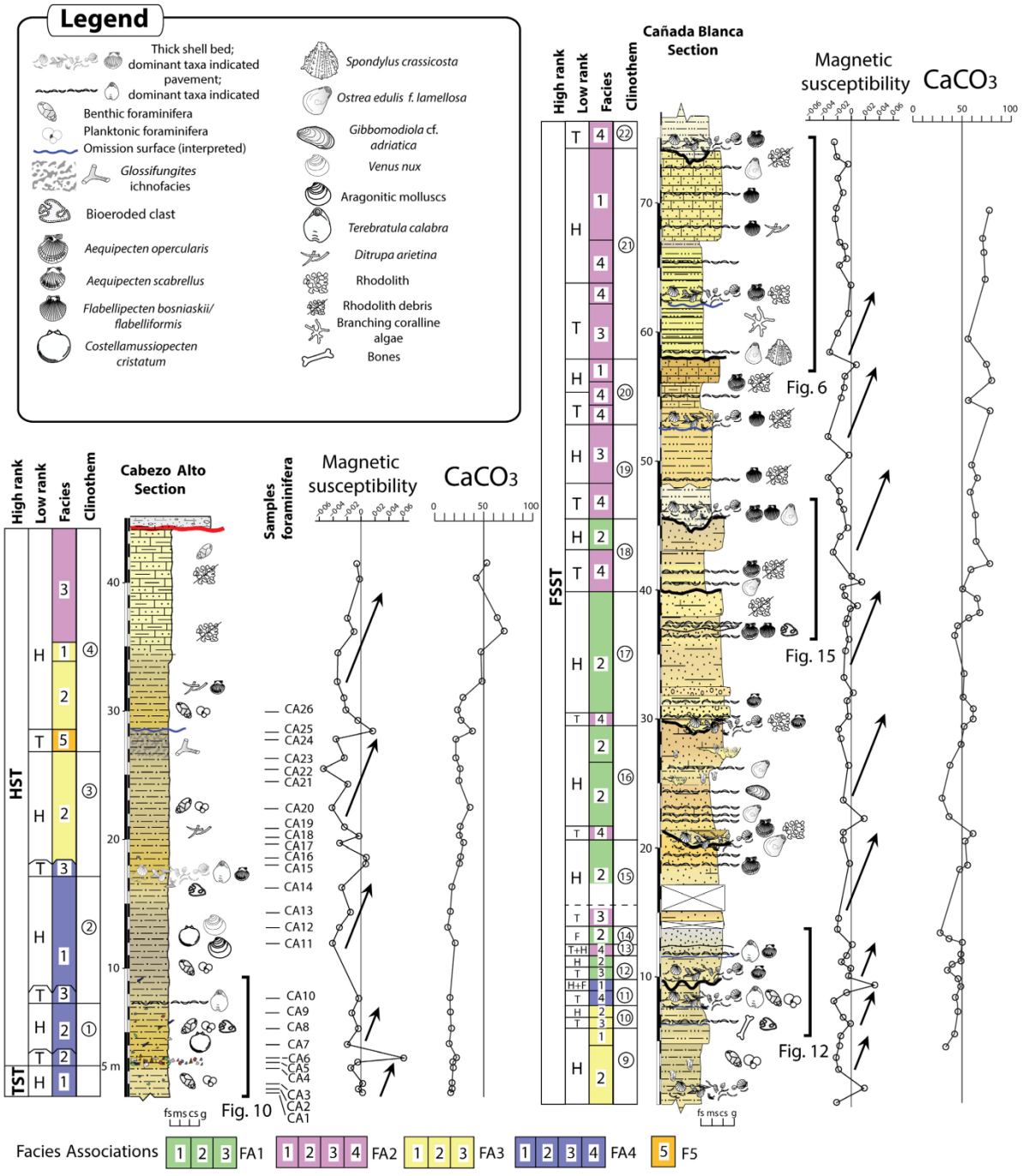

Fig. 4. Stratigraphic logs of the CA (clinothems 1 to 4) and CBL (clinothems 9 to 22) sections. The interpreted systems tracts of the high rank and low rank cycles are included, the latter with abbreviated letter codes; T (transgressive), H (highstand), F (falling stage) and L (lowstand). Numbers indicate the facies types of four facies associations (FA), the latter noted by colour code. The position of benthic foraminifera samples from the CA section is indicated. Skeletal concentrations were simplified to pavements and thick shell beds (dominant taxa indicated by the corresponding icon in the legend). Magnetic susceptibility and carbonate content trends are included. Possible cyclicity indicated by arrows. For a magnified zoom view of the interval including clinothems 9 to 14, see Fig. 12. TST or T, transgressive systems tract; FSST or F, falling stage systems tract; HST or H, highstand systems tract.

et al., 2007; Amorosi, 2012): (i) nascent (K_2O = 2 to 4%); (ii) slightly evolved (K_2O = 4 to 6%); (iii) evolved (K_2O = 6 to 8%); and (iv) highly evolved (K_2O > 8%). Glauconite K_2O content and colour are correlated: nascent to slightly evolved glauconite is light green – yellowish, mature glauconite is dark green. Glauconite composition was examined in one sample to determine its maturity. About 80 to 100 grains were picked from the 125 to 500 μm fraction, embedded in resin and polished on a slide. Glauconite analyses were performed at the Department of Lithospheric Research (University of Vienna) using a Cameca SXFive FE Electron Probe Microanalyzer (EPMA; CAMECA, Gennevilliers Cedex, France) equipped with five wavelength-dispersive and one energy-dispersive spectrometers. Well-characterized homogeneous natural and synthetic minerals were used as standards. All analyses were performed at 15 kV accelerating voltage and 20 nA beam current. Due to the K migration a defocused beam with 5 μm diameter and 10 sec counting time on peak position were used. For matrix corrections, the PAP method (Pouchou & Pichoir, 1991) was applied to all acquired data. The relative error of the laboratory internal standard is below 1%.

DESCRIPTION OF FACIES

Four main facies associations and one facies were recognized in the studied synthem. These are described in detail in Tables 1 to 4. Facies distributions are shown in stratigraphic logs and outcrop photomosaics to highlight vertical and lateral changes. In general, the facies grade into one another along a proximal-distal gradient.

Facies Association 1

The common feature of Facies Association 1 (FA1) is the occurrence of coarse-grained siliciclastics. Three facies are distinguished based on sorting, carbonate matrix and packing of macroinvertebrates.

Coarse-grained friable sandstone – F1.1
This facies was observed in only two clinothems of the Cañada Brusca W area. It consists of friable sandstone composed of well-sorted, coarse, angular grains (mainly of quartz and schists) (Fig. 5A and B). This sandstone is poorly cemented and pervasively bioturbated, therefore no physical sedimentary structures are preserved. In proximal parts it displays an intensely bioturbated ichnofabric dominated by vertically oriented *Macaronichnus* and subsidiary *Ophiomorpha* (Fig. 5A and D to H). It yields abraded and fragmented microfossils in low abundance, including ostracods (for example, *Aurila*) and benthic foraminifera, most notably *Elphidium crispum* and *Ammonia inflata* (Table 1).

Hybrid rhodolithic sandstone – F1.2
This facies mainly occurs in the Cañada Blanca section and the Cañada Brusca W sectors (Fig. 5I and J), in more distal positions than F1.1. It consists of poorly sorted coarse sandstone with a carbonate matrix. Granule-sized debris of coralline red algae is characteristic, albeit in varying proportions. The fabric in general is massive; locally, well-defined trace fossils are identifiable (Table 1).

Shell-rich hybrid sandstone – F1.3
This facies occurs in the Cañada Blanca section (clinothem 12). The matrix resembles that of F1.2 but it is distinguished by thick (>1 m), densely packed skeletal concentrations dominated by pectinids (*Aequipecten scabrellus*). It also displays a complex biofabric, with large gutter casts infilled with pectinids, and overlies an irregular erosive surface.

Interpretation of Facies Association 1
The well-sorted and winnowed texture of the coarse sands, selectively enriched in detrital quartz (Fig. 5B), suggests proximal environments affected by tidal and wave currents above the fair-weather wave base (Blomeier *et al.*, 2013). This interpretation is supported by the lateral facies change, in which beds displaying proximal facies F1.1 evolve distally into poorly-sorted and unwinnowed coarse sandstone facies F1.2 (Fig. 5I and J). The association of *Ophiomorpha* and dominant *Macaronichnus* in similar lithofacies (Fig. 5D to F) has been interpreted as either foreshore or upper shoreface environments (Frébourg *et al.*, 2012; Mayoral *et al.*, 2013; Uchman *et al.*, 2016). This is compatible with the impoverished benthic foraminiferal assemblage, with the poorly preserved shallow shelf species *Elphidium crispum* and *Ammonia inflata* (Sgarrella & Moncharmont Zei, 1993; Fiorini & Vaiani, 2001; Rasmussen, 2005). The low species richness, abundance and high taphonomic alteration of these microfossils can be

interpreted as an indication of onshore transportation (Davaud & Septfontaine, 1995). The dominance of *Flabellipecten bosniaskii* in some patches of facies F1.2 (Table 1) is consistent with proximal sandy environments (Aguirre *et al.*, 1996). The lack of physical sedimentary structures is most probably due to thorough bioturbation and/or cryptobioturbation (Pemberton *et al.*, 2008).

Facies Association 2

The main characteristic of Facies Association 2 (FA2) is the fine-grained carbonate-rich matrix ($CaCO_3$ *ca* 40 to 80%) (Fig. 4) and the frequent presence of coralline algae, either in the form of complete rhodoliths or rhodolith debris.

Calcarenite – F2.1
In contrast to other facies, this was found only in the upper two clinothems (Fig. 6A and B). The coarse-grained, well-sorted fabric is similar to F1.1 but is composed of carbonate lithoclasts. Small casts, probably of comminuted aragonitic shells, are visible. This facies is locally crudely stratified and can contain pavements of *Flabellipecten* and *Ostrea* (Table 2; Fig. 6). It has variable proportions of rhodolith debris and is pervasively bioturbated, with poorly defined trace fossils, except for intervals with well-defined *Thalassinoides* (Fig. 6B).

Hybrid rhodolithic calcirudite – F2.2
This facies only occurs locally, associated with F2.3. It consists of calcirudite mostly composed of rhodolithic debris and pectinids. It is often found infilling pods (like the ray pit trace *Piscichnus waitemata*). In clinothem 8, it forms a wedge, laterally interdigitating with facies F3.1.

Hybrid rhodolithic floatstone – F2.3
This facies is characteristic of the whole study area. The matrix consists of fine-grained siliciclastic material and micrite in variable proportions (up to 80% carbonate content). The dominant bioclastic material is rhodolith debris, which varies from coarse-grained to gravel size, but complete rhodoliths also occur and one locality exhibits pavements (Fig. 7). It is pervasively bioturbated with variable ichnoassemblages (Table 2); hence only one example of swaley cross-stratification (SCS) has been identified (Fig. 5K). In clinothem 21, however, it displays a crude stratification, forming tabular beds about 30 to 40 cm thick. The most characteristic macroinvertebrates are *Clypeaster* cf. *aegyptiacus* (often as complete tests), *Spondylus crassicosta* (often articulated), *Ostrea edulis* f. *lamellosa* and *Gigantopecten latissimus* (juveniles and adults). In some samples, coralline algae attributable to lithophylloid and melobesioid taxa were identified (Fig. 7D to F).

Shell-rich hybrid rhodolithic floatstone – F2.4
This is similar to F2.3 but contains densely packed concentrations of pectinids (*Aequipecten opercularis*) and rhodoliths and locally also *Ostrea* and *Spondylus*. This facies usually forms very thick (several metres) beds, often overlying an erosive or irregular surface. Coralline algae are sometimes present as rhodoliths or represented by small proportions of rhodolith debris.

Interpretation of Facies Association 2
The well-sorted, winnowed texture and coarse grain-size of F2.1, together with the dominance of *Flabellipecten* and *Ostrea*, points to high-energy proximal environments (Aguirre *et al.*, 1996; Blomeier *et al.*, 2013). The reduced grain-size of siliciclastics in F2.3 and F2.4 points to lower energy levels compared to FA1. The abundance of rhodoliths (Fig. 7) suggests background low-moderate energy conditions, good oxygenation, low sedimentation rates and low turbidity enabling suitable light penetration; the assemblage of melobesioids and lithophylloids (Fig. 7D to F) suggests depths in the order of several tens of metres (Aguirre *et al.*, 2012, 2017). Moreover, the characteristic macroinvertebrate species in this facies (Table 2; Fig. 5A) are common in shoreface environments (Malatesta, 1974; Ben Moussa, 1994; Mancosu & Nebelsick, 2017).

Swaley cross stratification (Fig. 5K) indicates storm deposition events (e.g. Myrow, 2005) in the offshore transitional zone (Dumas & Arnott, 2006). The occurrence of sporadic densely packed lenticular shell beds (Fig. 5), probably the product of 'cut and fill' structures, also points to major storm events (Zecchin *et al.*, 2017). The ichnoassemblage of F2.3 (*Ophiomorpha nodosa*, *Skolithos linearis* and *Planolites montanus*) (Table 2), combined with the features discussed above, is interpreted here to indicate an opportunistic response associated with storms or other high-energy disturbances (Pemberton *et al.*, 1992; Gani *et al.*, 2009; Buatois *et al.*, 2015), although individual ichnotaxa can occur under normal marine conditions. In the first scenario, *Palaeophycus* can be characteristic

Table 1. Main sedimentological and palaeontological features of Facies Association 1.

Facies	Lithology	Sedimentary structure	Ichnology	Macrofossils and taphonomy	Biofabric	Interpretation
F1.1	Coarse-grained, friable sands; moderately well-sorted; angulose grains, mainly of quartz, subordinately of schists and mica. Slightly cemented by sparite grains. Highly porous	Massive fabric	Intense bioturbation possibly responsible for the massive fabric. Only patches with preserved burrows of *Ophiomorpha* (BI = 3 to 6) associated with subvertically oriented *Macaronichnus* isp. traces. Low ichnodiversity	Strongly dominated by disarticulated, slightly fragmented valves of *Flabellipecten bosniaskii*. Subordinate articulated *Spondylus crassicosta*; fragmented *Ostrea edulis*, scarce rhodoliths, rare *Aequipecten scabrellus*	Barren to dispersed. In more distal parts there might be patches with densely packed *Flabellipecten* valves	Ichnofabrics with *Ophiomorpha* and *F. bosniaskii* indicate an upper shoreface. The *Ophiomorpha–Macaronichnus* ichnofabric, combined with the coarse-grained, well-winnowed sands, has been documented from upper-shoreface to foreshore settings. Microfossils are scarce and poorly preserved. Assemblage dominated by *Elphidium crispum* and *Ammonia inflata*. Subordinate taxa include: *Cibicidoides lobatulus*, *Neoconorbina terquemi*, *Reussella spinulosa* and *Spiroplectamina saggitula*. These taxa are typical of shallow water environments (Rasmussen, 2005)
F1.2	Hybrid grainstone and coarse-grained sand, poorly sorted (siliciclastic grains similar to those of F1.1). Small rhodolith fragments may be abundant. Poorly cemented; porous. This subfacies encompasses transitional types where the grain size of siliciclastic grains and proportion of carbonate matrix vary across a	Massive fabric	Intense bioturbation possibly responsible for the massive fabric. Burrows rarely preserved; attributable to *Ophiomorpha* and *Thalassinoides paradoxicus*. BI = 1 to 3	Occasional small aragonitic molluscs preserved as stein-kerns (shell hash). Macro-fossils scarce: disarticulated, abraded and bioeroded (*Entobia* isp.) shells of the dominant taxa *F. bosniaskii* and *A. scabrellus*. Rare *Pecten jacobaeus*. Complete rhodoliths occur rarely dis-persed in the matrix. The most distal subfacies types contain steinkerns of solitary corals (*Flabellum* sp.). Steinkerns of *Bulla* sp. are rare. Abraded small fragments of *Clypeaster* cf. *aegyptiacus* are common. Rare, nodular, massive zooaria of Celleporarian bryozoans. Tubes of *Ditrupa arietina* locally abundant. Rare *Schizechinus serialis*, *Spatangus*	Dispersed to loosely packed	This facies occurs in the top set, representing the middle shoreface. During forced regression, siliciclastic grains are transported down the foreset, mixing with reworked carbonate mud and bioclasts

Table 1. (continued)

Facies	Lithology	Sedimentary structure	Ichnology	Macrofossils and taphonomy	Biofabric	Interpretation
	proximal–distal gradient			*purpureus, Echinocyamus pusillus, Echinolampas sp. Cosmopolitodus hastalis/Isurus oxyrinchus, Sparus* sp., *Pinna* sp. Large acorn barnacles (*Concavus concavus*) occasionally encrusting echinoids, large bones, or large oysters in clusters of a few individuals		
F1.3	Matrix similar to F1.2 but rich in pectinids	Massive fabric	May contain poorly defined traces attributable to *Thalassinoides* isp	Dominated by disarticulated *Aequipecten scabrellus*, often complete valves. Different degrees of encrustation. Low bioerosion. Additional subsidiary taxa include *Cubitostrea frondosa* and *Spondylus crassicosta*	Densely packed, often infilling small channel-like structures, gutter casts and pods	Concentration of shoreface shells by storm-reworking and winnowing during forced regression. This facies is found only in clinothem 12 at the CBL section

of the fair-weather assemblage (Pemberton *et al.*, 1992). Finally, the rhodolith–pectinid rudstone infilling *Piscichnus* traces suggests trapping in burrows by passive filling when coarser particles are entrained during storm traction–transport (Wanless *et al.*, 1988; Zuschin & Stanton, 2002; Yesares-García & Aguirre, 2004).

The complex biofabric of thick, densely packed skeletal concentrations (facies F2.4) overlying erosive surfaces, together with the observation that they overlie FA1 (Fig. 5C to E) or F2.1 (Fig. 6), suggests that this facies formed under conditions of sediment bypass or starvation, promoting the amalgamation of event beds during transgressive phases (Kidwell, 1991; Abbott, 1997; Dattilo *et al.*, 2008; Zecchin *et al.*, 2017). They are therefore interpreted as onlap shell beds in line with conclusions drawn by Kidwell (1991) and Zecchin *et al.* (2017) elsewhere. The absence of physical sedimentary structures is interpreted here to be a result of thorough bioturbation. According to Zecchin (2007), this trait is typical of sheltered embayments.

Facies Association 3

The characteristic feature of Facies Association 3 (FA3) is the occurrence of the serpulid polychaete *Ditrupa arietina* in a fine-grained hybrid matrix. The carbonate content varies between about 30% and 50% (Fig. 4).

Hybrid packstone with Ditrupa and rhodolith debris – F3.1

Facies F3.1 is transitional between Facies Associations 2 and 3. It consists of hybrid fine-grained packstone to grainstone with small fragments of rhodolith debris. The main feature is the much smaller proportion of rhodolith debris compared to FA2. Locally it contains *Ditrupa*, pectinids or fragments of adeoniform zooaria (*Schizoretepora* sp.). Because of the high carbonate content (*ca* 50% $CaCO_3$), cementation locally defines beds varying from 30 to 40 cm to over 1 m in thickness. The fabric is massive.

Hybrid packstone with Ditrupa – F3.2

This is the most characteristic facies of FA3. *Ditrupa* is the dominant macroinvertebrate, often passively infilling pods (Fig. 8A) or forming loosely to densely packed concentrations. The grain-size of terrigenous particles is fine-grained and poorly sorted. *Macaronichnus – Teichichnus* and other traces are characteristic (Table 3). The bedding is completely disrupted by

Table 2. Main sedimentological and palaeontological features of Facies Association 2.

Facies	Lithology	Sedimentary structure	Ichnology	Macrofossils and taphonomy	Biofabric	Interpretation
F2.1	Coarse-grained calcarenite	Massive to crudely stratified in decimetre thick beds	Dominated by indistinct mottling. Well-defined *Thalassinoides* occur patchily. BI = 4 to 5	Dominated by complete, mostly disarticulated, complete valves in paucispecific beds. Either dominated by *Flabellipecten flabelliformis* or *Ostrea edulis*. Complete, rare *Ova canalifera*, *Clypeaster* cf. *aegyptiacus*, *Hinnites crispus*, and sparse rhodolith debris and/or complete rhodoliths; *Ditrupa* tubes may also occur	Molluscs occur in thin, densely packed pavements; convex-up orientation. Echinoids occur dispersed. The biofabric is otherwise dispersed	High-energy shallow-water environment (upper shoreface). The pavements with convex-up shells are similar to wave/current-winnowed shell bed taphofacies of Hendy *et al.* (2006)
F2.2	Hybrid rhodo lithic calcarenite/ calcirudite	Massive fabric	Discrete traces (BI = **1** to 2). Passively infilled with mud, vertical burrows dominate (*Skolithos* isp., *Ophiomorpha* isp.)	Dominated by small fragments of rhodoliths (rhodolith debris) and disarticulated, complete pectinids. *A. scabrellus*, common. Rare *Gigantopecten latissimus*, *Pecten jacobaeus*, *Gibbomodiola* cf. *adriatica*, *Talochamys multistriata*. Rare steinkerns of gastropods; rare epitoniid gastropods. Locally common *D. arietina*	Loosely packed	This facies occurs in the topset, often passively infilling *Piscichnus waitemata* traces. It also occurs as lenses in the upper portion of the foreset during forced regression, resulting from reworking and differential winnowing of fines under high-energy conditions, probably storms
F2.3	Hybrid rhodolith debris floatstone. Matrix of fine-grained mixed siliciclastic sand (poorly sorted) and carbonate mud	Massive fabric. Rare SCS	Variable intensity of bioturbation. BI = **1** to 5. Normally highly bioturbated. *Piscichnus waitemata* common in the first clinothems. *Thalassinoides* dominates the ichnofabrics in some clinothems. In others, *Ophiomorpha nodosa* and *Planolites montanus* or ?*Asterosoma* isp. cf. *ludwigae* dominate, with subordinate *Palaeophycus tubularis*, *Skolithos linearis*.	Dominated by rhodolith debris to complete rhodoliths. Disarticulated but complete *A. scabrellus* is frequent to abundant. Characteristic taxa are scarce *S. crassicosta* (often articulated); disarticulated, bioeroded *Gigantopecten latissimus*; rare *Calpensia nobilis* bryoliths; large disarticulated, bioeroded *Ostrea edulis*; fragments of *C.* cf. *aegyptiacus* (seldom complete tests). Scarce *P. jacobaeus*, *F. bosniaskii*, *Eucidaris desmoulinsi* (spines and disarticulated	Dispersed to loosely-packed. Except for pods and lenses with densely packed bioclast concentrations. Shell concentrations with a complex internal structure, random orientation of valves, occasionally with a trend to being concordant with the bedding plane, either con-	This facies is typical of the outer topset (lower shoreface). Some samples contain *Elphidium* sp. (thin sections) and *Planorbulina mediterranensis* (encrusting pectinids). A qualitative sample additionally contained *Biasterigerina planorbis*, *Cibicidoides lobatulus*, *Rosalina bradyi*, typical of inner shelf vegetated, sandy detritic bottoms (Sgarrella & Moncharmont Zei, 1993; Rasmussen, 2005). SCS suggests storm events in the

Table 2. (continued)

Facies	Lithology	Sedimentary structure	Ichnology	Macrofossils and taphonomy	Biofabric	Interpretation
			Sporadic *Diplocraterion parallelum*, *Cylindrichnus concentricus*. Some intervals are exclusively dominated by *Thalassinoides* isp.	ambulacral plates), *Schizechinus serialis*, *Spatangus purpureus*, *Arbacina romana*. Large shells are heavily bioeroded (most common traces are *Entobia* isp., subordinately *Caulostrepsis taeniola* and *Maeandropolydora* isp.)	cave-up or convex-up. Frequent examples of stacking and imbrication patterns (concave-up vertical stacking), rounded floating granules and clasts, and pod concentrations. In general, valves complete, disarticulated (except for *Spondylus crassicosta*)	OTZ. The densely packed lens-like skeletal concentrations are interpreted as shelly tempestites
F2.4	Shell-rich hybrid rhodolithic floatstone. Matrix as in F2.3	Massive fabric	Indistinct mottling in massive matrix	Dominated by disarticulated, complete to fragmented molluscs: *Aequipecten*, *Flabellipecten* or *Ostrea* and *Spondylus*; complete rhodoliths occasionally abundant. Additional uncommon to rare taxa may include bone fragments, steinkerns of gastropods, large acorn barnacles, membraniporiform zooaria encrusting shells, massive celleporarian zooaria, *Pecten jacobaeus*, *Gigantopecten latissimus*, vermitid gastropods, *Flabellum* sp., *Cubitostrea frondosa*, *Hyotissa* sp., *Eucidaris desmoulinsi* plates and spines and mostly disarticulated *Terebratula*. Large shells heavily bioeroded (mostly *Entobia* isp.)	Thick beds (up to 2 to 3 m), with densely packed skeletal concentrations with concordant to chaotic orientation	When this facies overlies F2.1 or F1.2 through an erosive surface, it is interpreted as a low rank onlap shell bed formed under low sedimentation rates, and subject to multi-episodic biotic and hydraulic reworking

Table 3. Main sedimentological and palaeontological features of Facies Association 3.

Facies	Lithology	Sedimentary structure	Ichnology	Macrofossils and taphonomy	Biofabric	Interpretation
F3.1	Hybrid packstone/grainstone and medium-sized siliciclastic sand	Massive fabric. Sometimes crudely stratified beds 30 to 50 cm thick	Poorly bioturbated (BI = 1). Indistinct mottling. Occassionally, isolated *O. nodosa* traces	Small rhodolith fragments rather less abundant than in previous facies. Macrofossils scarce to common: fragments of adeoniform bryozoan colonies (*Schizoretepora* sp. and other unidentified taxa), *D. arietina*, *A. scabrellus*, rare *P. jacobaeus*, *C. frondosa*, acorn barnacles	Dispersed to loosely packed	This facies occurs in the upper foreset close to the rollover zone during highstand. A qualitative micropalaeontological sample contained scarce foraminifera, with dominant *Biasteriger*ina *planorbis*, *Elphidium crispum*, *Cibicides refulgens*; subordinate *Dentalina* sp., *Uvigerina bononiensis*, *Hanzawaia boueana*, *Cibicidoides lobatulus*; very rare planktonics: *Globorotalia puncticulata*, *Globigerinoides obliquus*, *Globigerina bulloides*. The foraminiferal assemblage is typical of shallow shelf environments. *Uvigerina* and *Hanzawaia* indicate deeper settings, and organic-rich muddy substrates (Rasmussen, 2005). This facies is transitional to F2.3 proximally and F3.2 distally
F3.2	Hybrid packstone–fine-grained sand	Massive fabric	Proximal–distal gradient with bioturbation intensity and ichnodiversity increasing distally. Poximal (BI = 1): barren or rare isolated *O. nodosa*. Middle (BI = 1 to 3) *Macaronichnus segregatis – Palaeophycus heberti*, with subordinate *O. nodosa*, *Planolites montanus*, rare	Most characteristic in the oldest clinothems: *D. arietina*, often infilling pods. In distal sites a diverse calcitic assemblage can include complete, mainly disarticulated tests/valves, sometimes encrusted by bryozoans, cirripedes or serpulids, good preservation of ornamental details: *A. scabrellus*, *T. multistriata*, *Hinnites crispus*, *Flexopecten flexuosus*,	Loosely packed within clinothem, except for pod concentrations, often of *Ditrupa*	High sedimentation rates due to frequent siltation events and storm induced high-density gravity flows, in the foreset. Episodically organic rich substrates trigger opportunistic responses from taxa like *Ditrupa arietina*, and benthic foraminifera like *Cassidulina carinata*, *Bolivina* spp., *Bulimina aculeata*, *Globocassidulina subglobosa*. Decreased level of siltation distally favour more densely bioturbated ichnofabrics

Table 3. (continued)

Facies	Lithology	Sedimentary structure	Ichnology	Macrofossils and taphonomy	Biofabric	Interpretation
			Cylindrichnus concentricus, *Palaeophycus tubularis*. Distal (BI = 5 to 6): complex tiering, dominated by indistinct mottling. Discrete burrows dominated by *M. segregatis*, subordinately by *Teichichnus rectus* and unidentified, meniscate, back filled traces (?*Scolicia* isp.). Occasional traces: *C. concentricus*, *Diplocraterion* isp., *Scalichnus* isp. cf. *sursumdeorsum*, and rare isolated tubes of *Schaubcylindrichnus coronus*	*Limaria tuberculata*, *Gibbomodiola* cf. *adriatica*, *Pinna* sp., *Anomia ephippium*, *Cubitostrea frondosa*, *Scalina bronni*, *Epitonium* cf. *turtoni*, *Epitonium frondiculoides*, *Epitonium clathrus*, *Cirsotrema lamellosa*, *Cirsotrema pumiceum*, *Stenorhytis retusa*, *Concavus concavus*, *Solidobdanus mylensis*, *A. opercularis*, *Costellamussiopecten cristatum*, *Neopycnodonte cochlear*, *A. romana*, *S. seriatis*, *Ova canalifera*, ambulacral plates and spines of *E. desmoulinsi*. In shell beds, there are casts of infaunal bivalves: venerids, cardids, nuculanids; rare *Nototeredo* sp. (*Teredolites* isp.). Some of the above and the following probably transported from shallower settings: small, abraded fragments of *Clypeaster* sp., *P. jacobaeus*, celleporarian and vinculariiform bryozoan colonies, *Calpensia nobilis* bryoliths, *F. bosniaskii*, *G. latissimus*		

Table 3. (continued)

Facies	Lithology	Sedimentary structure	Ichnology	Macrofossils and taphonomy	Biofabric	Interpretation
F3.3	Shell-rich hybrid packstone	Massive fabric	No traces identified	Dominated by disarticulated, complete and well-preserved valves of *A. scabrellus*, fragments of adeoniform zooaria (*Schizoretepora* sp.), or disarticulated valves of *Gibbomodiola* cf. *adriatica*; other aragonitic bivalves are subsidiary	Skeletal concentrations can form (matrix-supported, densely packed *Aequipecten scabrellus*; clast-supported densely packed *Gibbomodiola* cf. *adriatica, Pinna* sp. and other aragonitic bivalves), and loosely to densely packed fragments of adeoniform zooaria (*Schizoretepora* sp.). Nesting and stacking patterns are frequent (concave-up vertical stacking). The *Gibbomodiola* bed thickens distally (*ca* 2 m thick) without erosive surface at the base or at the top	Typical of foreset settings. Assemblages dominated by suspension feeders interpreted to reflect a decrease in sedimentation rates. In proximal settings of this facies, densely packed biofabric and erosive surface may reflect differential winnowing and reworking by storm-induced currents

Table 4. Main sedimentological and palaeontological features of Facies Association 4 and Facies 5.

Facies	Lithology	Sedimentary structure	Ichnology	Macrofossils and taphonomy	Biofabric	Interpretation
F4.1	Hybrid packstone –fine-grained sand	Massive fabric	Variable intensity of bioturbation (BI = 1 to 5). Dominance of lined bur rows: *Cylindrichnus concentricus*, *Ophiomorpha nodosa* (burrows with a diameter about 3 cm), less frequent *Schaubcylindrichnus coronus*, *Skolithos linearis*, *Palaeophycus tubularis*. Also *Planolites* isp., *Trichichnus linearis* and unidentified meniscate traces (?*Scolicia* isp.) in some clinothems	Paucispecific assemblage dominated by complete, disarticulated valves of *Costellamussiopecten cristatum*. Aragonitic molluscs (*Venux nux*, *Ficus* sp.) or solitary corals are dissolved but are preserved as steinkerns. Macroscopic benthic foraminifera are frequent: *Pyramidulina raphanistrum* and keeled *Lenticulina* spp. (*L. calcar*, *L. cultrata*, *L. iota*)	Packing is barren to dispersed	In general, lower sedimentation rates than in foreset facies. Dominance of dwelling burrows point to background stable conditions with occasional high-density gravity flows that deliver outsized floating clasts and allochthonous shells from proximal environments. These events can trigger the response of deposit feeders (*Planolites* isp., ?*Scolicia* isp.)
F4.2	Paraconglomerate of floating metamorphic and bioclasts. Hybrid packstone–fine-grained sand matrix	Massive fabric	Numerous ferriginized subvertical traces and indistinct mottling. Also a similar assemblage as in F4.1	Most macrofossils are disarticulated. Mixture of complete, pristine shells and fragmented, bioeroded and encrusted ones. Characteristic and frequent macroinvertebrate taxa are: *Costellamussiopecten cristatum*, *Venus nux*, *Aequipecten opercularis*, *Flabellipecten bosniaskii* and *Cubitostrea frondosa*. The latter three are interpreted as transported from shallower settings and bear frequent encrustation by *Planorbulina mediterranensis*, *Cibicidoides lobatulus* and bryozoans. Also often bioeroded by clionaid sponges (*Entobia* isp.). Less frequent to rare taxa include: fish vertebrae, shark teeth (*Cosmopolitodus hastalis – Isurus oxyrhinchus*), crustacean dactylopodes, epitoniid gastropods (*Cirsotrema lamellosa*, *Stenorhytis retusa*, *Epitonium pseudoscalare*), bivalves (*Flex opecten flexuosus*, *Flexopecten*	Dispersing upward packing pattern, matrix-supported densely packed at the base of the paraconglomerate, to dispersed packing at the top	High rank backlap clast bed (maximum flooding zone). Similar to model III of Kidwell (1985). The bioclasts of species that occur characteristically in FA1 and FA2 are interpreted as allochthonous. These can include highly altered or well-preserved shells, as a result of being entrained in cohesive debris flows

Table 4. (continued)

Facies	Lithology	Sedimentary structure	Ichnology	Macrofossils and taphonomy	Biofabric	Interpretation
				glaber, *Talochlamys multistriata*, *Mimachlamys angelonii*, *Pseudamussium clavatum*, *Pecten jacobaeus*, *Limaria tuberculata*, *Neopycnodonte cochlear*), gastropods (*Aporrhais* sp. cf. *uttingeriana*, *Antisabia* sp.), echinoids (ambulacral plates and spines of *Eucidaris desmoulinsi* and other cidarids; fragments of *Ova candlifera*). Rare solitary corals (*Flabellum* sp.)		
F4.3	*Terebratula* pavements. Hybrid packstone – fine-grained sand matrix	Massive fabric	Indistinct mottling	Brachiopods occur in discrete levels about 10 to 20 cm thick, almost monospecific (mostly *Terebratula calabra*, and sometimes rare *Aphelesia bipartita*). More than 50% of specimens are articulated, complete, with well-preserved ornamental details. Barely microbioeroded or bioeroded (*Podichnus obliquus*). Rarely encrusted (*Concavus concavus*, and *Monia patelliformis*)	The terebratulid pavements dis play variable density of individuals possibly according to a proximal distal gradient, varying from loose to densely packed in the toesets. Clusters of two to four specimens are common	Low background sedimentation rates associated with pulses of relative sea rise facilitate development of terebratulid palaeocommu nities. These pavements are interpreted as mixed depos its (within habitat time-averaged and census assem blages extirpated by siltation)
F4.4	*Terebratula* biostrome. Hybrid packstone – fine-grained sand matrix	Massive fabric	*Glossifungites* ichnofacies dominated by *Thalassinoides suevicus*, with rare *Taenidium barretti* and *Skolithos linearis*. Also lined burrows (*Skolithos* isp. or *Ophiomorpha* isp.). The '*Terebratula* biostrome' contains a diversity of bioerosion traces with high dominance of *Entobia* isp., and less frequent *Podichnus obliquus*,	The '*Terebratula* biostrome' yields additional species of brachiopods but are rare (*Megerlia truncata*, *Megathiris detruncata*, *Terebratulina retusa* and *Aphelesia bipartita*, *Maltaia moysae*) or common (*Novocrania anomala* encrusting *Terebratula* shells). Mixture of pristine and altered shells (disarticulated, fragmented, abraded, encrusted and bioeroded). *Monia* spp. are very abundant, dominating *Monia squamma*, are always	The '*Terebratula* biostrome' dis plays variable and complex biofabrics: Packing is loose to dense. It records pod concentrations, imbrications and concave-up vertical stacking, gutter casts, and	The '*Terebratula* biostrome' indicates more sustained conditions of low sedimentation rates in time, with *Glossifungites* ichnofacies, higher diversity of bioerosion traces and brachiopods, and amalgamation of high-density gravity flows reworking and resediment-ing shells. Increased diversity of suspension feeder

Table 4. (continued)

Facies	Lithology	Sedimentary structure	Ichnology	Macrofossils and taphonomy	Biofabric	Interpretation
			Gnathichnus pentax, *Centrichnus* isp., *Renichnus arcuatus*, *Caulostrepsis taeniola*, *Anellusichnus circularis* and *Oichnus simplex*	associated with the 'Terebratula biostrome', found to live encrusting terebratulids. Occurrence of taxa interpreted as transported, most notably *Spondylus crassicosta* and worn out fragments of *Clypeaster*. Diverse and common membraniporiform zooaria	clumps of pristine specimens	epizoans due to taphonomic feedback
F5	Cemented burrowed hybrid packstone	Massive fabric	Dominated by dense networks of unlined burrows, mostly *Thalassinoides suevicus*. (BI = 6)	Except for the *Terebratula* biostrome, macrofossils are not abundant. It can include pectinids and echinoids (*Ova canalifera*). The sediment infilling the burrows is similar in composition to the encasing matrix	Barren to loosely packed	Formation of stiffgrounds due to sea-floor cementation during low sedimentation rates It develops either at the toesets–bottomsets or at the foresets

bioturbation and the fabric is massive. This facies is rich in benthic (Fig. 9) and planktonic foraminifera.

Shell-rich hybrid packstone – F3.3

The matrix, which is similar to F3.1 or F3.2, contains densely packed concentrations of macroinvertebrates, either fragments of adeoniform zooaria, pectinids (*A. scabrellus*), or the mytilid *Gibbomodiola* cf. *adriatica* (Fig. 8B). Pectinids most often occur as disarticulated, but complete valves, preserving the ornamental details. Erosive surfaces were observed only in the proximally positioned localities (*Gibbomodiola* and *Schizoretepora* beds). Well-preserved acorn barnacles (*Solidobalanus mylensis*), sometimes preserving scutal and tergal plates inside the corona, form clusters on *Aequipecten*.

Interpretation of Facies Association 3

This facies association is dominated by *D. arietina*, a short-lived, free-living suspension-feeder and opportunist that can attain high densities in fine sands and muddy substrates under high sedimentation rates, high turbidity and unstable conditions (Grémare *et al.*, 1998; Sanfilippo, 1999; Ceregato *et al.*, 2007; Scarponi *et al.*, 2014). The interpreted opportunistic behaviour agrees with its high dominance (Ceregato *et al.*, 2007), as in Pliocene outcrops in the Águilas and the neighboring Cope Basins (Martinell *et al.*, 2012). A review on its ecology by Hartley (2014) emphasizes two explanations for the high densities reported in modern environments, both associated with disturbances: (i) disruption of established benthic communities, enabling successful recruitment of high numbers of *Ditrupa* larvae; and (ii) post-settlement redistribution by storms and concentration in areas of deposition. It is therefore probable that the paucispecific fossil assemblages dominated by *Ditrupa* concentrations in FA3 are associated with the action of storms or internal waves, either by redeposition, by opportunistic responses to storm-induced siltation producing organic-rich substrates, or both (Ceregato *et al.*, 2007; Hartley, 2014). The abundance of the benthic foraminifera *Cassidulina carinata*, *Bolivina* spp., *Bulimina aculeata* and *Globocassidulina subglobosa* (Fig. 9) is consistent with the organic enrichment associated with siltation (Jorissen *et al.*, 2007; Abu-Zied *et al.*, 2008; Goineau *et al.*, 2012; Pérez-Asensio *et al.*, 2017). Ichnoassemblages support the interpretation of high sedimentation rates and nutrient contents,

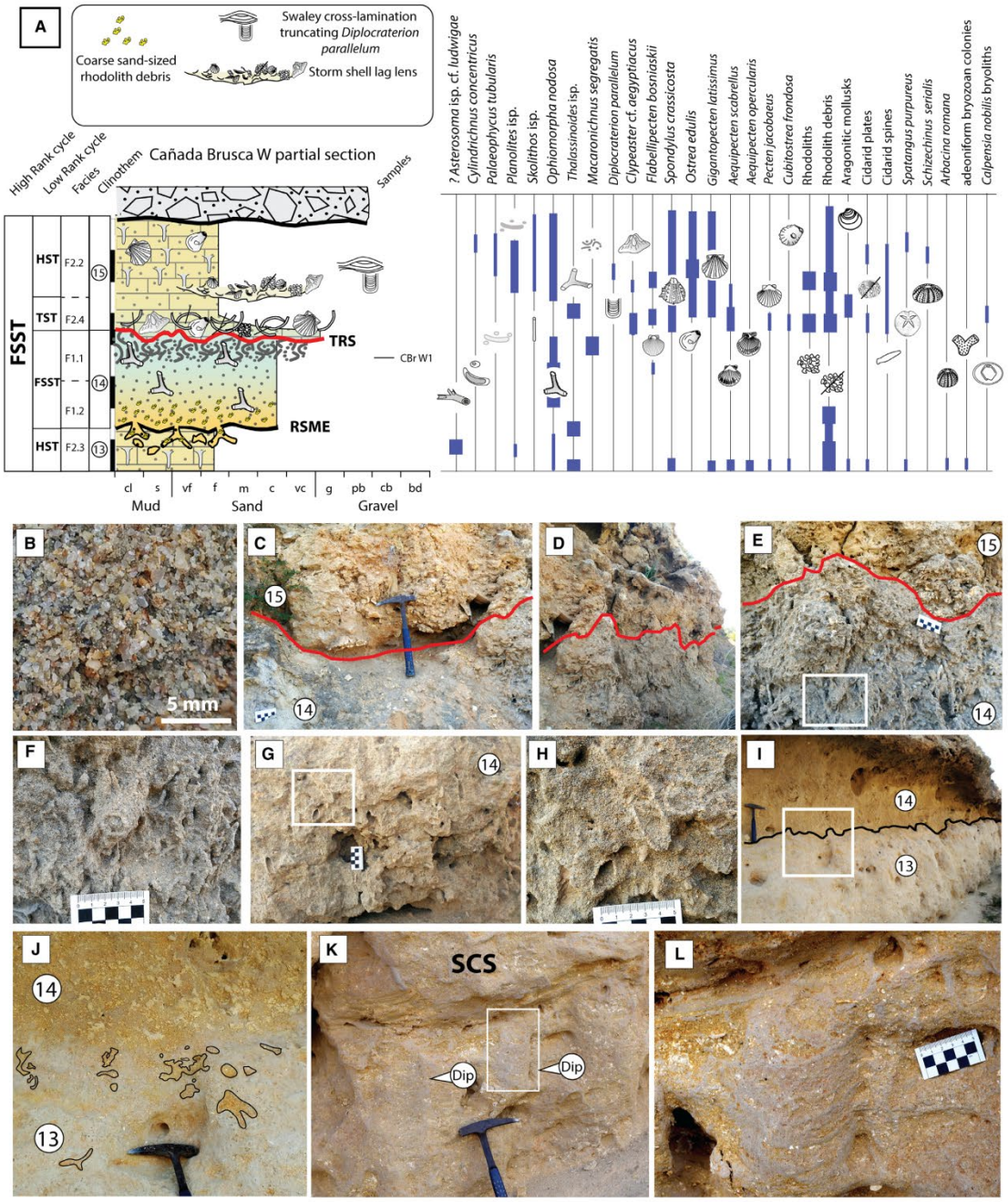

Fig. 5. Stratigraphic motif of low rank cycles from the CBr W sector. (A) Partial stratigraphic log with interpreted systems tracts (both high rank and low rank sequences), facies, clinothems and semi-quantitative abundance of traces and macrofossils. (B) Well-sorted, winnowed, coarse sandstone (F1.1) (clinothem 14). (C) to (E) Contact between clinothems 14 and 15 (red line), interpreted as a low rank transgressive ravinement surface (TRS). The shell bed overlying the TRS (facies F2.4) is interpreted as a low rank onlap shell bed (OSB). (E) Densely bioturbated *Macaronichnus* ichnofabric (clinothem 14). (F) *Ophiomorpha* burrow corresponding to the inset in (E). (G) to (H) *Ophiomorpha* ichnofabric (clinothem 14), *ca* 20 m basinward from the location shown in (C) to (F). (I) Irregular contact between clinothems 13 (facies F2.3) and 14 (black bold line), interpreted as a regressive surface of marine erosion. Hammer for scale is 33 cm long. (J) Detail from inset in (I), showing *Thalassinoides* burrows (*Glossifungites* ichnofacies) passively infilled with material from the base of clinothem 14 (facies 1.2). (K) Swaley-cross stratification (SCS) in facies F2.3, truncating two examples of *Diplocraterion parallelum*. (L) Detail of *D. parallelum* from inset in (K).

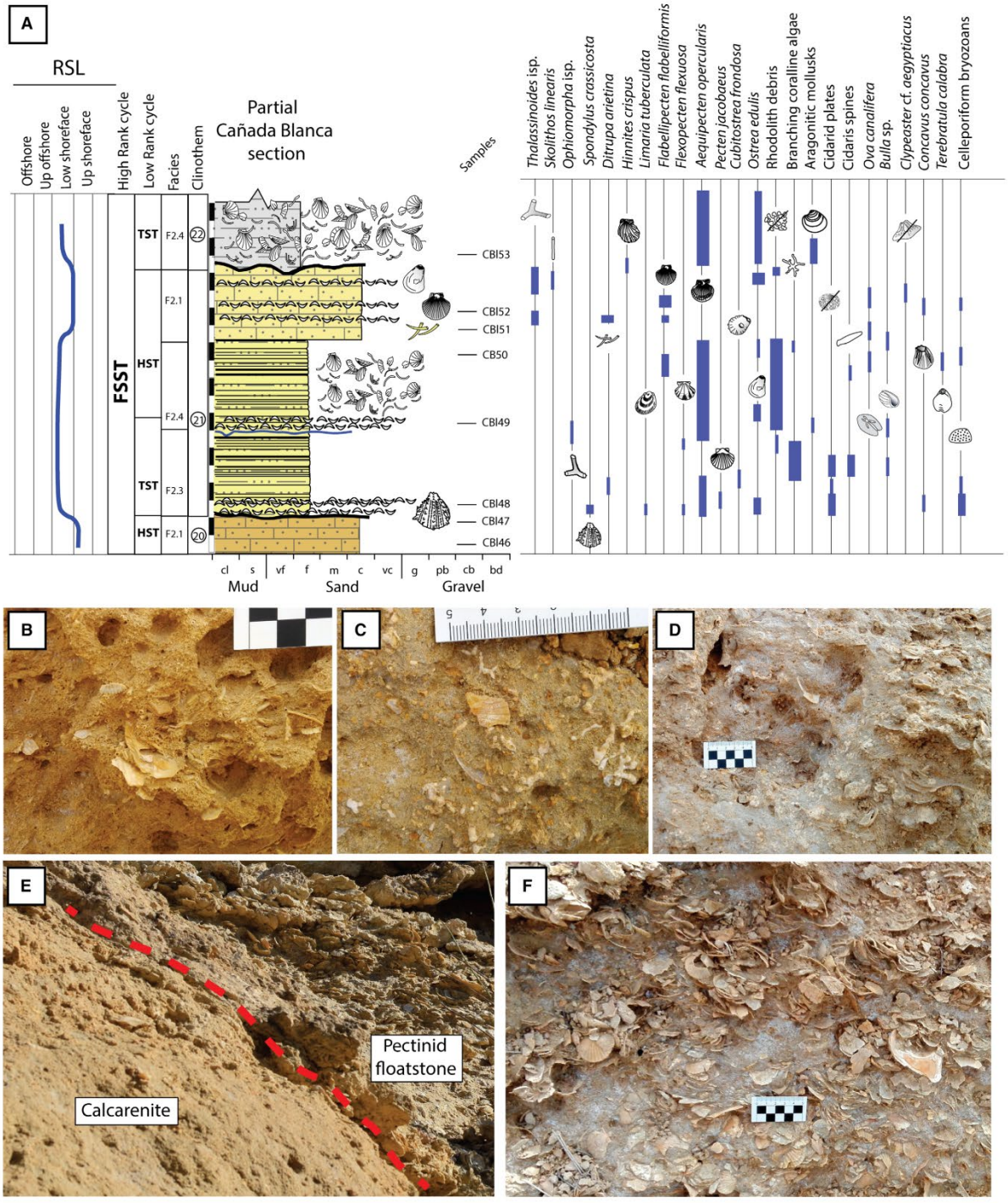

Fig. 6. Partial stratigraphic log of the Cañada Blanca section for clinothems 20 to 22. (A) Example of low rank sequence (clinothem 21). (B) Calcarenite (F2.1) with fragmented molluscs and tubes of *Ditrupa* (top of clinothem 21). (C) Hybrid coralline algal floatstone (F2.3) with branched coralline algae embedded in a fine-grained matrix (lower interval of clinothem 21). (D) Shell-rich rhodolithic floatstone (F2.4) with densely packed pectinids, rhodoliths and subsidiary oysters (middle of clinothem 21), interpreted as a low rank backlap shell bed. (E) Contact (red dashed line) between the calcarenite (top of clinothem 21) and the pectinid floatstone (F2.4) (base of clinothem 22), interpreted as a low rank onlap shell bed. (F) Detail of the pectinid floatstone of clinothem 22.

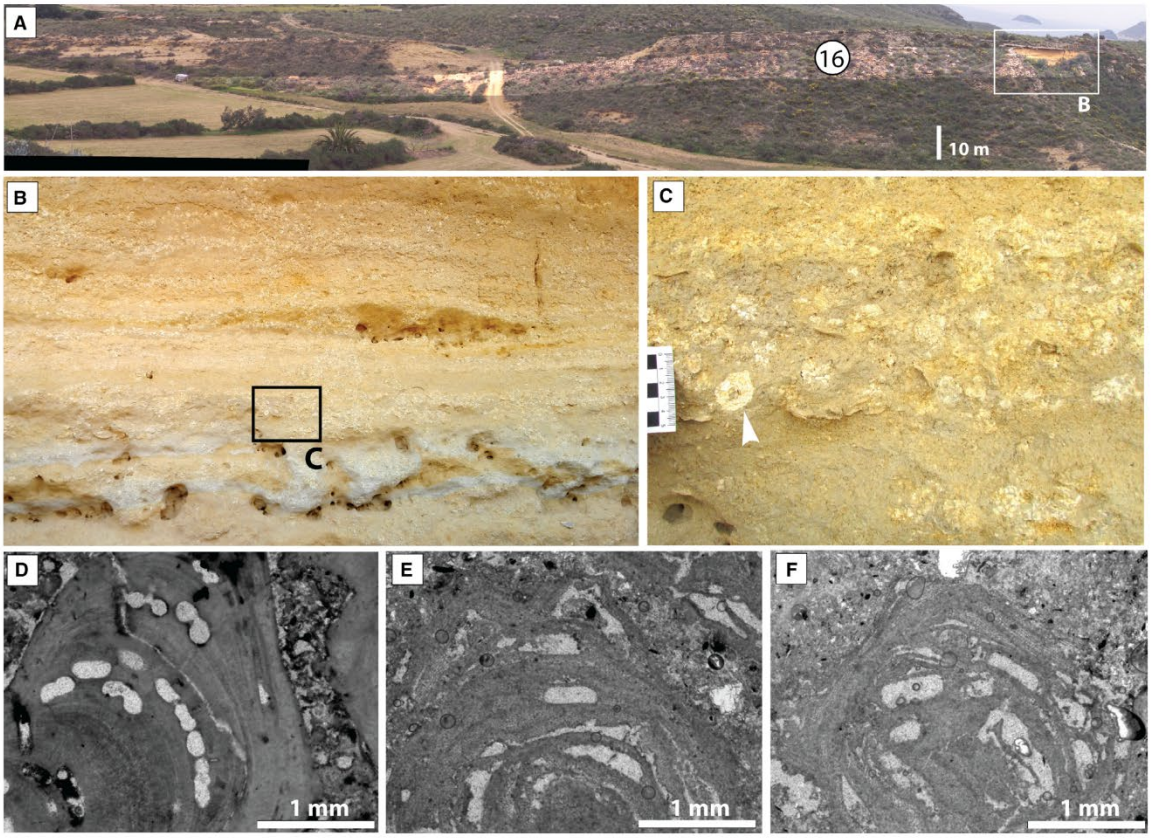

Fig. 7. Example of rhodolithic facies (FA2) in clinothem 16 (rollover zone) from the Cañada Brusca W sector. (A) Oblique view to depositional strike of clinothem 16, partially highlighted. (B) Rhodolith pavements in outer topset facies of clinothem 16. (C) Detail of a rhodolith pavement of (B), showing spheroidal growth forms (white arrowhead). Note the fine-grained hybrid carbonate matrix. (D) to (F) Thin sections of samples of FA1–FA2 facies displaying examples of coralline red algae. (D) Uniporate conceptacles of Lithophylloideae (clinothem 18). (E) and (F) Multiporate conceptacles of Melobesioideae (clinothem 17).

although there are variations in a proximal to distal gradient, with increasing ichnodiversity and density of traces towards distal positions. In general, facies F3.2 is dominated by *Macaronichnus*, which is the product of vagile, detritus-feeding worms (Bromley *et al.*, 2009; Pearson *et al.*, 2013). Such trace fossils are rarely reported from offshore settings (Aguirre *et al.*, 2010; Rodríguez-Tovar & Aguirre, 2014; Giannetti *et al.*, 2018) and their producers cope well with high sedimentation rates (Taylor *et al.*, 2003). In distal positions (the base of the Cañada Blanca section), other common ichnotaxa include *Teichichnus rectus*, attributed to a deposit-feeder in nutrient-rich sediments, which can re-equilibrate to the sediment-water interface (MacEachern *et al.*, 2012a). The intense bioturbation in distal positions (Table 3), however, suggests long colonization windows (Buatois *et al.*, 2015) under background fair-weather conditions, because the effects of siltation and/or gravity flows decrease both in intensity and frequency in these settings. The occurrence of the traces *Teichichnus*, *Diplocraterion* and *Scalichnus* in distal F3.2 (Table 3) points to re-equilibration in the aftermath of such sporadic, exceptional events (MacEachern *et al.*, 2012a).

Facies Association 4

The major characteristic of Facies Association 4 (FA4) is the presence of fine-grained hybrid packstone distally and the reduced carbonate content (*ca* 13 to 40%) (Fig. 4), characteristically dominated either by *Costellamussiopecten* or *Terebratula* (Figs 10B and 11).

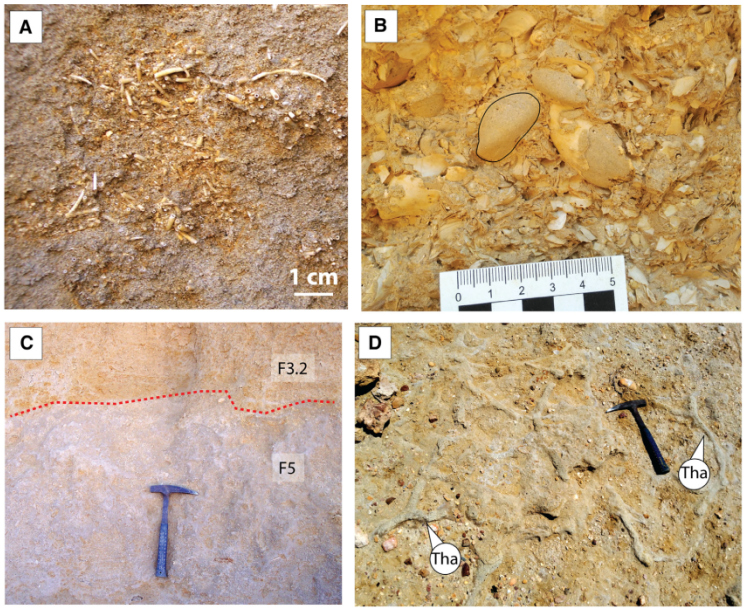

Fig. 8. Details of the main features in FA3 and F5. (A) A *Ditrupa* pod concentration in hybrid packstones. (B) Densely packed mollusc concentration (*Gibbomodiola* bed). (C) Contact (red dashed line) between F5 (*Glossifungites* ichnofacies; below red line) and the overlying *Ditrupa* rich friable hybrid packstones (F3.2) at the Cabezo Alto section. (D) *Glossifungites* ichnofacies (F5) with well-developed networks of *Thalassinoides suevicus* (marked 'Tha') in the Cañada Brusca sector.

Hybrid packstone with Costellamussiopecten – F4.1

Facies F4.1 consists of hybrid packstones with poorly sorted fine-grained sands to coarse silts (variable proportions of micrite and sparite depending on the locality). The terrigenous particles comprise angulose grains of quartz, schist and abundant mica flakes. Planktonic and benthic foraminifera (Fig. 9) are abundant, the latter including centimetre-sized tests of *Pyramidulina raphanistrum* and *Lenticulina* spp. As in the other facies, the fabric is massive and structureless. Macrofossils, most notably *Costellamussiopecten cristatum*, occur as dispersed, complete, disarticulated valves (Fig. 10B). The density of identifiable traces varies. Outsized, angular floating clasts of metamorphic material from the basement are very rare (Fig. 10C). Some of them are pebble-sized, rounded and bioeroded black dolostones (Fig. 10D).

Paraconglomerate of outsized floating clasts – F4.2

This facies occurs only at the base of the Cabezo Alto section (clinothem 1) (Fig. 10A). The matrix is similar to that of F4.1. It is characterized by a paraconglomerate of outsized, angular floating clasts and loosely packed to dispersed bioclasts (Fig. 10E). The richness of vertebrates and macroinvertebrates is the highest in the whole study area (including fish vertebrae, elasmobranch teeth, crustacean dactyla, wood remains bioeroded by *Nototeredo* sp., plant detritus and others; Fig. S2). Most shells are disarticulated, consisting of a mixture of pristine, fragmented and bioeroded/encrusted specimens of many species; some of them occur typically in FA1 and FA2 (Table 4; Fig. 10F). This facies is densely bioturbated (mostly indistinct mottling) and the richness of identifiable ichnotaxa is relatively high in comparison to other facies. The density of floating lithoclasts and bioclasts peaks at the base of clinothem 1 and decreases progressively upward (Fig. 10A and F). In the 125 to 500 μm fraction, yellowish to light-green glauconite grains (often preserved as foraminiferal casts) are frequent.

Terebratula pavements – F4.3

This facies is characteristic of the Cabezo Alto – Cañada Brusca area, where 13 outcrops were identified. They consist of *ca* 5 to 20 cm thick beds in which brachiopods appear embedded in a fine-grained matrix (Fig. 11A and B). Two outcrops showed two pavements separated by about 20 cm. These are referred to in this study as 'twin pavements' (Fig. 11C). No erosive or planar surfaces, either at the base or at the top of the skeletal concentration, were observed (Fig. 11A, B and G). No normal grading is visible in the matrix; the sediment is indistinguishable from that underlying and overlying the pavements; the shell orientation varies from random to umbo-down; bioclasts are well-preserved and only a few specimens show minor taphonomic alterations; more than 50% of the

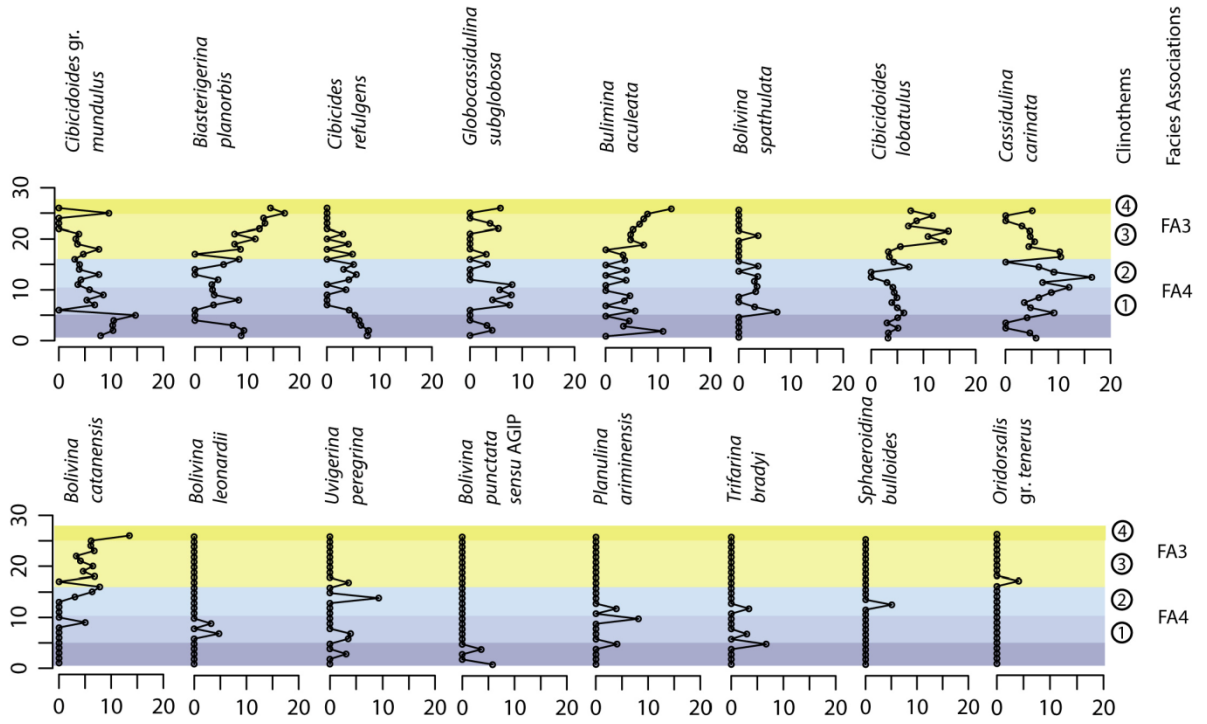

Fig. 9. Most abundant benthic foraminifera from the Cabezo Alto section in 26 samples encompassing FA4 and FA3. The position of the samples in the stratigraphic log is indicated in Fig. 4. Only peaks >3% are represented. Blue indicates FA4 (different grades for each clinothem) and yellow FA3.

specimens are articulated. Some pavements yield small juveniles. The packing of specimens is variable, from dense in the centre to loose towards distal and proximal positions of the pavement (Fig. 11G). In some cases, disrupted biological clumping occurs (Fig. 11B and F). All of the pavements studied yield yellowish to light-green glauconite grains. Chemical analysis of two glauconite grains from one sample showed a K_2O content of 4·4% and 4·3%. This facies is distributed cyclically, most often alternating with F4.1.

Terebratula biostrome – F4.4

This is one thick bed (>1 m) dominated by loosely to densely packed terebratulids (Fig. 12A). It contains a mixture of well-preserved, articulated specimens (Fig. 12B), sometimes devoid of sediment infill (Fig. 12C), and disarticulated valves (Fig. 12E and F). Many of the latter are fragmented, abraded, heavily bioeroded and encrusted by bryozoans, anomiid bivalves (Fig. 12D), serpulids and craniid brachiopods. The biofabric is variable and complex, with examples of *in situ Terebratula* clumps, pod concentrations and gutter casts (Fig. 12G). Outcrops of this single interval are recognizable for 850 m parallel to the strike, whilst at Cañada Brusca, a low abundance of additional brachiopod species (Table 4) was observed.

Interpretation of Facies Association 4

This facies association crops out in the more distal positions of the depositional profile, where the fine-grained sediment composition indicates low-energy background conditions. This is supported by the occurrence of *C. cristatum*, characteristic of F4.1, which is an extinct pectinid with delicate valves, frequently reported from offshore environments (Aguirre *et al.*, 1996; Robba, 1996; Yesares-García & Aguirre, 2004; Ceregato *et al.*, 2007). Extant species of the homeomorphic genus *Amusium* (Waller, 2011) inhabit quiet waters on fine sandy and muddy substrates of the Indo-Pacific region, at depths of 10 to 100 m (Fréneix *et al.*, 1987; Minchin, 2003). The benthic foraminiferal assemblage (Fig. 9) is also typical of offshore environments (Rasmussen, 2005). The massive

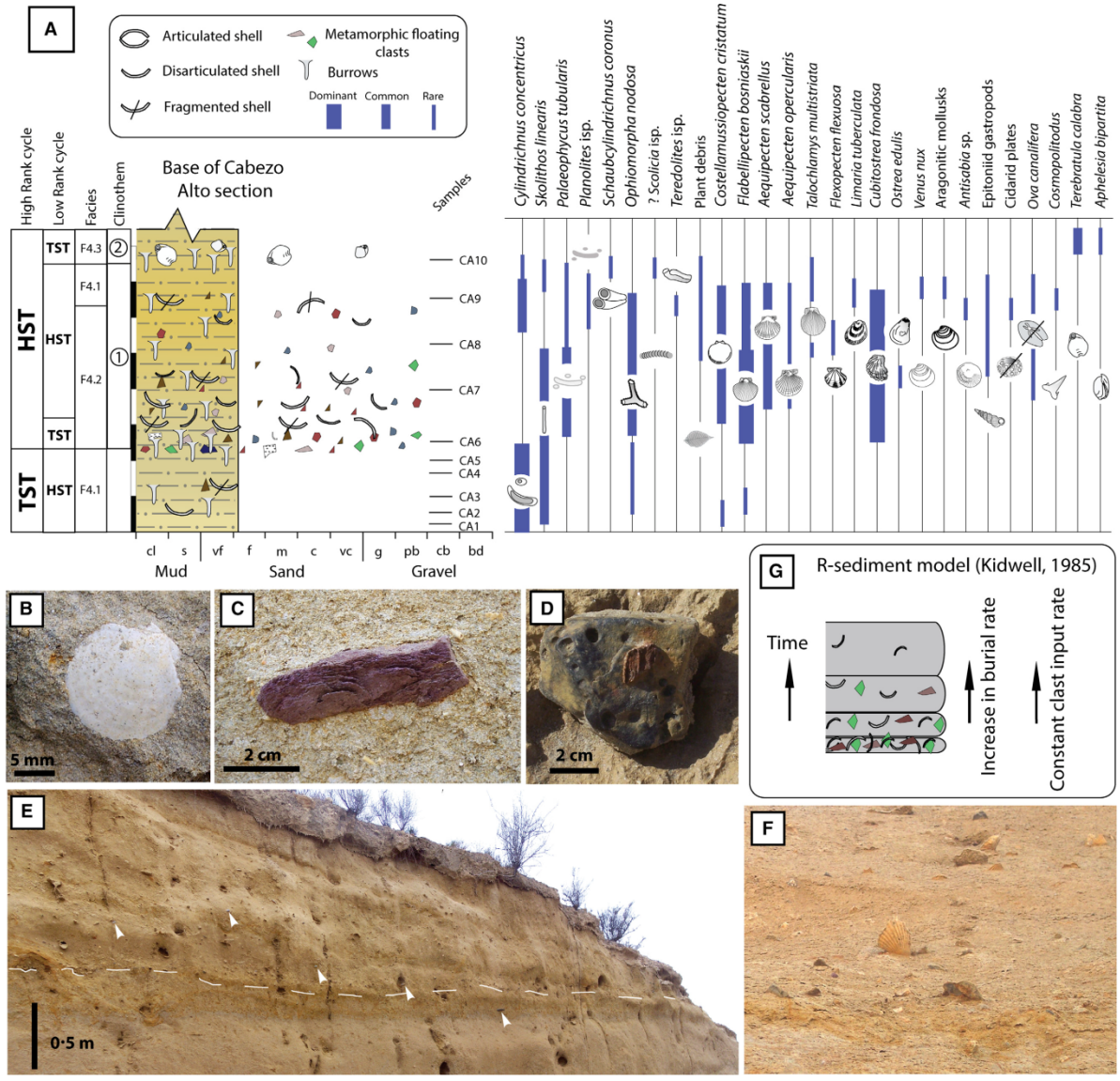

Fig. 10. Sedimentological and palaeontological features of FA4. (A) Stratigraphic log of the base of the Cabezo Alto section (clinothems 1 and 2). (B) Juvenile valve of *Costellamussiopecten cristatum*. (C) Example of cobble-sized angular, metamorphic floating clast. (D) Rounded and bioeroded dolostone clast. (E) Floating clast paraconglomerate at the base of clinothem 1 (examples with arrowheads). The dashed line highlights the base of the paraconglomerate. (F) Detail of the bioclasts in the paraconglomerate of clinothem 1 (*Flabellipecten bosniaskii* and *Cubitostrea frondosa*). (G) R-sediment model, adapted from Kidwell (1985) and Tomašových *et al.* (2006). It explains the fabric pattern with an upward decrease in density of floating clasts by a concomitant increase in burial rates.

fabric can be explained by intense bioturbation and deposition by suspension fall-out (García-García *et al.*, 2006; Longhitano, 2008). The barren to dispersed packing of F4.1 suggests high sedimentary dilution and/or low shell productivity (Tomašových *et al.*, 2006). The good taphonomic preservation of the autochthonous (and some allochthonous in F4.2) macrofossils (Table 4) fits the outer-shelf taphofacies model of Yesares-García & Aguirre (2004). The ichnofabrics also point to low–moderate background sedimentation rates probably affected episodically by high sedimentation rates, as in distal F3.2. Stable background conditions are

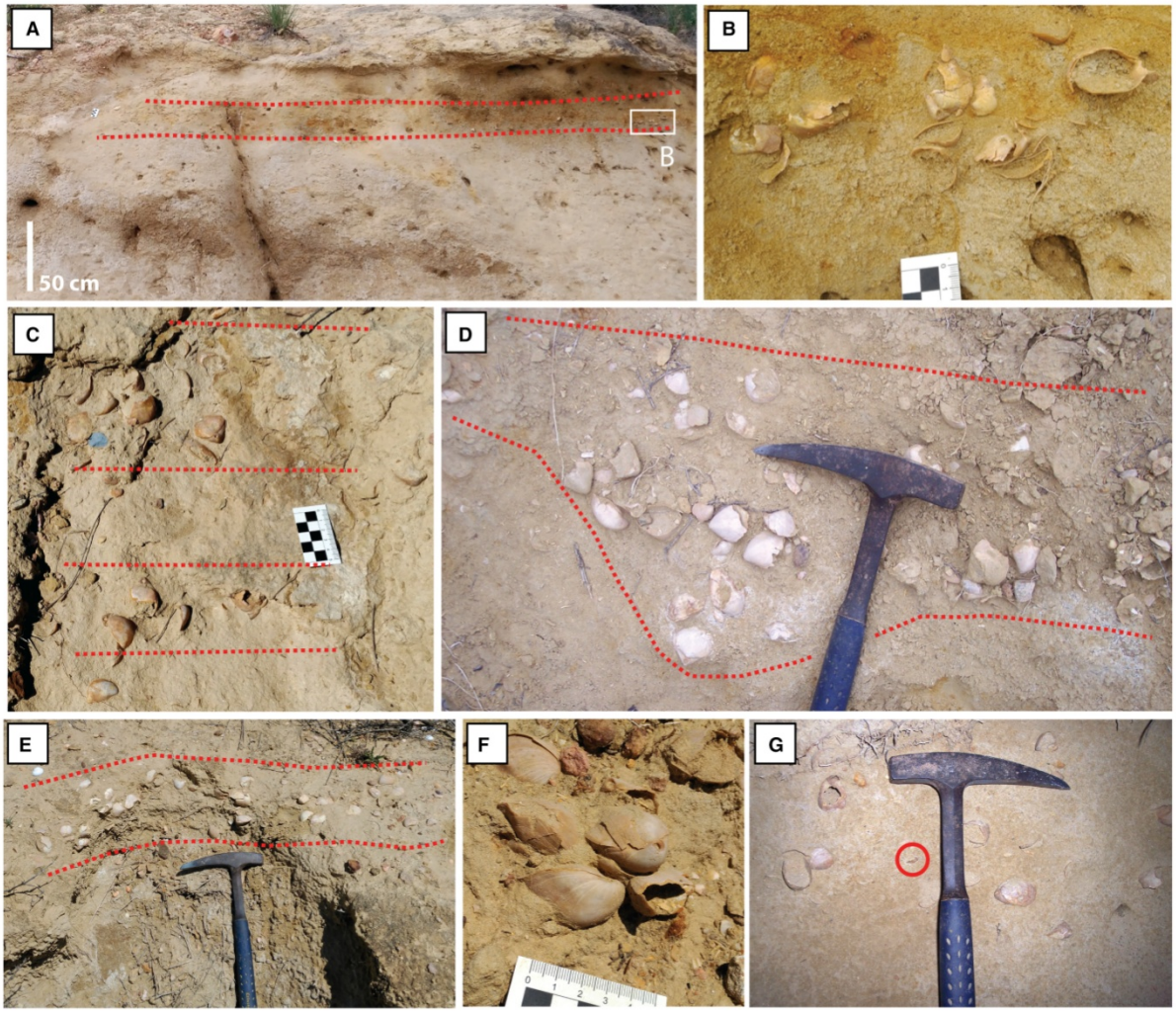

Fig. 11. Examples of facies F4.3 (*Terebratula* pavements; bounded by red dashed lines). (A) *Terebratula* pavement between clinothems 3 and 4 in the Cabezo Alto area. (B) Detail of the pavement shown in (A). Most specimens are articulated and distributed in small clusters of two to three specimens (possibly representing a disrupted biological clumping or patchiness). (C) 'Twin pavements' between clinothems 5 and 6. (D) and (E) Densely packed concentrations in the pavement between clinothems 9 and 10 in the Cañada Brusca sector. Hammer for scale is 33 cm long. (F) Possible *Terebratula* cluster. (G) Loosely packed pavement in more distal positions. The red circle pinpoints a juvenile specimen.

suggested by the dominance of lined burrows: such lining helps to stabilize burrows (constructed as permanent domiciles) in soft substrates (Bromley, 1996; Buatois & Mángano, 2011). The dominance of *Domichnia* therefore indicates well-oxygenated substrates and stable background conditions (Buatois & Mángano, 2011). The local occurrence of *Trichichnus* isp. at the CA section (clinothem 2) might be related to longer periods of stable conditions and a low food content at the sediment–water interface (Pervesler *et al.*, 2008). An event-bed suite can be interpreted based on the occurrence of some *Taenidium* and backfilled, unidentified meniscate traces (possibly *Scolicia* isp.), indicating the activity of deposit feeders. They probably reacted opportunistically to sporadic high-density gravity flows or siltation events associated with storms or other disturbances (de Gibert & Goldring, 2007).

The occurrence of outsized floating clasts (Fig. 10) across the depositional profile is interpreted as the product of storm-induced high-density gravity flows (Postma *et al.*, 1988;

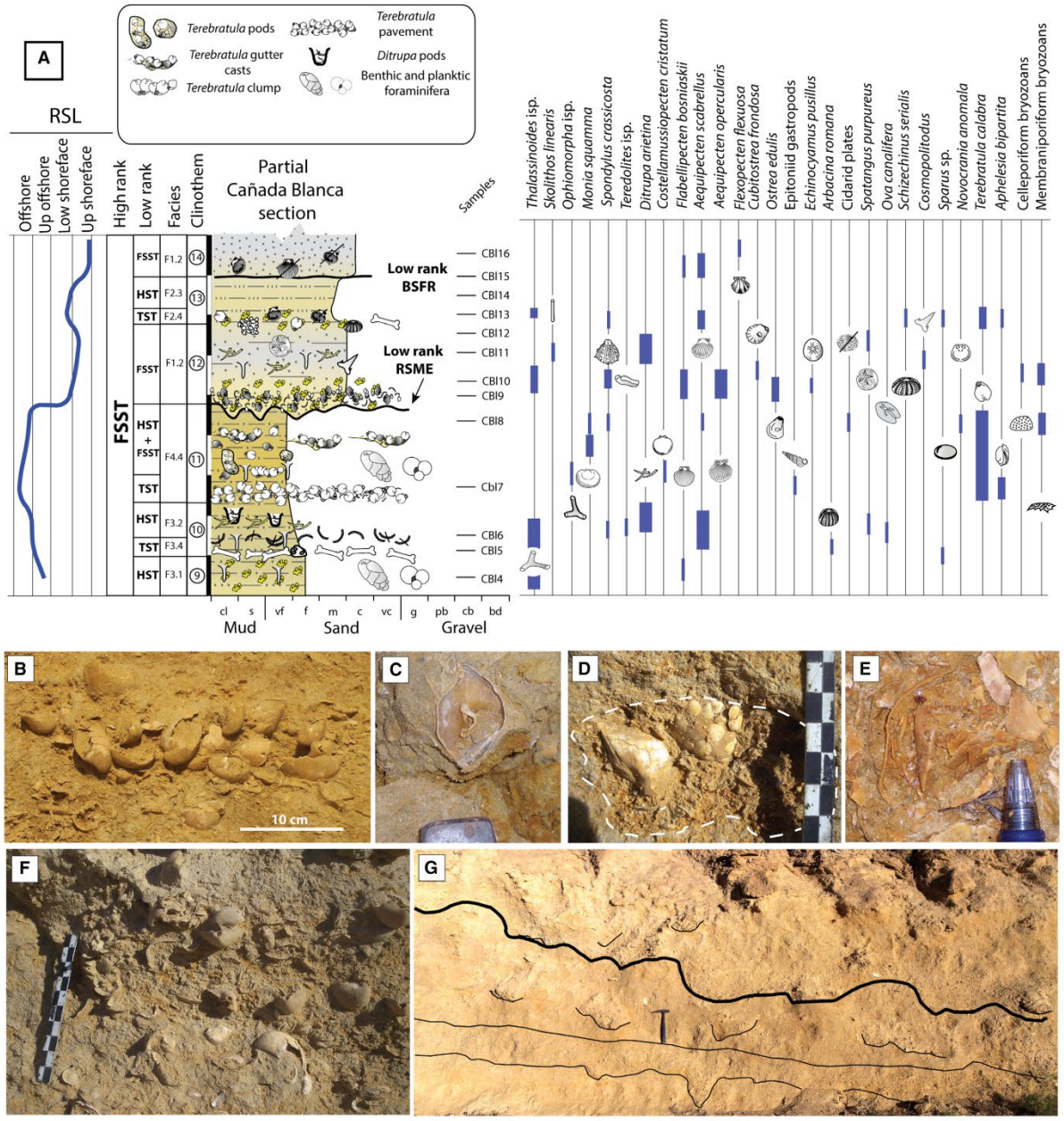

Fig. 12. Main features of FA3 and F4.4 at the Cañada Blanca section. (A) Detailed stratigraphic log for clinothems 9 to 14. (B) Clump of *in situ Terebratula* specimens. Note the articulated specimens, umbo-down orientation, presence of juveniles. (C) Void *Terebratula* displaying the brachidium (geopetal structure). Hammer tip for scale is 2 cm long. (D) Pod concentration filled with coarse siliciclastic grains, *Ditrupa* tubes and two articulated *Terebratula* specimens. Note the sharp-walled, unlined large burrow and numerous anomiid bivalves (*Monia squamma*) encrusting *Terebratula*. (E) Detail of imbricated, strongly altered *Terebratula* valves. Note the abraded foramen and right hinge-tooth in a fragmented ventral valve. Pen tip is 19 mm long. (F) Detail of gutter cast filled with disarticulated *Terebratula* shells. Concave-up, disarticulated ventral valves predominate. (G) View of the basal bed, overlain by gutter casts and the erosive surface separating clinothems 11 and 12. BSFR, basal surface of forced regression. Hammer is 33 cm long.

Mulder & Alexander, 2001; Talling *et al.*, 2012). This is consistent with source areas dominated by schists and phyllites, such as in the Águilas Basin. In particular, according to García-García (2004), the sensitivity of these lithologies to erosion favours the production of high volumes of fine fraction, which in turn enhances the formation of cohesive debris flows. The angularity of these clasts (some of which have weak lithologies) (Fig. 10C) suggests that they bypassed the depositional profile directly from the river or ephemeral stream mouth to reach the distal positions where FA4 was deposited, probably by hyperpycnal flows that transformed into cohesive debris flows. The roundness and the presence of *Gastrochaenolites* traces on the dolostone clasts suggest that the latter were stored in a delta plain, a beach or a cliff-toe (Uchman *et al.*, 2002; García-García *et al.*, 2011) and were incorporated into the flows during flash floods. The storage area would have been no further away than a few kilometres (Fig. 13), judging from the distribution and structure of the Palomas Unit (Álvarez & Aldaya, 1985). A possible alternative explanation for their occurrence is kelp or seaweed rafting as a main transportation means (Bennett *et al.*, 1994; Garden *et al.*, 2011; Frey & Dashtgard, 2012) but co-occurrence of the floating clasts with other allochthonous elements [out of habitat molluscs (Table 4), plant debris, *Teredolites* isp. and *Calpensia* bryoliths (Fig. S2)] supports the first hypothesis (MacEachern *et al.*, 2005; Ghinassi, 2007; Moissette *et al.*, 2010; Nalin *et al.*, 2010; Buatois *et al.*, 2011).

In facies F4.3, the frequent pristine preservation of terebratulids, the occurrence of juveniles and disrupted patchiness (Fig. 11A and B), together with the absence of diagnostic features for hydraulic reworking (e.g. Roetzel & Pervesler, 2004), suggest that these pavements probably represent obrution deposits of autochthonous palaeocommunities (Brett & Seilacher, 1991; Fürsich, 1995; Brett *et al.*, 2003). They can be interpreted as mixed assemblages, in part within-habitat time-averaged, and in part census death assemblages (Kidwell, 1998). The occurrence of glauconite in the terebratulid pavements points to conditions of very low terrigenous input (Odin & Fullagar, 1988; Harding *et al.*, 2014). Preservation of glauconite grains (often as well-preserved casts of foraminifera) points to their autochthonous or parautochthonous origin (Amorosi, 1997, 2012). Therefore, compared with F4.1, the *Terebratula* pavements (F4.3) indicate conditions of notably reduced sedimentation rates. The taphonomic traits and biofabric of these pavements suggest that the *Terebratula* palaeocommunities in the study area were extirpated by siltation events (Emig, 1989; Tomašových & Kidwell, 2017) because fine terrigenous particles clog the lophophore and smother these animals (He *et al.*, 2007). These siltation events probably represent the onset of the next cycle of F4.1 sedimentation. The interpretation here is, therefore, that the pattern of alternating F4.3 and F4.1 facies represents cyclical changes of decreased and increased sedimentation rates.

The '*Terebratula* biostrome' (F4.4) shares the dominance of terebratulids with F4.3 (Fig. 12). The variable taphofacies (Table 4) suggests complex taphonomic pathways of mixed biogenic–sedimentological origin (Kidwell *et al.*, 1986). The occurrence of *in situ* clumps (Fig. 12B) indicates that the terebratulids were autochthonous to the biotope where FA4 was being deposited. The dominance of *Terebratula* points to high shell productivity [high hard-part input rates *sensu* Tomašových *et al.* (2006)]. In contrast, pod concentrations, pristine void

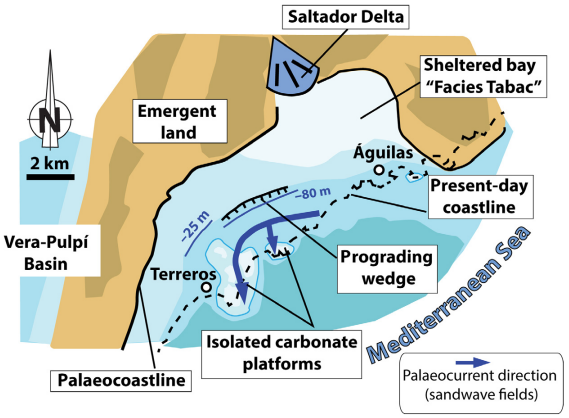

Fig. 13. Proposed palaeogeographic map of the Águilas Basin during deposition of synthem SP1 (Zanclean, MPl3 biozone). The exact position of the palaeocoastline in the western sector is tentative due to the paucity of shallow-water outcrops, and uncertainty as to their attribution to SP1. The indented black line indicates the rollover of the infralittoral prograding wedge and is shown with estimation of approximate inferred palaeobathymetry at the time of deposition of the oldest clinothems. The palaeocurrent direction is inferred from outcrops of stacked sandwave fields at the Terreros and La Carolina sectors (see Fig. 3), migrating seaward.

specimens (geopetal structures) and gutter casts infilled with highly altered and densely packed terebratulid shells, are all characteristic of episodes of rapid burial and hydraulic reworking *in situ* (Fig. 12C to F) (Baeza-Carratalá *et al.*, 2014). Hydraulic disturbances are also demonstrated by the occurrence of a few disarticulated valves of *Spondylus*, a typical element of FA2 (where it is often articulated), which suggests an allochthonous origin.

The abundant fragmented, abraded, bioeroded and encrusted shells (assemblage-level alteration) are typical for prolonged exposure at the sediment–water interface, which, together with the loose to dense packing (shelliness), points to reduced sedimentation rates (Kidwell, 1985, 1989). The rich ichnoassemblage of bioerosion traces (Table 4) is strongly uneven, dominated by *Entobia* isp. (clionaid sponges), highlighting strong hydrodynamics and background sedimentation rates between <1 g m^{-2} and *ca* 7 g m^{-2} (Carballo *et al.*, 1994). The rare occurrence of echinoid rasping traces *Gnathichnus pentax* coupled with the absence of *Radulichnus* (scratch marks by herbivorous gastropods and polyplacophorans) (de Gibert *et al.*, 2007) point to dim light or aphotic conditions (Bromley, 2005). The co-occurrence of the above taphonomically altered brachiopod bioclasts, together with abundant pristine specimens, demonstrates that the *Terebratula* palaeocommunity was able to recover from multiple episodic disturbances, where background conditions of strong hydrodynamics and low sedimentation rates were environmentally optimal for these brachiopods (Emig & García-Carrascosa, 1991; Reolid *et al.*, 2012). The co-occurrence of lined and sharp-walled, unlined burrows (Fig. 12D) suggests that the substrate within F4.4 evolved from a soft-ground to a stiffground, indicating a decrease in sedimentation rates (Taylor *et al.*, 2003; MacEachern *et al.*, 2012b).

Facies 5

Cemented burrowed hybrid packstone (Glossifungites ichnofacies)

This facies cannot be attributed to any particular facies association because in some places it adjoins FA4 but elsewhere adjoins FA3. It is treated here as a separate type. The matrix consists of a fine-grained hybrid packstone that is cemented (*ca* 40% $CaCO_3$) and completely bioturbated (Fig. 8C). In general, traces are poorly defined but some are attributable to non-compacted *Thalassinoides* burrows, except for one locality, where many well-defined, non-compacted *Thalassinoides suevicus* occur (Fig. 8D). The material infilling the burrows is similar to the surrounding matrix. In some localities, this facies displays loosely to densely packed skeletal concentrations, but *Ditrupa* is absent.

Interpretation of Facies 5

This facies, interspersed between either FA4 or FA3, is interpreted as the formation of stiff-grounds during phases of low sedimentation rates, which favoured cementation of the sea floor (Taylor *et al.*, 2003; MacEachern *et al.*, 2012b).

GEOMETRIC AND STRATIGRAPHIC STACKING PATTERNS

Geometry

The Cabezo-Alto and Cañada Brusca W sectors enable delta-scale clinoforms *sensu* Patruno *et al.* (2015) to be identified (Figs 1C, 14A and 14B). For example, the clinoform separating clinothems 5 and 6 extends for about 250 m from the toeset-point to the upper rollover (Fig. 1C). The clinoforms display a sigmoidal profile (*sensu* Adams & Schlager, 2000) where, in general, FA2 and facies 3.1 occur in the upper rollover, FA3 in the foreset and FA4 from the lower rollover basinward, in the bottomset. FA1 is best observed in the Cañada Brusca W sector where it occurs in the topset (Fig. 14D to F).

Stacking patterns

The mapping of stratigraphic surfaces on photomosaics, the outcrop study of bed surfaces and the facies distribution show that SP1 displays a south-east prograding and offlapping stacking pattern of sigmoidal clinothems. Twenty-two clinothems were identified in SP1 (numbering in Figs 4 and 14). In the Cabezo Alto (CA) sector, clinothems 1 to 6 display a forestepping pattern (progradation plus aggradation), evolving vertically from FA4 at the base to FA2 at the top; the latter is truncated and overlain by Quaternary deposits (Fig. 14A and B). The aggrading pattern is present in clinothems 5 and 6, which display facies 3.1 at the top of the sections; this contrasts with the adjacent clinothem 4, with facies 2.3 at the top (Fig. 14A and B). The contacts between these clinothems in distal positions consist of facies F4.2 (only at the base of the CA section),

F4.3 (red lines in Fig. 14A and B), or F5. Starting with clinothem 7, a downstepping pattern is visible, with strong shifts from facies F2.2 and F2.3 to F3.2 (Fig. 14A and B). The contact between these latter clinothems is erosive in the upper part of the sections (Fig. 14C). The offlapping trend is modulated by clinothem 11, which displays the more distal facies F3.1 at the Cañada Brusca W sector compared with adjacent older clinothems (Fig. 14D and E). Clinothem 11 is followed by strong shifts with facies F1.1 and F1.2 in clinothems 12 and 14, alternating with facies F2.3 in clinothems 13 and 15 through prominent erosive surfaces (Figs 5 and 14D to F). Clinothems 11 and 14 are very distinctive and make up marker beds recognized in the Cañada Brusca E, Cañada Brusca W and Cañada Blanca sectors. The Cañada Blanca section is characterized, in general, by alternating facies associations FA1 and FA2 and erosive contacts in between (Fig. 4). This pattern holds except at the base of the section which displays facies associations FA3 and FA4 up to clinothem 11, sharply overlain by facies association FA1 through an erosive surface (Figs 4 and 12).

MAGNETIC SUSCEPTIBILIY AND CARBONATE CONTENT

The overall carbonate content ranges from 13 to 80% (Fig. 4). Maximum values are attained in the rhodolith dominated facies of FA2; they decrease proximally and distally from this facies. In the CA section no cyclicity in $CaCO_3$ is recognizable, whereas in the CBL section the variation appears to roughly coincide with variation trends in magnetic susceptibility. Both the CA and CBL sections display very low magnetic susceptibility (MS) values, increasing only near the clinothem boundaries identified by sedimentological – palaeontological criteria. The maximum value in the whole studied area is recorded in the paraconglomerate interval at the base of section CA (Fig. 4).

DISCUSSION

Depositional model

Clinoforms of SP1 have the diagnostic features of sand-prone subaqueous delta-scale clinoforms (Patruno *et al.*, 2015), in particular: (i) steep foresets (≥7°, up to 14°) (Fig. 1C); (ii) a sigmoidal profile; (iii) development on a narrow shelf (an embayment about 14 km wide) (Fig. 13); and (iv) close proximity to the palaeocoast (indicated by bioeroded dolostone clasts of the Palomas Unit). Furthermore, the Pliocene Molino del Saltador delta occurs 6 km north-east from the base of the CA section. This implies that La Serrata and Los Melenchones (Fig. 3B), adjacent to where this delta developed, were already above sea-level during the early Pliocene (Fig. 13).

In general, the facies distribution in SP1 shows a proximal–distal energy gradient with decreasing grain-size distally, especially basinward, beyond the upper rollover (FA3 and FA4). This grain-size distribution matches systems dominated by physical accommodation in which facies belts reflect the hydraulic competence of the sedimentary particles (Pomar & Kendall, 2008). The geometry of the clinoforms is consistent with a prograding distally steepened ramp (Pomar, 2001; Pomar *et al.*, 2002; Martín *et al.*, 2004) or an infralittoral prograding wedge (IPW; Hernández-Molina *et al.*, 2000; Pomar *et al.*, 2015). In both cases, the rollover zone represents an energy threshold above which episodic high-energy conditions affect the topset and below which overall quiet conditions prevail offshore (seaward of the rollover). According to these genetic models, the upper rollover corresponds to the mean storm-weather wave base (SWWB), fostering sediment bypass at the topset and sediment shedding down on the foreset (Hernández-Molina *et al.*, 2000; Pomar *et al.*, 2015), the latter in the form of siltation/suspension fall-out and as sediment gravity-flows (Massari & Chiocci, 2006). Immediately offshore of the upper rollover zone, sedimentation rates peak (upper foreset) and gradually decrease distally, both in frequency and intensity (in the lower foreset and bottomset) (Walsh *et al.*, 2004; Mitchell, 2012). In the original example of an IPW from off Cabo de Gata (southern Spain) described by Hernández-Molina *et al.* (2000), the rollover lies at about 25 m water depth coincident with the mean SWWB. This bathymetry is compatible with the coralline algal assemblages in the study area (outer topset) (Fig. 7), although, during the early Pliocene, the storm intensities at this latitude were presumably stronger due to warmer sea-surface temperatures (SST) (Emanuel, 2005; Beltran *et al.*, 2011). A conservative depth of 25 to 30 m for the upper rollover zone of the Águilas subaqueous delta-scale clinoforms is, therefore, proposed. The location of the SP1 IPW in the south-western corner of the basin (Fig. 13) implies that it was probably the area most

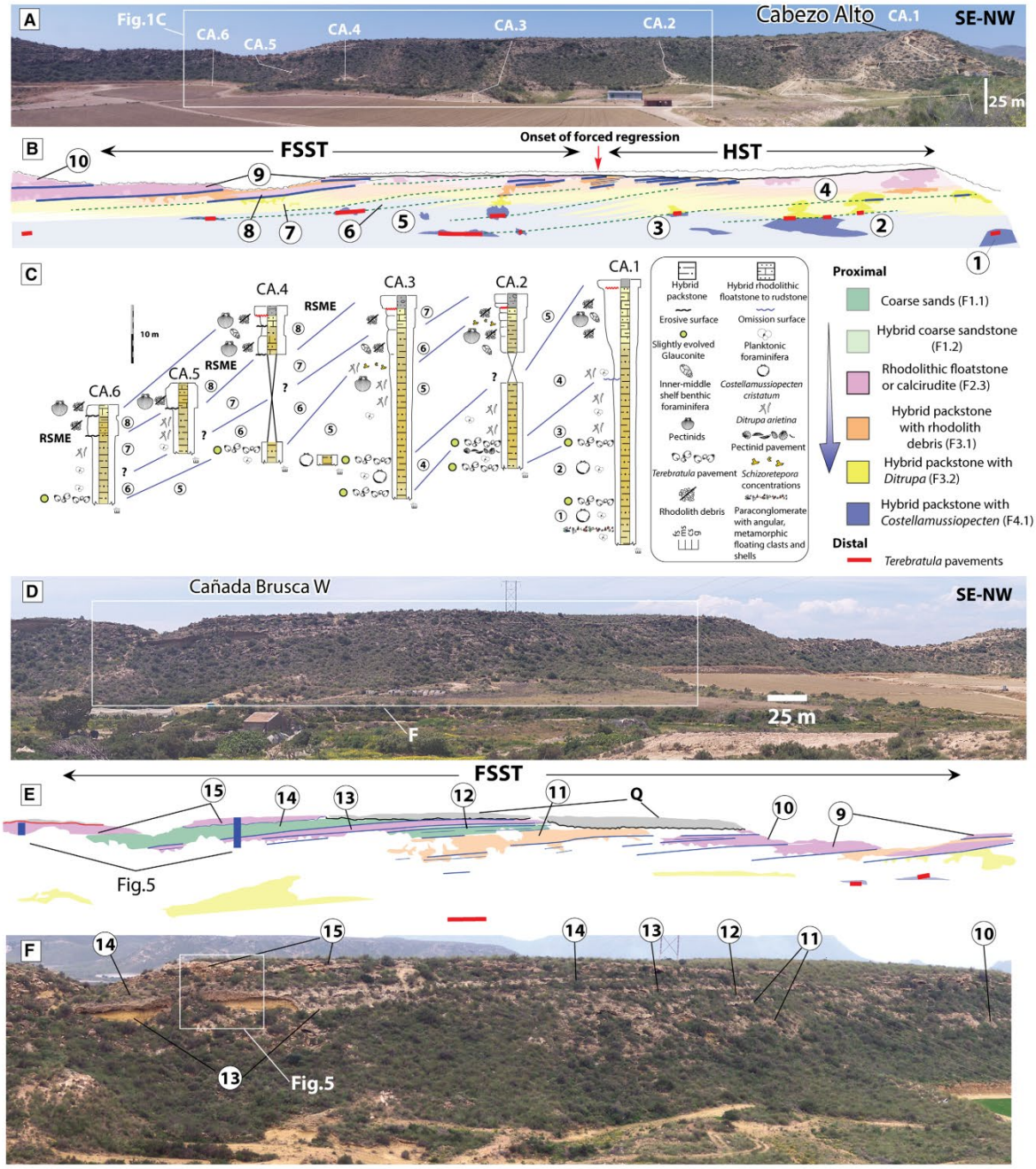

Fig. 14. Photomosaic of the early Pliocene infralittoral prograding wedge in the western sector of the Águilas Basin, synthem SP1. (A) Cabezo Alto (CA) sector (photograph parallel to depositional strike). White lines indicate the stratigraphic logs in (C). (B) Clinothems and facies indicated with colour code. Blue lines indicate beds identified in the field, red straight lines are *Terebratula* pavements, and dashed lines are the interpreted connection between beds in the topsets–foresets and terebratulid pavements at the toeset–bottomsets. Clinothems identified in the CA sector are indicated by encircled numbers. The topsets of clinothems 4 to 7 are truncated, and overlain by Quaternary conglomerates. (C) Synthetic stratigraphic logs (not composite; indicating dominant biofacies, stratigraphic contacts and correlation between adjacent sections). (D) The Cañada Brusca (CBr) sector viewed obliquely to depositional strike. Inset indicates the position of sector for details in (F). (E) Numbered clinothems and facies contacts as in (D). Colour code for facies as in (B) and (C). (F) Detail of the CBr sector from a view subparallel to depositional strike, with indication of clinothems 10 to 15.

exposed to easterly storms, as opposed to the laminated silty marls occurring in the north-eastern part of the basin, interpreted as a sheltered bay (Montenat *et al.*, 1978).

Sequence stratigraphy

Two hierarchical sequence ranks were here interpreted for the early Pliocene (late Zanclean, MPl3 biozone) SP1 synthem of the Águilas Basin. The low rank sequences (LRS) are the basic building blocks of the high rank sequence (HRS). In particular, the systems tracts of the HRS are defined both by the LRS stacking patterns and their bounding surfaces (Zecchin & Catuneanu, 2013). The LRS are represented by the identified outcropping clinothems (1 to 22); older ones were eroded, younger ones truncated or covered by colluviums.

Architecture of the high rank sequence

The interpreted HRS is bounded at the top by an extensive unconformity described by Dabrio *et al.* (1991). The basal unconformity is inferred at the Cabezo Alto sector based on changes in facies, strike, dip and micropalaeontological assemblages between the top of SP0 and base of SP1. This basal unconformity, however, crops out at the Terreros section (3·35 km to the southwest) (Fig. S1). Further work is necessary to confirm its presence throughout the study area.

The transgressive systems tract (TST) is interpreted here to crop out at the base of the CA section (only the youngest LRS) (Figs 4 and 10). Since the contact between synthems SP0 and SP1 in the Cabezo Alto does not crop out, the high rank transgressive ravinement surface has not been observed. The highstand systems tract (HST) is interpreted from the forestepping stacked clinothems 1 to 6 (Fig. 14A and B). These clinothems overlie the paraconglomerate at the base of the CA section (facies 4.2, clinothem 1) (Fig. 10), which is interpreted here as the maximum flooding zone (MFZ) (see below). Evidence for the falling stage systems tract (FSST) is shown by the generally downstepping facies stack of clinothems 7 to 22 (Fig. 14). The high rank lowstand systems tract (LST) has not been identified and is thought to occur in a deeper part in the basin, below the present-day sea-level. The general offlapping stacking pattern of the LRS in synthem SP1 (Fig. 14) indicates an overall regressive trend, typical for subaqueous deltas, which form during relative stillstands (highstands or lowstands) (Hernández-Molina *et al.*, 2000; Pepe *et al.*, 2014; Patruno *et al.*, 2015), or during falling stages of relative sea-level (RSL) (Hansen, 1999; Massari *et al.*, 1999).

High rank transgressive systems tract and maximum flooding zone

The high rank MFZ is interpreted to correspond to the paraconglomerate interval at the base of the CA section (facies 4.2) (Fig. 10), implying that most of the high rank TST does not crop out. According to Zecchin & Catuneanu (2013), the maximum flooding surface (MFS) may correspond to: "a 'cryptic' conceptual horizon within condensed deposits during the time of maximum transgression, without a clear physical expression". Condensation is interpreted here from the pattern of the dispersing upward packing of lithoclasts and bioclasts (Fig. 10), which can be explained by the R-sediment model of Kidwell (1985) (Fig. 10F). This model argues that clasts are increasingly dispersed upward concomitant with an increase in burial rates or higher sedimentary dilution (Dattilo *et al.*, 2012) at the onset of the HST, when sedimentation rates outpace accommodation space. This interpretation assumes a relatively constant frequency of the high-density gravity flow events that deliver allochthonous clasts to these depths (bottomset). In the rest of the synthem, floating lithoclasts in FA3–FA4 are rare and isolated, as expected from higher burial rates during the high rank HST and FSST (Neal & Abreu, 2009). Furthermore, the paraconglomerate interval is densely bioturbated (Zecchin & Catuneanu, 2013) and yields the deepest assemblage of benthic (Fig. 9) and planktonic foraminifera (Leckie & Olson, 2003). This includes frequent or common outer shelf taxa, such as *Planulina ariminensis* and *Uvigerina peregrina*. The high species richness of macrofossils also implies a longer window of time-averaging. Moreover, the position of this interval at the base of the prograding low rank clinothems reinforces its interpretation as the MFZ. Thus the paraconglomerate interval of clinothem 1 is here interpreted as a high rank backlap shell/clast bed. The paraconglomerate interval also coincides with the strongest magnetic susceptibility in the whole study area (Fig. 4).

High rank highstand and falling stage systems tracts

The forestepping stacking pattern (progradation plus aggradation) of clinothems 1 to 6, coupled with gradual facies changes, indicates a normal regression and are attributed to the high rank

HST (Catuneanu & Zecchin, 2016). In contrast, clinothems 7 to 22 display a general downstepping stacking pattern with strong shallowing-upward facies shifts and sharp erosional contacts. These traits are diagnostic for forced regression, and hence are interpreted as the FSST (Massari *et al.*, 2002; Massari & D'Alessandro, 2012). Forced regression is likewise indicated by frequent 'internal unconformity surfaces' (IUS) such as those reported by Massari & D'Alessandro (2012). The IUS in the study area are interpreted here to essentially represent low rank regressive surfaces of marine erosion (RSME) (Plint, 1988; Plint & Nummedal, 2000) (Figs 4 and 5). The contact between clinothems 13 and 14 in the outer topset and rollover zone is a good example of a surface interpretable as a RSME (Figs 5I and 14D to F). This surface records a strong facies shift from F2.3 (lower shoreface) to F1.2 (middle to upper shoreface), the latter prograding to F1.1 (upper shoreface to foreshore). The material of F1.2 passively filled truncated *Thalassinoides* burrows (*Glossifungites* ichnofacies) in clinohem 13 (Fig. 5J) (MacEachern *et al.*, 1992, 2012b). A subsequent low rank RSL rise partially eroded the upper shoreface–foreshore facies of clinothem 14 (F1.1) forming a low rank onlap shell bed (F2.4) (e.g. Zecchin, 2007). The lithofacies and biofacies F2.3 of clinothem 15 (Fig. 5) suggest an amplitude of about 15 to 20 m of sea-level rise with respect to clinothem 14.

The erosive surfaces at the CBL section (Figs 4, 6 and 15) are interpreted here to have formed by scouring associated with high-frequency variations of base level (Massari & D'Alessandro, 2012). However, the 'master RSME' or high rank RSME, which represents the onset of forced regression in the high rank sequence, is not the most prominent interpreted RSME in the study area. This can be explained by gradually stronger shoreface erosion at increasingly lower sea-levels (when the amplitude of the RSL fall of the low rank cycles is enhanced by the falling sea-level trend of the high rank cycle). In the Cabezo Alto sector, the erosive surfaces disappear distally and these distal portions are interpreted here as basal surfaces of forced regression.

Architecture of proximal low rank sequences

In the context of hierarchical sequence stratigraphy, Schlager (2004, 2010) recognized 'S-sequences and P-sequences'. The P-sequences have only TST and HST, while S-sequences also contain FSST and LST: P-sequences are equivalent to the small-scale cycles (metres to decametres in thickness) of Zecchin (2007), where R, T–R or T cycle types were recognized based on the predominant development of transgressive (T) or regressive (R) deposits. In general, the clinothems of SP1 can be interpreted as R and T–R cycles, with variations in the architecture depending on the position in the depositional profile and the systems tracts of the HRS. In the Cañada Blanca sector, the most common motif of LRS associated with the high rank FSST consists of R cycles bounded by erosive surfaces overlain by thick skeletal concentrations and a coarsening upward trend (Figs 4, 6 and 15). Some skeletal concentrations can be attributed to shelly tempestites because the texture and grain-size of the matrix is similar to or coarser than that of the material underlying the erosive surface (Figs 5A, 15A and 15B). Distinguishing low rank onlap shell beds (OSB) in shoreface environments from bedsets, which display tempestite amalgamation unrelated to shoreline shifts, is difficult (Zecchin *et al.*, 2017). This is because high-frequency, low-amplitude RSL fluctuations result in subtle facies variations in shoreface environments (Zecchin, 2007). Onlap shell beds form under low sedimentation rates when transgression creates accommodation space further onshore. Skeletal material then accumulates in the shoreface, producing loose to dense packing due to low sedimentary dilution (Fig. 15F). The resulting biofabric of the OSB thus reflects a complex history of multiple events of biotic (bulldozing organisms) and/or hydraulic reworking, along with differential winnowing by storms and tidal currents (Kidwell, 1991; Zecchin *et al.*, 2017). In the Cañada Blanca sector, erosive surfaces carved on coarse-grained F1.2 (Fig. 15C and D) and mantled by thick, shell-rich facies with fine-grained matrix (F2.4) (Fig. 15E) are interpreted to reflect RSL fluctuations (Massari *et al.*, 2002; Cattaneo & Steel, 2003). The abundance of complete rhodoliths in many of these shell beds (F2.4) (Fig. 6C) indicates low sedimentation rates (Aguirre *et al.*, 2017).

Architecture of distal low rank sequences

The interpretation here is that the internal architecture of the clinothems in FA4 consists of low rank TST formed by *Terebratula* pavements (F4.3) and the overlying hybrid packstone, with dispersed to barren packing (F4.1), represents the low rank HST. These cycles therefore conform to the structure of R cycles. In more proximal positions, the *Terebratula* pavements are

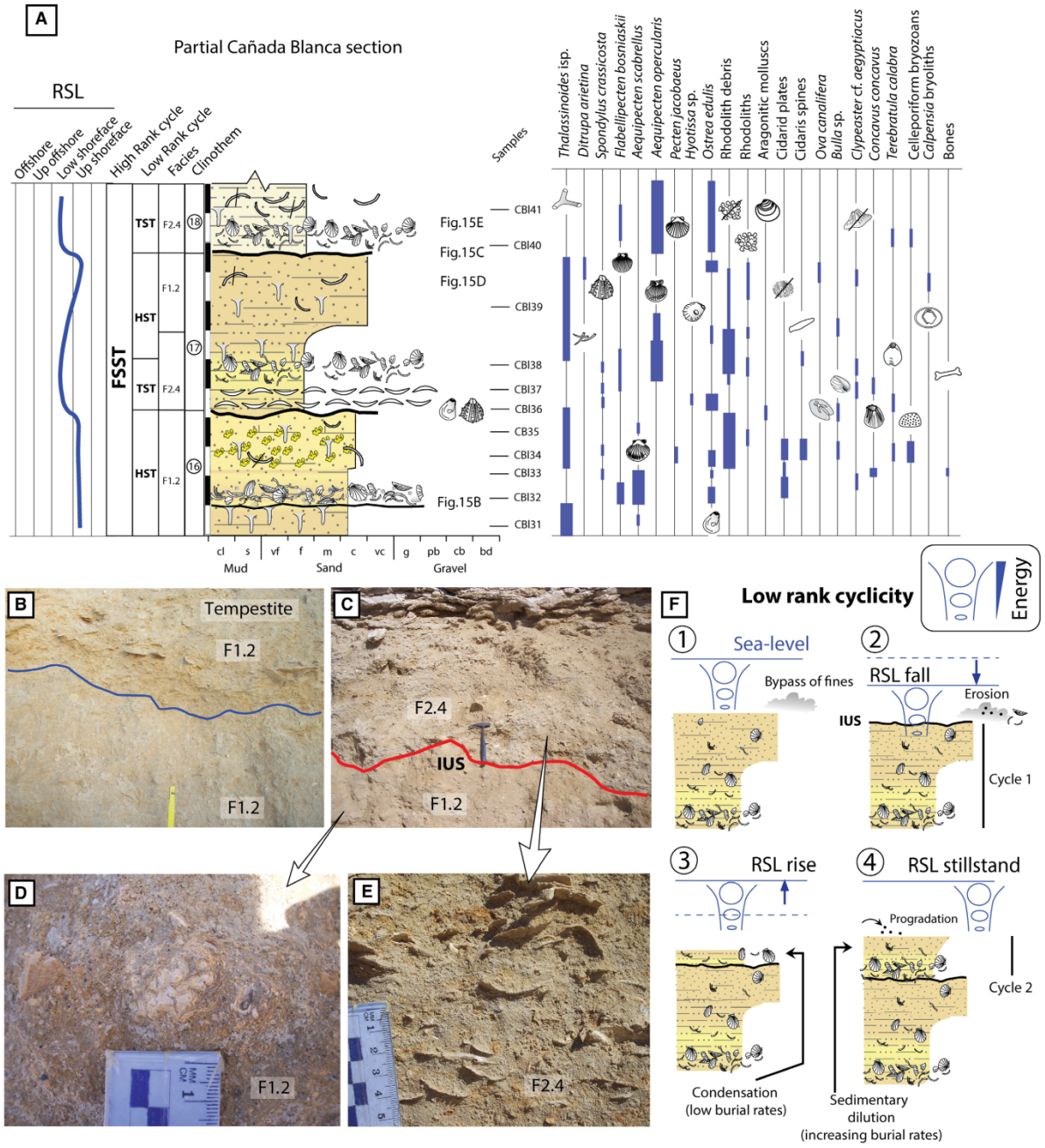

Fig. 15. Examples of low rank cycles in the Cañada Blanca section with alternating F1.2 and F2.4. (A) Detailed log for clinothem 17. (B) Example of tempestite in the upper part of clinothem 16. Yellow stick part for scale is 10 cm long. (C) Transition from clinothems 17 and 18 through an erosive surface (red line) interpreted as an 'internal unconformity surface' (IUS). Hammer is 33 cm long. (D) Rhodolith and *Clypeaster* fragment in coarse siliciclastic grains of F1.2, below the IUS. (E) Fine-grained hybrid matrix with loosely packed pectinid shells (F2.4). (F) Interpretation of the high-frequency cycle motifs at the Cañada Blanca section, bound by erosive surfaces overlain by shell-rich deposits and coarsening upward lithology.

occasionally replaced by the *Glossifungites* ichnofacies (F5) or shell beds (F3.4). A genetic model of these R cycles is presented below.

During stillstand stages of the low rank RSL, sediment aggraded in the topset until reaching the base level. Accommodation space thus

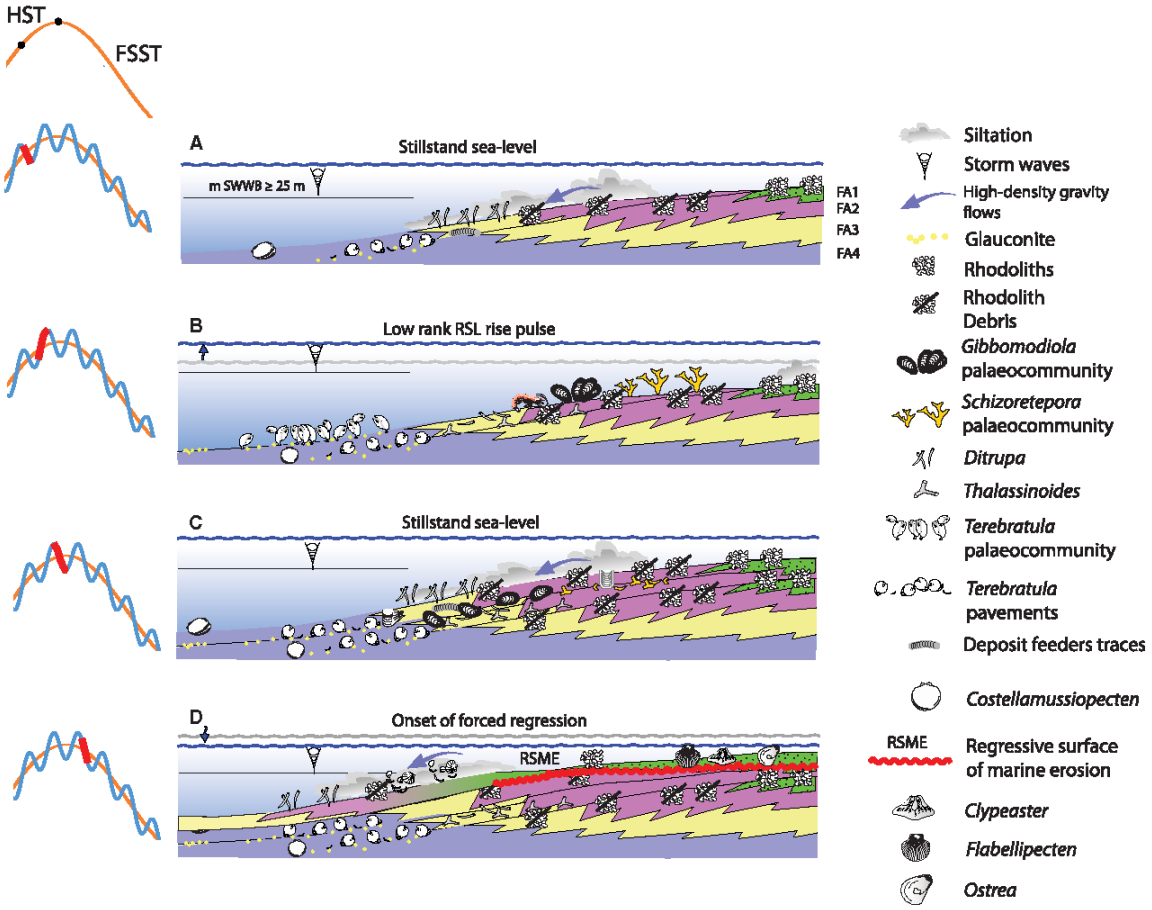

Fig. 16. Simplified depositional model for the infralittoral prograding wedge in the Águilas Basin. (A) Stillstand stage with no accommodation space at the topset. Storms sweep sediment downslope and clinothems prograde. (B) Low rank relative sea-level (RSL) rise creates accommodation space, sediments are trapped in nearshore environments. The sediment-starved distal areas are suitable for suspension feeder palaeocommunities. (C) Reduced rate of RSL rise is outpaced by sedimentation rate, filling up available space in the topset and resuming progradation in the foresets. Suspension feeder communities are extirpated or retreat offshore. *Ditrupa* and deposit feeders thrive. (D) The RSL fall produced forced regression. Base level intersects the sea floor, eroding the topset and leading to resedimentation and mixing up downslope.

became unavailable at the topset and progradation in the foreset resumed, eventually forming a new clinothem (Rich, 1951; Swift & Thorne, 1991; Pomar & Kendall, 2008; Pomar *et al.*, 2015) (Fig. 16A). Background conditions with frequent siltation events and high-density gravity flows in the foreset (F3.2) are indicated by opportunistic faunal responses, including the dominance of *Ditrupa*, infaunal benthic foraminifera and ichnoassemblages of vagile deposit feeders. During these stillstand stages, F4.1 was deposited at the lower rollover and bottomset.

During stages of low rank RSL rise (Fig. 16B), progradation in the foreset switched off and clinoforms developed as omission surfaces in the bottomsets and foresets, and often as transgressive lags or low rank OSB in the upper foresets and topsets (Massari *et al.*, 1999) (Fig. 5). This is because the base level rose concomitantly with the RSL, creating accommodation space in proximal settings of the topset. This was accompanied by reduced fluvial gradients and sediment trapping in nearshore environments, while more distal settings (mainly, foreset and bottomset) were left starved (Brett, 1998; Embry, 2009; Dattilo *et al.*, 2012). Compared with other examples of subaqueous delta-scale clinoforms (Pomar *et al.*, 2002), low rank RSL rise stages in the study area

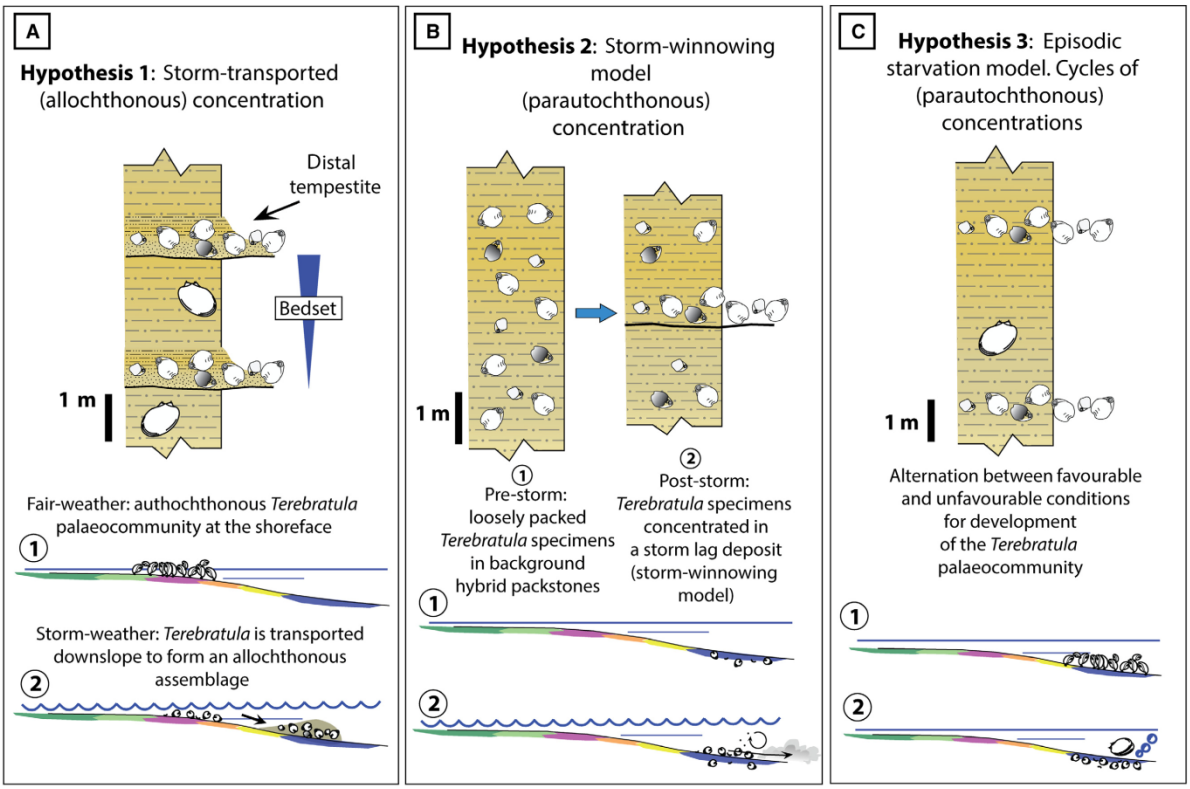

Fig. 17. Models to explain the *Terebratula* pavements in the study area. (A) The allochthonous concentration model. (B) The storm-winnowing model. (C) The episodic-starvation model.

did not result in aggrading clinothems. Rather, they were non-accretionary, forming only hiatal skeletal concentrations. This implies lower sedimentation rates of the Águilas subaqueous delta-scale clinoforms compared to those at Migjorn (Pomar *et al.*, 2002). The conditions of low-sedimentation rate fostered: (i) the colonization of the bottomsets–toesets and foresets by palaeocommunities of siltation-sensitive suspension feeders (Brett, 1998), in this case from proximal to distal: *Schizoretepora*, *Gibbomodiola* and *Terebratula* (Fig. 1C); (ii) the formation of authigenic minerals such as glauconite (Kidwell, 1991; Catuneanu, 2006; Amorosi, 2012); (iii) the development of densely packed shell beds in the middle–upper parts of the foresets (Fig. 8B) due to sediment starvation and differential winnowing (R-sediment model of Kidwell,1985); and (iv) the formation of firmgrounds associated with cementation, enabling colonization by callianassid shrimps and development of the *Glossifungites* ichnofacies (Taylor *et al.*, 2003; MacEachern *et al.*, 2012b) (Fig. 8C and D).

Hypotheses about the formation of the *Terebratula* pavements

Three main hypotheses are considered here to explain the genesis of the *Terebratula* pavements (Fig. 17):

1 The *allochthonous concentration* hypothesis (Kidwell *et al.*, 1986) envisages that the terebratulids were deposited at the lower rollover and bottomsets after being entrained in high-density gravity flows induced by storms or other disturbances (for example, internal waves). Their autochthonous habitat would be located in more proximal environments (for example, the upper rollover and outer topset) (Fig. 17A). This hypothesis is rejected because of: (i) the lack of diagnostic physical sedimentary structures for shelly tempestites (Einsele & Seilacher, 1991; Einsele, 2000; Flügel, 2004; Roetzel & Pervesler, 2004; Myrow, 2005); and (ii) the absence in nearly all pavements of other taxa that are abundant or dominant in more proximal environments of the depositional profile. An

allochthonous concentration would consist of a mixture of taxa entrained and mixed up from different habitats (Leighton & Schneider, 2004). Furthermore, to produce an allochthonous brachiopod-dominated concentration at the bottomsets, there should be high brachiopod productivity in the presumably autochthonous habitat in more proximal environments, which was not observed in the study area.

2 The *storm-winnowing model* (Dattilo *et al.*, 2008, 2012) considers that the *Terebratula* pavements are concentrated autochthonous shell lags that result from differential winnowing of the fine-grained sediment during storms (Fig. 17B). This hypothesis is rejected because, to produce such a dominance and abundance of terebratulids, high brachiopod productivity should occur throughout the stratigraphic intervals of FA4, between terebratulid pavements. These, instead, are barren or are characterized by dispersed *Costellamussiopecten*.

3 The *episodic starvation model* (Dattilo *et al.*, 2008, 2012) considers that the *Terebratula* concentrations are the result of biological processes during stages of low sedimentation rates (Fig. 17C). This hypothesis is supported by the disrupted biological patchiness, the presence of juveniles, the dominance of articulated, pristine shells and by the occurrence of glaucony, a typical proxy for condensed deposits. The occurrence of *Terebratula* clumps (*sensu* Kidwell *et al.*, 1986) in F4.4 demonstrates that *Terebratula* is autochthonous to FA4 (Hallam, 1961; Middlemiss, 1962; Fürsich, 1995).

Magnetic susceptibility and carbonate content

Quartz, calcite and organic compounds yield very weak to negative magnetic susceptibility (MS) values (diamagnetic minerals). In contrast, paramagnetic minerals such as clays (smectite, illite and chlorite); ferromagnesian minerals (biotite, tourmaline, pyroxenes and amphiboles); iron sulphides (pyrite and marcasite) and iron carbonates (siderite and ankerite), yield MS values several orders of magnitude higher than those of diamagnetic minerals, which dominate the signal when present in bulk samples (Davies *et al.*, 2013; Sullivan & Brett, 2013). Magnetic susceptibility in marine sedimentary rocks is usually considered as a proxy for the proportion of iron-rich sediments derived from terrestrial sources (Ellwood *et al.*, 2000; Sullivan & Brett, 2013). High MS values are considered to be attained during regressive stages, when increased erosion delivers proportionally higher amounts of terrestrial iron-rich sediments into the marine basin (Sullivan & Brett, 2013). This argument has been contradicted by the report of distinct MS peaks associated with surfaces of maximum starvation (Ellwood *et al.*, 2011). This can be explained by concentration of paramagnetic particles derived from aeolian sources (Reuter *et al.*, 2013). Likewise, very low to negative MS values, as in the Águilas Basin, SP1, may be explained by a very low terrigenous input and/or dilution of terrigenous particles in biogenic carbonate (Reuter *et al.*, 2013). When distinct positive MS peaks are the result of increased terrigenous input, MS trends anticorrelate with those of $CaCO_3$ (Davies *et al.*, 2013; Rothwell & Croudace, 2015). At the CA section, distinct MS peaks are coincident with a relative increase in $CaCO_3$ content (Fig. 4), suggesting that the MS values in such cases are associated with condensation. These peaks occur at the clinothem boundaries that were interpreted as omission surfaces (*Glossifungites* ichnofacies) or condensed intervals (paraconglomerate and *Terebratula* pavements) based on sedimentological and palaeontological features. The weak MS values are also potentially influenced by the slightly evolved glauconite content, which is paramagnetic (Amorosi, 1997).

Progradation rates of the lower rank cycles

Biostratigraphic data constrain the maximum possible duration of the HRS to somewhat less than 700 kyr. The yellowish to light green colour of the glauconite grains that separate the LRS in facies 4.3 suggests that, in terms of maturity, this is a slightly evolved stage. This was confirmed in one sample, where glauconite grains had a K_2O content of *ca* 4%. According to Amorosi (2012), the slightly evolved glaucony would indicate sediment-starved periods lasting about 10^4 years, implying that the LRS in the study area can be interpreted as high-frequency cycles in the Milankovitch band. The cyclicity in variation of terrigenous input is also recorded in the patterns of magnetic susceptibility and calcium carbonate content (Fig. 4). These patterns of magnetic susceptibility are similar to those reported by Davies *et al.* (2013) for the high-frequency cycles of the Llucmajor platform (Miocene, Spain), reinforcing the above interpretation. If this is true, the time-span encompassed by the HRS is considerably less than the 700 kyr suggested by biostratigraphic proxies.

CONCLUSIONS

The Águilas Basin records subaqueous delta-scale clinoforms that prograded during the early Pliocene (MPl3 biozone) in mixed temperate carbonate–siliciclastic environments. The sedimentological and palaeontological features of these clinoforms are compatible with the infralittoral prograding wedge model. The prograding units formed during the highstand and falling stages of a high rank relative sea-level cycle, and the biostratigraphic data indicate that this progradation lasted for less than 700 kyr. The basic building blocks of this sequence are clinothems whose internal architecture generally consists of skeletal concentrations overlain by a stratigraphic interval with a more disperse packing. In distal positions of the depositional profile, the skeletal concentrations consist of terebratulid brachiopod pavements. These pavements are distributed cyclically; they are interpreted here to have formed during high-frequency relative sea-level rise pulses that led to sediment starvation in these distal environments. During stillstand stages, accommodation space eventually became unavailable in the topset of the clinoforms, leading to a resumption in the progradation of the clinoform system, extirpating the brachiopod communities until the next cycle of relative sea-level rise. In other examples of subaqueous deltas, similar brachiopod assemblages bound the clinobedded unit at the base and the top, but did not occur on the clinoforms, as seen in the Águilas Basin. This implies lower progradation rates of the Águilas Basin clinoforms, allowing enough time for these benthic communities to develop. The occurrence of slightly evolved glauconite in the Águilas Basin suggests that these high-frequency cycles fall within the Milankovitch band, probably precession.

ACKNOWLEDGEMENTS

We thank Gregorio Romero Sánchez from the Paleontological Heritage Service of the Community of Murcia (Spain), for granting permits to conduct palaeontological fieldwork in the study area; Javier Souto-Derungs, Andrey Ostrovsky and Eric Wolfgring for their help with the SEM images and the identification of *Schizoretepora*. We thank Alfred Uchman for cross-checking identifications of certain trace fossils and for palaeoenvironmental suggestions about the *Macaronichnus–Ophiomorpha* ichnofabric. Thanks to Martin Maslo, Christa Hermann, Robert Peticzka and Theodoros Ntaflos for the analysis of carbonate content and glauconite. This work was inspired during fieldwork in the Águilas Arc with Jesús Soria, Hugo Corbí, Jordi Martinell, Rosa Domènech and Cristino Dabrio, all of whom are also thanked for providing literature and for discussions in the field. We thank Guillermo Díaz-Medina, Johann Hohenegger, Wolfgang Eder, Vlasta Ćosović, Adam Tomašových, Rafał Nawrot and many other colleagues for fruitful discussions and suggestions. Special thanks to Ildefonso Bajo and Enrico Borghi for their input about the taxonomy of Pliocene echinoids; to Julio Aguirre and Juan Carlos Braga for sending literature about rhodoliths and Andrés Guilabert for his help with Digital Terrain Models. We thank Michael Stachowitsch and Alexander Hugh Rice for improving the language. We thank the Editors Peir Pufahl and Christopher R. Fielding for the constructive comments during the review process. The stimulating reviews of Massimo Zecchin, Carlton Brett and an anonymous colleague significantly improved the final version of this manuscript. The authors declare that there is no conflict of interest.

REFERENCES

Abbott, S.T. (1997) Mid-cycle condensed shellbeds from mid-Pleistocene cyclothems, New Zealand: implications for sequence architecture. *Sedimentology*, **44**, 805–824.

Abu-Zied, R.H., Rohling, E.J., Jorissen, F.J., Fontanier, C., Casford, J.S. and **Cooke, S.** (2008) Benthic foraminiferal response to changes in bottom-water oxygenation and organic carbon flux in the eastern Mediterranean during LGM to Recent times. *Mar. Micropaleontol.*, **67**, 46–68.

Adams, E.W. and **Schlager, W.** (2000) Basic types of submarine slope curvature. *J. Sediment. Res.*, **70**, 814–828.

Aguirre, J., Braga, J.C., Jiménez, A.P. and **Rivas, P.** (1996) Substrate-related changes in pectinid fossil assemblages. *Palaeogeogr. Palaeoclimatol. Palaeoecol.*, **126**, 291–308.

Aguirre, J., de Gibert, J.M. and **Puga-Bernabéu, A.** (2010) Proximal–distal ichnofabric changes in a siliciclastic shelf, Early Pliocene, Guadalquivir Basin, southwest Spain. *Palaeogeogr. Palaeoclimatol. Palaeoecol.*, **291**, 328–337.

Aguirre, J., Braga, J.C., Martín, J.M. and **Betzler, C.** (2012) Palaeoenvironmental and stratigraphic significance of Pliocene rhodolith beds and coralline algal bioconstructions from the Carboneras Basin (SE Spain). *Geodiversitas*, **34**, 115–136.

Aguirre, J., Braga, J.C. and **Bassi, D.** (2017) Rhodoliths and Rhodolith beds in the rock record. In: *Rhodolith/Mäerl Beds: A Global Perspective* (Eds R. Riosmena-Rodríguez, W. Nelson and J. Aguirre), pp. 105–138. Springer International Publishing, Basel.

Álvarez, F. and **Aldaya, F.** (1985) Las unidades de la Zona Bética en la región de Águilas-Mazarrón (Prov. de Murcia). *Estud. Geol.*, **41**, 139–148.

Amorosi, A. (1997) Detecting compositional, spatial, and temporal attributes of glaucony: a tool for provenance research. *Sed. Geol.*, **109**, 135–153.

Amorosi, A. (2012) The occurrence of glaucony in the stratigraphic record: distribution patterns and sequence-stratigraphic significance. In: *Linking Diagenesis to Sequence Stratigraphy* (Eds S. Morad, J.M. Ketzerand and L.F. De Ros), pp. 37–53. John Wiley and Sons, West Sussex.

Amorosi, A., **Sammartino, I.** and **Tateo, F.** (2007) Evolution patterns of glaucony maturity: a mineralogical and geochemical approach. *Deep Sea Res. Part II*, **54**, 1364–1374.

Anell, I. and **Midtkandal, I.** (2015) The quantifiable clinothem–types, shapes and geometric relationships in the Plio-Pleistocene Giant Foresets Formation, Taranaki Basin, New Zealand. *Basin Res.*, **29**, 277–297.

Baeza-Carratalá, J.F., **Giannetti, A.**, **Tent-Manclús, J.E.** and **Joral, F.G.** (2014) Evaluating taphonomic bias in a storm-disturbed carbonate platform: effects of compositional and environmental factors in Lower Jurassic brachiopod accumulations (Eastern Subbetic Basin, Spain) Early Jurassic Brachiopod taphofacies. *Palaios*, **29**, 55–73.

Bardají, T., **Silva, P.**, **Goy, J.L.**, **Zazo, C.**, **Dabrio, C.** and **Civis, J.** (1999) Recent evolution of the Águilas Arc Basins (SE, Spain): Sea-level record and neotectonics. *M.B.S.S. Newletters*, **21**, 21–26.

Bardají, A.T., **Zazo, C.**, **Goy, J.L.**, **Silva, P.G.** and **Dabrio, C.J.** (2001) Registro de los cambios del nivel del mar en la Cuenca de Águilas (Murcia, SE de España). In: *V Iberian Quaternary Meeting and I Quaternary Congress of Countries of Iberian Languages* (Eds R. Taborda, J. Cascalho and L. Ortlieb), pp. 245–248. Sociedade Geológica de Portugal, Lisbon.

Beckvar, N. and **Kidwell, S.M.** (1988) Hiatal shell concentrations, sequence analysis, and sealevel history of a Pleistocene coastal alluvial fan, Punta Chueca, Sonora. *Lethaia*, **21**, 257–270.

Beltran, C., **Flores, J.A.**, **Sicre, M.A.**, **Baudin, F.**, **Renard, M.** and **De Rafélis, M.** (2011) Long chain alkenones in the Early Pliocene Sicilian sediments (Trubi Formation—Punta di Maiata section): Implications for the alkenone paleothermometry. *Palaeogeogr. Palaeoclimatol. Palaeoecol.*, **308**, 253–263.

Ben Moussa, A. (1994) Les bivalves néogènes du Maroc septentrional (façade atlantique et méditerranéenne). Biostratigraphie, Paléobiogéographie et Paléoécologie. Documents du Laboratoire de Géologie de Lyon (Fr), 132, 1–281.

Bennett, M.R., **Doyle, P.**, **Mather, A.E.** and **Woodfin, J.L.** (1994) Testing the climatic significance of dropstones: an example from southeast Spain. *Geol. Mag.*, **131**, 845–848.

Blomeier, D., **Dustira, A.M.**, **Forke, H.** and **Scheibner, C.** (2013) Facies analysis and depositional environments of a storm-dominated, temperate to cold, mixed siliceous-carbonate ramp: the Permian Kapp Starostin Formation in NE Svalbard. *Norw. J. Geol./Nor. Geol. Foren.*, **93**, 75–93.

Braga, J.C. and **Martín, J.M.** (1996) Geometries of reef advance in response to relative sea-level in a Messinian (uppermost Miocene) fringing reef (Cariatiz reef, Sorbas Basin, SE Spain). *Sed. Geol.*, **107**, 61–81.

Brett, C.E. (1998) Sequence stratigraphy, paleoecology, and evolution; biotic clues and responses to sea-level fluctuations. *Palaios*, **13**, 241–262.

Brett, C.E. and **Seilacher, A.** (1991) Fossil lagerstätten; a taphonomic consequence of event sedimentation. In: *Cycles and Events in Stratigraphy* (Eds G. Einsele, W. Ricken and A. Seilacher), pp. 283–297. Springer-Verlag, Berlin.

Brett, C.E., **Algeo, T.J.** and **McLaughlin, P.I.** (2003) The use of event beds and sedimentary cycles in high-resolution stratigraphic correlation of lithologically repetitive successions: the Upper Ordovician Kope Formation of Northern Kentucky and Southern Ohio. In: *High-Resolution Stratigraphic Approaches to Paleobiology* (Eds P. Harries and D. Geary), pp. 315–351. Kluwer Academic/Plenum Press, Boston.

Bromley, R.G. (1996) *Trace Fossils. Biology, Taphonomy and Applications*, 2nd edn, p. 361. Chapman and Hall, London.

Bromley, R.G. (2005) Preliminary study of bioerosion in the deep-water coral *Lophelia*, Pleistocene, Rhodes, Greece. In: *Cold-water Corals and Ecosystems* (Eds A. Freiwaldand and J.M. Roberts), pp. 895–914. Springer, Berlin.

Bromley, R.G., **Milan, J.**, **Uchman, A.** and **Hansen, K.S.** (2009) Rheotactic *Macaronichnus*, and human and cattle trackways in Holocene beachrock, Greece: reconstruction of paleoshoreline orientation. *Ichnos*, **16**, 103–117.

Buatois, L.A. and **Mángano, M.G.** (2011) *Ichnology. Organism-Substrate Interactions in Space and Time*, p. 358. Cambridge University Press, Cambridge.

Buatois, L.A., **Saccavino, L.L.** and **Zavala, C.** (2011) Ichnologic signatures of hyperpycnal flow deposits in Cretaceous river-dominated deltas, Austral Basin, southern Argentina, Sediment transfer from shelf to deep water—Revisiting the delivery system. *AAPG Studies in Geology*, **61**, 153–170.

Buatois, L.A., **Delgado, M.** and **Mángano, M.G.** (2015) Disappeared almost without a trace: Taphonomic pathways and the recognition of hidden bioturbation events in Eocene storm deposits (Paují Formation, Lake Maracaibo, Venezuela). *Ann. Soc. Geol. Pol.*, **85**, 473–479.

Carballo, J.L., **Sánchez-Moyano, J.E.** and **García-Gómez, J.C.** (1994) Taxonomic and ecological remarks on boring sponges (Clionidae) from the Straits of Gibraltar (southern Spain): tentative bioindicators? *Zool. J. Linn. Soc.*, **112**, 407–424.

Cattaneo, A. and **Steel, R.J.** (2003) Transgressive deposits: a review of their variability. *Earth Sci. Rev.*, **62**, 187–228.

Catuneanu, O. (2006) *Principles of Sequence Stratigraphy*, p. 386. Elsevier, Amsterdam.

Catuneanu, O. and **Zecchin, M.** (2016) Unique vs. non-unique stratal geometries: relevance to sequence stratigraphy. *Mar. Pet. Geol.*, **78**, 184–195.

Catuneanu, O., **Galloway, W.E.**, **Kendall, C.G.**, **St, C.**, **Miall, A.D.**, **Posamentier, H.W.**, **Strasser, A.** and **Tucker, M.E.** (2011) Sequence stratigraphy: methodology and nomenclature. *Newsl. Stratigr.*, **44**, 173–245.

Ceregato, A., **Raffi, S.** and **Scarponi, D.** (2007) The circalittoral/bathyal paleocommunities in the Middle Pliocene of Northern Italy: The case of the *Korobkovia oblonga–Jupiteria concava* paleocommunity type. *Geobios*, **40**, 555–572.

Coppier, G., **Griveaud, P.**, **de Larouziere, F.D.**, **Montenat, C.** and **Ott d'Estevou, P.** (1989) Example of Neogene tectonic indentation in the Eastern Betic Cordilleras: the Arc of Águilas (Southeastern Spain). *Geodin. Acta*, **3**, 37–51.

Corbí, H. and **Soria, J.M.** (2016) Late Miocene–early Pliocene planktonic foraminifer event-stratigraphy of the Bajo Segura basin: A complete record of the western Mediterranean. *Mar. Pet. Geol.*, **77**, 1010–1027.

Cuevas-Castell, J.M., **Betzler, C.**, **Roessler, J.**, **Hüssner, H.** and **Peinl, M.** (2007) Integrating outcrop data and forward computer modelling to unravel the development of a Messinian carbonate platform in SE Spain (Sorbas Basin). *Sedimentology*, **54**, 423–441.

Dabrio, C.J., **Bardají, T.**, **Zazo, C.** and **Goy, J.L.** (1991) Effects of sea-level changes on a wave-worked Gilbert-type delta (Late Pliocene, Águilas Basin, SE Spain). *Cuad. Geol. Ibérica*, **15**, 103–137.

Dattilo, B.F., **Brett, C.E.**, **Tsujita, C.J.** and **Fairhurst, R.** (2008) Sediment supply versus storm winnowing in the development of muddy and shelly interbeds from the Upper Ordovician of the Cincinnati region, USA. *Can. J. Earth Sci.*, **45**, 243–265.

Dattilo, B.F., **Brett, C.E.** and **Schramm, T.J.** (2012) Tempestites in a teapot? Condensation-generated shell beds in the Upper Ordovician, Cincinnati Arch, USA. *Palaeogeogr. Palaeoclimatol. Palaeoecol.*, **367**, 44–62.

Davaud, E. and **Septfontaine, M.** (1995) Post-mortem onshore transportation of epiphytic foraminifera: recent example from the Tunisian coastline. *J. Sediment. Res.*, **65**, 136–142.

Davies, E.J., **Ratcliffe, K.T.**, **Montgomery, P.**, **Pomar, L.**, **Ellwood, B.B.** and **Wray, D.S.** (2013) Magnetic susceptibility (χ) stratigraphy and chemostratigraphy applied to an isolated carbonate platform reef complex; Llucmajor Platform, Mallorca. In: *Deposits, Architecture, and Controls of Carbonate Margin, Slope and Basinal Settings* (Eds K. Verwer, T.E. Playton and P.M. Harris), SEPM Spec. Publ., **105**, 142–156.

Di Celma, C., **Ragaini, L.**, **Cantalamessa, G.** and **Landini, W.** (2005) Basin physiography and tectonic influence on the sequence architecture and stacking pattern: Pleistocene succession of the Canoa Basin (central Ecuador). *Geol. Soc. Am. Bull.*, **117**, 1226–1241.

Drummond, C.N. and **Wilkinson, B.H.** (1996) Stratal thickness frequencies and the prevalence of orderedness in stratigraphic sequences. *J. Geol.*, **104**, 1–18.

Dumas, S. and **Arnott, R.W.C.** (2006) Origin of hummocky and swaley cross-stratification—The controlling influence of unidirectional current strength and aggradation rate. *Geology*, **34**, 1073–1076.

Einsele, G. (2000) *Sedimentary Basins: Evolution, Facies, and Sediment Budget*, p. 792. Springer-Verlag, Berlin.

Einsele, G. and **Seilacher, A.** (1991) Distinction of tempestites and Turbidites. In: *Cycles and Events in Stratigraphy* (Eds G. Einsele, W. Rickenand and A. Seilacher), pp. 377–382. Springer-Verlag, Berlin.

Ellwood, B.B., **Crick, R.E.**, **Hassani, A.E.**, **Benoist, S.L.** and **Young, R.H.** (2000) Magnetosusceptibility event and cyclostratigraphy method applied to marine rocks: detrital input versus carbonate productivity. *Geology*, **28**, 1135–1138.

Ellwood, B.B., **Algeo, T.J.**, **El Hassani, A.**, **Tomkin, J.H.** and **Rowe, H.D.** (2011) Defining the timing and duration of the Kačák Interval within the Eifelian/Givetian boundary GSSP, Mech Irdane, Morocco, using geochemical and magnetic susceptibility patterns. *Palaeogeogr. Palaeoclimatol. Palaeoecol.*, **304**, 74–84.

Emanuel, K. (2005) Increasing destructiveness of tropical cyclones over the past 30 years. *Nature*, **436**, 686.

Embry, A.F. (1993) Transgressive–regressive (T–R) sequence analysis of the Jurassic succession of the Sverdrup Basin, Canadian Arctic Archipelago. *Can. J. Earth Sci.*, **30**, 301–320.

Embry, A.F. (1995) Sequence boundaries and sequence hierarchies: problems and proposals. In: *Sequence Stratigraphy on the Northwest European Margin* (Eds R.J. Steel, F.L. Felt, E.P. Johannessen and C. Mathieu), NPF Spec. Publ., **5**, 1–11.

Embry, A.F. (2009) Practical sequence stratigraphy. *Can. Soc. Petrol. Geol.*, 81. Available at www.cspg.org

Emig, C.C. (1989) Observations préliminaires sur l'envasement de la biocoenose à *Gryphus vitreus* (Brachiopoda), sur la pente continentale du Nord de la Corse (Méditerranée). Origines et conséquences. *C. R. Acad. Sci. IIb. Mec.*, **309**, 337–342.

Emig, C.C. and **García-Carrascosa, M.A.** (1991) Distribution of *Gryphus vitreus* (Born, 1778) (Brachiopoda) on transect P 2 (Continental margin, French Mediterranean coast) investigated by submersible. *Sci. Mar.*, **55**, 385–388.

Fiorini, F. and **Vaiani, S.C.** (2001) Benthic foraminifers and transgressive-regressive cycles in the Late Quaternary subsurface sediments of the Po Plain near Ravenna (Northern Italy). *Bollettino della Societa Paleontologica Italiana*, **40**, 357–404.

Flügel, E. (2004) *Microfacies Analysis of Carbonate Rocks. Analysis, Interpretation and Application*, p. 976. Springer-Verlag, Berlin.

Franseen, E.K. and **Mankiewicz, C.** (1991) Depositional sequences and correlation of middle (?) to late Miocene carbonate complexes, Las Negras and Níjar areas, southeastern Spain. *Sedimentology*, **38**, 871–898.

Frébourg, G., **Hasler, C.A.** and **Davaud, E.** (2012) Uplifted marine terraces of the Akamas Peninsula (Cyprus): evidence of climatic conditions during the Late Quaternary highstands. *Sedimentology*, **59**, 1409–1425.

Frey, S.E. and **Dashtgard, S.E.** (2012) Seaweed-assisted, benthic gravel transport by tidal currents. *Sed. Geol.*, **265**, 121–125.

Fürsich, F.T. (1995) Shell concentrations. *Eclogae Geol. Helv.*, **88**, 643–655.

Fürsich, F.T., **Oschmann, W.**, **Jaitly, A.K.** and **Singh, I.B.** (1991) Faunal response to transgressive-regressive cycles: example from the Jurassic of western India. *Palaeogeogr. Palaeoclimatol. Palaeoecol.*, **85**, 149–159.

Gani, M.R., **Bhattacharya, J.P.** and **MacEachern, J.A.** (2009) Using ichnology to determine relative influence of waves, storms, tides, and rivers in deltaic deposits: examples from Cretaceous Western Interior Seaway, USA. In: *Applied Ichnology* (Eds J.A. MacEachern, K.L. Bann, M.K. Gingras and S.G. Pemberton), SEPM Short Course Notes, **52**, 209–225.

García-García, F. (2004) Sedimentary models of coarse-grained deltas in the Neogene basins of the Betic Cordillera (SE Spain): Tortonian and Pliocene examples. *Bol. Geol. Min.*, **115**, 469–494.

García-García, F., **Fernández, J.**, **Viseras, C.** and **Soria, J.M.** (2006) High frequency cyclicity in a vertical alternation of Gilbert-type deltas and carbonate bioconstructions in the late Tortonian, Tabernas Basin, Southern Spain. *Sed. Geol.*, **192**, 123–139.

García-García, F., **Corbí, H.**, **Soria, J.M.** and **Viseras, C.** (2011) Architecture analysis of a river flood-dominated delta during an overall sea-level rise (early Pliocene, SE Spain). *Sed. Geol.*, **237**, 102–113.

García-Ramos, D.A., **Corbí, H.A.**, **Pina, J.A.G.** and **Soria, J.M.M.** (2012) Bioestratigrafía de alta resolución basada en foraminíferos planctónicos para el Plioceno inferior del arco de Águilas (cordillera Bética oriental). In: *XXVIII*

Jornadas de la Sociedad Española de Paleontología y Simposios de los Proyectos n. 587 y 596 del PICG. Valencia y Sóller 1-6 de octubre de 2012. Homenaje a Guillem Colom Casasnovas (1900–1993) (Eds J.-C. Liao, J.A. Gámez Vintaned, J.J. Valenzuela-Ríos and A. García-Forner), pp. 67–39. Libro de Resúmenes. Universitat de València. Valencia; Sociedad Española de Paleontología, Madrid.

García-Ramos, D.A., **Corbí, H.** and **Soria, J.M.M.** (2014) Paleoenvironmental analysis of an Early Pliocene section in the Águilas Basin (Eastern Betic Cordillera). *Geogaceta*, **56**, 123–126.

Garden, C.J., **Craw, D.**, **Waters, J.M.** and **Smith, A.** (2011) Rafting rocks reveal marine biological dispersal: A case study using clasts from beach-cast macroalgal holdfasts. *Estuar. Coast. Shelf Sci.*, **95**, 388–394.

Ghinassi, M. (2007) The effects of differential subsidence and coastal topography on high-order transgressive–regressive cycles: Pliocene nearshore deposits of the Val d'Orcia Basin, Northern Apennines, Italy. *Sed. Geol.*, **202**, 677–701.

Giannetti, A., **Baeza-Carratalá, J.F.**, **Soria-Mingorance, J.M.**, **Dulai, A.**, **Tent-Manclús, J.E.** and **Peral-Lozano, J.** (2018) New paleobiogeographical and paleoenvironmental insight through the Tortonian brachiopod and ichnofauna assemblages from the Mediterranean-Atlantic seaway (Guadix Basin, SE Spain). *Facies*, **64**, 24.

de Gibert, J.M. and **Goldring, R.** (2007) An ichnofabric approach to the depositional interpretation of the intensely burrowed Bateig Limestone, Miocene, SE Spain. *Sed. Geol.*, **194**, 1–16.

de Gibert, J.M., **Domènech, R.** and **Martinell, J.** (2007) Bioerosion in shell beds from the Pliocene Roussillon Basin, France: Implications for the (macro) bioerosion ichnofacies model. *Acta Palaeontol. Pol.*, **52**, 783–798.

Gilbert, G.K. (1885) The topographic feature of lake shores. *U.S. Geol. Sur.*, Annual Report, **5**, 104–108.

Goineau, A., **Fontanier, C.**, **Jorissen, F.**, **Buscail, R.**, **Kerhervé, P.**, **Cathalot, C.**, **Pruski, A.M.**, **Lantoine, F.**, **Bourgeois, S.**, **Metzger, E.**, **Legrand, E.** and **Rabouille, C.** (2012) Temporal variability of live (stained) benthic foraminiferal faunas in a river-dominated shelf-faunal response to rapid changes of the river influence (Rhône prodelta, NW Mediterranean). *Biogeosciences*, **9**, 1367–1388.

Grémare, A., **Sardá, R.**, **Medernach, L.**, **Jordana, E.**, **Pinedo, S.**, **Amouroux, J.M.**, **Martin, D.**, **Nozais, C.** and **Charles, F.** (1998) On the dramatic increase of *Ditrupa arietina* O.F. Müller (Annelida: Polychaeta) along both the French and the Spanish Catalan coasts. *Estuar. Coast. Shelf Sci.*, **47**, 447–457.

Griveaud, P., **Coppier, G.**, **Montenat, C.** and **Ott d'Estevou, P.** (1990) Le Néogène des Sierras D'Águilas. In: Les Bassins Néogènes du Domaine Bétique Oriental (Espagne): Tectonique et sédimentation dans un couloir de décrochement. Première partie: Etude Régionale. Doc et Trav. Inst. Geol. Albert-de-Lapparent, Paris no. 12–13, 221–238.

Hallam, A. (1961) Brachiopod life assemblages from the marlstone rock-bed of Leicestershire. *Palaeontology*, **4**, 653–659.

Hansen, K.S. (1999) Development of a prograding carbonate wedge during sea level fall: Lower Pleistocene of Rhodes, Greece. *Sedimentology*, **46**, 559–576.

Harding, S.C., **Nash, B.P.**, **Petersen, E.U.**, **Ekdale, A.A.**, **Bradbury, C.D.** and **Dyar, M.D.** (2014) Mineralogy and geochemistry of the Main Glauconite Bed in the Middle Eocene of Texas: Paleoenvironmental implications for the Verdine Facies. *PLoS One*, **9**, 1–26.

Hartley, J.P. (2014) A review of the occurrence and ecology of dense populations of *Ditrupa arietina* (Polychaeta: Serpulidae). *Mus. Victoria Mem.*, **71**, 85–95.

He, W., **Shi, G.R.**, **Feng, Q.**, **Campi, M.J.**, **Gu, S.**, **Bu, J.**, **Peng, Y.** and **Meng, Y.** (2007) Brachiopod miniaturization and its possible causes during the Permian-Triassic crisis in deep water environments, South China. *Palaeogeogr. Palaeoclimatol. Palaeoecol.*, **252**, 145–163.

Helland-Hansen, W., **Steel, R.J.** and **Sømme, T.O.** (2012) Shelf genesis revisited. *J. Sediment. Res.*, **82**, 133–148.

Hendy, A.J., **Kamp, P.J.** and **Vonk, A.J.** (2006) Cool-water shell bed taphofacies from Miocene-Pliocene shelf sequences in New Zealand: Utility of taphofacies in sequence stratigraphic analysis. In: *Cool-Water Carbonates: Depositional Systems and Palaeoenvironmental Controls* (Eds H.M. Pedley and G. Carannante), Geological Society, London, Special Publications, **255**, 283–305.

Hernández-Molina, F.J., **Fernández-Salas, L.M.**, **Lobo, F.**, **Somoza, L.**, **Díaz-del-Río, V.** and **Dias, J.A.** (2000) The infralittoral prograding wedge: a new large-scale progradational sedimentary body in shallow marine environments. *Geo-Mar. Lett.*, **20**, 109–117.

Iaccarino, S., **Premoli-Silva, I.**, **Biolzi, M.**, **Foresi, L.M.**, **Lirer, F.**, **Turco, E.** and **Petrizzo, M.R.** (2007) *Practical Manual of Neogene Planktonic Foraminifera*. International School on Planktonic Foraminifera, 6th Course. Università degli Studi di Perugia, Perugia, 140 pp.

Jorissen, F.J., **Fontanier, C.** and **Thomas, E.** (2007) Paleoceanographical proxies based on deep-sea benthic foraminiferal assemblage characteristics. *Dev. Mar. Geol.*, **1**, 263–325.

Kidwell, S.M. (1985) Palaeobiological and sedimentological implications of fossil concentrations. *Nature*, **318**, 457–460.

Kidwell, S.M. (1989) Stratigraphic condensation of marine transgressive records: origin of major shell deposits in the Miocene of Maryland. *J. Geol.*, **97**, 1–24.

Kidwell, S.M. (1991) The stratigraphy of shell concentrations. In: *Taphonomy: Releasing the Data Locked in the Fossil Record* (Eds P.A. Allison and D.E.G. Briggs), p. 211–290. Plenum Press, New York, 560 pp.

Kidwell, S.M. (1998) Time-averaging in the marine fossil record: overview of strategies and uncertainties. *Geobios*, **30**, 977–995.

Kidwell, S.M. and **Holland, S.M.** (1991) Field description of coarse bioclastic fabrics. *Palaios*, **6**, 426–434.

Kidwell, S.M., **Fürsich, F.T.** and **Aigner, T.** (1986) Conceptual framework for the analysis and classification of fossil concentrations. *Palaios*, **1**, 228–238.

Kleipool, L.M., **Jong, K.**, **Vaal, E.L.** and **Reijmer, J.J.** (2017) Seismic characterization of switching platform geometries and dominant carbonate producers (Miocene, Las Negras, Spain). *Sedimentology*, **64**, 1676–1707.

Kondo, Y., **Abbott, S.T.**, **Kitamura, A.**, **Kamp, P.J.J.**, **Naish, T.R.**, **Kamataki, T.** and **Saul, G.S.** (1998) The relationship between shellbed type and sequence architecture: examples from Japan and New Zealand. *Sed. Geol.*, **122**, 109–127.

Leckie, R.M. and **Olson, H.C.** (2003) Foraminifera as proxies for sea-level change on siliciclastic margins. In: *Micropaleontologic Proxies for Sea-Level Change and Stratigraphic Discontinuities* (Eds H.C. Olson and R.M. Leckie), Spec. Publ. SEPM Soc. Sediment. Geol., **75**, 5–19.

Leighton, L.R. and **Schneider, C.L.** (2004) Neighbor proximity analysis, a technique for assessing spatial patterns in the fossil record. *Palaios*, **19**, 396–407.

Longhitano, S.G. (2008) Sedimentary facies and sequence stratigraphy of coarse-grained Gilbert-type deltas within the Pliocene thrust-top Potenza Basin (Southern Apennines, Italy). *Sed. Geol.*, **210**, 87–110.

MacEachern, J.A., Raychaudhuri, I. and **Pemberton, S.G.** (1992) Stratigraphic applications of the *Glossifungites* ichnofacies: delineating discontinuities in the rock record. In: *Applications of Ichnology to Petroleum Exploration* (Ed. S.G. Pemberton), pp. 169–198. Society of Economic Paleontologists and Mineralogists, Core Workshop Notes 17, Tulsa.

MacEachern, J.A., Bann, K.L., Bhattacharya, J.P. and **Howell, C.D. Jr** (2005) Ichnology of deltas: organism responses to the dynamic interplay of rivers, waves, storms, and tides. In: *River Deltas: Concepts, Models and Examples* (Eds L. Giosan And J.P. Bhattacharya), SEPM Special Publication **83**, 49–85.

MacEachern, J., Bann, K., Gingras, M., Zonneveld, J., Dashtgard, S. and **Pemberton, S.** (2012a) The ichnofacies paradigm. In: *Trace Fossils as Indicators of Sedimentary Environments* (Eds D. Knaust and R.G. Bromley), pp. 103–138. Elsevier, Amsterdam.

MacEachern, J.A., Dashtgard, S.E., Knaust, D., Catuneanu, O., Bann, K.L. and **Pemberton, S.G.** (2012b) Sequence stratigraphy. In: *Trace Fossils as Indicators of Sedimentary Environments* (Eds D. Knaust, R.G. Bromley), pp. 157–194. Elsevier, Amsterdam.

Malatesta, A. (1974) Malacofauna pliocenica umbra. *Memorie per Servire alla Carta Geologica d'Italia*, **13**, 1–498.

Mancosu, A. and **Nebelsick, J.H.** (2017) Ecomorphological and taphonomic gradients in clypeasteroid-dominated echinoid assemblages along a mixed siliciclastic-carbonate shelf from the early Miocene of northern Sardinia, Italy. *Acta Palaeontol. Pol.*, **62**, 627–646.

Martín, J.M., Braga, J.C., Aguirre, J. and **Betzler, C.** (2004) Contrasting models of temperate carbonate sedimentation in a small Mediterranean embayment: the Pliocene Carboneras Basin, SE Spain. *J. Geol. Soc.*, **161**, 387–399.

Martinell, J., Kowalewski, M. and **Domènech, R.** (2012) Drilling predation on serpulid polychaetes (*Ditrupa arietina*) from the Pliocene of the Cope Basin, Murcia region, southeastern Spain. *PLoS One*, **7**, 1–14.

Massari, F. and **Chiocci, F.** (2006) Biocalcarenite and mixed cool-water prograding bodies of the Mediterranean Pliocene and Pleistocene: architecture, depositional setting and forcing factors. In: *Cool-Water Carbonates: Depositional Systems and Palaeoenvironmental Controls* (Eds H.M. Pedley and G. Carannante), Geol. Soc. London Spec. Publ., **255**, 5–120.

Massari, F. and **D'Alessandro, A.** (2012) Facies partitioning and sequence stratigraphy of a mixed siliciclastic-carbonate ramp stack in the Gelasian of Sicily (S Italy): a potential model for Icehouse, distally-steepened Heterozoan ramps. *Rivista Italiana di Paleontologia e Stratigraphia*, **118**, 503–534.

Massari, F., Sgavetti, M., Rio, D., D'Alessandro, A. and **Prosser, G.** (1999) Composite sedimentary record of falling stages of Pleistocene glacio-eustatic cycles in a shelf setting (Crotone basin, south Italy). *Sed. Geol.*, **127**, 85–110.

Massari, F., Rio, D., Sgavetti, M., Prosser, G., D'Alessandro, A., Asioli, A., Capraro, L., Fornaciari, E. and **Tateo, F.** (2002) Interplay between tectonics and glacio-eustasy: Pleistocene succession of the Crotone basin, Calabria (southern Italy). *Geol. Soc. Am. Bull.*, **114**, 1183–1209.

Mayoral, E., Ledesma-Vazquez, J., Baarli, B.G., Santos, A., Ramalho, R., Cachão, M. and **Johnson, M.E.** (2013) Ichnology in oceanic islands; case studies from the Cape Verde Archipelago. *Palaeogeogr. Palaeoclimatol. Palaeoecol.*, **381**, 47–66.

Middlemiss, F.A. (1962) Brachiopod ecology and lower greensand palaeogeography. *Palaeontology*, **5**, 253–267.

Minchin, D. (2003) Introductions: some biological and ecological characteristics of scallops. *Aquat. Living Resour.*, **16**, 521–532.

Mitchell, N.C. (2012) Modeling the rollovers of sandy clinoforms from the gravity effect on wave-agitated sand. *J. Sediment. Res.*, **82**, 464–468.

Mitchum, R.M. and **Van Wagoner, J.C.** (1991) High-frequency sequences and their stacking patterns: sequence-stratigraphic evidence of high-frequency eustatic cycles. *Sed. Geol.*, **70**, 131–160.

Moissette, P., Cornée, J.J. and **Koskeridou, E.** (2010) Pleistocene rolling stones or large bryozoan nodules in a mixed siliciclastic-carbonate environment (Rhodes, Greece). *Palaios*, **25**, 24–39.

Montenat, C., de Reneville, P. and **Bizon, G.** (1978) Le Néogène des environs d'Aguilas (provinces de Murcia et d'Almeria) Cordilleres bétiques, Espagne. *Bulletin Musée National d'Histoire Naturelle, Sciences de la Terre*, **68**, 37–54.

Mount, J.F. (1984) Mixing of siliciclastic and carbonate sediments in shallow shelf environments. *Geology*, **112**, 432–435.

Mulder, T. and **Alexander, J.** (2001) The physical character of subaqueous sedimentary density flows and their deposits. *Sedimentology*, **48**, 269–299.

Myrow, P.M. (2005) Storms and storm deposits. In: *Encyclopedia of Geology* (Eds R.C. Selley, R. Cocks and I. Pilmer), pp. 580–587. Elsevier Limited, Oxford.

Naish, T.R. and **Kamp, P.J.J.** (1997) Sequence stratigraphy of sixth-order (41 k.y.) Pliocene-Pleistocene cyclothems, Wanganui basin, New Zealand: a case for the regressive systems tract. *Geol. Soc. Am. Bull.*, **109**, 978–999.

Nalin, R., Ghinassi, M. and **Basso, D.** (2010) Onset of temperate carbonate sedimentation during transgression in a low-energy siliciclastic embayment (Pliocene of the Val d'Orcia Basin, Tuscany, Italy). *Facies*, **56**, 353–368.

Nalin, R., Ghinassi, M., Foresi, L.M. and **Dallanave, E.** (2016) Carbonate Deposition in Restricted Basins: A Pliocene Case Study From the Central Mediterranean (Northwestern Apennines), Italy. *J. Sed. Res.*, **86**, 236–267.

Neal, J. and **Abreu, V.** (2009) Sequence stratigraphy hierarchy and the accommodation succession method. *Geology*, **37**, 779–782.

Odin, G.S. and **Fullagar, P.D.** (1988) Geological significance of the glaucony facies. In: *Green Marine Clays* (Ed. G.S. Odin), Developments in Sedimentology, **45**, 295–332.

ÖNORM L 1084 (2006) Chemical analyses of soils—determination of carbonate. In: *Austrian Standards Institute* (Ed. ÖNORM L 1084), pp. 2–8. Austrian Standards Institute, Vienna.

Patruno, S., Hampson, G.J. and **Jackson, C.A.-L.** (2015) Quantitative characterisation of deltaic and subaqueous clinoforms. *Earth Sci. Rev.*, **142**, 79–119.

Pearson, N.J., Gabriela Mángano, M., Buatois, L.A., Casadío, S. and **Raising, M.R.** (2013) Environmental variability of

Macaronichnus ichnofabrics in Eocene tidal-embayment deposits of southern Patagonia, Argentina. *Lethaia*, **46**, 341–354.

Pemberton, S.G., MacEachern, J.A. and **Ranger, M.J.** (1992) Ichnology and event stratigraphy: the use of trace fossils in recognizing tempestites. In: *Applications of Ichnology to Petroleum Exploration: A Core Workshop* (Ed. S.G. Pemberton), Society for Sedimentary Geology Core Workshop, **17**, 85–118.

Pemberton, S.G., MacEachern, J.A., Gingras, M.K. and **Saunders, T.D.** (2008) Biogenic chaos: Cryptobioturbation and the work of sedimentologically friendly organisms. *Palaeogeogr. Palaeoclimatol. Palaeoecol.*, **270**, 273–279.

Pepe, F., Bertotti, G., Ferranti, L., Sacchi, M., Collura, A.M., Passaro, S. and **Sulli, A.** (2014) Pattern and rate of post-20 ka vertical tectonic motion around the Capo Vaticano Promontory (W Calabria, Italy) based on offshore geomorphological indicators. *Quatern. Int.*, **332**, 85–98.

Pérez-Asensio, J.N., Aguirre, J. and **Rodríguez-Tovar, F.J.** (2017) The effect of bioturbation by polychaetes (Opheliidae) on benthic foraminiferal assemblages and test preservation. *Palaeontology*, **60**, 807–827.

Pervesler, P., Uchman, A. and **Hohenegger, J.** (2008) New methods for ichnofabric analysis and correlation with orbital cycles exemplified by the Baden-Sooss section (Middle Miocene, Vienna Basin). *Geol. Carpath.*, **59**, 395–409.

Pirmez, C., Pratson, L.F. and **Steckler, M.S.** (1998) Clinoform development by advection-diffusion of suspended sediment: Modeling and comparison to natural systems. *J. Geophys. Res.*, **103**, 24141–24157.

Plint, A.G. (1988) Sharp-based shoreface sequences and 'offshore bars' in the Cardium Formation of Alberta: their relationship to relative changes in sea level. In: *Sea-level Changes: An Integrated Approach* (Eds C.K. Wilgus, B.S. Hastings, C.G.St.C. Kendall, H.W. Posamentier, C.A. Rossand and J.C. Van Wagoner), Society of Economic Paleontologists and Mineralogists Special Publications, **42**, 357–370.

Plint, A.G. and **Nummedal, D.** (2000) The falling stage systems tract: recognition and importance in sequence stratigraphic analysis. *Geol. Soc., London, Spec. Pub.*, **172**, 1–17.

Pomar, L. (2001) Types of carbonate platforms: a genetic approach. *Basin Res.*, **13**, 313–334.

Pomar, L. and **Kendall, C.G.C.** (2008) Architecture of carbonate platforms: a response to hydrodynamics and evolving ecology. In: *Controls on Carbonate Platform and Reef Development* (Eds J. Lukasik and J. A Simo), SEPM Special Publication, **89**, 187–216.

Pomar, L. and **Ward, W.C.** (1994) Response of a late Miocene Mediterranean reef platform to high-frequency eustasy. *Geology*, **22**, 131–134.

Pomar, L., Obrador, A. and **Westphal, H.** (2002) Sub-wavebase cross-bedded grainstones on a distally steepened carbonate ramp, Upper Miocene, Menorca, Spain. *Sedimentology*, **49**, 139–169.

Pomar, L., Aurell, M., Bádenas, B., Morsilli, M. and **Al-Awwad, S.F.** (2015) Depositional model for a prograding oolitic wedge, Upper Jurassic, Iberian basin. *Mar. Pet. Geol.*, **67**, 556–582.

Postma, G. (1990) An analysis of the variation in delta architecture. *Terra Nova*, **2**, 124–130.

Postma, G., Nemec, W. and **Kleinspehn, K.L.** (1988) Large floating clasts in turbidites: a mechanism for their emplacement. *Sed. Geol.*, **58**, 47–61.

Pouchou, J.L. and **Pichoir, F.** (1991) Quantitative analysis of homogeneous or stratified microvolumes applying the model "PAP". In: *Electron Probe Quantitation* (Eds K.F.J. Heinrich and D.E. Newbury), pp. 31–75. Plenum Press, New York, NY.

Rasmussen, T.L. (2005) Systematic paleontology and ecology of benthic foraminifera from the Plio-Pleistocene Kallithea Bay section, Rhodes, Greece. *Cushman Foun. Spec. Pub.*, **39**, 53–157.

Read, J.F. (1985) Carbonate platform facies models. *Am. Assoc. Petrol. Geol. Bulletin*, **69**, 1–21.

Reolid, M., García-García, F., Tomašových, A. and **Soria, J.M.** (2012) Thick brachiopod shell concentrations from prodelta and siliciclastic ramp in a Tortonian Atlantic-Mediterranean strait (Miocene, Guadix Basin, southern Spain). *Facies*, **58**, 549–571.

Reuter, M., Piller, W.E., Brandano, M. and **Harzhauser, M.** (2013) Correlating Mediterranean shallow water deposits with global Oligocene-Miocene stratigraphy and oceanic events. *Global Planet. Change*, **111**, 226–236.

Rich, J.L. (1951) Three critical environments of deposition, and criteria for recognition of rocks deposited in each of them. *Geol. Soc. Am. Bull.*, **62**, 1–20.

Robba, E. (1996) Autoecology of some Pliocene thin-shelled pectinids. In: *Autecology of Selected Fossil Organisms: Achievements and Problems* (Ed. A. Cherchi), Bollettino della Società Paleontologica Italiana, Special Volume **3**, 159–174.

Rodríguez-Tovar, F.J. and **Aguirre, J.** (2014) Is *Macaronichnus* an exclusively small, horizontal and unbranched structure? *Macaronichnus segregatis degiberti* isubsp. nov. *Spanish J. Palaeontol.*, **29**, 131–142.

Roetzel, R. and **Pervesler, P.** (2004) Storm-induced event deposits in the type area of the Grund Formation (Middle Miocene, Lower Badenian) in the Molasse Zone of Lower Austria. *Geol. Carpath.*, **55**, 87–102.

Rothwell, R.G. and **Croudace, I.W.** (2015) Twenty years of XRF core scanning marine sediments: What do geochemical proxies tell us? In: *Micro-XRF Studies of Sediment Cores: Applications of a Non-Destructive Tool for the Environmental Sciences* (Eds I.W. Croudace and R.G. Rothwell), pp. 25–102. Springer, Dordrecht.

Ruban, D.A. (2015) Worldwide application of synthem stratigraphy in the 21st century: a bibliographical survey. *Proc. Geol. Assoc.*, **126**, 307–313.

Ruffell, A. and **Wach, G.** (1998) Firmgrounds–key surfaces in the recognition of parasequences in the Aptian Lower Greensand Group, Isle of Wight (southern England). *Sedimentology*, **45**, 91–107.

Sanfilippo, R. (1999) *Ditrupa brevis* n. sp., a new serpulid from the Mediterranean Neogene with comments on the ecology of the genus. *Riv. Ital. Paleontol. Stratigr.*, **105**, 455–463.

Scarponi, D., Huntley, J.W., Capraro, L. and **Raffi, S.** (2014) Stratigraphic paleoecology of the Valle di Manche section (Crotone Basin, Italy): a candidate GSSP of the Middle Pleistocene. *Palaeogeogr. Palaeoclimatol. Palaeoecol.*, **402**, 30–43.

Schlager, W. (2004) Fractal nature of stratigraphic sequences. *Geology*, **32**, 185–188.

Schlager, W. (2010) Ordered hierarchy versus scale invariance in sequence stratigraphy. *Int. J. Earth Sci.*, **99**, 139–151.

Sgarrella, F. and **Moncharmont Zei, M.** (1993) Benthic Foraminifera of the Gulf of Naples (Italy): systematics and

autoecology. *Bollettino della Società Paleontologica Italiana*, **32**, 145–264.

Silva, P.G., **Goy, J.L.**, **Somoza, L.**, **Zazo, C.** and **Bardají, T.** (1993) Landscape response to strike-slip faulting linked to collisional settings: Quaternary tectonics and basin formation in the Eastern Betics, Southeast Spain. *Tectonophysics*, **224**, 289–303.

Soria, J.M., **Fernández, J.**, **García, F.** and **Viseras, C.** (2003) Correlative lowstand deltaic and shelf systems in the Guadix Basin (Late Miocene, Betic Cordillera, Spain): the stratigraphic record of forced and normal regressions. *J. Sediment. Res.*, **73**, 912–925.

Sullivan, N.B. and **Brett, C.E.** (2013) Integrating magnetic susceptibility data with sequence stratigraphy in the ironstone bearing successions (Lower Silurian) of eastern North America. *Stratigraphy*, **10**, 261–280.

Swift, D.J.P. and **Thorne, J.A.** (1991) Sedimentation on continental margins, I: a general model for shelf sedimentation. In: *Shelf Sand and Sandstone Bodies* (Eds D.J.P. Swift, G.F. Oertel, R.W. Tillman and J.A. Thorne), IAS Special Publication, **14**, 3–31.

Talling, P.J., **Masson, D.G.**, **Sumner, E.J.** and **Malgesini, G.** (2012) Subaqueous sediment density flows: depositional processes and deposit types. *Sedimentology*, **59**, 1937–2003.

Taylor, A., **Goldring, R.** and **Gowland, S.** (2003) Analysis and application of ichnofabrics. *Earth Sci. Rev.*, **60**, 227–259.

Thorne, J. (1995) On the scale independent shape of prograding stratigraphic units. In: *Fractals in Petroleum Geology and Earth Processes* (Eds C.C. Barton and P.R. La Pointe), pp. 97–112. Springer, Boston, MA.

Tomašových, A. and **Kidwell, S.M.** (2017) Nineteenth-century collapse of a benthic marine ecosystem on the open continental shelf. *Proc. R. Soc. B*, **284**, 20170328.

Tomašových, A., **Fürsich, F.T.** and **Olszewski, T.D.** (2006) Modeling shelliness and alteration in shell beds: variation in hardpart input and burial rates leads to opposing predictions. *Paleobiology*, **32**, 278–298.

Tomassetti, L. and **Brandano, M.** (2013) Sea level changes recorded in mixed siliciclastic–carbonate shallow-water deposits: The Cala di Labra Formation (Burdigalian, Corsica). *Sed. Geol.*, **294**, 58–67.

Uchman, A., **Demírcan, H.**, **Toker, V.**, **Derman, A.S.**, **Sevim, S.** and **Szulc, J.** (2002) Relative sea-level changes recorded in borings from a Miocene rocky shore of the Mut Basin, southern Turkey. *Ann. Soc. Geol. Pol.*, **72**, 263–270.

Uchman, A., **Johnson, M.E.**, **Rebelo, A.C.**, **Melo, C.**, **Cordeiro, R.**, **Ramalho, R.S.** and **Ávila, S.P.** (2016) Vertically-oriented trace fossil *Macaronichnus segregatis* from Neogene of Santa Maria Island (Azores; NE Atlantic) records vertical fluctuations of the coastal groundwater mixing zone on a small oceanic island. *Geobios*, **49**, 229–241.

Vail, P.R., **Audemard, F.**, **Bowman, S.A.**, **Eisner, P.N.** and **Pérez-Cruz, G.** (1991) The stratigraphic signatures of tectonics, eustasy and sedimentology – an overview. In: *Cycles and Events in Stratigraphy* (Eds G. Einsele, W. Ricken and A. Seilacher), pp. 617–659. Springer-Verlag, Berlin.

Violanti, D. (2012) Pliocene Mediterranean foraminiferal biostratigraphy: a synthesis and application to the paleoenvironmental evolution of Northwestern Italy. In: *Stratigraphic Analysis of Layered Deposits* (Ed. Ö. Elitok), pp. 123–160. InTech Open Access Publisher: Rijeka. Available at: https://www.intechopen.com/books/stratigraphic-analysis-of-layered-deposits/pliocene-mediterranean-foraminiferal-biostratigraphy-a-synthesis-and-application-to-the-paleoenviro

Waller, T.H. (2011) Neogene Paleontology of the Northern Dominican Republic. 24. *Propeamussiidae* and *Pectinidae* (Mollusca: Bivalvia: Pectinoidea) of the Cibao Valley. *Bull. Am. Paleontol.*, **381**, 1–198.

Walsh, J.P., **Nittrouer, C.A.**, **Palinkas, C.M.**, **Ogston, A.S.**, **Sternberg, R.W.** and **Brunskill, G.J.** (2004) Clinoform mechanics in the Gulf of Papua, New Guinea. *Cont. Shelf Res.*, **24**, 2487–2510.

Wanless, H.R., **Tedesco, L.P.** and **Tyrrell, K.M.** (1988) Production of subtidal and surficial tempestites by hurricane Kate, Caoicos platform, British West Indies. *J. Sediment. Petrol.*, **58**, 739–750.

Yesares-García, J. and **Aguirre, J.** (2004) Quantitative taphonomic analysis and taphofacies in lower Pliocene temperate carbonate–siliciclastic mixed platform deposits (Almería-Níjar basin, SE Spain). *Palaeogeogr. Palaeoclimatol. Palaeoecol.*, **207**, 83–103.

Zecchin, M. (2007) The architectural variability of small-scale cycles in shelf and ramp clastic systems: the controlling factors. *Earth Sci. Rev.*, **84**, 21–55.

Zecchin, M. and **Catuneanu, O.** (2013) High-resolution sequence stratigraphy of clastic shelves I: units and bounding surfaces. *Mar. Pet. Geol.*, **39**, 1–25.

Zecchin, M. and **Catuneanu, O.** (2017) High-resolution sequence stratigraphy of clastic shelves VI: Mixed siliciclastic-carbonate systems. *Mar. Pet. Geol.*, **88**, 712–723.

Zecchin, M., **Caffau, M.**, **Catuneanu, O.** and **Lenaz, D.** (2017) Discrimination between wave-ravinement surfaces and bedset boundaries in Pliocene shallow-marine deposits, Crotone Basin, southern Italy: an integrated sedimentological, micropaleontological and mineralogical approach. *Sedimentology*, **64**, 1755–1791.

Zuschin, M. and **Stanton, R.J. Jr** (2002) Paleocommunity reconstruction from shell beds: a case study from the Main Glauconite Bed, Eocene, Texas. *Palaios*, **17**, 602–614.

Manuscript received 3 November 2017; revision accepted 20 September 2018

Supporting Information

Additional information may be found in the online version of this article:

Fig. S1. Photomosaic of the base of the Terreros section, showing the cyclically bedded synthem SP0 (Zanclean, MPl1 MPl2 biozones) and the overlying calcirudites of SP1 (MPl3 biozone *fide* Montenat *et al.*, 1978) on top, resting on an erosion surface (SP0 SP1 unconformity).

Fig. S2. Some examples of allochthonous elements in FA4 and FA3.

SUPPORTING INFORMATION

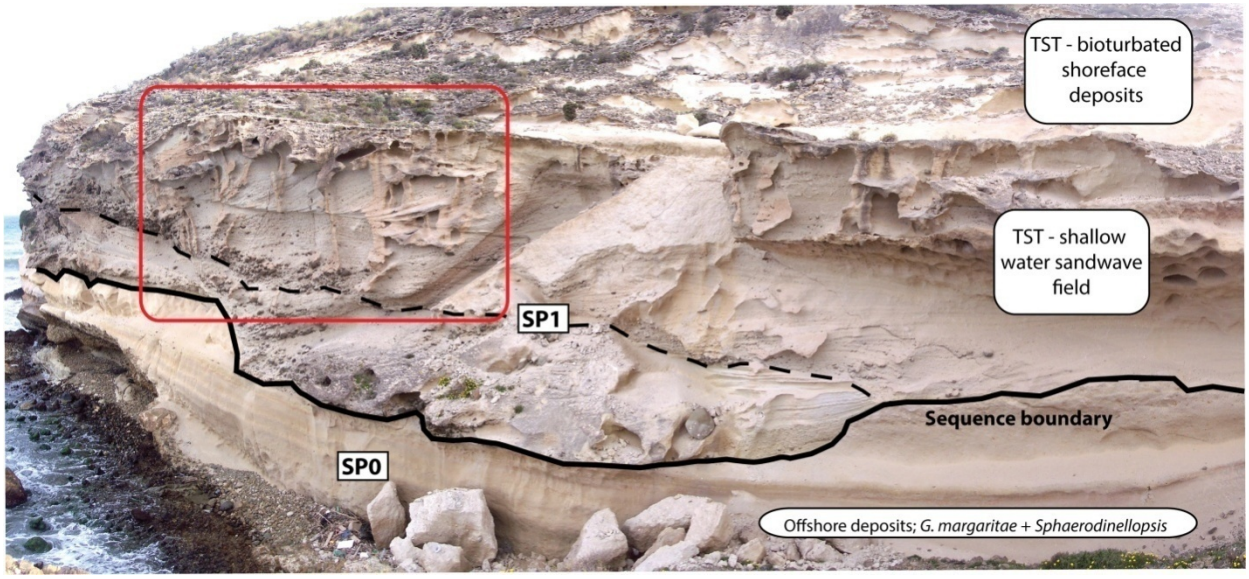

Fig. S1. Photomosaic of the base of the Terreros section, showing the cyclically bedded synthem SP0 (Zanclean, MPl1–MPl2 biozones) and the overlying calcirudites of SP1 (MPl3 biozone *fide* Montenat *et al*.,1978) on top, resting on an erosion surface (SP0–SP1 unconformity).

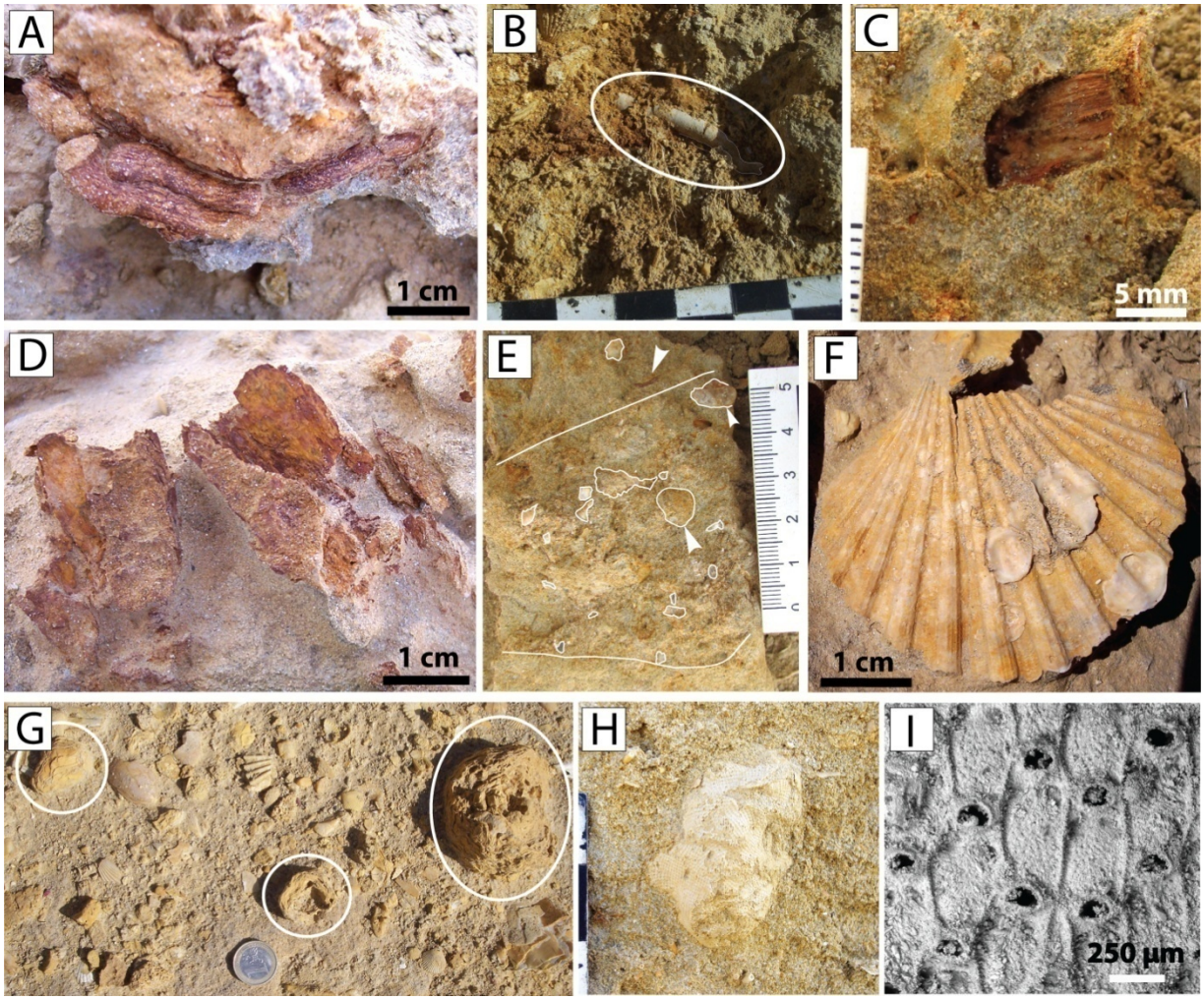

Fig. S2. Some examples of allochthonous elements in FA4 and FA3.

Chapter 3

MANUSCRIPT 2

The environmental factors limiting the distribution of shallow-water terebratulid brachiopods

Authors: Diego A. García-Ramos, Stjepan Ćorić, Michael Joachimski and Martin Zuschin

Publication status: accepted on the 12th January 2020 in *Paleobiology*

The environmental factors limiting the distribution of shallow-water terebratulid brachiopods

Diego A. García-Ramos, Stjepan Ćorić, Michael M. Joachimski, and Martin Zuschin

Abstract.—The Cenozoic genus *Terebratula* seems to be an exception to the post-Permian trend in brachiopod retreat to offshore habitats, because it was species rich and numerically abundant in warm-temperate shallow-water environments in the Mediterranean and the Paratethys realms. This was so despite the general dominance of bivalves and the pervasive bioturbation and predation pressure during the Neogene. *Terebratula*, however, went extinct in the Calabrian (Pleistocene). The optimal environmental conditions for *Terebratula* during its prime are poorly known. The Águilas Basin (SE Spain) is an ideal study area to investigate the habitat of *Terebratula*, because shell beds of this brachiopod occur there cyclically in early Pliocene deposits. We evaluate the paleoecological boundary conditions controlling the distribution of *Terebratula* by estimating its environmental tolerances using benthic and planktic foraminiferal and nannoplanktic assemblages and oxygen isotopes of the secondary layer brachiopod calcite. Our results suggest that *Terebratula* in the Águilas Basin favored oligotrophic to mesotrophic, well-oxygenated environments at water depths of 60–90 m. Planktic foraminiferal assemblages and oxygen isotopes point to sea-surface temperatures between ~16°C and 22°C, and bottom-water temperatures between 17°C and 24°C. The analyzed proxies indicate that *Terebratula* tolerated local variations in water depth, bottom temperature, oxygenation, productivity, and organic enrichment. *Terebratula* was probably excluded by grazing pressure from well-lit environments and preferentially occupied sediment-starved, current-swept upper offshore habitats where coralline red algae were absent. Narrow temperature ranges of *Terebratula* species might have been a disadvantage during the high-amplitude seawater temperature fluctuations that started about 1 Ma, when the genus went extinct.

Diego A. García-Ramos and Martin Zuschin. Department of Paleontology, University of Vienna,

Althanstrasse, 14, A-1090, Vienna, Austria. E-mail: garcia.ramosda@univie.ac.at, martin.zuschin@univie.ac.at

Stjepan Ćorić. Geological Survey of Austria, Neulinggasse, 38, A-1030, Vienna, Austria. E-mail: stjepan.coric@geologie.ac.at

Michael M. Joachimski. GeoZentrum Nordbayern, Universität Erlangen-Nürnberg, Schlossgarten 5, 91054 Erlangen, Germany. E-mail: michael.joachimski@fau.de

Accepted: 8 February 2020

Data available from the Dryad Digital Repository: https://doi.org/10.5061/dryad.h9w0vt4dz

Introduction

Brachiopods were the most successful benthic marine animals during the Paleozoic (Thayer 1986), with about 400 species remaining today (Emig et al. 2013). In Recent seas, terebratulids are by far the most successful of all brachiopod clades (Lee 2008). Like other representatives of the subfamily Terebratulinae, such as *Pliothyrina* and *Maltaia*, some species of "*Terebratula*" appear to stand as an exception to the general progressive trend of brachiopod retreat to deep and/or cryptic habitats after the Permian–Triassic mass extinction (Tomašových 2006). This is because Terebratulinae were numerically abundant above the storm-weather wave base (Kroh et al. 2003; Gramigna et al. 2008; Pervesler et al. 2011), much like other Terebratulida can dominate in present-day, shallow-water hard-bottom environments (Logan and Noble 1971; Richardson 1981; Försterra et al. 2008; Tomašových 2008). European Terebratulinae, however, went extinct in the Calabrian (approximately during or shortly after the Jaramillo Subchron), not surviving beyond the Sicilian (D'Alessandro et al. 2004; Taddei Ruggiero and Taddei 2006; La Perna and Vazzana 2016; Crippa et al. 2019), with the last species being *Terebratula terebratula* and *Terebratula scillae*. Although Neogene and Pleistocene *Terebratula* had to cope with specialized predators, niche competitors (bivalves), and bulldozing and grazing marine organisms (Thayer 1983), it thrived mainly in warm-temperate shallow-water detritic-bottom habitats in the Paratethys and the Mediterranean realms

(Pedley 1976; Bitner and Pisera 2000; Reolid et al. 2012). There are also reports from subtropical environments, where species of *Terebratula* infilled cavities in *Porites–Tarbellastraea* reefs during the Tortonian (Barbera et al. 1995) or were present on the distal slope of *Porites* fringing reefs during the lower Messinian (Llompart and Calzada 1982; Obrador et al. 1983; Videt 2003). Little is known, however, about the paleoecology of *Terebratula* (Benigni and Robba 1990; Pavia and Zunino 2008). Narrowing down the factors that led European Terebratulinae to extinction calls for improving our knowledge about the habitats and the ecological niche occupied by these terebratulids in their prime. This study is designed to help fill this gap by evaluating the environmental conditions in the subenvironments where the *Terebratula* populations were at their optimum in the Pliocene outcrops of the Águilas Basin (SE Spain), as well as the paleoecological boundary conditions onshore and offshore of this optimum. More specifically, we estimate environmental tolerances of this brachiopod with respect to water depth, bottom oxygenation, bottom temperature, productivity, and organic enrichment. This study area is among the most suitable for this purpose, because abundant and almost monospecific shell beds of *Terebratula* occur here cyclically in a mixed temperate carbonate–siliciclastic system (García-Ramos and Zuschin 2019).

Study Area and Paleoenvironmental Setting

The Águilas Basin (SE Spain) is located in the southwestern inner sector of the tectonic Águilas Arc (Fig. 1A,B), in the Internal Betic Zone (Coppier et al. 1989). The Águilas Basin was a small embayment (about 14 km wide) during the early Pliocene (Fig. 1C) (García-Ramos and Zuschin 2019).

The studied brachiopods belong to a sequence of late Zanclean age (MPl3 planktic foraminiferal biozone of the Mediterranean Pliocene; for the biozonation, see Iaccarino et al. [2007] and Corbí and Soria [2016]). The present study also yielded scarce specimens of the nannoplankton species *Reticulofenestra* cf. *cisnerosi* at the base of the sequence. This occurrence, together with the absence of *Discoaster tamalis* and the association with *Globorotalia puncticulata* and *Globorotalia*

margaritae, constrains the age of the base of the sequence to the older part of Subchron C3n.1r (between 4.52 and 4.42 Ma), according to the biostratigraphic scheme of Lancis et al. (2015).

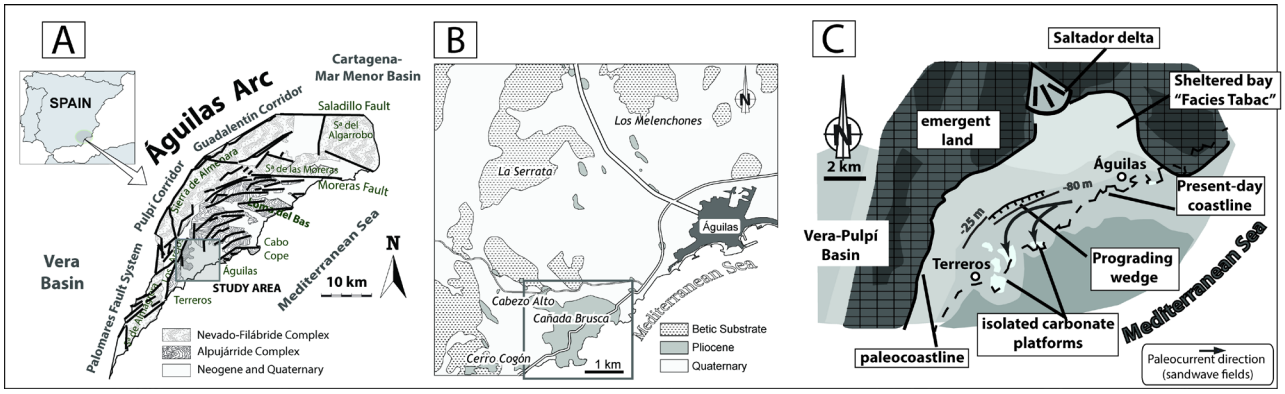

FIGURE 1. A, Location of the Águilas Arc in southeast Spain (adapted from Bardají et al. 2001). B, Location of the Cabezo Alto–Cañada Brusca area in the Águilas Basin. C, Paleogeographic map of the Águilas Basin during the Zanclean (adapted from García-Ramos and Zuschin 2019).

The studied strata define originally inclined units that were deposited on a slope (termed "clinobeds"), which were interpreted to reflect high-frequency and low-amplitude relative sea-level changes (García-Ramos and Zuschin 2019). Sedimentologically, these clinobedded units are consistent with sand-prone subaqueous delta-scale clinoforms (sensu Patruno et al. 2015), which developed entirely below sea level. The most proximal deposits are bioturbated coarse sands, followed distally by rhodolith-rich finer-grained sediments (rhodalgal facies). Both facies correspond to the topset of the clinoforms (Fig. 2A). Following a biological benthic zonation (i.e., Gili et al. 2014), these environments were interpreted as mediolittoral to infralittoral (foreshore to upper shoreface) and lower infralittoral to upper circalittoral (lower shoreface) (García-Ramos and Zuschin 2019). The rhodolith debris disappears gradually toward the basin, giving way to fine-grained sands rich in the polychaete *Ditrupa arietina* along with benthic and planktic foraminifera. The disappearance of the rhodoliths distally can be interpreted as a transition zone from the upper circalittoral to the lower circalittoral (Basso 1998; Cameron and Askew 2011; Gili et al. 2014). This

facies transition between rhodalgal and *Ditrupa*-rich deposits was also interpreted as the offshore

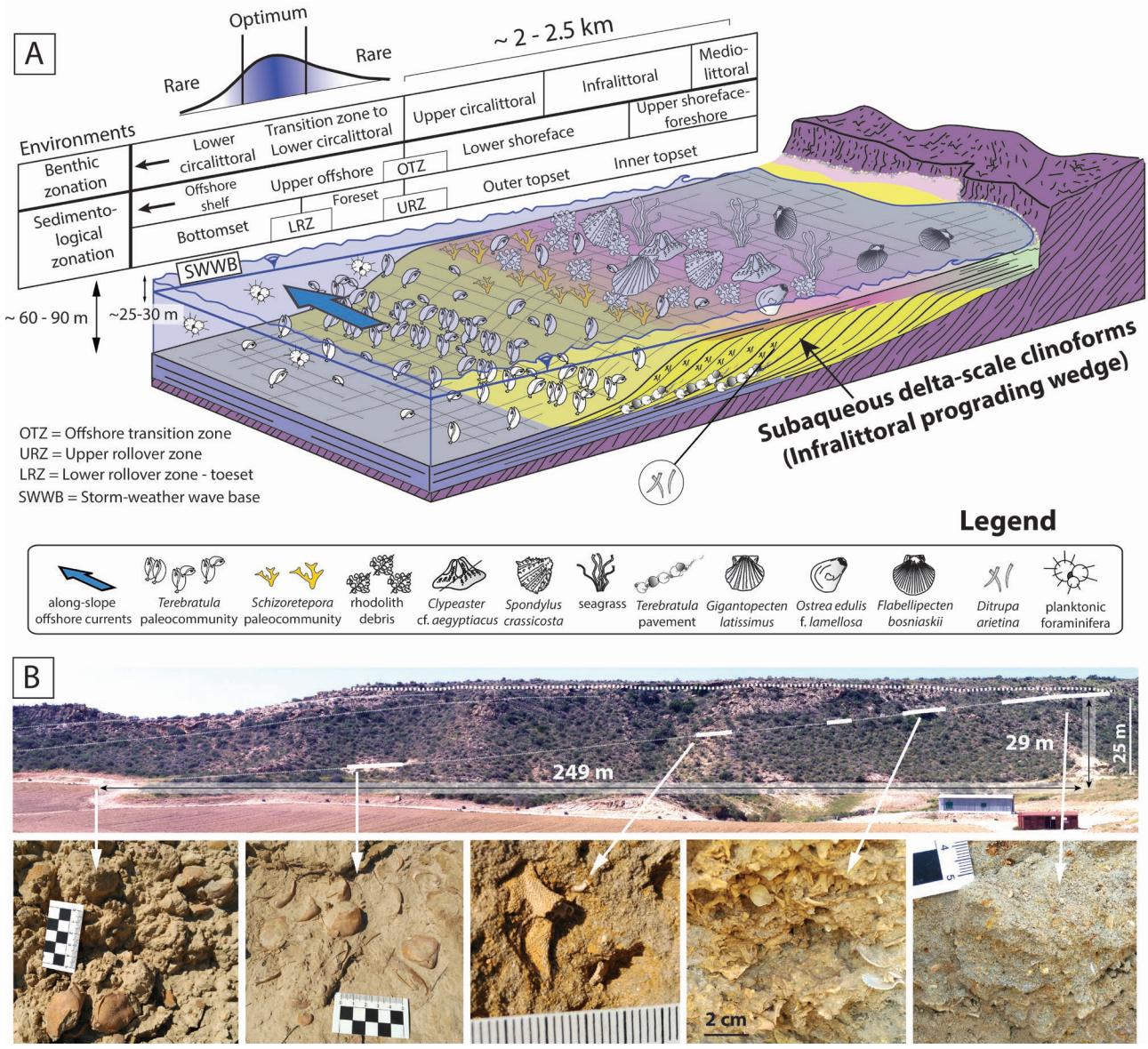

FIGURE 2. A, Depositional setting of the late Zanclean sediments in the study area and the paleoenvironmental distribution of *Terebratula* across the depositional profile. Included are a biological benthic zonation slightly modified from Gili et al. (2014) and a sedimentological zonation based on Pomar and Tropeano (2001) and García-Ramos and Zuschin (2019). The depositional profile is adapted from Pomar et al. (2015). B, Field photo of subaqueous delta-scale clinoforms, with outcrop photos of biofacies along a proximal–distal gradient: *Schizoretepora*-rhodolith debris, *Schizoterepora* and *Terebratula* biofacies (adapted from García-Ramos and Zuschin 2019).

transition zone (OTZ) based on sedimentological evidence; it coincides with the topset–foreset transition (i.e., upper rollover) of the clinoforms (García-Ramos and Zuschin 2019). The *Ditrupa* facies in this transition zone to the lower circalittoral corresponds to the foreset of the clinoforms (Fig. 2A). The most distal facies in our area is fine-grained muddy sands with the characteristic pectinid *Costellamussiopecten cristatum* occurring as dispersed, disarticulated shells (Fig. 2A, bottomset of the clinoforms). These deposits can be interpreted as formed in upper offshore environments, also within the transition zone to the lower circalittoral.

In the above facies, 5- to 20-cm-thick monospecific pavements of *Terebratula calabra* (Figs. 2B and 3A,B) are interspersed cyclically (Fig. 2A). Locally the pavements also yield rare specimens of the rhynchonellid *Aphelesia bipartita*. As a rule, the greatest *Terebratula* concentrations occur in the transition between the foreset and the bottomset (the lower rollover zone) (Fig. 2A,B), where the *Terebratula* pavements show loosely to densely packed biofabrics (Figs. 2B and 3B). The density of *Terebratula* decreases toward more proximal (foreset) and more distal positions (bottomset) (Figs. 2A and 3C) in the depositional profile. The rhodalgal facies (lower shoreface) also contains rare, isolated specimens of *Terebratula* (Fig. 3D,E). The shells in the pavements are mostly complete, articulated, and minimally encrusted by epizoans or bioeroded (recording rare traces of *Podichnus obliquus* produced by conspecifics). These concentrations were interpreted as parautochthonous assemblages in relatively shallow-water but offshore (circalittoral) environments during stages of reduced sedimentation rates (for details, see García-Ramos and Zuschin 2019). A recognizable 1.5- to 2-m-thick bed dominated by *Terebratula* in the study area shows loose to densely packed biofabrics (Fig. 3F–J). The taxonomic richness in this bed is distinctly higher than in the pavements. In this bed, the "*Terebratula* biostrome," highly altered shells occur admixed with clusters of well-preserved terebratulids, some of which can be interpreted as biological clumps (sensu Kidwell et al. 1986). This suggests that the terebratulids were autochthonous (García-Ramos and Zuschin 2019). Many shells in the biostrome are bioeroded by

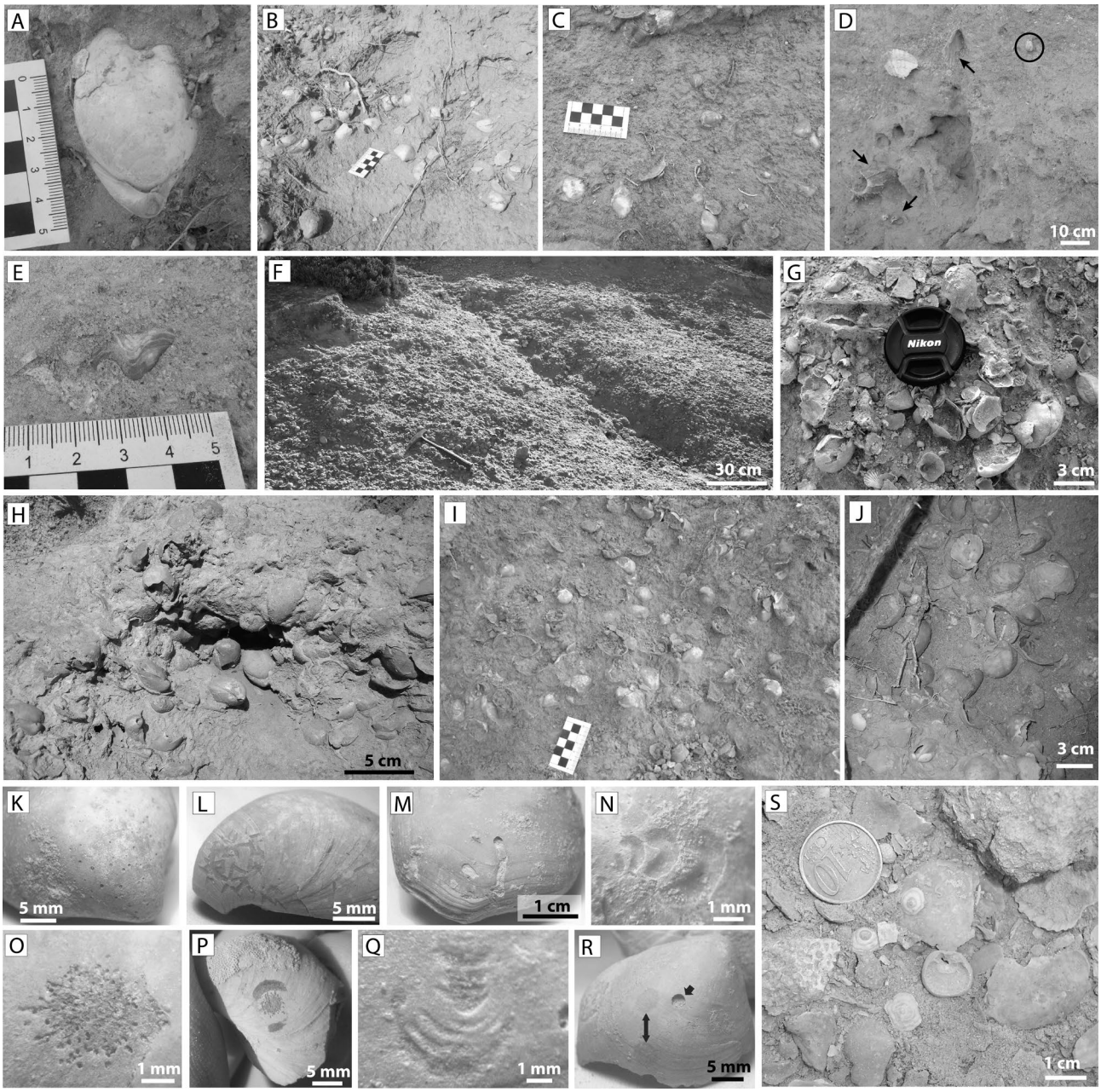

FIGURE 3. Paleoenvironmental features of *Terebratula calabra* outcrops in the Águilas Basin. A, An articulated specimen of *T. calabra*. B, Densely packed pavement TP1 at the toeset subenvironment. C, Loosely packed biofabrics on a plane bed at the bottomset. D, E, isolated *Terebratula* specimens in the rhodolithic hybrid floatstone facies. The arrows in D pinpoint typical shoreface taxa: *Gigantopecten latissimus*, *Spondylus crassicosta*, and *Aequipecten opercularis*, while the circle in D highlights a *Terebratula* specimen. F–J, Densely packed biofabrics from the "*Terebratula* biostrome." K–R, Macrobioerosion traces on specimens from the biostrome: *Entobia* isp. (K), *Gnathichnus pentax* (L), *Caulostrepsis taeniola* (M), *Renichnus arcuatus* (N), *Podichnus obliquus*

(O), same ichnospecies with abrasion marks from the foramen rims (P), *Centrichnus eccentricus*(Q), *Anellusichnus* isp. and *Oichnus simplex* indicated by arrows (R), specimens of *Novocrania anomala* from the biostrome (S).

clionaid sponges (Fig. 3K), although other traces also occur in low abundance (Fig. 3L–R). The rasping trace *Gnathichnus pentax* (Fig. 3L) is represented, whereas the rasping trace *Radulichnus* isp. is absent (García-Ramos and Zuschin 2019). Molinu et al. (2013), who studied microbioerosion traces affecting *Terebratula* specimens from the biostrome at the Cañada Brusca E-2 section, reported that the traces produced by fungi were dominant, although the microendolith trace *Rhopalia clavigera* (the product of chlorophytes) is also represented. The "*Terebratula* biostrome," compared with the pavements, yields additional brachiopod taxa: the craniid *Novocrania anomala* (Fig. 3S), often encrusting disarticulated shells of *Terebratula*, is relatively common. In contrast, *Megathiris detruncata*, *Megerlia truncata*, *Terebratulina retusa*, *A. bipartita*, and *Maltaia moysae* are rare or very rare.

From a morpho-sedimentary viewpoint, these clinoform systems have also been referred to as "infralittoral prograding wedges" (Hernández-Molina et al. 2000; Pomar and Tropeano 2001). Assuming the latter genetic model, the transition between the topset and the foreset of the clinoforms (i.e., the upper rollover) is coincident with the storm-weather wave base (lower shoreface–offshore transition) (Fig. 2A). A minimum water depth for this environment was probably about 25–30 m, in line with data from Recent examples from the Western Mediterranean (Hernández-Molina et al. 2000; Betzler et al. 2011) and the coralline algal assemblage (García-Ramos and Zuschin 2019). The vertical distance between the lower and upper rollover in the clinoform between clinothems 5 and 6 (García-Ramos and Zuschin 2019) is 29 m (Fig. 2B). This suggests a water depth of 54–59 m for the foreset–bottomset transition of the clinoforms (i.e., the lower rollover), without considering lithostatic compaction. During stages of low-amplitude (~15–20 m) relative sea-level rise pulses (García-Ramos and Zuschin 2019), the water depth of the lower

rollover and bottomset was an estimated 70–80 m (Fig. 2A).

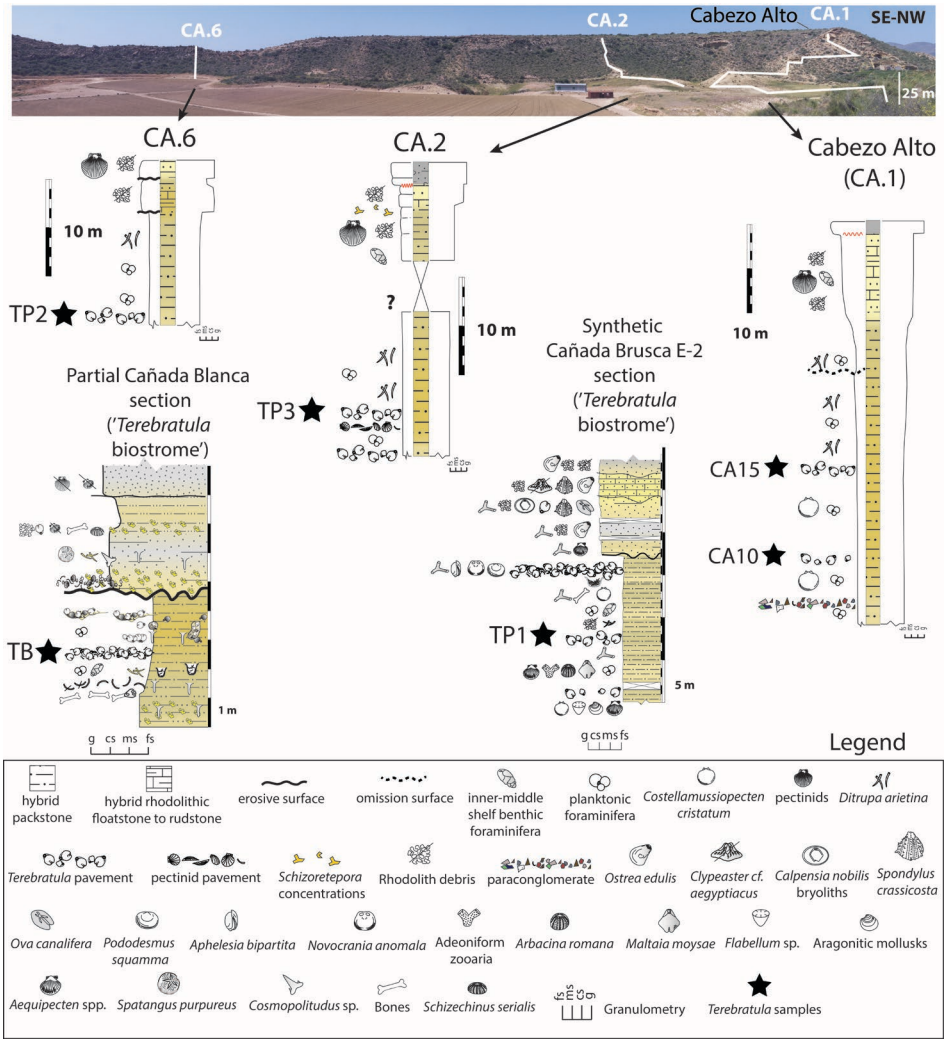

FIGURE 4. Synthetic sections from the Cabezo Alto, Cañada Brusca, and Cañada Blanca areas (adapted from García-Ramos and Zuschin 2019). The Cabezo Alto section, the focus of this study, is also indicated as CA.1. The studied *Terebratula* samples are indicated with black stars. fs = fine sand; ms = medium sand; cs = coarse sand; g = gravel.

Material and Methods

Brachiopod assemblages are well represented, and crop out cyclically, in the Águilas Basin (SE Spain) (Fig. 1A,B). To evaluate the range of paleoenvironmental conditions, we studied the micropaleontological content of 26 bulk samples of friable sediment from the Cabezo Alto (CA) section (Fig. 4). The CA section was chosen because it records a vertical succession continuously

exposing the main facies in the study area (including two *Terebratula* pavements: samples CA10 and CA15) (Fig. 4). The CA section is a suitable template for comparison with other *Terebratula* outcrops from the same stratigraphic sequence (three additional samples from *Terebratula* pavements [TP1, TP2, and TP3] and one from the "*Terebratula* biostrome" [sample TB]). Comparison between CA and other outcrops helps assess the variability of the environmental conditions associated with the presence and absence of *Terebratula* in the studied localities.

The samples were screened to study benthic and planktic foraminifera and calcareous nannoplankton. Each of the three taxonomic groups was studied and analyzed as separate data sets. For each sample, >200 specimens of benthic foraminifera (>100 in the case of planktics) in the 125–500 μm fraction (Weinkauf and Milker 2018) were identified to species level whenever possible and counted. Only tests >50% complete, which included diagnostic features, were considered. For calcareous nannoplankton, smear slides were prepared using standard procedures and examined under the light microscope (cross and parallel nicols) at 1000× magnification. The occurrence of ascidian spicules was noted. Quantitative data were obtained by counting at least 300 specimens from each smear slide. A further 100 view squares were checked for important species to interpret the biostratigraphy and paleoecology of the calcareous nannoplankton. Among reticulofenestrids, we followed the general distinction based on size (Young 1998): *Reticulofenestra minuta* (<3 μm), *Reticulofenestra haqii* (3–5 μm), *Reticulofenestra pseudoumbilica* (5–7 μm), and *R. pseudoumbilica* (>7 μm).

Before subsequent analyses, differences in sample size were accounted for by rarefying the Q × R matrix with count abundance data of benthic foraminifera so that each sample contained 200 specimens (100 specimens in the planktic foraminiferal data set). This was accomplished using the function *rrarefy* of the package vegan (Oksanen et al. 2018). All subsequent analyses were conducted in the R statistical environment, v. 3.5 (R Development Core Team 2018). The resampling process was repeated 100 times, and the mean data set was used for further analysis. For benthic foraminifera, species with relative abundances below 3% were discarded. The variability of

the environmental parameters is shown in box plots by comparing samples where *Terebratula* was abundant, rare, or formed the biostrome. Samples lacking *Terebratula* were segregated between bottomset and foreset subenvironments (both in the transition zone from upper to lower circalittoral) (Fig. 2A) based on facies analysis conducted by García-Ramos and Zuschin (2019).

Benthic Foraminiferal Assemblages and Bathymetry

We used a Q-mode nonmetrical multidimensional scaling (NMDS) as an ordination method to visualize in the Bray-Curtis multivariate space the position of the samples containing *Terebratula* along the environmental gradient encompassing bottomset and foreset subenvironments at the CA section. Differences in the composition of benthic foraminiferal assemblages among bottomset, foreset, and *Terebratula* samples were additionally evaluated with a test of permutational multivariate analysis of variance (PERMANOVA, function *adonis* in package vegan). The variation in composition of such assemblages was examined with a permutational analysis of multivariate dispersions (PERMDISP, function *betadisper* in package vegan). Facies occurring in shallower environments (e.g., the rhodalgal facies) were excluded from the analysis, because this facies consists of hardened rock that hampers the extraction of foraminiferal tests. The composition of benthic foraminifera in the samples containing *Terebratula* is shown in bar plots. The composition of the remaining samples can be checked in a two-way cluster analysis (Supplementary Fig. 1).

Additionally, we provide estimates for bathymetry using the transfer function proposed by Báldi and Hohenegger (2008). This approach was applied using benthic foraminiferal species with both non-overlapping and overlapping depth ranges. The depth ranges of benthic foraminifera were mainly compiled from Sgarrella and Moncharmont Zei (1993), Altenbach et al. (2003), Hohenegger (2005), Rasmussen (2005), Spezzaferri and Tamburini (2007), Sen Gupta et al. (2009), Phipps et al. (2010), and Milker and Schmiedl (2012). The same transfer function, weighted by the mean, was applied on the vertical distribution range of planktic foraminiferal species to estimate minimum water-column depth. The depth ranges of planktic foraminifera were compiled from Rebotim et al. (2017). For comparison, we also computed depth estimates based on the plankton/benthic ratio

(P/B) using the regression function by Van der Zwaan et al. (1990).

Ecological Groups of Benthic Foraminifera as Proxies for Oxygenation and Organic Enrichment

Changes in organic matter content are often coupled with reduced oxygen concentrations at the seafloor (Jorissen et al. 1995; Koho et al. 2008). An increase in organic matter is evaluated by analyzing changes in the proportional abundance of foraminiferal species assigned to five ecological groups (EG1 to EG5). These groups were proposed based on different degrees of opportunistic species' response to varying levels of organic matter enrichment (Alve et al. 2016; Jorissen et al. 2018). We used only species whose proportional abundance was >3%, because ecological information on rare species is often not available. For visualization in box plots, percentages were recalculated after discarding rare species (Dominici et al. 2008). For some quantitatively important species (e.g., *Planulina ariminensis*) not listed by Alve et al. (2016) and Jorissen et al. (2018), a tentative attribution to a category of EG was attempted based on literature evidence (e.g., Rasmussen 2005). In this study, for each EG, we report the proportion of taxa, including unlisted species that were tentatively attributed to a corresponding group. We denoted this as the "aggregated ecological group" (AEG). To visualize the results, we used the conceptual TROX model (Jorissen et al. 1995), representing the *Terebratula* samples in a scheme adapted from Koho et al. (2008) by incorporating the main benthic foraminiferal species found in our samples.

Productivity and Water Temperature

The ecological and environmental distribution of extant species of planktic foraminifera is associated with levels of primary productivity and temperature (roughly warm-oligotrophic vs. cold-eutrophic species) (Hemleben et al. 1989; Sierro et al. 2003). The taxonomy generally follows the concepts of Kennett and Srinivasan (1983) with consideration of other sources (e.g., Poore and Berggren 1975; Malgrem and Kennett 1977; Darling et al. 2006; Schiebel and Hemleben 2017). Productivity based on planktic foraminiferal assemblages was assessed by comparing samples

containing *Terebratula* with those where it was absent. The attribution of the planktic species to a category (warm-oligotrophic vs. cold-eutrophic) was based on information provided by Spezzaferri et al. (2002), Sierro et al. (2003), and Incarbona et al. (2013). We performed a modern analogue technique (MAT) with the packages analogue and analogueExtra (Simpson 2007) to estimate sea-surface temperature (SST) from the Águilas Zanclean samples. As a training data set, we used the modern North Atlantic planktic foraminiferal data set from Kucera et al. (2005), available at the Pangaea repository. The fossil species were standardized with the closest extant relatives using the morphogroups proposed by Serrano et al. (2007). The exception was that we included *Globorotalia hirsuta* as a proxy for *G. margaritae* (e.g., *Globoturborotalita rubescens* was taken as a proxy for *Globoturborotalita* gr. *apertura*; *Globorotalia inflata* for *G. puncticulata*; *Globigerinoides ruber* [lumping pink and white types] for *Globigerinoides obliquus* and *Globigerinoides extremus*). We computed an NMDS ordination of the modern data set and the Águilas samples, and we superimposed the calculated SST isotherms on the ordination plot using the function *ordisurf* from vegan. The variance of the Kucera et al. (2005) data set explained by SST was calculated with canonical correspondence analysis (CCA).

To evaluate bottom-water temperatures, we selected 12 specimens of *Terebratula calabra* collected from different stratigraphic intervals and shell beds from the Águilas Basin for oxygen isotope analysis. The specimens were embedded in resin and cut along a longitudinal axis to produce thin sections, which were subsequently screened for diagenetic alteration with the cathodoluminescence microscope Technosyn 8200 MK II at the GeoZentrum Nordbayern, University Erlangen–Nuremberg. Selected samples of nonluminescent *Terebratula* shells were polished, etched in 5% HCl solution for 15 seconds (Crippa et al. 2016), sputtered with gold, and photographed under a scanning electron microscope (Jeol JSM 6400) at the University of Vienna. Carbonate powders extracted with a microdrill from the secondary layer somewhat posterior to the middle part of the shell were reacted with 100% phosphoric acid at 70°C using a Gasbench II connected to a Thermo Fisher Delta V Plus mass spectrometer at the GeoZentrum Nordbayern,

University Erlangen–Nuremberg. All values are reported in per mil relative to VPDB. Reproducibility and accuracy were monitored by replicate analysis of laboratory standards calibrated by assigning $\delta^{13}C$ values of +1.95‰ to NBS19 and −47.3‰ to IAEA-CO9 and $\delta^{18}O$ values of −2.20‰ to NBS19 and −23.2‰ to NBS18. Reproducibility for $\delta^{13}C$ and $\delta^{18}O$ was ±0.09 and ±0.08 (1 SD), respectively. To estimate temperatures from oxygen isotopes, we used the equation from O'Neil et al. (1969). We assumed a seawater $\delta^{18}O_{sw}$ = +1.5‰ VSMOW for the western Mediterranean in the late Zanclean, based on Recent seawater composition in the eastern Mediterranean (Schmidt 1999; Rohling 2013). Sample S104 was identified as an outlier and was excluded from analysis.

Results

Benthic Foraminiferal Assemblages and Bathymetry of the *Terebratula* Samples

The Q-mode NMDS ordination plot (Fig. 5A) shows that the samples with *Terebratula* occupy a transitional position between *Terebratula*-barren bottomset and foreset samples, as was already observed from lateral facies variations in the field (Fig. 2B). The exceptions are CA10 (a bottomset sample with rare *Terebratula*) and TB ("*Terebratula* biostrome"), which shows affinity

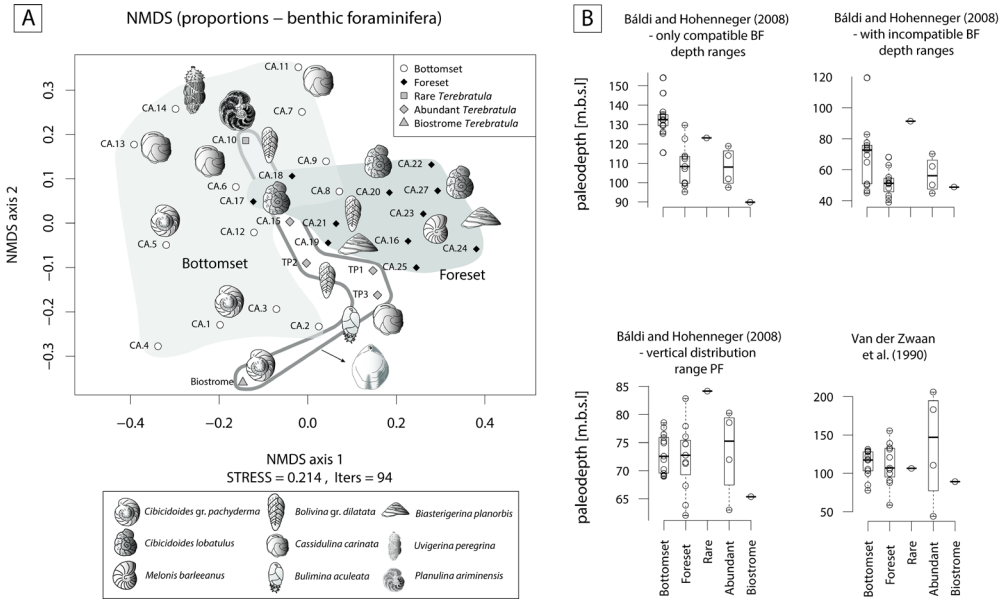

FIGURE 5. A, Q-mode nonmetrical multidimensional scaling (NMDS) ordination. Samples

containing *Terebratula* mostly occur at the transition from foreset to bottomset. B, Box plots of depth estimates using the transfer function from Báldi and Hohenegger (2008) and the regression equation for planktic/benthic ratio from van der Zwaan et al. (1990). BF stands for Benthic Foraminifera and PF stands for Planktic Foraminifera.

with the samples at the base of the CA section. PERMANOVA finds a significant difference among bottomset, foreset, and *Terebratula* samples, but only ~19% of the total variance is explained by these groups. Permutation tests applied on PERMDISP find a significant although moderate compositional variation between the bottomset and foreset samples (permutest: $F = 4.77$, df $= 2$, $p = 0.022$), whereas a post hoc Tukey's honest significant difference test for multiple comparisons among groups indicates a significant compositional difference only between bottomset and foreset samples ($p = 0.013$). The benthic foraminiferal composition of the samples containing *Terebratula* is characterized, in general, by the dominance of *Bolivina* gr. *dilatata* and *Cassidulina carinata*,

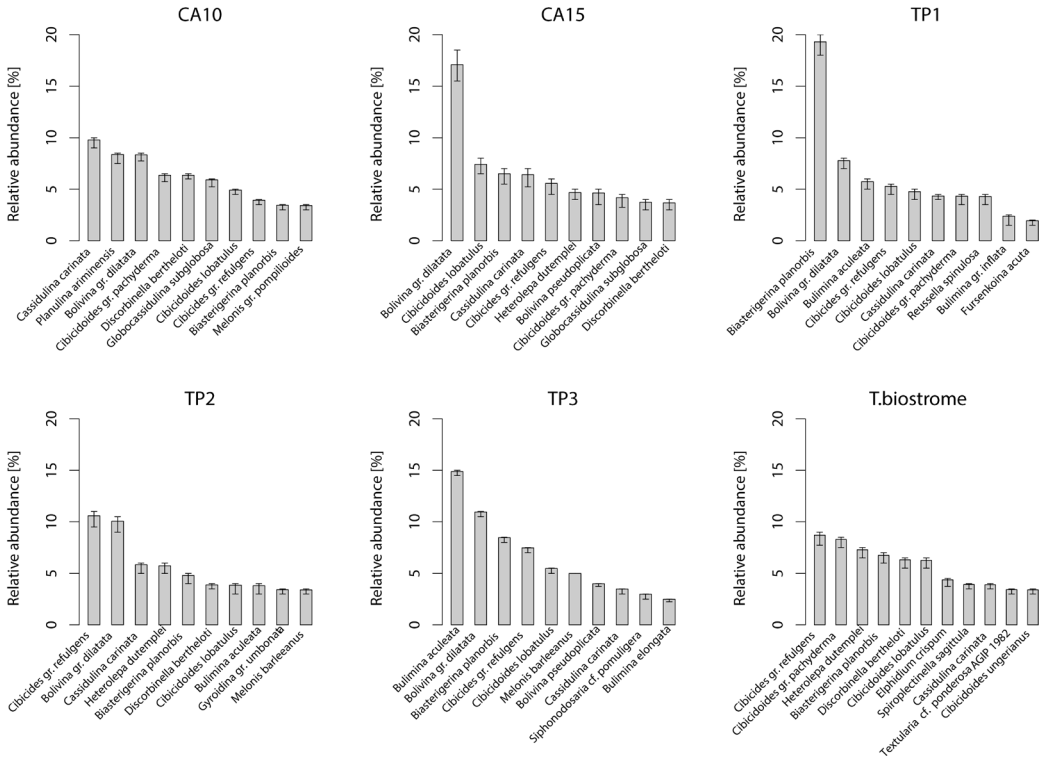

FIGURE 6. Relative abundane of benthic foraminiferal species in the *Terebratula* samples with 95% confidence intervals (percentile method). Only species with relative abundance higher than ~3% are

shown. CA, Cabezo Alto; TP, *Terebratula* pavement.

followed by cibicidids and asterigerinids (Fig. 6). The TB sample is dominated by cibicidids. The equation of Báldi and Hohenegger (2008) yielded depth estimates of ~50 to 90 m for the *Terebratula* samples when including non-overlapping shallow-water species and the vertical distribution range of planktic foraminifera (Fig. 5B). These values are consistent with estimates based on sedimentological models. Removing non-overlapping shallow-water species yielded bathymetric estimates of ~90 to 125 m. The regression function by Van der Zwaan et al. (1990) returned unrealistic depth estimates for the *Terebratula* samples (50–200 m), most probably because of onshore transportation of planktic foraminifera by currents (Murray 1976).

Organic Carbon Enrichment and Oxygenation

The box plots show that samples with *Terebratula* contain a slightly higher proportion of benthic foraminifera belonging to the EG of "sensitive species" (AEG1) compared with samples where *Terebratula* is absent (Fig. 7). The *Terebratula*-containing samples vary between ~35% to ~60% of AEG1 (in the TB sample), the latter being the maximum value in the data set. All these samples fall within the range shown by samples devoid of *Terebratula* with regard to the proportion of benthic species belonging to the EGs of "indifferent species" (AEG2), "tolerant" (AEG3), and "second-order opportunists" (EG4). Most *Terebratula* samples, however, display low proportions (~10%) of benthic species of EG4 (Fig. 7). The exception is sample CA10, a bottomset sample, which contains ~20% of EG4 species and rare *Terebratula*. In the whole data set, "first-order opportunists" (EG5) were absent.

Productivity

The *Terebratula* samples fall within the ranges of cold-eutrophic and warm-oligotrophic species contained in the *Terebratula*-barren samples (Fig. 8A). Sample CA10 displays the

maximum proportion of cold-eutrophic species (~60%), whereas TB yields a relatively low proportion (~30%) (Fig. 8A). Overall, the *Terebratula* samples are dominated by warm-oligotrophic species, except for sample CA10 (Fig. 8A). The NMDS ordination of the nannoplankton (Fig. 8B) shows that the sample with rare *Terebratula* is associated with a *Calcidiscus leptoporus–Coccolithus pelagicus* assemblage, whereas the sample with abundant *Terebratula* is included in the *Reticulofenestra* small assemblage. In six additional *Terebratula* outcrops, nannoplankton were rare in four samples and absent in the other two. The samples with rare nannoplankton, however, contain the *Calcidiscus leptoporus–Coccolithus pelagicus* assemblage.

Seawater Temperature

The MAT analysis using data from Kucera et al. (2005) shows that SST ranges from ~16°C (for sample CA10) to ~22°C (samples TP1, TP3, and *Terebratula* biostrome) (Fig. 9). The

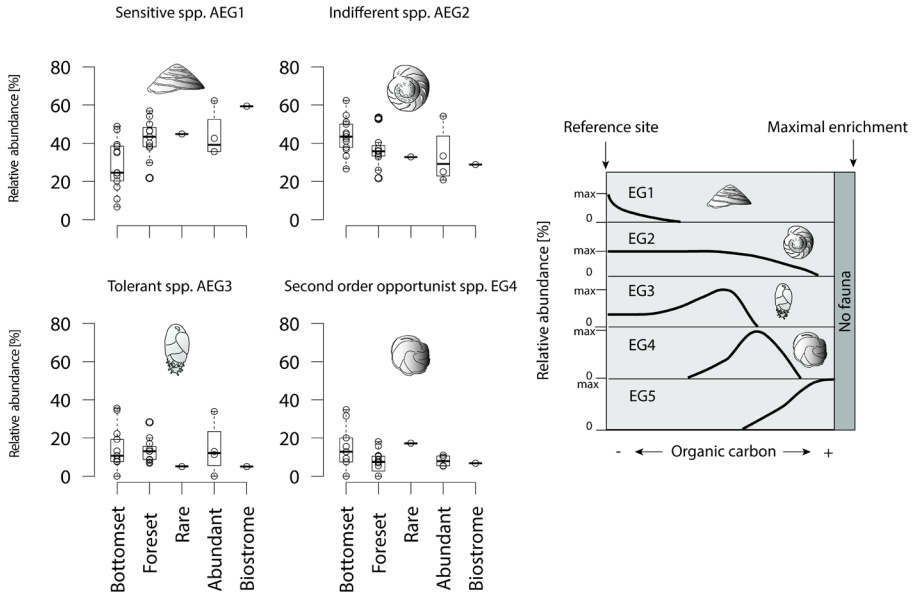

FIGURE 7. Relative abundance of aggregate ecological groups (AEG) of benthic foraminifera, partitioned into *Terebratula*-barren bottomset and foreset samples and those samples with rare, abundant, or biostrome-forming *Terebratula*. The conceptual scheme regarding the faunal response of benthic foraminiferal ecological groups (EG) to organic enrichment is based on Alve et al. (2016) and Jorissen et al. (2018).

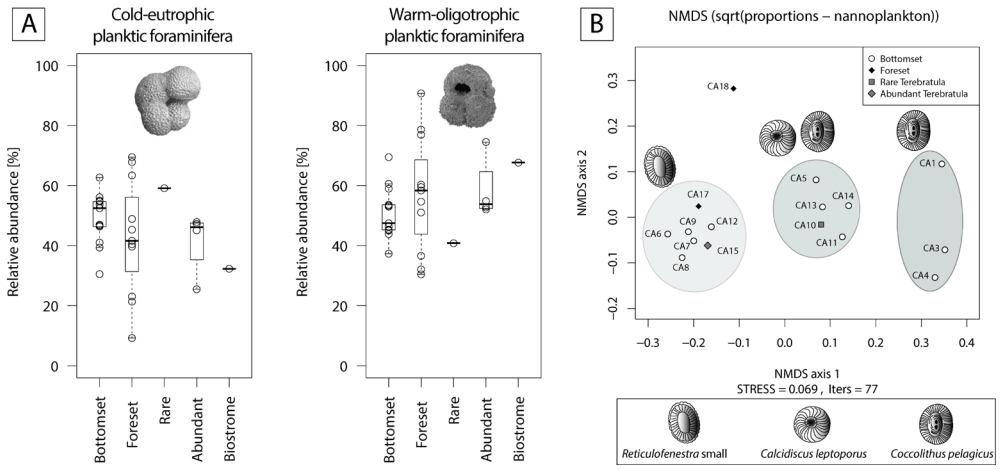

FIGURE 8. A, Relative abundance of cold-eutrophic and warm-oligotrophic species of planktonic foraminifera, partitioned into *Terebratula*-barren bottomset and foreset samples and those samples with rare, abundant, or biostrome-forming *Terebratula*. B, Q-mode nonmetric multidimensional scaling (NMDS) of the Cabezo Alto (CA) section nannoplankton samples.

Terebratula samples CA15 and TP2 fall within the range of 17°C to 19°C. CCA estimates that SST explains 39% of the variance (permutation test: $F = 540.46$, df = 1, $p = 0.001$) in the Kucera et al. (2005) data set.

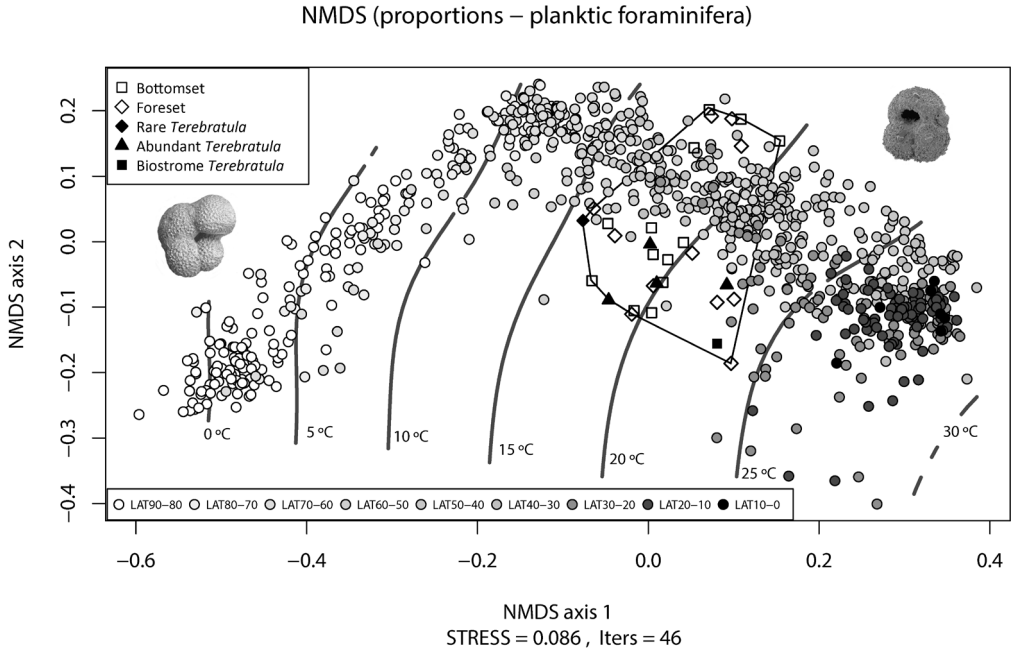

FIGURE 9. Nonmetric multidimensional scaling (NMDS) of planktonic foraminifera performed on

the standardized Pliocene samples from the Águilas Basin (squares, diamonds, and triangles) and the Kucera et al. (2005) extant data set (circles). The calculated sea-surface temperature (SST) for the Pliocene samples is based on the modern analogue technique. SST isotherms are superimposed on the NMDS plot with the *ordisurf* function in R. Black line: the range of SST covered by the Pliocene samples.

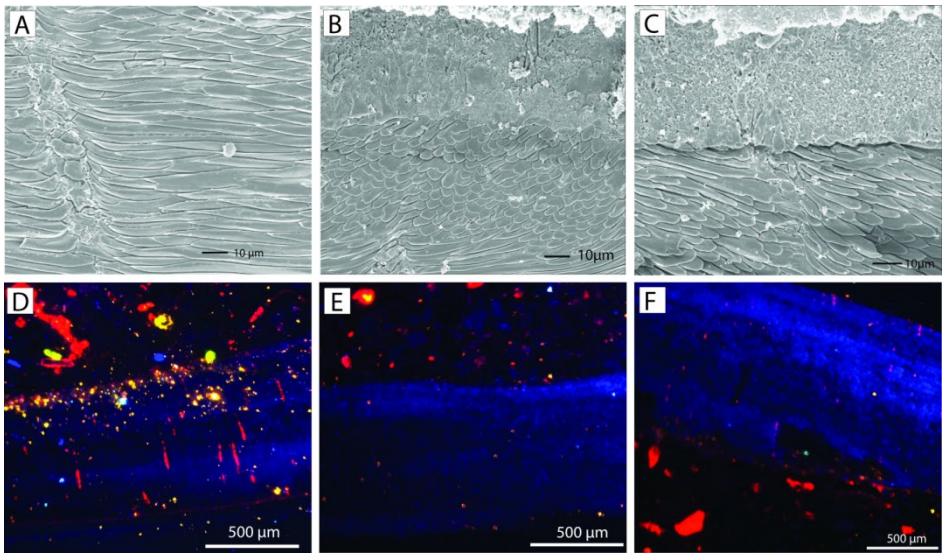

FIGURE 10. A–C, Scanning electron microscope (SEM) images of ultrastructural details of *Terebratula* from the study area. The shells display good preservation of the fibers in the secondary layer. D–F, Nonluminescent shells of *Terebratula*, although some of the punctae are luminescent.

Table 1. Oxygen isotope values from the secondary layer of *Terebratula* specimens from the study area, with estimation of the temperature.S104 is an outlier and not considered for the interpretation.

Sample	Outcrop	$\delta^{18}O_{calc}$ (‰ V-PDB)	$\delta^{18}O_w$ (‰ VSMOW) (Rohling, 2013)	T_{calc} °C (O'Neil et al., 1969)	$\delta^{18}O_w$ (‰VSMOW)	T_{calc} °C (O'Neil et al., 1969)
S74	**CBl.Tereb.Biost.**	1.16	1.5	17.1	0	10.7
S75	**CBl.Tereb.Biost.**	0.83	1.5	18.6	0	12.1
S77	**TP2**	0.97	1.5	17.9	0	11.5
S78	**CBrE1.Tere.Biost.**	0.43	1.5	20.4	0	13.8
S79	**Tere.pav.Balsa**	1.16	1.5	17.1	0	10.7
S80	**TP1**	0.92	1.5	18.2	0	11.7
S81	**CA.28**	0.71	1.5	19.1	0	12.6
S83	**Ter.pav.Balsa**	0.91	1.5	18.2	0	11.7
S85	**TP3**	0.53	1.5	19.9	0	13.3
S86	**TP2**	0.36	1.5	20.7	0	14.1
S87	**CA.15**	0.84	1.5	18.5	0	12
S88	**CBl.Tereb.Biost**	-0.32	1.5	23.8	0	17
S102	**CA.28**	0.91	1.5	18.2	0	11.7
S103	**CA.28**	0.57	1.5	19.7	0	13.2
S104	**CA.28**	-1.91	1.5	31.6	0	24.3

Regarding the oxygen isotopes, the *Terebratula* samples displayed a good preservation of the secondary layer fibers (Fig. 10A–C). The exception is sample S86, which shows cracks in the fibers. All analyzed *Terebratula* samples were nonluminescent, except for the punctae in some specimens (Fig. 10D–F). The volume of nonluminescent shell material is far greater than that of the sediment infilling the punctae. We therefore assume that the oxygen isotopic signal represents primary, diagenetically unaltered values. The $\delta^{18}O_{calc}$ of the 12 *Terebratula* samples varies between −0.32 and 1.16, with a mean value of 0.71 (Table 1). Assuming that the seawater $\delta^{18}O$ in the Águilas Basin during the late Zanclean was +1.5‰ by analogy with the warmer Recent eastern Mediterranean (Schmidt 1999; Rohling 2013), then the $\delta^{18}O_{calc}$ values translate into temperatures between 17.1°C and 23.8°C (mean: 19.1°C). Three measurements, done along the posterior–anterior axis of an isolated *Terebratula* shell from the foreset facies (sample CA28) (measurements S81, S102, S103), yield $\delta^{18}O_{calc}$ values of 0.71, 0.91, and 0.57 VPDB. The calculated temperatures are 19.1°C, 18.2°C, and 19.7°C, respectively. A fourth measurement from the anterior part of the shell (S104) is considered to be an outlier (Table 1).

Discussion

Bathymetric Distribution

Terebratula calabra in the studied sequence of the Águilas Basin is very rare or absent in the rhodalgal facies (lower shoreface; ~25–30 m depth) (Figs. 2A and 4D,E) and in the deepest fine-grained sandy facies (offshore) (Figs. 2A, 4C, and 5). The maximum population density occurs close to (but notably below) the shoreface–offshore transition in fine-grained sands at estimated paleodepths of about 60 to 90 m (Figs. 2A,B, 4B, and 5B). The benthic foraminiferal assemblage of the *Terebratula* samples (Fig. 6) characterizes an offshore environment (e.g., Sgarrella and Moncharmont Zei 1993; Rasmussen 2005; Milker et al. 2009; Frezza et al. 2010; Mojtahid et al. 2010).

Substrate

Modern Terebratulida bathymetrically equivalent to *Terebratula* mostly occur in shallow rocky habitats in bays and fjords (Supplementary Table 1). *Terebratula* species, instead, were abundant in soft sediments: coarse to muddy sands (e.g., Gaetani 1986; Barrier et al. 1987; Dominici 2001; Gramigna et al. 2008). *Terebratula*, like certain other brachiopods (Rudwick 1961; Richardson 1981; Llompart and Calzada 1982), was potentially attached to ascidians, whose spicules are pervasive in section CA. We did not quantify the percentage of *Terebratula* shells affected by pedicle attachment traces (*P. obliquus*), but this trace is rare. This matches previous reports on several species of *Terebratula*, in which 1% or less were affected by *P. obliquus* (Taddei Ruggiero and Bitner 2008). Other members of Terebratulinae are known to facultatively form clusters, such as *Pliothyrina* (Bell and Bell 1872; Rudwick 1961) and *Liothyrella* (Foster 1974; Richardson 1981; Peck et al. 1997). A cluster of *Terebratula calabra* from the Águilas Basin was illustrated by García-Ramos and Zuschin (2019).

Oxygenation, Organic Enrichment, and Productivity

Among the dominant benthic foraminifera in the *Terebratula* samples, a first group of species (*B.* gr. *dilatata*, *Bulimina aculeata*, *C. carinata*) suggests that *Terebratula* in this basin was subject to seasonal inputs of labile organic matter, possibly associated with episodes of dysoxia at the seafloor (Barmawidjaja et al. 1992; Fontanier et al. 2003; Langezaal et al. 2006; Abu-Zied et al. 2008; Mendes et al. 2012). This interpretation is reinforced by the presence of the *Calcidiscus leptoporus–Coccolithus pelagicus* nannoplankton assemblage in several *Terebratula* samples, suggesting productivity pulses triggered by coastal upwelling (Silva et al. 2009; Auer et al. 2014). In contrast, the "*Reticulofenestra* small" nannoplankton assemblage in sample CA15 points to an opportunistic response to increased eutrophic levels, environmental disturbance, or water stratification related to continental runoff or riverine input (Wade and Bown, 2006; Ćorić and

Hohenegger 2008; Auer et al. 2014). This latter assemblage correlates with warmer-water SST

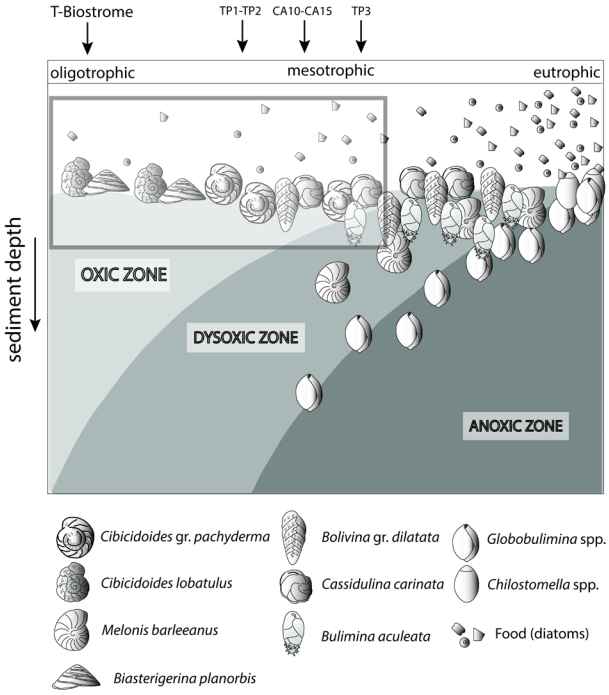

FIGURE 11. TROX model (adapted from Koho et al. 2008) conceptually representing the range of conditions interpreted for the *Terebratula* samples, marked by an inset. CA, Cabezo Alto; TP, *Terebratula* pavement.

indicated by planktic foraminiferal assemblages (Supplementary Fig. 2). A second group of benthic foraminifera (*Heterolepa dutemplei*, *P. ariminensis*, *Ccibicides* gr. *refulgens*, *Discorbinella bertheloti*, *Cibicidoides* gr. *pachyderma*, *Biasterigerina planorbis,* and *Cibicidoides lobatulus*) suggests oligotrophic, well-oxygenated background conditions under the influence of strong bottom currents (Donnici and Barbero 2002; Schönfeld 2002; Szarek et al. 2006; Fontanier et al. 2008; Koho et al. 2008; Schweizer et al. 2009; Frezza et al. 2010; Buosi et al. 2012). Background oligotrophism and high oxygen levels are suggested by the proportional dominance of the "sensitive" and "indifferent" EGs of benthic foraminifera (Fig. 7) and warm-oligotrophic planktic foraminifera (Fig. 8A). Note here that the sample from the *Terebratula* biostrome (TB), however, is mostly characterized by oxiphylic species such as *C.* gr. *pachyderma* and *C.* gr. *refulgens*, which are

suspension-feeding epizoans (Koho et al. 2008; Schweizer et al. 2009). Our data from the Águilas Basin suggest, overall, that *Terebratula* preferred oligotrophic and well-oxygenated habitats, under moderate to strong currents, but tolerated mesotrophic conditions and fluctuating concentrations of oxygen levels at the seafloor (Fig. 11).

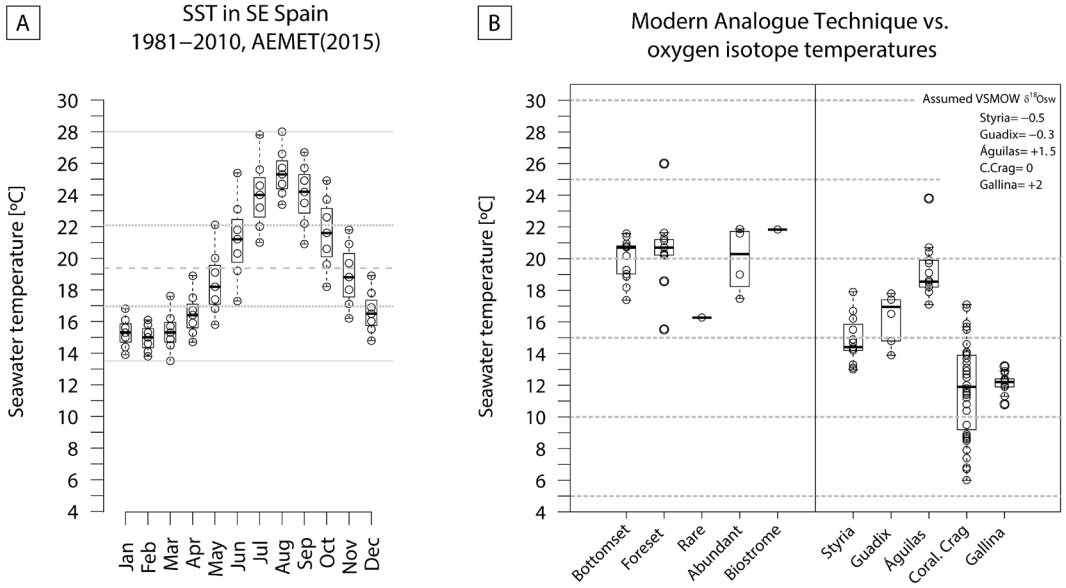

FIGURE 12. A, Monthly sea-surface temperatures (SST) off Águilas for the period 1981–2010 (data from Guijarro et al. 2015). B, Comparison between SST estimated from modern analogue technique using the Kucera et al. (2005) data set of planktonic foraminifera and bottom temperatures from oxygen isotopes of *Terebratula* shells from the Águilas Basin. *Terebratula* oxygen isotopes from Styria, Guadix, and Gallina and *Pliothyrina* from the Coralline Crag are included for comparison. The data were taken from Bojar et al. (2004), Clark et al. (2016), Rollion-Bard et al. (2016), and Vignols et al. (2018). All temperatures were calculated using the equation given by O'Neil et al. (1969). $\delta^{18}O_{sw}$ was assumed based on the values proposed by Lear et al. (2000) for the Styria and Guadix samples. For the *Pliothyrina* samples, $\delta^{18}O_{sw}$ was assumed as 0‰ VSMOW.

Seawater Temperature

Modern (1981–2010) water temperatures off Águilas (SE Spain) range from 13.5°C to 28°C (range = 14.5°C). The monthly averages are between 17°C and 22°C, and the annual mean is

19.4°C (Guijarro et al. 2015) (Fig. 12A). The temperatures calculated from the oxygen isotope ratios (min = 17.1°C; max = 23.8°C; mean = 19.1°C; Table 1), as well as MAT (min = 16.3°C; max = 21.9°C; mean = 19.7°C), are consistent with the modern average temperatures. The MAT results are similar for the *Terebratula*-barren and *Terebratula*-bearing samples (Fig. 12B). This suggests that temperature alone does not explain the presence/absence distribution patterns of *Terebratula* during the Zanclean. Given that *Terebratula* lived in offshore environments, the temperatures derived from oxygen isotope ratios would not be representative of sea-surface conditions. The assumption is that, for the Zanclean, Mediterranean SST was higher than today (Templado 2014; Tindall and Haywood 2015). In the Águilas Basin, during the late Zanclean, other paleoclimatic proxies are the species *Clypeaster* cf. *aegyptiacus*, *Echinolampas* spp., *Hyotissa* sp., *Talochlamys ercolaniana*, *Hinnites crispus*, *Spondylus crassicosta*, and *Gigantopecten latissimus* (García-Ramos and Zuschin 2019). These species are considered to be warm-temperate to subtropical taxa (Brébion et al. 1978; Ávila et al. 2015). For these species, Monegatti and Raffi (2001) proposed monthly average SST of 24°C–25°C for at least five to six months. The relatively narrow range of temperatures obtained from oxygen isotopes (6.7°C; 3.6 °C without the 23.8 outlier; Fig. 12B) suggests that *Terebratula* either preferentially lived below the thermocline (cf. Houpert et al. [2015] for the seasonal thermoclines in the modern Mediterranean) or grew during particular seasons of the year. "*Terebratula*" sp. from Styria (Langhian, Austria), *T.* cf. *calabra* from Guadix (Tortonian, Spain), and *T. scillae* from Gallina (Calabrian, Italy) (Bojar et al. 2004; Clark et al. 2016; Rollion-Bard et al. 2016) also display relatively narrow temperature ranges: 4.9°C, 3.9°C, and 2.4°C, respectively. An exception is *Pliothyrina maxima*, another member of Terebratulinae, from the Coralline Crag (Zanclean, UK), showing a large range of 11.1°C (Vignols et al. 2018). Importantly, however, the data in those studies are derived from a sclerochronological approach on one or two specimens, sometimes mixing signals from the primary and secondary brachiopod shell layers. Oxygen isotope ratios measured on the primary shell layer and posterior and anterior parts of the shell should be interpreted with caution, because

they are likely affected by nonequilibrium isotope fractionation (e.g., Romanin et al. 2018). The similar brachiopod species *Liothyrella uva* from Antarctic waters is subject to temperature ranges of only 2°C–3°C, not surviving above 4.5 °C (Peck 2005). In contrast, the cool-temperate *Liothyrella neozelanica* experiences values between 8°C and 18°C (Lee 1991). The relatively narrow temperature ranges of different *Terebratula* species should be further investigated as a possible cause for their extinction during the dramatic climate changes of the late Pleistocene, which would have left them insufficient time to adapt (Peck 2007). Note also that *Terebratula* not surviving beyond the Jaramillo Subchron coincides with the onset of the strongest glacial–interglacial shifts during the Pleistocene (e.g., Rohling et al. 2014).

Environmental Factors Limiting the Distribution of *Terebratul*a in the Águilas Basin

Terebratula had an optimum close to the OTZ, but why was the genus rare or absent in the shoreface and basinward beyond the OTZ? Our data suggest that oxygenation levels, food availability, or temperature—which have been invoked to explain the distribution of some brachiopod species (e.g., Tunnicliffe and Wilson 1988; Kowalewski et al. 2002; Tomašových et al. 2006; Peck 2007)—might not have acted as limiting factors in the Águilas Basin. This is because *Terebratula* appeared to be fairly tolerant to local variations in these parameters.

Preferred Habitat of Terebratula: Upper Offshore.—The consistent pattern in the Águilas Basin is the peak abundance of *Terebratula* in sediments devoid of coralline algae. Accordingly, light penetration might have exerted an important influence on the distribution of *Terebratula* in relation to grazing pressure (Noble et al. 1976; Witman and Cooper 1983; Asgaard and Stenthoft 1984; Asgaard and Bromley 1991; Tomašových 2008; Zuschin and Mayrhofer 2009; Radley 2010). The bioerosion assemblages in the *Terebratula* biostrome are interesting because they display affinity with the *Gnathichnus* ichnofacies (Bromley and Asgaard 1993; De Gibert et al. 2007). Bromley and Asgaard (1993) proposed the *Entobia* ichnofacies for deep tier–dwelling borings in

littoral rocky substrates subject to long exposure. The *Gnathichnus* ichnofacies, instead, characterizes shallow-tier structures on briefly exposed substrates (i.e., shells) in deeper water (De Gibert et al. 2007). The outcrop from the Pliocene Roussillon Basin (De Gibert et al. 2007), for example, was a shoreface environment whose shell beds are mostly composed of ostreids and pectinids. There, the dominant traces are *G. pentax* (rasping traces produced by regular echinoids feeding on algae) and *Radulichnus inopinatus* (produced by the radular grazing activity of gastropods or polyplacophorans) (De Gibert et al. 2007). In contrast, the dominant macrobioerosion trace in the *Terebratula* biostrome is *Entobia* isp., whereas other traces such as *G. pentax* (Fig. 4L) are rare (Molinu et al. 2013). García-Ramos and Zuschin (2019) argued that the rare occurrence of the bioerosion trace *Gnathichnus* on *Terebratula* shells, coupled with the absence of *Radulichnus*, may indicate dim light or aphotic conditions, in line with interpretations elsewhere (Bromley 2005). This interpretation is consistent with the microendolith assemblages reported by Molinu et al. (2013) from the *Terebratula* biostrome. That assemblage is dominated by fungal traces (*Saccomorpha clava*, *Orthogonum lineare*, *Flagrichnus* isp.), whose producers are more common in relatively deep aphotic environments (e.g., Glaub 2004; Wisshak 2012). The microendolith trace *R. clavigera* is also present in the *Terebratula* biostrome. The producer of this trace characterizes the euphotic zone (Golubić and Radtke 2008), but can also be common in deep euphotic habitats (Wisshak 2012). Overall, the microendolith assemblages suggest irradiances around 0.01% or less (Wisshak 2012), which classifies the habitat from the *Terebratula* biostrome as a transition from upper to lower circalittoral (Cameron and Askew 2011). Such microendolith ichnoassemblages pointing to dim light are consistent with the absence of coralline algae in the *Terebratula* samples. The dysphotic zone (1–0.01% irradiance) can occur at depths between 40 and 120 m in some Mediterranean localities (Ballesteros 2006). Recent shells of the brachiopod *Gryphus vitreus* are affected by the endolithic green alga *Ostreobium queketti* (which is adapted to extremely low light conditions) to a depth of 130–135 m off Corsica (Emig 2018). Similar benthic foraminiferal assemblages as in the "*Terebratula* biostrome" (Fig. 6) occur at 70–80 m depth in the Strait of

Bonifaccio (Buosi et al. 2012), which supports the above interpretation based on microendolith ichnoassemblages.

Exclusion of Terebratula Offshore: The Upper Foreset.—The rarity or absence of *Terebratula* in shoreface environments was discussed earlier, but in the Águilas Basin the distribution of this brachiopod in upper offshore (circalittoral) environments is not homogeneous (Fig. 2A). The peak density occurs in the foreset–bottomset transition (i.e., the lower rollover of the clinoforms). Why was *Terebratula* rare or absent in the upper foreset? The rhodalgal facies disappears basinward beyond the OTZ (coincident with the topset–foreset transition; i.e., upper rollover zone) (Fig. 2A). This suggests that the upper foreset was already under poorly lit conditions or other excluding environmental factors for coralline algae were present. *Terebratula* could have potentially colonized this habitat, which was safe from high grazing pressure, but it was absent. This pattern can be explained by peak sedimentation rates at the upper foreset (upper offshore, circalittoral) due to its proximity to the upper rollover, which is a threshold between high and low hydrodynamic conditions (from sediment advection and bypass at the topset to sedimentation at the foreset) (Driscoll and Karner 1999; Cattaneo et al. 2007; Mitchell 2012). Thus, the environmental conditions at the upper foreset likely surpassed the physiological capacity of *Terebratula* to cope with sedimentation (Williams et al. 2018). Sedimentation rates decrease gradually down the foreset (Mitchell 2012). Accordingly, the facies belt at the foreset–bottomset transition marks the threshold of sedimentation rates tolerated by *Terebratula*.

Exclusion of Terebratula Offshore: Beyond the Lower Rollover.—*Terebratula* density rapidly decreases beyond the lower rollover basinward (Figs. 2A and 3C). This is coincident with Gaetani (1986) and Barrier et al. (1987), who report *T. calabra* as being restricted to proximal circalittoral environments, whereas other Terebratulidina such as *T. scillae*, *G. vitreus*, and *Stenosarina sphenoidea* display a deeper optimum in the lower circalittoral and bathyal (Gaetani

and Saccà 1985). A common pattern of subaqueous delta-scale clinoform systems is the association with offshore currents running parallel to the shoreline along the foreset–bottomset transition (e.g., Pomar et al. 2002; Cattaneo et al. 2007; Patruno and Helland-Hansen 2018). The occurrence of aggrading sandwave fields migrating basinward at the localities of Terreros and La Carolina (García-Ramos and Zuschin 2019) demonstrates the sustained development of cyclonic current systems during the late Zanclean in the Águilas Basin (Fig. 1C). This interpretation is supported by the dominance in the benthic foraminiferal assemblages of suspension-feeding species that favor vigorous currents and by the abundance in the *Terebratula* biostrome of clionaid sponges, which cannot cope with high levels of turbidity (Carballo et al. 1994; Taylor et al. 2003). This pattern does not seem unique to the Águilas Basin, because records of *Terebratula* at the lower rollover and adjacent bottomset of delta-scale clinoforms are described elsewhere (e.g., Llompart and Calzada 1982; Pomar and Tropeano 2001; Soria et al. 2003; Videt 2003; Gramigna et al. 2012; Massari and D'Alessandro 2012; Reolid et al. 2012). As brachiopods are facultatively active suspension feeders (La Barbera 1977; Wildish and Kristmanson 1997), the attenuation or disappearance of the along-slope currents basinward possibly affected the *Terebratula* paleocommunity; this reflects the physiological cost of shifting from passive to permanently active suspension feeding (La Barbera 1977; James et al. 1992). An analogous case of offshore and onshore decrease in population density as a function of bottom current velocity has been described for extant communities of the terebratulidine *G. vitreus* (Emig 1989; Emig and García-Carrascosa 1991).

Environmental Distribution of Terebratulinae in Other Studies

Cenozoic to Quaternary Terebratulinae have often been found in relatively shallow-water environments, from boulders at the toe of beach cliffs (Aigner 1983; Dixon 2011; Betancort et al. 2014) to intertidal and very shallow subtidal gravelly bottoms (Diedrich 2012). They often occur adjacent to sandwave fields where tidal or other types of currents are present but attenuated (Barrier

et al. 1987; Roetzel et al. 1999; Pomar and Tropeano 2001; Courville and Crônier 2003; Kroh et al. 2003; Bosselaers et al. 2004; Calvo et al. 2012; Reolid et al. 2012). Such conditions prevent burial of the brachiopod paleocommunity by migrating subaqueous sandwaves. These brachiopods have also been found close to submarine hard-bottom structures that they possibly colonized, including shallow-water submarine cliffs (Kroh et al. 2003; Pervesler et al. 2011). Smaller species, such as *Maltaia maltensis* and *"Terebratula" styriaca*, were able to inhabit crevices and sheltered microenvironments in coralline algal buildups (e.g., Bianucci et al. 2011; M. Harzhauser personal communication, 2019), cavities in coral reefs (Barbera et al. 1995), or in parareefal environments (Conesa et al. 2007). In the Pleistocene, some species colonized dykes in seamounts and walls on paleocliffs at bathyal depths (Ietto and Bernasconi 2005; Titschack et al. 2005). Other species have also been reported from muddy bottoms at bathyal depths (Thomsen et al. 2005; Rögl et al. 2008), but it remains to be determined whether these assemblages were transported. Most occurrences, however, are associated with environments close to the lower shoreface–offshore transition and upper offshore settings, often co-occurring with bryozoans and/or acorn barnacles (De Porta et al. 1979; D'Alessandro and Iannone 1982; Gaetani 1986; Studencki 1988; Taddei Ruggiero 1996; Bitner and Pisera 2000; Montenat et al. 2000; Gramigna et al. 2008; Pavia and Zunino 2008; Puga-Bernabéu et al. 2008; Di Stefano and Longhitano 2009; Messina et al. 2009; Long and Zalasiewicz 2011; Giannetti et al. 2018; 2019; Crippa et al. 2019). Terebratulid colonization of the photic zone and their co-occurrence with coralline algae have sometimes been explained by the onset of eutrophic conditions triggered by upwelling, which can be deleterious for phototrophic and mixotrophic organisms (Brandano et al. 2016). Other authors interpreted that *Terebratula*, which is often typical of monospecific to paucispecific assemblages, was an opportunist able to colonize environments subject to disturbance associated with mesotrophic conditions (Massari and D'Alessandro 2012). Overall, the available evidence points to *Terebratula* preferring habitats where grazing disturbance was reduced because of poorly lit environments (e.g., Pedley and Grasso 2002; Brandano et al. 2015).

Conclusions

The late Zanclean deposits of the Águilas Basin record cycles of *Terebratula* paleocommunities that developed offshore (circalittoral) on fine-grained sediments deposited at the foreset–bottomset transition of subaqueous delta-scale clinoforms. These deposits therefore provide a good scenario to understand the paleoenvironmental distribution of this taxon in space and time. The analysis of benthic and planktic foraminiferal and nannoplankton assemblages suggests that, overall, *Terebratula* thrived in relatively warm, oligotrophic to mesotrophic, well-oxygenated environments influenced by strong bottom currents. The oxygen isotopes showed that *Terebratula* in this basin lived in a relatively narrow range of temperatures (6.7°C). Such narrow ranges have also been reported for other species, potentially helping explain their extinction during the abrupt climate changes of the late Pleistocene: these brachiopods may have been unable to adapt quickly enough to such high-amplitude seawater temperature fluctuations after the Jaramillo Subchron. The consistent occurrence of terebratulids in sediments devoid of coralline red algae, combined with the bioerosion assemblages in the *Terebratula* biostrome, suggest that the limiting factor affecting the onshore distribution of *Terebratula* was light penetration and the associated high grazing pressure. This would explain the virtual absence of *Terebratula* in shoreface environments. Higher sedimentation rates at the shoreface–offshore transition also excluded the *Terebratula* paleocommunity in the upper foreset. In contrast, further offshore beyond the foreset–bottomset transition, we conclude that the attenuation or disappearance of along-slope currents was responsible for the lack of *Terebratula* populations.

Acknowledgments

We thank G. Romero Sánchez from the Paleontological Heritage Service of the Community of Murcia (Spain) for granting permits to conduct paleontological fieldwork in the study area. We also thank P. Bukenberger and J. Souto-Derungs (University of Vienna) for their help with SEM

images and M. Bošnjak (Croatian Natural History Museum, Zagreb) for suggesting improvements to an earlier version of the article. E. Borghi, G. Díaz-Medina, M. Harzhauser (Natural History Museum of Vienna), and A. Giannetti (University of Alicante) are acknowledged for providing paleoenvironmental information on Terebratulinae from certain localities; E. Borghi and G. Crippa (University of Milan) also for sending literature. Special thanks to A. Tomašových (Slovak Academy of Sciences) for his help with technical aspects. D.A.G.-R. wishes to thank Y. Sun and E. Jarochowska (University of Erlangen–Nuremberg) for support in Erlangen. The authors thank M. Stachowitsch (University of Vienna) for proofreading and improving the language. We thank the editor J. Crampton for constructive comments during the review process. The insightful reviews of two anonymous reviewers substantially improved the final version of this article.

Literature Cited

Abu-Zied, R. H., E. J. Rohling, F. J. Jorissen, C. Fontanier, J. S. Casford, and S. Cooke. 2008. Benthic foraminiferal response to changes in bottom-water oxygenation and organic carbon flux in the eastern Mediterranean during LGM to Recent times. Marine Micropaleontology 67:46–68.

Aigner, T. 1983. A Pliocene cliff-line around the Giza pyramids plateau, Egypt. Palaeogeography, Palaeoclimatology, Palaeoecology 42:313–322.

Altenbach, A. V., G. F. Lutze, R. Schiebel, and J. Schönfeld. 2003. Impact of interrelated and interdependent ecological controls on benthic foraminifera: an example from the Gulf of Guinea. Palaeogeography, Palaeoclimatology, Palaeoecology 197:213–238.

Alve, E., S. Korsun, J. Schönfeld, N. Dijkstra, E. Golikova, S. Hess, K. Husum, and G. Panieri. 2016. Foram-AMBI: a sensitivity index based on benthic foraminiferal faunas from North-East Atlantic and Arctic fjords, continental shelves and slopes. Marine Micropaleontology 122:1–12.

Asgaard, U., and R. G. Bromley. 1991. Colonization by micromorph brachiopods in the shallow

subtidal of the eastern Mediterranean Sea. Pp. 261–264 *in* D.I. MacKinnon, D.E. Lee, and J.D. Campbell, eds. Brachiopods through time. Balkema, Rotterdam.

Asgaard, U., and N. Stentoft. 1984. Recent micromorph brachiopods from Barbados: palaeoecological and evolutionary implications. Geobios 17:29–37.

Auer, G., W. E. Piller, and M. Harzhauser. 2014. High-resolution calcareous nannoplankton palaeoecology as a proxy for small-scale environmental changes in the Early Miocene. Marine Micropaleontology 111:53–65.

Ávila, S. P., R. S. Ramalho, J. M. Habermann, R. Quartau, A. Kroh, B. Berning, M. Johnson, et al. 2015. Palaeoecology, taphonomy, and preservation of a lower Pliocene shell bed (coquina) from a volcanic oceanic island (Santa Maria Island, Azores). Palaeogeography, Palaeoclimatology, Palaeoecology 430:57–73.

Báldi, K., and J. Hohenegger. 2008. Paleoecology of benthic foraminifera of the Baden-Sooss section (Badenian, Middle Miocene, Vienna Basin, Austria). Geologica Carpathica 59:411–424.

Ballesteros, E. 2006. Mediterranean coralligenous assemblages. Pp. 297–317 *in* R. N. Gibson, R. J. A. Atkinson, and J. D. M. Gordon, eds. Oceanography and marine biology—an annual review. Taylor and Francis.

Barbera, C., F. Bilancio, and P. Giordano. 1995. A miocenic reef near Catanzaro, Calabria, South Italy. Bollettino della Società dei Naturalisti in Napoli 102:49–56.

Bardají A. T., C. Zazo, J. L. Goy, P. G. Silva, and C. J. Dabrio. 2001. Registro de los cambios del nivel del mar en la Cuenca de Águilas (Murcia, SE de España). Pp. 245–248 *in* R. Taborda, J. Cascalho, and L. Ortlieb, eds. V Iberian Quaternary Meeting and I Quaternary Congress of Countries of Iberian Languages, Portugal (23/07/2001).

Barmawidjaja, D. M., F. J. Jorissen, S. Puskaric, and G. J. van der Zwaan. 1992. Microhabitat selection by benthic Foraminifera in the northern Adriatic Sea. Journal of Foraminiferal Research 22:297–317.

Barrier, P., V. Casale, B. Costa, I. Di Geronimo, O. Olivieri, and A. Rosso. 1987. La sezione plio-pleistocenica di Pavigliana (Reggio Calabria). Bollettino della Società Paleontologica Italiana 25:107–144.

Basso, D. 1998. Deep rhodolith distribution in the Pontian Islands, Italy: a model for the paleoecology of a temperate sea. Palaeogeography, Palaeoclimatology, Palaeoecology 137:173–187.

Bell, A., and R. Bell. 1872. On the English Crags and the stratigraphical divisions indicated by their invertebrate fauna. Proceedings of the Geologists' Association 2:185–218.

Benigni, C., and E. Robba. 1990. A Pliocene Micromorph Brachiopod-Pectinid Community. Atti del Quarto Simposio di Ecologia e Paleoecologia delle Communità Bentoniche, Sorrento, 1–5 Novembre 1988. Museo Regionale di Scienze Naturali Torino, new series 604:341–356.

Betancort, J. F., A. Lomoschitz, and J. Meco. 2014. Mio-Pliocene crustaceans from the Canary Islands, Spain. Rivista Italiana di Paleontologia e Stratigrafia (Research In Paleontology and Stratigraphy) 120:337–349.

Betzler, C., J. C. Braga, D. Jaramillo-Vogel, M. Roemer, C. Huebscher, G. Schmiedl, and S. Lindhorst. 2011. Late Pleistocene and Holocene cool-water carbonates of the Western Mediterranean Sea. Sedimentology 58:643–669.

Bianucci, G., M. Gatt, R. Catanzariti, S. Sorbi, C. G. Bonavia, R. Curmi, and A. Varola. 2011. Systematics, biostratigraphy and evolutionary pattern of the Oligo-Miocene marine mammals from the Maltese Islands. Geobios 44:549–585.

Bitner, M. A., and A. Pisera. 2000. Brachiopod fauna from the Middle Miocene deposits of Niechobrz, south-eastern Poland. Tertiary Research 20: 7–15.

Bojar, A. V., H. Hiden, A. Fenninger, and F. Neubauer. 2004. Middle Miocene seasonal temperature changes in the Styrian basin, Austria, as recorded by the isotopic composition of pectinid and brachiopod shells. Palaeogeography, Palaeoclimatology, Palaeoecology 203:95–105.

Bosselaers, M., J. Herman, K. Hoedemakers, O. Lambert, R. Marquet, and K. Wouters. 2004. Geology and palaeontology of a temporary exposure of the late Miocene Deurne sand in Antwerpen (N. Belgium). Geologica Belgica 7:27–39.

Brandano, M., L. Tomassetti, and V. Frezza. 2015. *Halimeda* dominance in the coastal wedge of Pietra di Finale (Ligurian Alps, Italy): the role of trophic conditions. Sedimentary Geology 320:30–37.

Brandano, M., L. Tomassetti, R. Sardella, and C. Tinelli. 2016. Progressive deterioration of trophic conditions in a carbonate ramp environment: the Lithothamnion Limestone, Majella Mountain (Tortonian–early Messinian, central Apennines, Italy). Palaios 31:125–140.

Brébion, P., A. Lauriat-Rage, D. Pajaud, S. Pouyet, and J. Roman. 1978. Les faunes pliocènes des environs d'Aguilas (provinces d'Almeria et de Murcia, Espagne méridionale). Bulletin du Muséum National d'Histoire Naturelle 68:55–76.

Bromley, R. G. 2005. Preliminary study of bioerosion in the deep-water coral *Lophelia*, Pleistocene, Rhodes, Greece. Pp. 895–914 *in* A. Freiwald and J. M. Roberts, eds. Cold-water corals and ecosystems. Springer, Berlin.

Bromley, R. G., and U. Asgaard. 1993. Two bioerosion ichnofacies produced by early and late burial associated with sea-level change. Geologische Rundschau 82:276–280.

Buosi, C., E. A. D. Châtelet, and A. Cherchi. 2012. Benthic foraminiferal assemblages in the current-dominated Strait of Bonifacio (Mediterranean Sea). Journal of Foraminiferal Research 42:39–55.

Calvo, J. P., M. V. Triantaphyllou, M. Regueiro, and M. G. Stamatakis. 2012. Alternating diatomaceous and volcaniclastic deposits in Milos Island, Greece. A contribution to the upper Pliocene–lower Pleistocene stratigraphy of the Aegean Sea. Palaeogeography, Palaeoclimatology, Palaeoecology 321–322:24–40.

Cameron, A., and N. Askew, eds. 2011. EUSeaMap—preparatory action for development and assessment of a European broad-scale seabed habitat map final report.

http://jncc.gov.uk/euseamap.

Carballo, J. L., J. E. Sánchez-Moyano, and J. C. García-Gómez. 1994. Taxonomic and ecological remarks on boring sponges (Clionidae) from the Straits of Gibraltar (southern Spain): tentative bioindicators?. Zoological Journal of the Linnean Society 112:407–424.

Cattaneo, A., F. Trincardi, A. Asioli, and A. Correggiari. 2007. The Western Adriatic shelf clinoform: energy-limited bottomset. Continental Shelf Research 27:506–525.

Clark, J. V., A. Pérez-Huerta, D. P. Gillikin, A. E. Aldridge, M. Reolid, and K. Endo. 2016. Determination of paleoseasonality of fossil brachiopods using shell spiral deviations and chemical proxies. Palaeoworld 25:662–674.

Conesa, G., F. Demory, J. Oudet, J. J. Cornée, P. Münch, and J. L. Rubino. 2007. Journée 1—l'Oligo-aquitanien de la Côte Bleue: les systèmes récifaux et bioclastiques du littoral méditerranéen entre l'Estaque et la Couronne. Pp. 1–19 *in* O. Parize and J.-L. Rubino, eds. Les systèmes oligo-miocènes carbonatés et clastiques de Basse-Provence. Des témoins de l'évolution géodynamique de la marge provençale et du bassin d'avant-pays alpin. Excursion commune 10ième congrès ASF–GDR " Marges Golfe du Lion."

Coppier, G., P. Griveaud, F. D. de Larouziere, C. Montenat, and P. Ott d'Estevou. 1989. Example of Neogene tectonic indentation in the Eastern Betic Cordilleras: the Arc of Águilas (southeastern Spain). Geodinamica Acta 3:37–51.

Corbí, H., and J. M. Soria. 2016. Late Miocene–early Pliocene planktonic foraminifer event-stratigraphy of the Bajo Segura basin: a complete record of the western Mediterranean. Marine and Petroleum Geology 77:1010–1027.

Ćorić, S., and J. Hohenegger. 2008. Quantitative analyses of calcareous nannoplankton assemblages from the Baden−Sooss section (Middle Miocene of Vienna Basin, Austria). Geologica Carpathica 59:447–460.

Courville, P., and C. Crônier. 2003. Les faluns tortoniens (Miocène supérieur) de Noyant-la-Plaine, (Ouest de la France). Nouvelles données lithologiques et paléontologiques. Annales de la

Société Géologique du Nord10:275–284.

Crippa, G., F. Ye, C. Malinverno, and A. Rizzi. 2016. Which is the best method to prepare invertebrate shells for SEM analysis?: Testing different techniques on recent and fossil brachiopods. Bollettino della Società Paleontologica Italiana 55:111–125.

Crippa, G., M. Azzarone, C. Bottini, S. Crespi, F. Felletti, M. Marini, M. R. Petrizzo, D. Scarponi, S. Raffi, and G. Raineri. 2019. Bio- and lithostratigraphy of lower Pleistocene marine successions in western Emilia (Italy) and their implications for the first occurrence of *Arctica islandica* in the Mediterranean Sea. Quaternary Research 92:549–569.

D'Alessandro, A., and A. Iannone. 1982. Pleistocene carbonate deposits in the area of Monopoli (Bari province): sedimentology and palaeoecology. Geologica Romana 21:603–653.

D'Alessandro, A., F. Massari, E. Davaud, and G. Ghibaudo. 2004. Pliocene–Pleistocene sequences bounded by subaerial unconformities within foramol ramp calcarenites and mixed deposits (Salento, SE Italy). Sedimentary Geology 166:89–144.

Darling, K.F., M. Kucera, D. Kroon, and C.M. Wade. 2006. A resolution for the coiling direction paradox in *Neogloboquadrina pachyderma*. Paleoceanography 21:1–14.

De Gibert, J. M., R. Domènech, and J. Martinell. 2007. Bioerosion in shell beds from the Pliocene Roussillon Basin, France: implications for the (macro) bioerosion ichnofacies model. Acta Palaeontologica Polonica 52:783–798.

De Porta, J., J. Martinell, and J. Civis Llovera. 1979. Datos paleontológicos y tafonómicos de la formación Turre en Cortijada de Arejos (Almería). Studia Geologica Salmanticensia 15:63–84.

Diedrich, C. G. 2012. Palaeoecology, facies and stratigraphy of shallow marine macrofauna from the Upper Oligocene (Palaeogene) of the southern Pre-North Sea Basin of Astrup (NW Germany). Open Geosciences 4:163–187.

Di Stefano, A., and S. G. Longhitano. 2009. Tectonics and sedimentation of the Lower and Middle Pleistocene mixed siliciclastic/bioclastic sedimentary successions of the Ionian Peloritani

Mts (NE Sicily, southern Italy): the onset of opening of the Messina Strait. Central European Journal of Geosciences 1:33–62.

Dixon, R. 2011. Field meeting to the Bawdsey Peninsula, Suffolk, England, 22nd May 2010, to examine London Clay, Coralline Crag and Red Crag deposits: Leaders: Roger Dixon and Bob Markham. Proceedings of the Geologists' Association 122:514–523.

Dominici, S. 2001. Taphonomy and paleoecology of shallow marine macrofossil assemblages in a collisional setting (late Pliocene–early Pleistocene, western Emilia, Italy). Palaios 16:336–353.

Dominici, S., C. Conti, and M. Benvenuti. 2008. Foraminifer communities and environmental change in marginal marine sequences (Pliocene, Tuscany, Italy). Lethaia 41:447–460.

Donnici, S., and R. S. Barbero. 2002. The benthic foraminiferal communities of the northern Adriatic continental shelf. Marine Micropaleontology 44:93–123.

Driscoll, N. W., and G. D. Karner. 1999. Three-dimensional quantitative modeling of clinoform development. Marine Geology 154:383–398.

Emig, C. C. 1989. Distributional patterns along the Mediterranean continental margin (Upper Bathyal) using *Gryphus vitreus* (Brachiopoda) densities. Palaeogeography, Palaeoclimatology, Palaeoecology 71:253–256.

Emig, C. C. 2018. Brachiopodes récoltés lors de campagnes (1976–2014) dans l'étage Bathyal des côtes françaises méditerranéennes. Redéfinition des limites du système phytal dans le domaine marin benthique. Carnets de Géologie, Madrid, CG2018_B01.

Emig, C. C., and M. A. García-Carrascosa. 1991. Distribution of *Gryphus vitreus* (Born, 1778) (Brachiopoda) on transect P2 (Continental margin, French Mediterranean coast) investigated by submersible. Scientia Marina 55:385–388.

Emig, C. C., M. A. Bitner and F. Álvarez. 2013. Phylum Brachiopoda. Zootaxa 3703:75–78.

Fontanier, C., F. J. Jorissen, G. Chaillou, C. David, P. Anschutz, and V. Lafon. 2003. Seasonal and interannual variability of benthic foraminiferal faunas at 550 m depth in the Bay of Biscay.

Deep Sea Research, part I (Oceanographic Research Papers) 50:457–494.

Fontanier, C., F. J. Jorissen, B. Lansard, A. Mouret, R. Buscail, S. Schmidt, P. Kerhervé, et al. 2008. Live foraminifera from the open slope between Grand Rhône and Petit Rhône Canyons (Gulf of Lions, NW Mediterranean). Deep Sea Research, part I (Oceanographic Research Papers) 55:1532–1553.

Försterra, G., V. Häussermann, and C. Lüter. 2008. Mass occurrence of the recent brachiopod *Magellania venosa* (Terebratellidae) in the fjords Comau and Renihue, northern Patagonia, Chile. Marine Ecology 29:342–347.

Foster, M.W. 1974. Recent Antarctic and subantarctic brachiopods. Antarctic Research Series 21. American Geophysical Union, Washington, D.C.

Frezza, V., J. S. Pignatti, and R. Mateucci. 2010. Benthic foraminiferal biofacies in temperate carbonate sediment in the Western Pontine Archipelago (Tyrrhenian Sea, Italy). Journal of Foraminiferal Research 40:313–326.

Gaetani, M. 1986. Brachiopod palaeocommunities from the Plio/Pleistocene of Calabria and Sicily (Italy). Pp. 477–483 *in* P. R. Racheboeuf and C. C. Emig, eds. Les Brachiopodes fossiles et actuels. Biostratigraphie du Paléozoïque 4.

Gaetani, M., and D. Saccà. 1985. Brachiopodi neogenici e pleistocenici della provincia di Messina e della Calabria meridionale. Geologica Romana 22:1–43.

García-Ramos, D. A., and M. Zuschin. 2019. High-frequency cycles of brachiopod shell beds on subaqueous delta-scale clinoforms (early Pliocene, south-east Spain). Sedimentology 66:1486–1530.

Giannetti, A., J. F. Baeza-Carratalá, J. M. Soria-Mingorance, A. Dulai, J. E. Tent-Manclús, and Peral-Lozano, J. 2018. New paleobiogeographical and paleoenvironmental insight through the Tortonian brachiopod and ichnofauna assemblages from the Mediterranean–Atlantic seaway (Guadix Basin, SE Spain). Facies 64:24.

Giannetti, A., P. Monaco, S. Falces-Delgado, F. G. La Iacona, and H. Corbí. 2019. Taphonomy,

ichnology, and palaeoecology to distinguish event beds in varied shallow-water settings (Betic Cordillera, SE Spain). Journal of Iberian Geology 45:47–61.

Gili J. M., R. Sardà, T. Madurell, and S. Rossi. 2014. Zoobenthos. Pp. 213–236 *in* S. Goffredo and Z. Dubinsky, eds. The Mediterranean Sea: its history and present challenges. Springer, Dordrecht, Netherlands.

Glaub, I. 2004. Recent and sub-recent microborings from the upwelling area off Mauritania (West Africa) and their implications for palaeoecology. *In* D. McIlroy, ed. The application of ichnology to palaeoenvironmental and stratigraphic analysis. Geological Society of London Special Publication 228:63–67.

Golubić, S., and G. Radtke. 2008. The trace *Rhopalia clavigera* isp. n. reflects the development of its maker *Eugomontia sacculata* Kornmann 1960. Pp. 95–108 *in* M. Wisshak and L. Tapanila, eds. Current developments in bioerosion. Springer, Berlin.

Gramigna, P., A. Guido, A. Mastandrea, and F. Russo. 2008. The paleontological site of Cessaniti: a window on a coastal marine environment of seven million years ago (southern Calabria, Italy). Geologica Romana 41:25–34.

Gramigna, P., D. Bassi, and F. Russo. 2012. An upper Miocene siliciclastic-carbonate ramp: depositional architecture, facies distribution, and diagenetic history (Capo Vaticano area, southern Italy). Facies 58:191–215.

Guijarro, J. A., J. Conde, J. Campins, M. L. Orro, and M. A. Picornell. 2015. Atlas de clima marítimo 0-52°N, 35°W-12°E 1981–2010. Agencia Estatal de Meteorología, Madrid.

Hemleben, C., M. Spindler, and O. R. Anderson. 1989. Modern planktonic foraminifera. Springer, New York.

Hernández-Molina, F. J., L. M. Fernández-Salas, F. Lobo, L. Somoza, V. Díaz-del-Río, and J.A. Dias. 2000. The infralittoral prograding wedge: a new large-scale progradational sedimentary body in shallow marine environments. Geo-Marine Letters 20:109–117.

Hohenegger, J., 2005. Estimation of environmental paleogradient values based on presence/absence

data: a case study using benthic foraminifera for paleodepth estimation. Palaeogeography, Palaeoclimatology, Palaeoecology 217:115–130.

Iaccarino, S., I. Premoli-Silva, M. Biolzi, L. M. Foresi, F. Lirer, E. Turco, and M. R. Petrizzo. 2007. Practical manual of Neogene planktonic foraminifera. International School on Planktonic Foraminifera, 6th Course. Universita degli Studi di Perugia, Perugia.

Ietto, F., and M. P. Bernasconi. 2005. The cliff bordering the northwestern margin of the Mesima basin (southern Calabria) is of Pleistocene age. Geografia Fisica e Dinamica Quaternaria28:205–210.

Incarbona, A., J. Dinarès-Turell, E. Di Stefano, G. Ippolito, N. Pelosi, and R. Sprovieri. 2013. Orbital variations in planktonic foraminifera assemblages from the Ionian Sea during the Middle Pleistocene Transition. Palaeogeography, Palaeoclimatology, Palaeoecology 369:303–312.

James, M. A., A. D. Ansell, M. J. Collins, G. B. Curry, L. S. Peck, and M. C. Rhodes. 1992. Biology of living brachiopods. Advances in Marine Biology 28:175–387.

Jorissen, F. J., H. C. de Stigter, and J. G. V. Widmark. 1995. A conceptual model explaining benthic foraminiferal microhabitats. Marine Micropaleontology 26:3–15.

Jorissen, F. J., M. P. Nardelli, A. Almogi-Labin, C. Barrasa, L. Bergamin, E. Bicchia, A. El Katebe, et al.. 2018. Developing Foram-AMBI for biomonitoring in the Mediterranean: species assignments to ecological categories. Marine Micropaleontology 140:33–45.

Kennett, J. P., and M. S. Srinivasan. 1983. Neogene planktonic foraminifera: a phylogenetic atlas. Hutchinson Ross, Stroudsburg, Penn.

Kidwell, S. M., F. T. Fürsich, and T. Aigner. 1986. Conceptual framework for the analysis and classification of fossil concentrations. Palaios 1:228–238.

Koho, K. A., R. García, H. C. de Stigter, E. Epping, E. Koning, T. J. Kouwenhoven, and G. J. van der Zwaan. 2008. Sedimentary labile organic carbon and pore water redox control on species distribution of benthic foraminifera: a case study from Lisbon–Setúbal Canyon

(southern Portugal). Progress in Oceanography 79:55–82.

Kowalewski, M., M. G. Simões, M. Carroll, and D. L. Rodland. 2002. Abundant brachiopods on a tropical, upwelling-influenced shelf (Southeast Brazilian Bight, South Atlantic). Palaios 17:277–286.

Kroh, A., M. Harzhauser, W. E. Piller, and F. Rögl. 2003. The Lower Badenian (Middle Miocene) Hartl Formation (Eisenstadt-Sopron Basin, Austria). Pp. 87–109 *in* W. E. Piller, ed. Stratigraphia Austriaca. Schriftenreihe Erdwissenschaftliche Kommissionen, Vol. 16. Österreichische Akademie der Wissenschaften, Vienna.

Kucera, M., M. Weinelt, T. Kiefer, U. Pflaumann, A. Hayes, M. Weinelt, M.-T. Chen, et al. 2005. Reconstruction of sea-surface temperatures from assemblages of planktonic foraminifera: multi-technique approach based on geographically constrained calibration data sets and its application to glacial Atlantic and Pacific Oceans. Quaternary Science Reviews 24:951–998.

LaBarbera, M. 1977. Brachiopod orientation to water movement. 1. Theory, laboratory behavior, and field orientations. Paleobiology 3:270–287.

Lancis, C. S., J. E. Tent-Manclús, J. A. Flores, and J. M. Soria Mingorance. 2015. The Pliocene Mediterranean infilling of the Messinian erosional surface: new biostratigraphic data based on calcareous nannofossils (Bajo Segura basin, SE Spain). Geologica Acta 13:211–228.

Langezaal, A. M., F. J. Jorissen, B. Braun, G. Chaillou, C. Fontanier, P. Anschutz, and G. J. van der Zwaan, G. J. 2006. The influence of seasonal processes on geochemical profiles and foraminiferal assemblages on the outer shelf of the Bay of Biscay. Continental Shelf Research 26:1730–1755.

La Perna, R., and A. Vazzana. 2016. On the last occurrence of Marginella Lamarck, 1799 (Gastropoda, Marginellidae) in the Mediterranean: description of a new species from the Early Pleistocene and paleoceanographic implications. Geodiversitas 38:451–462.

Lear, C. H., H. Elderfield, and P. A. Wilson. 2000. Cenozoic deep-sea temperatures and global ice volumes from Mg/Ca in benthic foraminiferal calcite. Science 287:269–272.

Lee, D. E., 1991. Aspects of the ecology and distribution of the living Brachiopoda of New Zealand. Pp. 273–279 *in* D. L. MacKinnon, D. E. Lee, and J. D. Campbell, eds. Brachiopods through time. Balkema, Rotterdam.

Lee, D. E. 2008. The terebratulides: the supreme brachiopod survivors. Fossils and Strata 54:241–249.

Llompart, C., and S. Calzada. 1982. Braquiópodos messinienses de la isla de Menorca. Boletín de la Real Sociedad Española de Historia Natural. Sección geológica 80:185–206.

Logan, A., and J. P. A. Noble. 1971. A Recent shallow-water brachiopod community from the Bay of Fundy. Maritime Sediments 7:85–91.

Long, P. E., and J. A. Zalasiewicz. 2011. The molluscan fauna of the Coralline Crag (Pliocene, Zanclean) at Raydon Hall, Suffolk, UK: palaeoecological significance reassessed. Palaeogeography, Palaeoclimatology, Palaeoecology 309:53–72.

Malgrem, B. A., and J. P. Kennett. 1977. Biometric differentiation between Recent *Globigerina bulloides* and *Globigerina falconensis* in the southern Indian Ocean. Journal of Foraminiferal Research 7:130–148.

Massari, F., and A. D'Alessandro. 2012. Facies partitioning and sequence stratigraphy of a mixed siliciclastic-carbonate ramp stack in the Gelasian of Sicily (S Italy): a potential model for Icehouse, distally-steepened Heterozoan ramps. Rivista Italiana di Paleontologia e Stratigrafia 118:503–534.

Mendes, I., J. D. Alveirinho, J. Schönfeld, and O. Ferreira. 2012. Distribution of living benthic foraminifera on the northern Gulf of Cádiz Continental Shelf. Journal of Foraminiferal Research 42:18–38.

Messina, C., M. A. Rosso, F. Sciuto, I. D. Geronimo, W. Nemec, T. D. Dio, R. D. Geronimo, R. Maniscalco, and R. Sanfilippo. 2009. Anatomy of a transgressive systems tract revealed by integrated sedimentological and palaeoecological study: the Barcellona Pozzo Di Gotto Basin, northeastern Sicily, Italy. Pp. 367–400 *in* G. Nichols, E. Williams, and C. Paola, eds.

Sedimentary processes, environments and basins. Wiley-Blackwell, Oxford.

Milker, Y., and G. Schmiedl. 2012. A taxonomic guide to modern benthic shelf foraminifera of the western Mediterranean Sea. Palaeontologia Electronica 15:1–134.

Milker, Y., G. Schmiedl, C. Betzler, M. Roemer, D. Jaramillo-Vogel, and M. Siccha. 2009. Distribution of recent benthic foraminifera in shelf carbonate environments of the western Mediterranean Sea. Marine Micropaleontology 73:207–225.

Mitchell, N. C. 2012. Modeling the rollovers of sandy clinoforms from the gravity effect on wave-agitated sand. Journal of Sedimentary Research 82:464–468.

Mojtahid, M., F. Jorissen, B. Lansard, and C. Fontanier. 2010. Microhabitat selection of benthic foraminifera in sediments off the Rhône River mouth (NW Mediterranean). Journal of Foraminiferal Research 40:231–246.

Molinu A. R., R. Domènech, D. A. García-Ramos, and J. Martinell. 2013. Microbioerosión en esqueletos de invertebrados marinos del Plioceno temprano de la región de Murcia. Libro de resúmenes de las XXIX Jornadas de la Sociedad Española de Paleontología. Córdoba:97–98.

Monegatti, P., and S. Raffi. 2001. Taxonomic diversity and stratigraphic distribution of Mediterranean Pliocene bivalves. Palaeogeography, Palaeoclimatology, Palaeoecology 165:171–193.

Montenat, C., P. Barrier, and L. Garnier. 2000. La sédimentation miocène au nord des massifs de Ventoux-Lure (chaînes subalpines méridionales). Géologie de la France 3:3–32.

Murray, J. W. 1976. A method of determining proximity of marginal seas to an ocean. Marine Geology 22:103–119.

Noble, J. P. A., A. Logan, and G. R. Webb. 1976. The Recent Terebratulina community in the rocky subtidal zone of the Bay of Fundy, Canada. Lethaia 9:1–18.

Obrador, A., L. P. i Gomà, A. R. Perea, and M. J. Jurado. 1983. Unidades deposicionales del Neógeno menorquín. Acta geológica hispánica 18:87–97.

Oksanen, J. F., G. Blanchet, R. Kindt, P. Legendre, P. R. Minchin, R. B. O'Hara, G. L. Simpson, P. Solymos, M. H. H. Stevens, and H. Wagner. 2018. Vegan: community ecology package, R package version 2.5-2. **https://cran.r-project.org/web/packages/vegan/index.html**.

O'Neil, J. R., R. N. Clayton, and T. K. Mayeda. 1969. Oxygen isotope fractionation in divalent metal carbonates. Journal of Chemical Physics 51:5547–5558.

Patruno, S., and W. Helland-Hansen. 2018. Clinoforms and clinoform systems: Review and dynamic classification scheme for shorelines, subaqueous deltas, shelf edges and continental margins. Earth-Science Reviews 185:202–233.

Patruno, S., G. J. Hampson, and C. A. -L. Jackson. 2015. Quantitative characterisation of deltaic and subaqueous clinoforms. Earth-Science Reviews 142:79–119.

Pavia, G., and M. Zunino. 2008. Progetti di conservazione del sito a Brachiopodi del Pliocene Inferiore di Capriglio (Asti). Geologica Romana 41:19–24.

Peck, L. S. 2005. Prospects for survival in the Southern Ocean: vulnerability of benthic species to temperature change. Antarctic Science 17:497–507.

Peck, L. S. 2007. Brachiopods and climate change. Earth and Environmental Science Transactions of the Royal Society of Edinburgh 98:451–456.

Peck, L. S., S. Brockington, and T. Brey. 1997. Growth and metabolism in the Antarctic brachiopod *Liothyrella uva*. Philosophical Transactions of the Royal Society of London B 352:851–858.

Pedley, H. M. 1976. A palaeoecological study of the Upper Coralline Limestone, *Terebratula-Aphelesia* Bed (Miocene, Malta) based on bryozoan growth-form studies and brachiopod distributions. Palaeogeography, Palaeoclimatology, Palaeoecology 20:209–234.

Pedley, H. M., and M. Grasso. 2002. Lithofacies modelling and sequence stratigraphy in microtidal cool-water carbonates: a case study from the Pleistocene of Sicily, Italy. Sedimentology 49:533–553.

Pervesler, P., R. Roetzel, and A. Uchman. 2011. Ichnology of shallow sublittoral siliciclastics of the Burgschleinitz Formation (Lower Miocene, Eggenburgian) in the Alpine-Carpathian

Foredeep (NE Austria). Austrian Journal of Earth Sciences 104:81–96.

Phipps, M., M. A. Kaminski, and A. E. Aksu. 2010. Calcareous benthic foraminiferal biofacies on the southern Marmara Shelf. Micropaleontology 56:377–392.

Pomar, L., and M. Tropeano. 2001. The Calcarenite di Gravina Formation in Matera (southern Italy): new insights for coarse-grained, large-scale, cross-bedded bodies encased in offshore deposits. AAPG Bulletin 85:661–690.

Pomar, L., A. Obrador, and H. Westphal. 2002. Sub-wavebase cross-bedded grainstones on a distally steepened carbonate ramp, Upper Miocene, Menorca, Spain. Sedimentology 49:139–169.

Pomar, L., M. Aurell, B. Bádenas, M. Morsilli, and S. F. Al-Awwad. 2015. Depositional model for a prograding oolitic wedge, Upper Jurassic, Iberian basin. Marine and Petroleum Geology 67:556–582.

Poore, R. Z., and W. A. Berggren. 1975. The morphology and classification of *Neogloboquadrina atlantica* (Berggren). Journal of Foraminiferal Research 5:76–84.

Puga-Bernabéu, A., J. M. Martín, and J. C. Braga. 2008. Sistemas de canales submarinos en una rampa de carbonatos templados, Cuenca de Sorbas, sureste de España. Geogaceta 44:203–206.

R Development Core Team, 2018. Version 3.5, R: a language and environment for statistical computing: R Foundation for Statistical Computing, Vienna. http://www.R-project.org

Radley, J. D. 2010. Grazing bioerosion in Jurassic seas: a neglected factor in the Mesozoic marine revolution? Historical Biology 22:387–393.

Rasmussen, T. L. 2005. Systematic paleontology and ecology of benthic foraminifera from the Plio-Pleistocene Kallithea Bay section, Rhodes, Greece. Cushman Foundation for Foraminiferal Research, Special Publication 39:53–157.

Rebotim, A., A. H. L. Voelker, L. Jonkers, J. J. Waniek, H. Meggers, R. Schiebel, I. Fraile, M. Schulz, and M. Kucera. 2017. Factors controlling the depth habitat of planktonic foraminifera in the subtropical eastern North Atlantic. Biogeosciences 14:827–859.

Reolid, M., F. García-García, A. Tomašových, and J. M. Soria. 2012. Thick brachiopod shell concentrations from prodelta and siliciclastic ramp in a Tortonian Atlantic–Mediterranean strait (Miocene, Guadix Basin, southern Spain). Facies 58:549–571.

Richardson, J. R. 1981. Distribution and orientation of six articulate brachiopod species from New Zealand. New Zealand Journal of Zoology 8:189–196.

Roetzel, R., P. Pervesler, O. Mandic, and M. Harzhauser. 1999. B5 Limberg-Steinbrüch Hengl. Pp. 290–293 *in* R. Roetzel, ed. Arbeitstagung der Geologischen Bundesanstalt 1999—Retz-Hollabrunn. Geologische Bundesanstalt, Vienna.

Rögl, F., S. Ćorić, M. Harzhauser, G. Jimenez-Moreno, A. Kroh, O. Schultz, G. Wessely, and I. Zorn. 2008. The Middle Miocene Badenian stratotype at Baden-Sooss (Lower Austria). Geologica Carpathica 59:367–374.

Rohling, E. J. 2013. Oxygen isotope composition of seawater. Pp. 915–922 *in* S. A. Elias ed. The encyclopedia of Quaternary science. Elsevier, Amsterdam.

Rohling, E. J., G. L. Foster, K. M. Grant, G. Marino, A. P. Roberts, M. E. Tamisiea, and F. Williams. 2014. Sea-level and deep-sea-temperature variability over the past 5.3 million years. Nature 508:477–482.

Rollion-Bard C., S. Saulnier, N. Vigier, A. Schumacher, M. Chaussidon, and C. Lécuyer. 2016. Variability in magnesium, carbon and oxygen isotope compositions of brachiopod shells: implications for paleoceanographic studies. Chemical Geology 423:49–60.

Romanin, M., G. Crippa, F. Ye, U. Brand, M.A. Bitner, D. Gaspard, V. Häussermann, and J. Laudien. 2018. A sampling strategy for recent and fossil brachiopods: selecting the optimal shell segment for geochemical analyses. Rivista Italiana di Paleontologia e Stratigrafia 124:343–359.

Rudwick, M. J. S. 1961. The anchorage of articulate brachiopods on soft substrata. Palaeontology 4:475–476.

Schiebel, R., and C. Hemleben. 2017. Planktic foraminifers in the modern ocean. Springer, Berlin.

Schmidt, G. A. 1999. Forward modeling of carbonate proxy data from planktonic foraminifera

using oxygen isotope tracers in a global ocean model. Paleoceanography 14:482–497.

Schönfeld, J. 2002. Recent benthic foraminiferal assemblages in deep high-energy environments from the Gulf of Cadiz (Spain). Marine Micropaleontology 44:141–162.

Schweizer, M., J. Pawlowski, T. Kouwenhoven, and B. van der Zwaan. 2009. Molecular phylogeny of common cibicidids and related Rotaliida (Foraminifera) based on small subunit rDNA sequences. Journal of Foraminiferal Research 39:300–315.

Sen Gupta, B. K., L. E. Smith, and M. L. Machain-Castillo. 2009. Foraminifera of the Gulf of Mexico. Pp. 87–129 *in* D. L. Felder and D. K. Camp eds. Gulf of Mexico—origins, waters, and biota. Biodiversity, Vol. 1. Texas A&M University Press, College Station, Tex.

Serrano, F., J. M. González-Donoso, P. Palmqvist, A. Guerra-Merchán, D. Linares, and J. A. Pérez-Claros. 2007. Estimating Pliocene sea-surface temperatures in the Mediterranean: an approach based on the modern analogs technique. Palaeogeography, Palaeoclimatology, Palaeoecology 243:174–188.

Sgarrella, F., and M. Moncharmont Zei. 1993. Benthic Foraminifera of the Gulf of Naples (Italy): systematics and autoecology. Bollettino della Società Paleontologica Italiana 32:145–264.

Sierro, F. J., J. A. Flores, G. Francés, A. Vazquez, R. Utrilla, I. Zamarreño, H. Erlenkeuser, and M. A. Barcena. 2003. Orbitally-controlled oscillations in planktic communities and cyclic changes in western Mediterranean hydrography during the Messinian. Palaeogeography, Palaeoclimatology, Palaeoecology 190:289–316.

Silva, A., S. Palma, P. B. Oliveira, and M. T. Moita. 2009. *Calcidiscus quadriperforatus* and *Calcidiscus leptoporus* as oceanographic tracers in Lisbon Bay (Portugal). Estuarine, Coastal and Shelf Science 81:333–344.

Simpson, G. L. 2007. Analogue methods in palaeoecology: using the analogue package. Journal of Statistical Software 22:1–29.

Soria, J. M., J. Fernández, F. García, and C. Viseras. 2003. Correlative lowstand deltaic and shelf systems in the Guadix Basin (Late Miocene, Betic Cordillera, Spain): the stratigraphic

record of forced and normal regressions. Journal of Sedimentary Research 73:912–925.

Spezzaferri, S., and F. Tamburini. 2007. Paleodepth variations on the Eratosthenes Seamount (Eastern Mediterranean): sea-level changes or subsidence? eEarth Discussions 2:115–132.

Spezzaferri, S., S. Ćorić, J. Hohenegger, and F. Rögl. 2002. Basin-scale paleobiogeography and paleoecology: an example from Karpatian (Latest Burdigalian) benthic and planktonic foraminifera and calcareous nannofossils from the Central Paratethys. Geobios 35:241–256.

Studencki, W. 1988. Facies and sedimentary environment of the Pinczow limestones (Middle Miocene; Holy cross mountains, central Poland). Facies 18:1–25.

Szarek, R., W. Kuhnt, H. Kawamura, and H. Kitazato. 2006. Distribution of recent benthic foraminifera on the Sunda Shelf (South China Sea). Marine Micropaleontology 61:171–195.

Taddei Ruggiero, E. 1996. Biostratigrafia e paleoecologia delle Calcareniti di Gravina nei dintorni di Cerignola (brachiopodi e foraminiferi). Memorie della Società Geologica Italiana 51:197–207.

Taddei Ruggiero, E., and M. A. Bitner. 2008. Bioerosion on brachiopod shells—a Cenozoic perspective. Earth and Environmental Science Transactions of the Royal Society of Edinburgh 98:369–378.

Taddei Ruggiero, E., and R. Taddei. 2006. I brachiopodi delle calcareniti di Castro Marina (Lecce). Thalassia Salentina 29(Suppl.):301–310.

Taylor, A., R. Goldring, and S. Gowland. 2003. Analysis and application of ichnofabrics. Earth-Science Reviews 60:227–259.

Templado, J. 2014. Future trends of Mediterranean biodiversity. Pp. 479–498 *in* S. Goffredo and Z. Dubinsky, eds.The Mediterranean Sea: its history and present challenges. Springer, Dordrecht, Netherlands.

Thayer, C. W. 1983. Sediment-mediated biological disturbance and the evolution of marine benthos. Pp. 479–629 *in* M. J .S. Tevesz and P. L. McCall, eds. Biotic interactions in Recent and fossil benthic communities. Plenum, New York.

Thayer, C. W. 1986. Are brachiopods better than bivalves? Mechanisms of turbidity tolerance and their interaction with feeding in articulates. Paleobiology 12:161–174.

Thomsen, E., T. L. Rasmussen, and A. Hastrup. 2005. Overview of the Plio-Pleistocene geology of Rhodes, Greece. Lithology, calcareous nannofossil biostratigraphy, and sampling of the Kallithea Bay section. Cushman Foundation for Foraminiferal Research, Special Publication 39:3–13.

Tindall, J. C., and A. M. Haywood. 2015. Modeling oxygen isotopes in the Pliocene: large scale features over the land and ocean. Paleoceanography 30:1183–1201.

Titschack, J., R. G. Bromley, and A. Freiwald. 2005. Plio-Pleistocene cliff-bound, wedge-shaped, warm-temperate carbonate deposits from Rhodes (Greece): sedimentology and facies. Sedimentary Geology 180:29–56.

Tomašových, A. 2006. Brachiopod and Bivalve ecology in the Late Triassic (Alps, Austria): onshore-offshore replacements caused by variations in sediment and nutrient supply. Palaios 21:344–368.

Tomašových, A. 2008. Substrate exploitation and resistance to biotic disturbance in the brachiopod *Terebratalia transversa* and the bivalve *Pododesmus macrochisma*. Marine Ecology Progress Series 363:157–170.

Tomašových, A., F. T. Fürsich, and M. Wilmsen. 2006. Preservation of autochthonous shell beds by positive feedback between increased hard part-input rates and increased sedimentation rates. Journal of Geology 114:287–312.

Tunnicliffe, V., and K. Wilson. 1988. Brachiopod populations: distribution in fjords of British Columbia (Canada) and tolerance of low oxygen concentration. Marine Ecology Progress Series 47:117–128.

van der Zwaan, G. J., F. J. Jorissen, and H. C. de Stigter. 1990. The depth dependency of planktonic/benthic foraminiferal ratios: constraints and applications. Marine Geology 95:1–16.

Videt, B. 2003. Dynamique des paléoenvironnements à huîtres du Crétacé supérieur nord-aquitain (SO France) et du Mio-Pliocène andalou (SE Espagne): biodiversité, analyse séquentielle, biogéochimie. Ph.D. dissertation, Université Rennes 1, Rennes, France.

Vignols, R. M., A. M. Valentine, A. G. Finlayson, E. M. Harper, B. R. Schöne, M. J. Leng, H. J. Sloane, and A. L. A Johnson. 2018. Marine climate and hydrography of the Coralline Crag (early Pliocene, UK): isotopic evidence from 16 benthic invertebrate taxa. Chemical Geology. doi: 10.1016/j.chemgeo.2018.05.034.

Wade, B. S., and P. R. Bown. 2006. Calcareous nannofossils in extreme environments: the Messinian salinity crisis, Polemi Basin, Cyprus. Palaeogeography, Palaeoclimatology, Palaeoecology 233:271–286.

Weinkauf, M., and Y. Milker. 2018. The effect of size fraction in analyses of benthic foraminiferal assemblages: a case study comparing assemblages from the >125 and >150 μm size fractions. Frontiers in Earth Science 37:1–10.

Wildish, D., and D. Kristmanson. 1997. Benthic suspension feeders and flow. Cambridge University Press, New York.

Williams, U-M. M-C., J. Robinson, D. Lee, and M. Lamare. 2018. Investigating the ecology and environmental tolerance to sedimentation of the brachiopod *Calloria inconspicua* in Otago Harbour, New Zealand. Permophiles 66(Suppl. 1):123–124.

Wisshak, M. 2012. Microbioerosion. Pp. 213–243 *in* D. Knaust, and R. G. Bromley, eds. Trace fossils as indicators of sedimentary environments. Developments in Sedimentology 64. Elsevier, Amsterdam.

Witman, J. D., and R. A. Cooper. 1983. Disturbance and contrasting patterns of population structure in the brachiopod *Terebratulina septentrionalis* (Couthouy) from two subtidal habitats. Journal of Experimental Marine Biology and Ecology 73:57–79.

Young, J. R., 1998. Neogene. Pp. 225–265 *in* P. R. Bown, ed. Calcareous nannofossil biostratigraphy. Chapman & Hall, Cambridge.

Zuschin, M., and S. Mayrhofer. 2009. Brachiopods from cryptic coral reef habitats in the northern Red Sea. Facies 55:335–344.

SUPPORTING INFORMATION

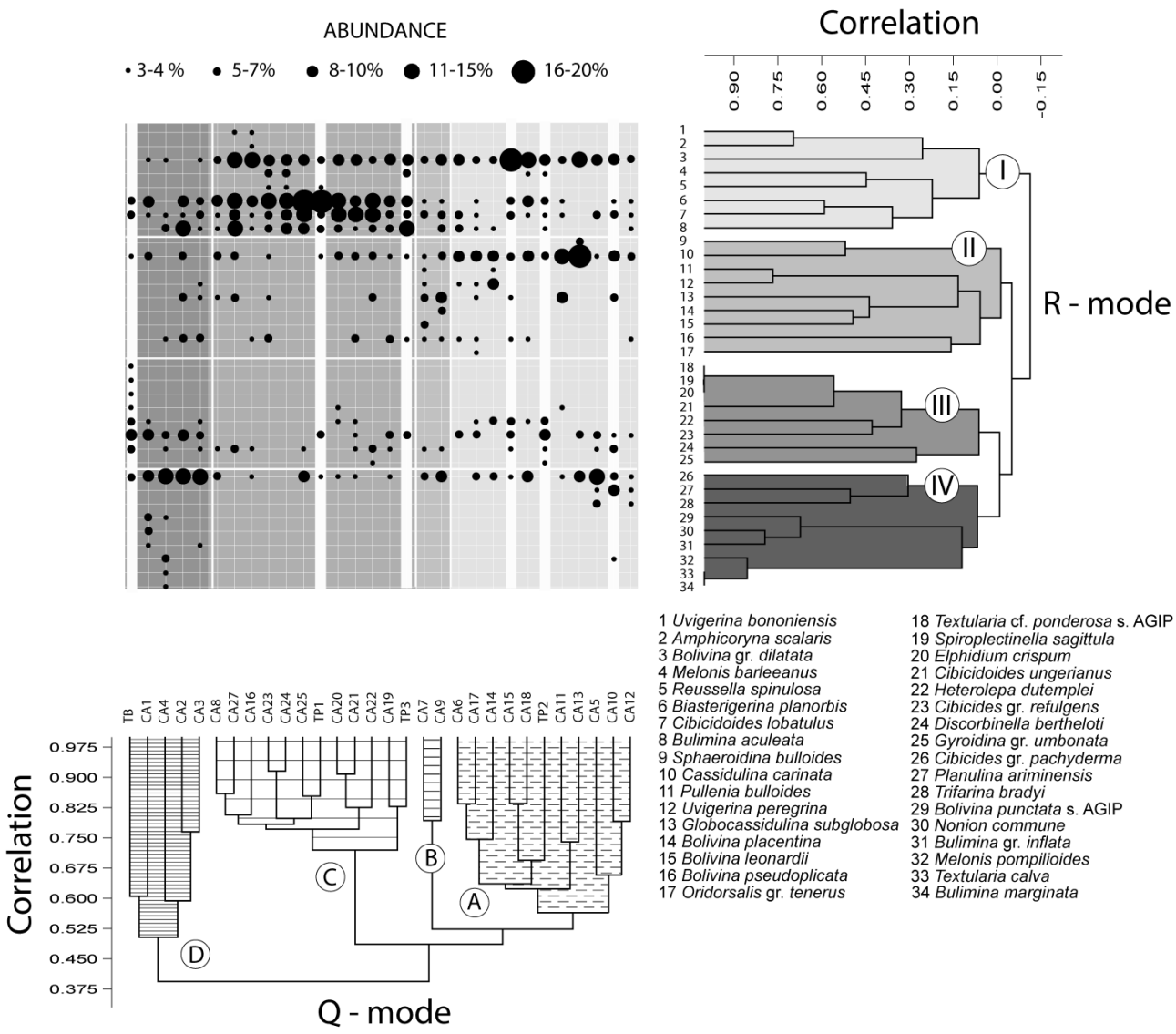

SUPPLEMENTARY FIGURE 1. Two-way (Q-mode, R-mode) Paired Group Average (UPGMA) cluster analysis. The samples associated with *Terebratula* are indicated by thick white vertical lines.

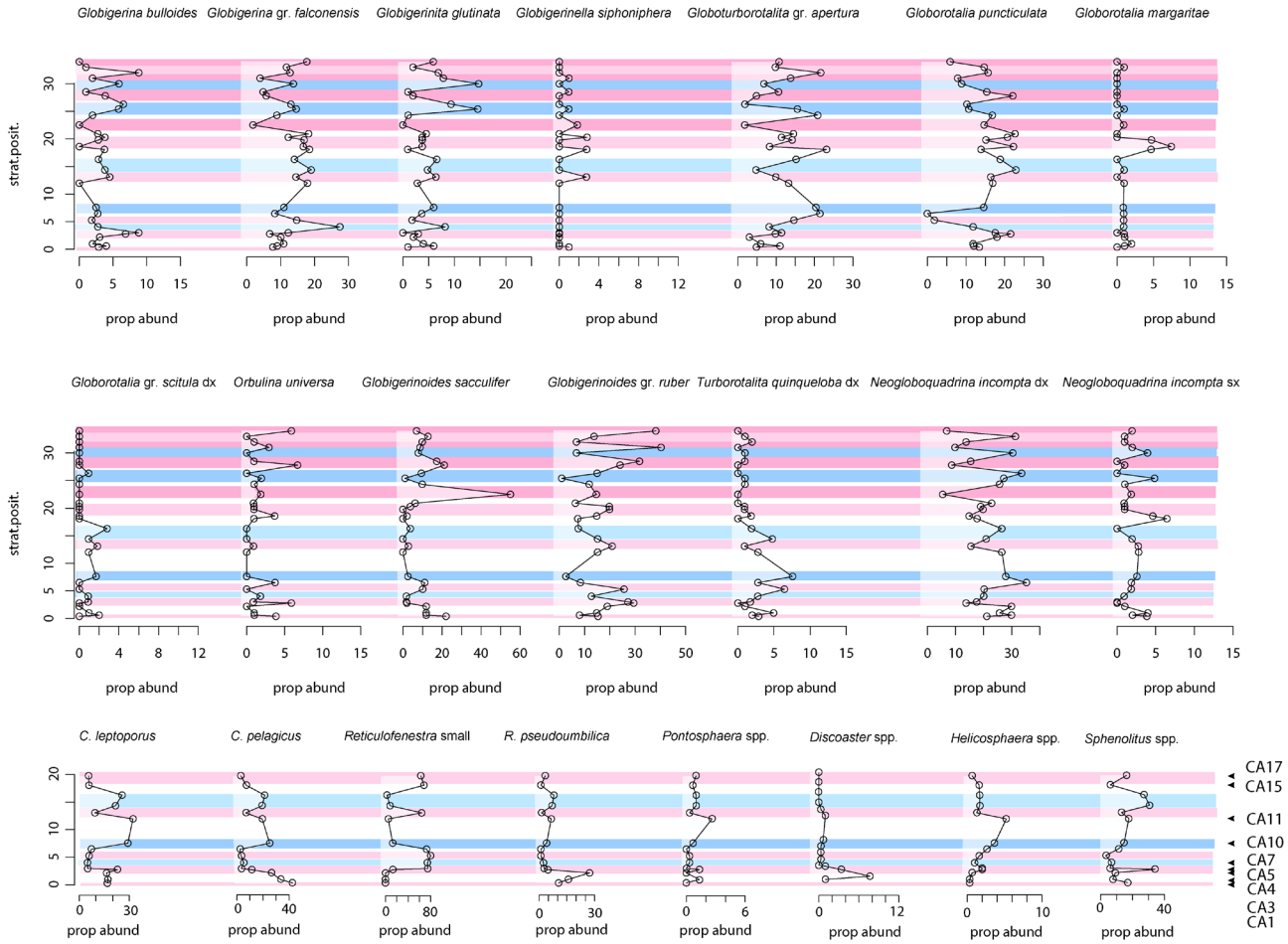

SUPPLEMENTARY FIGURE 2. Distribution of the main planktonic foraminifera (first two rows) and calcareous nannoplankton (last row) taxa in the Cabezo Alto section. The red and blue bands represent warm and cold periods identified with transfer functions of planktonic foraminifera. *Globigerinoides* gr. *ruber* includes *G. ruber*, *G. obliquus* and *G. extremus*.

SUPPLEMENTARY TABLE 1. Habitats features of modern Terebratulida bathymetrically equivalent to *Terebratula*.

Species	**Bathymetry**	**Environment**	**Type of substrate**	**Reference**
Terebratalia transversa	Shallow (intertidal down to 110 m; optimum >20 m)	Small bays and marine channels	Rocky habitats	Tomašových (2008)
Terebratulina septentrionalis	Mainly shallow (0-750; optimum 35 m)	Bay	Rocks or boulders; rarely shell fragments	Logan and Noble (1971)
Magellania venosa	Shallow (2 – 35 m; optimum 15-20 m)	Fjord	Solitary or clustered; Mainly rocky (overhangs at 2 m depth); rarely soft sediments (attached to coarse sand grains)	Försterra et al. (2008)
Liothyrella neozelanica	Mainly shallow (predominantly between 10 to 40 m, but recorded down to 805 m)	Fjord	Solitary and clustered; Rocky habitats and sessile animals on the substrate (also conspecifics)	Foster (1974); Richardson (1981)
Calloria inconspicua	Shallow (intertidal to subtidal)	Fjord	Solitary and clustered; Rock to soft bottoms (mud to shell-gravel; attached to molluscan, worm, brachiopod shells and crustose algae).	Richardson (1981)
Magasella sanguinea	Shallow (subtidal)	Fjord	Solitary; rock surfaces to soft bottoms (mud to shell gravel; attached to molluscan, worm, brachiopod shells and crustose algae).	Richardson (1981)

Collective Conclusion

In southern Spain, and elsewhere in the Mediterranean, there are numerous outcrops from relatively shallow-water environments that record *Terebratula* concentrations in the form of pavements. An interesting observation is that these pavements occur embedded in facies which, to the base or the top of the same unit, appear the same but otherwise lack brachiopods. Therefore at close-up outcrop scale, facies of brachiopod-bearing units, *per se*, offer insufficient information to explain the presence-absence patterns of this brachiopod. This dissertation presents the results of the detailed studies on the important lower Pliocene outcrops in the Águilas Basin (SE Spain). The aim was to elucidate the habitat and the paleoenvironmental factors that shaped the distribution of *T. calabra* in different facies belts along a proximal-distal gradient.

Chapter 2 gathers integrative stratigraphic, sedimentological and paleontological features of the SP1 informal stratigraphic sequence of the Águilas Basin (SE Spain), which is exposed in the Cabezo Alto – Cañada Brusca – Cañada Blanca landscapes. Vertical and lateral continuity of different outcrops in the study area, close inspection of stratigraphic surfaces and stacking patterns of different stratigraphic units enabled the interpretation of subaqueous delta-scale clinoforms separating clinothems. Four main facies associations were found. Proximal deposits are characterized by bioturbated coarse friable sands which grade distally into mixed carbonate-siliciclastic finer-grained deposits rich in coralline red algae. These first two facies occur at the topset of the clinoforms. Further distally, red algae disappear and sediments become finer-grained, strikingly characterized by the dominance of polychaete tubes of *Ditrupa arietina*. This latter facies corresponds with the foreset of the clinoforms. Finally, the *Ditrupa* facies gradually disappears and gives way to a fine-grained facies characterized by dispersed *C. cristatum*. These latter materials are the most distal facies belt recognized in the study area, and correspond with the lower rollover and bottomset of the clinoforms. The *Terebratula* pavements occur interspersed in the *C. cristatum* facies. A first obvious conclusion from this inhomogeneous presence-absence pattern of *Terebratula* is that, whatever the environmental conditions conducive to the formation of the

pavements, these were changing cyclically. The stratigraphic intervals immediately associated with the *Terebratula* pavements contain K-poor glaucony which suggests that the pavements formed sometime during periods when that particular environment was subject to low sedimentation rates. The stages of low sedimentation rates were, however, not long enough as to allow maturation of glaucony. This suggests that the *Terebratula* pavements were linked to high-frequency cycles of decreased sedimentation rates. In outcrops recording shallower facies belts, it is possible to recognize regressive surfaces of marine erosion, which conform with an overall falling stage systems tracts. These shallower deposits, however, also record ravinement surfaces overlain by shell-clast lags interpretable as transgressive surfaces. It can be concluded that despite an overall regressive trend, the basin was punctuated by high-frequency pulses of relative sea-level rise. The *Terebratula* paleocommunities were likely favored by the low sedimentation rates derived from these pulses, when accomodation space was created further onshore and the bottomset of the clinoforms periodically became sediment starved.

Low sedimentation rates alone, however, do not explain why the peak abundance of *Terebratula* specimens was attained at the lower rollover of the clinoforms, because the transgressive lags at the topset facies contain rare and disperse, or absent *Terebratula*. The following step, attained in **Chapter 3**, tackled the analysis of seafloor oxygenation, nutrient availability, temperature and light as possible factors influencing the distribution patterns of *Terebratula*. These parameters were assessed in samples both containing and lacking *Terebratula*, based on the integrative study of benthic and planktic foraminiferal, and nannoplankton assemblages, and oxygen isotopes of the secondary layer of brachiopod calcite.

Results from microfossil assemblages show that the differences between *Terebratula*-barren and *Terebratula*-abundant samples are not striking . It can be concluded that *Terebratula* in the Águilas Basin lived under background conditions of oxic seafloors and oligotrophism, although this brachiopod was tolerant to seasonal variations of increased nutrient inputs and the associated possible decrease in oxygen levels at the seafloor. Local temperature variations inferred from

planktic foraminiferal assemblages did not likely affect the presence-absence patterns of *Terebratula* in the study area.

The most obvious distributional pattern of *Terebratula* in the analyzed outcrops was its abundance in sediments invariably lacking coralline red algae, which might indicate dim or aphotic conditions or other environmental factors deleterious for coralline red algae. Previous studies on the microbioerosion ichnoassemblages recorded in *Terebratula* shells from the biostrome, together with the record of rare *Gnathichnus* and absence of *Radulichnus* macrobioerosion traces, also suggest dim light or aphotic conditions, pointing to light irradiances of 0.01% or less. Turbid conditions as an explanation for the low light levels are unlikely because the abundance of clionaid sponges, as evidenced by their bioerosion traces on disarticulated *Terebratula* shells, indicates otherwise. It is concluded that *Terebratula* was likely excluded from well-lit shoreface environments by grazing pressure. Benthic foraminiferal assemblages in the *Terebratula*-containing samples are richer in suspension feeding, current-loving species, compared with *Terebratula*-barren samples. The peak density of *Terebratula* at the lower rollover of the clinoforms is interesting because there is cogent evidence from recent and fossil examples of prograding wedges where the lower rollover is swept by offshore along-slope currents. This distribution pattern has been recorded in some other outcrops elsewhere in Spain and the Mediterranean region.

Oxygen isotope ratios from twelve samples of *Terebratula* shells from the study area show a temperature range of about 7ºC. This narrow range fits the findings for other species, which suggests that *Terebratula* was probably vulnerable to sudden and dramatic temperature drops during glaciations. The extinction of *Terebratula* coinciding approximately with the Jaramillo Subchron supports the hypothesis of a glaciation-mediated extinction mechanism, because the onset of the strongest streak of temperature drops during the Pleistocene started approximately after the Jaramillo Subchron. The conclusion from the research presented in this dissertation is that the main limiting factors for the distribution of *Terebratula calabra* were low sedimentation rates, dim light or aphotic conditions (leading to little or no grazing pressure) and the presence of vigorous offshore

currents which favoured suspension feeding with minimal energetic costs.

Abstract

The brachiopod genera *Terebratula*, *Pliothyrina* and *Maltaia*, belonging to the subfamily Terebratulinae, were species-rich and numerically abundant from the Oligocene to the Pleistocene in relatively shallow-water environments in Europe: the pre-North Sea Basin, the Paratethys, the Mediterranean, and some localities of Portugal, SW Spain, Morocco and the Canary Islands. Despite their success in cool-temperate to subtropical environments during the Cenozoic, overcoming competition and disturbance from mollusks, predators, grazers, bulldozing and bioturbating organisms, the last representatives of the subfamily went extinct in the Pleistocene (Calabrian). The optimal environmental conditions for *Terebratula* and its preferred habitat are currently poorly known. The present dissertation presents the results about the investigation of the stratigraphic and paleoenvironmental distribution of the terebratulidine brachiopod *Terebratula calabra* from the lower Pliocene deposits in the Águilas Basin (south-east Spain). This is an ideal area to investigate the paleoecology of *Terebratula* because 1) outcrops are widespread and often continuous vertically and horizontally, enabling the study of the variability of facies belts, the recognition of important stratigraphic surfaces and the associated stacking patterns of the stratigraphic units; 2) *Terebratula* skeletal concentrations are numerous and occur cyclically, forming disperse to thin, densely packed pavements, and a biostrome (a 2-m-thick densely packed *Terebratula*-dominated concentration cropping out along 850 m in the study area). The second chapter of this dissertation presents sequence stratigraphic and sedimentological models of the lower Pliocene sequence in the study area. The small-scale stratigraphic units were identified as clinothems bounded by subaqueous delta-scale clinoforms. Regressive surfaces of marine erosion coupled with downstepping stacking patterns point to a general trend of relative sea-level fall. It is concluded that *Terebratula* paleocommunities thrived cyclically as a response to high-frequency pulses of relative sea-level rise, due to an increase in accommodation space associated with an onshore expansion of the coastal facies belts and the concomitant sediment starvation in offshore environments occupied by the *Terebratula* paleocommunities. The third chapter of this

dissertation focuses on paleoecological factors (bottom oxygenation, productivity, temperature and light irradiance) as explanatory variables for the success of *Terebratula* along a proximal-distal gradient. These factors were assessed by investigating the benthic and planktic foraminiferal, and calcareous nannoplankton assemblages, and oxygen isotope ratios from the secondary layer of *Terebratula* shell calcite. It is concluded that *Terebratula* was versatile, preferring well-oxygenated, oligotrophic environmental regimes, but was able to tolerate fluctuating pulses of increased organic matter input and the associated reduced oxygen levels at the seafloor. Paleotemperature derived from planktic foraminiferal assemblages suggests that this parameter was not important at the local scale for the success of *Terebratula*. *Terebratula* was rare or absent in shoreface environments. Peak abundances of *Terebratula* were consistently found close to, but below, the offshore transition zone where coralline red algae were absent. Previous investigations on microbioerosion ichnoassemblages recorded in *Terebratula* shells, together with rare echinoid rasping trace *Gnathichnus pentax* and the absence of shallower *Radulichnus*, suggest that *Terebratula* thrived in dim light or aphotic conditions, probably excluded from shallower, better lit environments by grazing disturbance. The disproportional distribution of *Terebratula* in offshore environments can be explained by a combination of sedimentation rate gradients and offshore shore-parallel current systems. The narrow range of paleotemperatures exhibited by different species of Terebratulinae, derived from oxygen isotope ratios, suggests that the last members of the subfamily could not survive the conspicuous temperature drops that occurred approximately during or after the Jaramillo Subchron.

Zusammenfassung

Die zur Unterfamilie Terebratulinae gehörenden Brachiopodengattungen *Terebratula*, *Pliothyrina* und *Maltaia* waren artenreich und vom Oligozän bis zum Pleistozän im relativ flachen Meeresbereich in Europa häufig: das Paläo-Nordseebecken, die Paratethys, das Mittelmeer, und einige Orte in Portugal, Südwestspanien, Marokko und den Kanarischen Inseln. Trotz ihres Erfolgs in kühl-gemäßigten bis subtropischen Umgebungen während des Känozoikums, der Überwindung der Konkurrenz und der Beeinträchtigung durch Mollusken, Räuber, Weidegänger, Bulldozer und bioturbierende Organismen, starben die letzten Vertreter der Unterfamilie im Pleistozän (Kalabrium) aus. Die optimalen Umweltbedingungen für *Terebratula* und seinen bevorzugten Lebensraum sind derzeit kaum bekannt. Die vorliegende Dissertation präsentiert die Ergebnisse zur Untersuchung der stratigraphischen und paläoökologischen Verteilung des Terebratuliden Brachiopodenart *Terebratula calabra* aus den unteren Pliozänsedimenten im Águilas-Becken (Südostspanien). Dies ist ein idealer Bereich, um die Paläoökologie von *Terebratula* zu untersuchen, da 1) Aufschlüsse weit verbreitet und häufig vertikal und horizontal verfolgbar sind, was die Charakterisierung und Variabilität von Faziesgürteln ermöglicht; das Erkennen wichtiger stratigraphischer Oberflächen und der damit verbundenen Stapelmuster der stratigraphischen Einheiten; 2) Die *Terebratula*-Schalenkonzentrationen sind zahlreich, treten zyklisch auf und bilden dispergierte, dünne, dicht gepackte Pflaster und ein Biostrom (eine 2 m dicke, dicht gepackte *Terebratula*-dominierte Konzentration, die über 850 m im Untersuchungsgebiet verfolgbar ist). Das zweite Kapitel dieser Dissertation präsentiert sequenzstratigraphische und sedimentologische Modelle der unteren Pliozänsequenz im Untersuchungsgebiet. Die kleinen stratigraphischen Einheiten wurden als Klinotheme identifiziert, die durch subaquatische Klinoformen im Delta-Maßstab begrenzt sind. Regressive Oberflächen der Meereserosion in Verbindung mit absteigenden Stapelmustern deuten auf einen allgemeinen Trend des relativen Meeresspiegelabfalls hin. Es wird der Schluss gezogen, dass die Paläocommunities von *Terebratula* als Reaktion auf hochfrequente Impulse desrelativen Anstieg des Meeresspiegels zyklisch erfolgte, da der Akkomodationsraum im

Zusammenhang mit der Ausdehnung der Küstenfaziesgürtel zumLand hin und dem damit einhergehenden Sedimentmangel in den von den *Terebratula*-Paläocommunities besetzten Offshore-Umgebungen zunahm. Das dritte Kapitel dieser Dissertation befasst sich mit paläoökologischen Faktoren (Sauerstoffanreicherung des Bodens, Produktivität, Temperatur und Lichtintensität) als erklärende Variablen für den Erfolg von *Terebratula* entlang eines proximal-distalen Gradienten. Diese Faktoren wurden durch Untersuchung der benthischen und planktischen Foraminiferen- und kalkigen Nannoplankton-Vergesellschaftungen sowie der Sauerstoffisotopenverhältnisse aus der sekundären Schalenlage von *Terebratula*-Schalenkalzit bewertet. Es wird der Schluss gezogen, dass Terebratula vielseitig war und sauerstreiche, oligotrophe Umweltbedingungen bevorzugte, jedoch schwankende Impulse mit erhöhtem Eintrag organischer Stoffe und den damit verbundenen verringerten Sauerstoffwerten am Meeresboden tolerieren konnte. Die aus planktischen Foraminiferen-Vergesellschaftungenabgeleitete Paläotemperatur legt nahe, dass dieser Parameter auf lokaler Ebene für den Erfolg von Terebratula nicht wichtig war. *Terebratula* war in Küstengebieten selten oder nicht vorhanden. Spitzenhäufigkeiten von *Terebratula* wurden konsistent in der Nähe, jedoch unterhalb der Offshore-Übergangszone gefunden, in der keine korallinen Rotalgen vorhanden waren. Frühere Untersuchungen zurIchnovergesellschaftung von Mikrobioerodierern, die in *Terebratula*-Schalen gefundenwurden, zusammen mit der seltenen Seeigel-Raspelspur *Gnathichnus pentax* und dem Fehlen von flacherem *Radulichnus*, legen nahe, dass *Terebratula* in schwachem Licht oder aphotischen Bedingungen gedieh, wahrscheinlich ausgeschlossen von flacheren, besser durchlichtetenUmgebungen durch Weidedruck. Die überproportionale Verteilung von *Terebratula* in küstenfernenUmgebungen kann durch eine Kombination von Sedimentationsratengradienten und küstenparallelen Strömungen erklärt werden. Der enge Bereich der Paläotemperaturen verschiedener Arten von Terebratulinae, abgeleitet von Sauerstoffisotopenverhältnissen, legt nahe, dass die letzten Mitglieder der Unterfamilie die auffälligen Temperaturabfälle, die um den Jaramillo Subchron auftreten, nicht überleben konnten.